


Spring 5-9-2020

## Characterization of Novel Animal Models for Parkinson's Disease

Mohannad Almikhlafi  
*University of Nebraska Medical Center*

Tell us how you used this information in this [short survey](#).

Follow this and additional works at: <https://digitalcommons.unmc.edu/etd>

 Part of the [Disease Modeling Commons](#), and the [Nervous System Diseases Commons](#)

---

### Recommended Citation

Almikhlafi, Mohannad, "Characterization of Novel Animal Models for Parkinson's Disease" (2020). *Theses & Dissertations*. 445.  
<https://digitalcommons.unmc.edu/etd/445>

This Dissertation is brought to you for free and open access by the Graduate Studies at DigitalCommons@UNMC. It has been accepted for inclusion in Theses & Dissertations by an authorized administrator of DigitalCommons@UNMC. For more information, please contact [digitalcommons@unmc.edu](mailto:digitalcommons@unmc.edu).

CHARACTERIZATION OF NOVEL ANIMAL MODELS  
FOR PARKINSON'S DISEASE

By

Mohannad A. Almikhlafi

A DISSERTATION

Presented to the Faculty of  
The University of Nebraska Graduate Collage  
In Partial Fulfillment of the Requirements  
For the Degree of Doctor of Philosophy  
Pharmacology and Experimental Neuroscience

Under the Supervision of Professor Howard S. Fox

University of Nebraska Medical Center

Omaha, Nebraska

March, 2020

Supervisory Committee

Myron Toews, Ph.D.

Matthew Zimmerman, Ph.D.

Keshore Bidasee, Ph.D.

Siddappa Byrareddy, Ph.D.

## Acknowledgments

In the Name of God, the Most Gracious, the Most Merciful

As the “graduate student” part of my life draws to a close, I cannot help but to look back and express my gratitude for many people who provided aid during my time in graduate school. Without all of you, my journey would have been very difficult.

First and foremost, I have to mention and express my gratitude to my mentor, Dr. Howard S. Fox for many things. Dr. Fox is one of the smartest people I have ever known. He took me as a mentee after leaving my previous lab. In the beginning, I had a hard time fitting into the research that was going in the lab. However, he assisted me a lot to find myself. Not only that, but he was very open to my ideas and I can still remember the excitement in his face when I told him that we can build our own gait machine, or we that can do stereology. He is one of the only people that I know that never lost ambition about science and the more we discover, the more ambitious he becomes to know more. He always encourages us to be curious in science and a good example of this is encouraging me to explore the physiological differences in rat reproductive organs. Dr. Fox’s work ethic and attitude made him a role model to me. Besides science, he successfully created a big lovely family within the lab. From all my heart, thank you, Dr. Fox.

Thank you to the members of my advisory committee, Dr. Matthew Zimmerman, Dr. Keshore Bidasee, Dr. Myron Toews, and Dr. Siddappa Byraredy for their time, guidance, and comments.

I would like also to express gratitude to Dr. Kelly L. Stauch who is not from West Des Moines. Kelly is more than a colleague, she is a friend and I consider her as my co-mentor and, in the near future, a collaborator. I learned a lot from discussing things with Kelly, from designing experiments to structuring a project. I am very honored to know Kelly and to work with her.

Thank you to my friends in Fox lab. Benjamin Lamberty, who helped maintain our growing rat colony and helped greatly in the development of behavioral protocols. Steven Totusek, who has added so much to my project by developing and building behavior equipment, as well as, helping with software. I also would like to thank all Fox and Stauch laboratory personnel: Brenda Morsey, Jenny Brady, Kathleen Emanuel, Joseph George (Runza buddy), Shannon Callen (Second place fantasy football), Anna Fangmeier, Dr. Andrew Trease, Eliezer Lichter, and Jane Mattingly.

I will forever be thankful to my former mentor during my Master's, Dr. Alice Gardner. Alice was a great mentor who was helpful in providing advice many times during my graduate school career. She was and remains a role model as a passionate scientist, mentor, and teacher. I still think fondly of my time as a graduate student in her lab. Her enthusiasm and love for teaching is contagious.

I am very, very grateful to my lovely wife, Amjad Amoudi. She is the mitochondrion of my life and the source of my happiness. Since beginning my journey of pursuing higher education in the United States in 2011, Amjad has always been by my side. She always motivates, encourages, and cheers me up.



She has faith in me and my intellect, even when I felt like digging hole and crawling into one because I didn't have faith in myself. The past ten years have not been an easy ride, both academically and personally. I truly thank Amjad for sticking by my side, even when I was irritable and depressed. Without your presence in my life, I would have quit five years ago. I am very pleased, grateful and lucky to have you in my life.

I am very grateful to my kids, Emar, Awab, Omar, and Adam; your presence in our lives was the best thing that happened to us. Your presence gave us power and strength. Awab, I feel that I lost a part of my heart the moment we lost you. I know for a fact that you are in a better place with better people. You will never be forgotten and will always be in our minds and hearts.

I would like to acknowledge my parents, Najiah Amoudi and Abdu Almikhlaifi for their unconditional love and support. My siblings Mohammed, Mowaffaq, Maysam, Ghalib, and Shaker. Also, my brother-in-law, Amro Barashi. I am also very grateful to my extended family Enam Istanbuli and Tariq Amoudi and my in-laws, Jihad, Eyad, Mohammed, Jawad, and Joud.

Finally, I would like to express my gratitude to King Abdullah Bin Abdul Aziz Al-Saud "May God mercy may be on his Soule" and King Salman Bin Abdul Aziz Al-Saud and the Crown Prince HRH Mohammed Bin Salman for giving us the Saudi students the opportunity to receive this quality of higher education through the Kings scholarship program. Thank you to UNMC for the high-quality education I have received. Thank you to my scholarship sponsors: Taibah

University and the Ministry of Education represented by the Saudi Arabian  
Cultural Mission in the United States of America.

## Abstract

# CHARACTERIZATION OF A NOVEL ANIMAL MODEL OF PARKINSON'S DISEASE: PINK1/PARKIN DOUBLE KNOCKOUT RATS

Mohannad A. Almikhlaifi, Ph.D.

University of Nebraska, 2020

Supervisor: Dr. Howard S. Fox, M.D., Ph.D.

Parkinson's disease (PD) is neurodegenerative disorder characterized by dopaminergic neuronal loss in the substantia nigra (SN) pars compacta. Mutations in DJ-1, PINK1 and Parkin lead to PD in humans; however, in mice, mutations or knockout of these genes do not lead to disease. Development of small animal models mimicking PD pathogenesis would enable better understanding of the disease. Here, we examined two approaches using laboratory rats. First, DJ-1 knockout rats have been reported to develop movement disorders and loss of neurons similar to human PD. Comprehensive analysis of mitochondrial proteomic alteration in isolated synaptic mitochondria from DJ-1 knockout rats using mass spectrometry revealed that proteins perturbed by the loss of DJ-1 were involved in several mitochondrial functional pathways, including the TCA cycle and the electron transport chain. In addition,

synaptic mitochondrial respiration was measured to assess mitochondrial function, which showed a significant change due to DJ-1 knockout.

Second, we generated a novel model of Parkinson's disease by combining PINK1 and Parkin knockouts to create a PINK1/Parkin double knockout (DKO) rat. To characterize the model, behavioral testing was used to assess motor function and stereological counting to quantify assessed neurons. PINK1/Parkin DKO at 6 months showed a 23% reduction in dopaminergic neurons in the SN relative to wild-type rats. Neuronal loss increased to 45% in older rats (8 months of age). To understand the impact of degeneration of neurons on behavior, gait was measured using a device developed in the lab and called the RatWalker. Gait abnormalities were present at 8 months. Abnormalities were present in different gait parameters, including a reduction in hind-limb step length, a reduction in fore- and hind-limb step pressure, and an increase in step angle. Bradykinesia and agility were tested by pole test, which showed an increase in the time required to turn and to walk down the pole in 6- and 9-month old rats. Hind-limb strength assessed by cylinder test showed a significant drop in the rearing frequency at 6 and 8 months of age. Together, these projects demonstrate the importance of these genes and proteins affecting mitochondria in Parkinson's disease in terms of both function and proteomics that would help improving our understanding of the underlying mechanisms of disease.

## Table of Contents

<b>Acknowledgments .....</b>	<b>i</b>
<b>Abstract .....</b>	<b>i</b>
<b>Table of Contents .....</b>	<b>v</b>
<b>Table of Figures .....</b>	<b>x</b>
<b>List of abbreviations .....</b>	<b>xiv</b>
<b>1 Chapter 1 .....</b>	<b>1</b>
<b>1.1 History .....</b>	<b>2</b>
<b>1.2 Etiology and risk factors of Parkinson's disease .....</b>	<b>3</b>
<b>1.3 Clinical symptoms and stages of Parkinson's disease: .....</b>	<b>6</b>
1.3.1 Motor symptoms: .....	6
<b>1.4 Neurochemical and Neuropathological Features of PD .....</b>	<b>10</b>
<b>1.5 Mitochondrial Functions: .....</b>	<b>12</b>
<b>1.6 Mitophagy .....</b>	<b>13</b>
<b>1.7 Animal models to study Parkinson's disease .....</b>	<b>14</b>
1.7.1 Neurotoxin model: .....	14
1.7.2 Genetic models .....	18
<b>1.8 PINK1 and Parkin importance beyond Parkinson's disease .....</b>	<b>28</b>

1.8.1	Cancer .....	28
1.8.2	Heart Disease .....	29
1.8.3	Liver disease .....	30
<b>1.9</b>	<b>Current Therapies for PD.....</b>	<b>30</b>
1.9.1	Medication.....	30
1.9.2	Deep Brain Stimulation (DBS).....	31
<b>1.10</b>	<b>Ideal animal model .....</b>	<b>205</b>
<b>2</b>	<b>Chapter 2.....</b>	<b>46</b>
<b>2.1</b>	<b>Abstract.....</b>	<b>47</b>
<b>2.2</b>	<b>Introduction .....</b>	<b>48</b>
<b>2.3</b>	<b>Materials and Methods.....</b>	<b>49</b>
2.3.1	Animals .....	49
2.3.2	Brain dissection and synaptic mitochondrial isolation .....	50
2.3.3	Sample preparation for SWATH-MS proteomics.....	51
2.3.4	SWATH data acquisition .....	52
2.3.5	Bioinformatic analysis .....	52
2.3.6	Mitochondrial bioenergetics assays .....	53
2.3.7	Statistical analysis.....	54
<b>2.4</b>	<b>Results .....</b>	<b>54</b>

2.4.1	Proteomic alterations in striatal synaptic mitochondria from DJ-1 deficient rats .....	54
2.4.2	Loss of DJ-1 alters striatal mitochondria in rats .....	57
<b>2.5</b>	<b>Discussion: .....</b>	<b>58</b>
<b>3</b>	<b>Chapter 3.....</b>	<b>120</b>
<b>3.1</b>	<b>Abstract.....</b>	<b>121</b>
<b>3.2</b>	<b>Introduction .....</b>	<b>123</b>
<b>3.3</b>	<b>MATERIALS AND METHODS.....</b>	<b>126</b>
3.3.1	Generation of DKO rats.....	126
3.3.2	Weight.....	126
3.3.3	Brain collection for stereology .....	127
3.3.4	Stereology tissue processing .....	127
3.3.5	Stereology .....	128
3.3.6	Nerve terminal isolation.....	128
3.3.7	Mitochondrial Respiration.....	129
3.3.8	Cylinder Test.....	130
3.3.9	Gait .....	131
3.3.10	Pole test .....	131
3.3.11	Accelerating Rotarod.....	132

3.3.12	Statistical analysis .....	133
<b>3.4</b>	<b>RESULTS .....</b>	<b>133</b>
3.4.1	Behavioral characteristics of DKO rats.....	133
3.4.2	Effect of aging on DKO behavior.....	135
3.4.3	Pathological phenotyping of DKO rats. ....	136
3.4.4	Functional assessment of the mitochondria .....	137
<b>3.5</b>	<b>DISCUSSION.....</b>	<b>137</b>
<b>4</b>	<b>Chapter 4.....</b>	<b>168</b>
<b>4.1</b>	<b>Introduction .....</b>	<b>169</b>
<b>4.2</b>	<b>Methods .....</b>	<b>170</b>
4.2.1	Animals .....	170
4.2.2	Immunoblotting.....	170
4.2.3	DNA extraction .....	171
4.2.4	Real Time PCR (RT-PCR) .....	171
4.2.5	Fluorescence immunostaining.....	172
4.2.6	Rearing test.....	173
<b>4.3</b>	<b>Results .....</b>	<b>173</b>
4.3.1	Striatal and cortical dopaminergic neurons terminal.....	173
4.3.2	Striatal mtDNA .....	174



4.3.3	Longitudinal behavior examination in female DKO.....	174
<b>5</b>	<b>Chapter 5.....</b>	<b>200</b>
5.1	Conclusions.....	201
5.2	Stress .....	203
5.3	Exercise .....	204
	Appendix .....	206
<b>6</b>	<b>References:.....</b>	<b>210</b>

## Table of Figures

Figure 1.1 Breakthroughs in PD history. ....	33
Figure 1.2 Neuropathology of Parkinson's Disease. ....	35
Figure 1.3 The PINK1–Parkin pathway of mitophagy. ....	38
Figure 1.4 MPTP metabolism in the brain.....	41
Figure 1.5 Dopamine synthesis and common pharmacological therapeutics for PD.....	43
Figure 1.6 Electrode Implantation for Deep-Brain Stimulation.....	45
Figure 2.1 Identification of the differentially expressed proteins in the striatal synaptic mitochondria from DJ-1 KO rats. ....	63
Figure 2.2 Significant differentially expressed proteins in the striatal synaptic mitochondria from DJ-1 KO rats.....	65
Figure 2.3 Overview of pathways altered in DJ-1 KO rats.....	67
Figure 2.4 Centrality analysis among synaptic mitochondrial proteins differentially expressed in DJ-1 KO rats.....	69
Figure 2.5 Mitochondrial bioenergetic analysis.....	71
Figure 2.6 Quantitative analysis reveals changes in the expression of protein subunits in the ETC and TCA due to DJ-1 deficiency. ....	73
Figure 2.7 DJ-1 protein expression.....	75
Figure 2.8 Reproducibility of SWATH-MS proteomics between biological replicates of WT and DJ-1 KO synaptic mitochondria. ....	77
Figure 3.1 Genotyping of DKO rats.....	143
Figure 3.2 Weight change in WT and PINK1/Parkin DKO rats. ....	145

<b>Figure 3.3 Reduction hind-limb strength and presence of fore-limb asymmetry.....</b>	<b>147</b>
<b>Figure 3.4 Gait abnormality of fore- and hind-limbs of DKO. ....</b>	<b>149</b>
<b>Figure 3.5 Increase in bradykinesia and decrease in the agility in DKO. ..</b>	<b>151</b>
<b>Figure 3.6 Motor coordination deficit in DKO. ....</b>	<b>153</b>
<b>Figure 3.7 Progressive loss of dopaminergic neuron in the SNpC and the VTA. ....</b>	<b>155</b>
<b>Figure 3.8 Effect of PINK1/Parkin deletion on mitochondrial respiration at the nerve terminal.....</b>	<b>157</b>
<b>Figure 3.9 Supplement stereology counting areas.....</b>	<b>159</b>
<b>Figure 3.10 Supplement walking floor design.....</b>	<b>161</b>
<b>Figure 3.11 Supplement walking floor cover design. ....</b>	<b>163</b>
<b>Figure 3.12 Supplement mirror holder design. ....</b>	<b>165</b>
<b>Figure 3.13 Supplement background light design.....</b>	<b>167</b>
<b>Figure 4.1 Western blot and quantification of cortical homogenate of 3 month old rats.....</b>	<b>177</b>
<b>Figure 4.2 Western blot and quantification of cortical homogenate of 6 month old rats.....</b>	<b>179</b>
<b>Figure 4.3 Western blot and quantification of cortical homogenate of 8 month old rats.....</b>	<b>181</b>
<b>Figure 4.4 Western blot and quantification of striatal homogenate of 3 month old rats.....</b>	<b>183</b>

<b>Figure 4.5 Western blot and quantification of striatal homogenate of 6 month old rats.....</b>	<b>185</b>
<b>Figure 4.6 Western blot and quantification of striatal homogenate of 8 month old rats.....</b>	<b>187</b>
<b>Figure 4.7 Absence of mtDNA alterations. ....</b>	<b>189</b>
<b>Figure 4.8 Upregulation in the expression of dopamine transporter in the SNpc. ....</b>	<b>191</b>
<b>Figure 4.9 Weight change in WT and PINK1/Parkin DKO females. ....</b>	<b>193</b>
<b>Figure 4.10 Agility and bradykinesia in DKO females. ....</b>	<b>195</b>
<b>Figure 4.11 Motor coordination in DKO females.....</b>	<b>197</b>
<b>Figure 4.12 Reduction in hind-limb strength of female DKO. ....</b>	<b>199</b>

**List of tables**

<b>Table 1.1 Familial Parkinson's Disease .....</b>	<b>5</b>
<b>Table 2.1 A total of 932 proteins were quantified by SWATH-MS in all samples from synaptic mitochondria from the striatum of 3-month-old WT and DJ-1 KO rats. ....</b>	<b>78</b>
<b>Table 2.2 The complete list of the 371 proteins identified and the quantification values for each biological replicate.....</b>	<b>105</b>
<b>Table 2.3 differentially expressed proteins found in striatal mitochondria of DJ-1 KO rats.....</b>	<b>116</b>

## List of abbreviations

6-OHDA	6-hydroxydopamine
AADC	aromatic L-amino acid decarboxylase
AAV	adeno-associated virus
ALT	alanine aminotransferase
AR-JP	autosomal-recessive juvenile parkinsonism
ARM	armadillo domain
ATP	adenosine triphosphate
BBB	blood-brain barrier
BNIP3	BCL2 interacting protein 3
CE	coefficient of error
CHCHD2	coiled-coil-helix-coiled-coil-helix domain containing 2
COMT	catecholamine-O-methyltransferase
COR	C-terminal of ROC
DA	dopamine
DAT	dopamine transporter
DBS	Deep Brain Stimulation
DIA	data-independent acquisition
DKO	PINK1/Parkin double-knockout
DUB	de-ubiquitinating
ETC	electron transport chain
FAF	fatty acid free

FASP	filter-aided sample preparation
FCCP	carbonylcyanide-p-triflouromethoxyphenylhydrazone
FDA	U.S. Food and Drug Administration
FUNDC1	FUN14 domain-containing protein 1
GO	Gene Ontology
IACUC	Institutional Animal Care and Use Committee
Idh2	isocitrate dehydrogenase 2
IHC	Immunohistochemical
KO	knockout
L-DOPA	L-3,4-dihydroxyphenylalanine
LARR2	Leucine-rich repeat kinase 2
LB	Lewy Bodies
LC-3	light chain 3
LEH	Long Evans Hooded
LRRK2	Leucine-rich repeat kinase 2
MAO B	monoamine oxidase B
MAPKKK	mitogen-activated protein kinase kinase kinase
MLDA	mesolimbic dopaminergic neurons
MPP+	1-methyl-4-phenylpyridine
MPTP	1-methyl-4-phenyl-1,2,3,6-tetrahydropyridine
mRNA	Messenger ribonucleic acid
NAK	ankyrin repeat
NGS	normal goat serum

NINDS	National Institute of Neurological Disorders and Stroke
NIX	NIP3-like protein X
NSDA	Nigrostriatal dopaminergic neuron
OCR	oxygen consumption rate
Ogdh	oxoglutarate dehydrogenase
OMM	outer mitochondria membrane
OTP	ovarian tumor protease
OXPHOS	oxidative phosphorylation
PBS	phosphate buffer saline
PCR	Polymerase Chain Reaction
PD	Parkinson's disease
PET	Positron transmission tomography
PI-3K	phosphatidyl-inositol-3 kinase
PINK1	PTEN induced putitive kinase 1
RBR	RING1-IN-Between-RING2
ROC	Ras of complex protein domain
ROS	reactive oxygen species
Sdha	succinate dehydrogenase complex flavoprotein subunit A
SNPC	Substantia nigra pars compacta
SRC	spare respiratory capacity
SWATH-MS	sequential window acquisition of all theoretical fragment-ion spectra mass spectrometry
TCA	Tricarboxylic acid



T <sub>Des</sub>	time to descend
TH	tyrosine hydroxylase
TMPD	tetramethylphenylenediamine
T <sub>turn</sub>	time to turn
Ubl	ubiquitin-like
UCH	ubiquitin carboxy-terminal hydrolase
UCH-L1	ubiquitin carboxy-terminal hydrolase L1
US	United States
USP	ubiquitin-specific protease
VTA	ventral tegmental area
WT	wild-type
$\Delta\Psi_{\mu}$	mitochondrial membrane potential

# Chapter 1

## Parkinson's Disease

## 1.1 History

Two centuries ago, the British physician James Parkinson wrote a seminal essay reporting his clinical observations of six individuals with “paralysis agitans” or ‘the shaking palsy.’ James Parkinson described the clinical picture of the disease as: ‘Involuntary tremulous motion, with lessened muscular power, in parts not in action and even when supported; with a propensity to bend the trunk forwards, and to pass from a walking to a running pace: the senses and intellects being uninjured’ [1]. Sixty years later, Jean-Martin Charcot made the next important contribution by differentiating the disease from other disorders associated with tremors such as multiple sclerosis. Also, he explained in detail some of the changes that occur with the disease, e.g., arthritic changes, dysautonomia, and pain. In order to honor James Parkinson, his name became a term that describes the disease ‘Parkinson’s disease (PD)’ by Charcot, who found that PD patients do not necessarily have tremors [2]. In 1880, William Gowers, who worked in London with 80 patients with PD, was the first to correctly identify the slight predominance of the male in his study “Manual of Disease of the Nervous System.” Clinical and morphological details of the progressive stages of disabilities associated with PD were reported by French neurologists Henri Meige and Paul Richer in 1895 [3]. Motor fluctuations were noted in 1921 by Joseph Babinski [4].

The pathology of the disease was first proposed by Brissaud, who proposed damage to the substantia nigra in 1925 [5], followed by further studies demonstrating the involvement of the substantia nigra in the disease [6, 7].

Biochemical changes in the brain were identified in the 1950s after a large amount of work by Arvid Carlsson, Oleh Hornykiewicz, and Isamu Sano. The most comprehensive analysis of PD pathology was performed by Greenfield and Bosanquet in 1953 [8]. Since the pathology of the disease is associated with dopamine, extended and short-term benefits of oral levo-dopa were confirmed, which made levo-dopa the primary medication for those with PD in 1969 [9-11]. In 2000, Arvid Carlsson was awarded the Nobel Prize in Physiology or Medicine for his work on dopamine and PD (Figure 1.1).

## **1.2 Etiology and risk factors of Parkinson's disease**

The etiology of PD is not fully understood despite almost 200 years of research. The risk of developing PD is associated with several epidemiological factors. (1) Age: The risk of developing PD rises with aging since the disease affects around 1% of individuals over the age of 65, and the risk increases as the individuals become older [12]. (2) Gender: PD incidence rate is higher in males than in females with a ratio of 2 to 1 [13]. In males, the incidence rate rises from 3.6 per 100,000 between the ages of 40-49 to around 258 per 1000,000 for those over 80. At the same time, the incidence rate in females over the age of 80 is approximately 66 per 100,000 [14]. In 2010, there were around 680,000 individuals in the United States (US) with PD, and this number will rise to approximately 930,000 in 2020 and 1,238,000 in 2030 based on the US Census Bureau population projections [15]. (3) Race/Ethnicity: Epidemiological studies that took place in the US concluded that Hispanics have the highest risk of

developing PD, followed by non-Hispanic White, Asian, finally African American persons, the latter having been found to be at low risk to develop PD [16, 17]. (4) Environmental factors: Investigation of environmental toxins linked insecticides, pesticides, and herbicides to PD causes. In 1996 a study in Germany involving 380 PD patients and 379 healthy subjects concluded that exposure to preservatives of wood and to heavy metals had a significant correlation with the development of the disease [18]. Additionally, rural well water drinking for more than five years showed an increase in the risk of developing PD by around 90% in rural California. The reason is believed to be due to contamination of the well water by pesticides, which explains the increase in the incidence rate in rural and agricultural states. [19].

In the late 1970s and early 1980s, self-administration of contaminated synthetic heroin led to severe and permanent movement disorders resembling PD [20, 21]. Samples of the synthetic heroin revealed that it was comprised of almost pure 1-methyl-4-phenyl-1,2,3,6-tetrahydropyridine (MPTP) that was identified as the likely reason for developing permanent PD [22]. Subsequent work revealed that MPTP is metabolized in astrocytes to MPP<sup>+</sup>, which poisons complex I of the mitochondrial electron transport chain, leading to death of dopaminergic neurons [23]. (5) Genetic factors: A large number of genetic studies on families with a high prevalence of PD revealed several genes linked to PD. Among those genes, the mutations in  $\alpha$ -synuclein, leucine-rich repeat kinase 2 (LRRK2), parkin, PTEN-induced putative kinase 1 (PINK1), and DJ-1 are now well documented to be linked to PD (**Table 1.1**).

**Table 1.1 Familial Parkinson's Disease**

Locus	Gene	Chromosomal location	Inheritance	Onset	Reference
PARK1	$\alpha$ -synuclein	4q21	AD	Mid-late	[24]
PARK2	Parkin	6q25.2-q27	AR	Early	[25]
PARK3	Unknown	2q13	AD	Late	[26]
PARK4	$\alpha$ -synuclein	4q21	AD	Late	[27]
PARK5	UCHL1	4q13	AD	Mid-late	[28]
PARK6	PINK1	1p36	AR	Early	[29]
PARK7	DJ-1	1p36	AR	Early	[30]
PARK8	LARRK2	12q12	AD	Late	[31]
PARK9	Unknown	1p36	AD and AR	Juvenile	[32]
PARK10	Unknown	1p	AD	Late	[33]
PARK11	Unknown	2q39-q37	AD	Late	[34]
PARK12	Unknown	Xq21-q25	X-Lined	Unknown	[33]
PARK13	Htra2	2p12	AD	Late	[35]
PARK22	CHCHD2	7p11.2	AD	Late	[36]

### **1.3 Clinical symptoms and stages of Parkinson's disease:**

James Parkinson inaccurately emphasized that non-motor abilities, including sensory and cognitive abilities, are not affected in patients with PD. Since then, the main focus of research has been on the motor symptomology of PD.

#### **1.3.1 Motor symptoms:**

According to the National Institute of Neurological Disorders and Stroke (NINDS) [37, 38], cardinal signs of PD can be grouped under the acronym TRAP:

1. Tremor 4-6 Hz (Shaking of hands, arms, legs, and face, especially during rest)
2. Rigidity of the muscle in the limbs and trunk
3. Akinesia/Bradykinesia (i.e., slowness of initiating a voluntary movement)
4. Postural instability (impairment in coordination and balance)

Besides these symptoms, there are secondary motor features that were reported in PD [38] including:

- Dystonia
- Fatigue
- Fine motor tasks impairment
- Gross motor coordination impairment
- Decreased arm swing while moving
- Speech problems e.g. softness of voice
- Masking (loss of facial expression)
- Micrographia (small size and cramping in handwriting)

- Difficulty swallowing
- Sexual dysfunction
- Cramping
- Drooling

Based on the UK Parkinson's Disease Society Brain Bank clinical diagnosis criteria, the presence of one or more of the cardinal symptoms, in addition to family history in the patient's family, is used to diagnose the disease. Also, responsiveness to levodopa, a chemical precursor of dopamine used in managing PD symptoms, is considered confirmation of PD diagnosis [39].

According to the Hoehn and Yahr scale [40], there are five different stages in PD that the patient goes through:

Stage I: Minimal or no functional motor impairment; if present, it will be unilateral.

Stage II: Bilateral existence of cardinal symptoms and some secondary symptoms may appear without balance impairment.

Stage III: Increase in the severity of stage II symptoms. In addition, balance impairment becomes blatant. At this stage, the patient is still independent with mild to moderate disability.

Stage IV: The patient becomes severely disabled due to motor symptoms, leading to an exacerbation in need of assistance in routine activities.

Stage V: The patient is entirely disabled, confined to bed or wheelchair, and needs full assistance.



### 1.3.1.1 Non-motor symptoms:

Reports have confirmed the existence of many non-motor symptoms in patients with PD [41-44]. However, clinicians commonly overlook non-motor symptoms of PD and do not discuss them or fail to diagnose them [45]. These symptoms include depression, cognitive changes, pain, hyposmia, anxiety, sleep disturbance, gastrointestinal problems (constipation and acid reflux), and urinary problems (increase the frequency of urination and incontinence).

### 1.3.1.2 Pre-motor Symptoms

Currently, PD is diagnosed when the previously mentioned motor symptoms appear. Those motor symptoms occur as a result of the degeneration of DA neurons in the substantia nigra pars compacta (SNpc) [46]. However, other neurons and pathways are also affected. Emerging information by Braak et al. demonstrated the involvement of the mesocortical and the cortico-limbic pathways in the progression of the disease [47]. The presence of Lewy bodies and Lewy neurites, as well as significant neurodegeneration in different sites including the olfactory bulb, anterior olfactory nucleus, dorsal motor nucleus, and pons, have been found in post-mortem studies [48]. The association between early-stage PD and smell dysfunction is now well recognized, and the prevalence in sporadic PD is approximately 80-90% [49]. Also, reports strongly correlate hyposmia and excessive daytime sleepiness with the onset of motor symptoms in PD [50, 51]. Braak et al. proposed neuropathological mapping for PD, signs of which begin almost 20 years before the appearance of motor symptoms [48, 52].

#### 1.3.1.3 Pre-symptomatic

Stage 1: This stage is characterized by gastrointestinal symptoms where Lewy bodies deposits were found, especially in the colon [53]. Change in bowel movements to less than 1/day imply that constipation is the premotor phase of PD [54]. Also, changes in hyposmia, bladder, and erectile function have been linked to early signs of PD [52].

Stage 2: This stage involves the coeruleus/subcoeruleus complex, which controls food intake, vigilance, sleep-wake cycle, mood, and sensory response to stimuli [55-58]. Also, it involves a raphe nucleus that plays roles in learning and memory. Patients in this stage of the disease exhibit some of the following symptoms: excessive daytime sleepiness, depression, obesity, and maybe cognitive deficits [52].

#### 1.3.1.4 Classic motor symptoms

Stage 3: Unilateral motor deficits (i.e., tremor, rigidity, and bradykinesia) and depression are the main characteristic features of this stage. Here, Lewy body deposits migrate to the SNpc and pedunculopontine tegmental nucleus and subnucleus of the amygdala [59].

Stage 4: This stage is characterized by an increase in the extent of Lewy bodies in multiple sites, including interstitial nucleus of the stria terminalis, the accessory cortical and basolateral nuclei of the amygdala, ventral claustrum, intralaminar nuclei of the thalamus, the second sector of the Ammon's horn, and the

anteromedial temporal mesocortex. Defects in this circuit may lead to a change in impulse control, hypersexuality, and compulsive gambling [60, 61].

#### 1.3.1.5 Disability motor symptoms

Stage 5 and 6: These stages represent the late stages of the disease when PD patients require full assistance due to disability. In these stages, motor deficits become severe, accompanied by cortical damage. Lewy body inclusions become more extreme than in the previously mentioned regions in stages 1 to 4.

However, in stages 5 and 6, they spread to insular, subgenual mesocortex, anterior cingulate regions extending to pre-motor areas of neocortex, primary, and sensory-motor areas [62].

### 1.4 Neurochemical and Neuropathological Features of PD

Major pathological hallmarks of PD include the loss of dopaminergic neurons in the SNpc and the presence of intraneural cytoplasmic inclusions, known as “Lewy Bodies” (LBs), which are proteinaceous deposits of  $\alpha$ -synuclein [63, 64] and ubiquitin (**Error! Reference source not found.**) [65]. The cell bodies of nigrostriatal dopaminergic neurons (NSDA) are located in the SNpc, and they project terminals to the striatum. Degeneration of these neurons, which contain a brown pigment known as neuromelanin, produces the pathological clinical features of SNpc depigmentation. In patients with PD, this loss pattern was parallel to a 57% reduction in the expression of dopamine (DA) transporter (DAT) messenger ribonucleic acid (mRNA) compared to age-matched healthy

controls [66, 67]. In addition, [ $^{11}\text{C}$ ]FeCIT positron emission tomography (PET) scans of DAT in patients with PD revealed 25% reductions of DAT in the SN and 41% reductions in the striatum [68]. At the onset of clinical features, ~80% of striatal DA is depleted, and ~60% of dopaminergic neurons in the SNpc have died [69].

To understand the pathology of PD, the anatomy and the changes in the structure of different parts of the SNpc are crucial. In this context, the SN is divided into two zones – black (pars compacta) and red (pars reticulata). Pars compacta is divided into ventral and dorsal tiers [70]. Ventral tiers project to the striatal striosomes that project back to the cell body and the proximal dendrites of the ventral tiers, while dorsal tiers project to the matrix that projects back to the pars reticulata and distal dendrites of the ventral tiers. Striatal striosomes and matrix are histochemically unique. In PD, neuronal loss is concentrated in the ventral tiers of the SNpc. However, in healthy aging, the dorsal tiers of the SNpc are affected [59].

Dopaminergic neurons that project from the SNpc to the striatum express two populations of dopamine receptors. D1 receptor neurons form inhibitory projections to the globus pallidus internus, known as the “direct pathway”. Another population is the D2-receptor neurons that project through the globus pallidus externa, which controls the activity of the subthalamic nucleus that synapses on the globus pallidus interna. This pathway is known as the “indirect pathway” because the stimulation of the globus pallidus interna was not direct, unlike the direct pathway. In normal individuals, the direct pathway and the

indirect pathway are in balance. In PD, degeneration of DA neurons in the SNpc reduces the DA receptors in the striatum leading to an imbalance between the direct and the indirect pathways resulting in locomotor abnormalities [71].

### **1.5 Mitochondrial Functions:**

One billion years ago, bacteria invaded single-cell anaerobic organisms and established a mutual relationship that was maintained during the evolution of multicellular organisms [72]. Mitochondria, the successors of the original bacterial symbiont, are complex, multifaceted organelles essential for cellular physiology. One essential mitochondrial function is adenosine triphosphate (ATP) production, which provides energy to maintain cellular functionality [73]. In organs experiencing constant intercellular signaling, such as the heart or brain, healthy mitochondria are important for ATP production. The heavy dependence of the brain on ATP produced by oxidative phosphorylation causes elevation in the sensitivity of the mitochondria to damage [74-76]. Impaired mitochondria lead to a reduction in cellular energy levels and excessive production of reactive oxygen species (ROS), which exacerbate mitochondrial damage, that if not cleared, would lead to cell and tissue damage [77]. As a result, damaged mitochondria activate mitophagy, which is an evolutionarily conserved cellular process targeting and clearing dysfunctional or damaged mitochondria, which tend to accumulate as a result of stress or damage [78]. Dysfunctional mitochondria have been implicated in numerous neurodegenerative disorders, including Parkinson's disease.

## 1.6 Mitophagy

Mitophagy was first discovered by Lewis and Lewis in 1914 in isolated cells [79]. Mitochondrial debris thought to be from mitophagy was seen by electron microscopy in 1962 by Ashford and Porter [80]. The term mitophagy has been used since 1998, where mito means mitochondria and phagy is derived from the Greek word for eating [81]. Mitophagy takes place once damage occurs to the mitochondria that cannot be corrected; cells conduct mitophagy by different mechanisms depending on the stimuli, which can promote mitophagy through multiple signaling cascades. Mitochondria can undergo mitophagy in a ubiquitin-dependent or -independent manner [82]. Ubiquitin-dependent mitophagy involves PINK1 and Parkin, which were previously discussed. Once mitochondria become depolarized, PINK1 accumulates and is stabilized on the outer mitochondria membrane (OMM) of damaged mitochondria. Auto-phosphorylation activates PINK1 in order to recruit and phosphorylate ubiquitin and Parkin. Phosphorylation of Parkin activates ubiquitin E3-ligase activity that ubiquitinates multiple OMM components, which can be detected by autophagosome light chain 3 (LC-3), leading to autophagosome formation [78]. On the other hand, ubiquitin-independent mitophagy involves mitochondrial proteins that serve as mitophagy receptors that directly interact with LC3, including the OMM proteins NIX (NIP3-like protein X), BNIP3 (BCL2 interacting protein 3), and FUNDC1 (FUN14 domain-containing protein 1) (Figure 1.3).

Alterations in mitophagy proteins and their contribution to PD are described later on in this chapter.

## **1.7 Animal models to study Parkinson's disease**

Recent genetic discoveries have improved our understanding of the molecular pathways that contribute to the pathogenesis of PD. However, those discoveries did not shed light on other important aspects of the disease, including the following questions. Why are dopaminergic neurons more prone to degradation. What is the role of aging in genetic and sporadic PD? Can we reverse the disease or slow its progression? What is the impact of PD on organs other than the brain? To answer those questions, we need a valid animal model that shows neuronal loss that correlates with behavioral abnormalities.

### **1.7.1 Neurotoxin model:**

#### **1.7.1.1 MPTP Model**

MPTP is highly lipophilic, which allows it to pass the blood-brain barrier. Once MPTP is in the brain, it is rapidly metabolized into 1-methyl-4-phenylpyridine (MPP<sup>+</sup>) by monoamine oxidase B (MAO B) [21]. MPP<sup>+</sup> is taken up by dopaminergic neurons, since MPP<sup>+</sup> is a substrate for DAT that leads to the accumulation of MPP<sup>+</sup> [83]. The neurotoxic effect of MPP<sup>+</sup> primarily occurs by inhibiting complex 1 of the mitochondrial respiratory chain leading to impaired production of ATP, elevated intracellular calcium concentration, and free radical generation that causes oxidative stress and thus cell death [84-86].

Given how MPTP can induce similar effects to typical PD in humans, MPTP was used to generate animal models to study the pathophysiological changes, behavioral abnormalities, and the effect of drugs on the symptoms. Various mammalian species were treated with MPTP to model PD, including sheep, dogs guinea pigs, cats, mice, and monkeys [87, 88]. The first attempts to generate PD with MPTP in monkeys in 1984 showed all motor symptoms typically seen in PD patients, and these were responsive to levodopa treatment. Also, MPTP was able to induce a loss in the dopaminergic neurons in the SNpc, which terminates in the putamen [89, 90]. MPTP treatment was also able to induce similar effects in mice, but not in rats. The reason why rats are resistant to MPTP toxicity was found to be due to the very high level of MAO in their blood-brain barrier that converts MPTP to MPP<sup>+</sup>, which is not lipophilic and thus MPP<sup>+</sup> cannot permeate into the rat brain [91, 92]. In summary, with the caveat of MPTP acute toxicity as seen with other neurotoxic animal models of PD, it will proceed to play a significant role in research based on its reproducibility, ability to produce PD-like effects, and responsiveness to dopamine replacement therapies, e.g. L-3,4-dihydroxyphenylalanine (L-DOPA) (Figure 1.4).

#### 1.7.1.2 6-Hydroxydopamine Model

In 1968, 6-hydroxydopamine (6-OHDA) was introduced as the first neurotoxin to induce dopaminergic neuronal death in the SNpc [93]. To date, 6-OHDA has been widely used to lesion the nigrostriatal pathway to produce a PD animal model. However, it is not specific for DA neurons only, but it can induce degeneration of noradrenergic neurons as well [93]. It exerts its toxic



effect when it accumulates in the cytosol by generating reactive oxygen species and, as a result, oxidative stress-related toxicity [94]. In order to bypass the blood-brain barrier, 6-OHDA is usually injected using stereotactically into a specific region of the brain to induce the desired effect. In addition, 6-OHDA was found to successfully induce PD in rats, cats, guinea pigs, dogs, and monkeys [87, 95]. 6-OHDA is most commonly injected unilaterally to different areas of the brain, e.g., SN, medial forebrain bundle, or striatum [96]. Generally, 6-OHDA is more toxic to nerve terminals than the axon and cell body, but when injected into the SN, it produces a complete and rapid degeneration of the nigrostriatal pathway in ~2-3 days [97, 98]. Like any other model, 6-OHDA has advantages as well as disadvantages. The main advantages of this model were fast induction of neuronal degeneration, a handy tool to assess anti-parkinsonian effects and neuroprotective therapies, and useful to test new therapeutic strategies, e.g. cell transplantation. On the other hand, this model lacks a progressive and aging effect of PD, and there are no Lewy bodies present.

#### 1.7.1.3 Rotenone

Rotenone is a widely used pesticide to kill insects. It is naturally found in the Leguminosa family of plants such as *Derris elliptica*, *Lonchocarpus nicou*, and *Tephrosia vogelii* [99]. Rotenone can cross the blood-brain barrier rapidly due to its high lipophilicity and does not require a specific transporter to cross into the cell. Rotenone is a selective inhibitor of complex I that can reduce its activity by 75% without affecting the enzymatic activity of succinate dehydrogenase (complex II) or cytochrome oxidase (complex IV) [100, 101].

Rotenone was first used to generate a PD model in 1985 when Hiekkilä injected a 5 mM solution directly into a rat brain, which is approximately 500,000 fold higher than the  $IC_{50}$  of 10 nM [102]. However, at that high concentration, any toxin might induce similar results. Besides, it was reported that it also produces nonspecific peripheral toxicity in addition to nonspecific brain lesions [103]. Greenmyre and colleagues later developed a low-dose chronic regimen [100]. Jugular vein infusion of rotenone produced selective nigrostriatal neurodegeneration in addition to  $\alpha$ -synuclein inclusions. Despite rotenone advantages over other neurotoxins, it has not been widely used. The main reason is related to its high variability that depends on animal sensitivity [104].

#### 1.7.1.4 Paraquat

Paraquat (1,1'-dimethyl-4,4'-bipyridine) is a bipyridylium compound that is commonly used as a herbicide in several crops, such as soybeans, sugar cane, cotton, corn, apple, and others. The use of paraquat has already been banned in many countries due to its pulmonary-induced lesions, which are often fatal [105]. It is still unclear how paraquat affects dopaminergic neurons, but it is believed that paraquat toxic effects are primarily through oxidative stress by depleting glutathione and increasing the level of oxidized glutathione [106, 107]. Paraquat accumulation in the brain is age-dependent, which was confirmed when 2-week and 3-, 12- and 24-month-old rats received subcutaneous injection of paraquat and were euthanized after 1 hour. Results demonstrated higher concentrations in the 2 week-old animals, suggesting a role of the blood-brain barrier [108]. Motor

deficits and dopaminergic neuron degeneration in mice were found to be induced in a dose- [109] and age- [109, 110] dependent manner.

### 1.7.2 Genetic models

#### 1.7.2.1 PARK1/4 ( $\alpha$ -synuclein)

Although the function of  $\alpha$ -synuclein is not clear, the presence of various mutations in synuclein in familial as well as sporadic PD was detected [64].  $\alpha$ -synuclein is routinely expressed in the brain; however, over-expression and mutations of the protein have been linked to dopaminergic neuronal loss in the striatum and abnormalities in motor function [111, 112]. Overexpression of human  $\alpha$ -synuclein in rats was found to cause 50% loss of dopaminergic neurons in the SN 13 weeks after recombinant adenovirus infection. Also, the level of DA in the striatum was down-regulated. Degeneration of the neurons is believed to be mediated by the activation of caspase-9 as a result of oxidative stress in order to activate apoptosis [113, 114]. Additionally, overexpression of  $\alpha$ -synuclein was reported to induce mitochondrial dysfunction by binding to OMM. There is also growing evidence to suggest that  $\alpha$ -synuclein can affect mitochondrial dynamics, in particular mitochondrial fusion leading to mitochondrial fragmentation in a *Caenorhabditis elegans* model [115].

In contrast, missense mutations in  $\alpha$ -synuclein gene were previously explored, which occur in familial PD (A53T and A30P). Mice expressing A53T exhibited larger axonal swelling in brainstem and spinal cord. Also, eosinophilic

Lewy body-like inclusions were found in the cytoplasm of cortical and spinal motor neurons. In vitro, A53T and A30P showed an increase in the tendency for self-aggregation and oligomerization of  $\alpha$ -synuclein into protofibrils, but only A53T mutation promotes fibril formation. Finally, motor neurons were depleted in A53T mice but were less affected in A30P mice [116, 117]. A53T mutant mice motor behavior assessment revealed progressive difficulties maintaining their balance, postural reflex difficulties, and grip strength impairment similar to what is seen in PD [118].

#### 1.7.2.2 PARK8 (Leucine-rich repeat kinase 2)

Leucine-rich repeat kinase 2 (LRRK2) is the best known genetic contributor to an autosomal dominant PD. About 10% of PD is due to genetic causes???, and LRRK2 mutation is the most common genetic cause of the disease. LRRK2 is a multi-domain protein composed of several functional domains including armadillo domain (ARM), ankyrin repeat (ANK), leucine-repeat-rich (LRR), Ras of complex protein domain (ROC), C-terminal of ROC (COR), mitogen-activated protein kinase kinase kinase (MAPKKK), and a WD40 domain. An autosomal dominant form of PD was first identified in an extended family in Western Nebraska, then in a German-Canadian lineage, and then in a large Japanese family, leading to the identification of PARK8 [119-121]. PARK8 was later determined to be the LRRK2 gene.

More than 40 missense mutations in LRRK2 have been discovered, but only 8 of them caused PD [122]. LRRK2 is highly expressed in different brain

regions, including the cortex, striatum, hippocampus, cerebellum and in the dopaminergic neurons of the SNpc [123]. LRRK2's exact function in the body is not well understood although it has been identified as a tyrosine kinase-like protein. In the brain, LRRK2 has been reported to promote microglial proinflammatory responses, regulating cytoskeleton, MAPK kinase signaling, or synaptic vesicle storage and mobilization within the recycling pool [124-126]. Some of the mutations appear to increase the kinase activity. It was also reported that LRRK2 has the ability to interact with other PD proteins, such as  $\alpha$ -synuclein and Parkin. The effect of LRRK2 mutations was determined in different animal models. In G2019S LRRK2 transgenic rats, mutation did not cause nigrostriatal neurodegeneration, but they displayed modest behavioral alteration [127]. Similarly, G2019S LRRK2 mice didn't display remarkable neuropathological changes or nigrostriatal dopaminergic neuronal loss [128]. However, G2019S in vitro studies have reported neuronal death in human neuroblastoma SH-SY5Y cells and in primary neurons [129, 130].

#### 1.7.2.3 PARK2 (Parkin)

In 1973, autosomal-recessive juvenile parkinsonism (AR-JP) was first described in 13 Japanese families [131]. Parkin, a 465-amino acid protein, is an E3 ubiquitin ligase that is composed of an N-terminal ubiquitin-like (Ubl) domain linked to four zinc-finger domains, three of which form a RING1-IN-Between-RING2 (RBR) motif [132]. The age of onset in this type of PD typically ranges between childhood and the 4<sup>th</sup> decade of life [133]. More than 100 Parkin

mutations, including point mutations, exotic rearrangements, and small deletions or insertions, lead Parkin to be the most common genetic cause of early onset PD, which was reported to account for 6-37% of these cases [134, 135].

Postmortem studies verified that loss of Parkin function selectively led to the loss of dopaminergic neurons in the SNpc and locus ceruleus, without any presence of Lewy bodies or neurofibrillary tangles. More than 100 mutations of Parkin have been reported. Patients with mutations are more likely to have asymmetric involvement and dystonia at the onset; later or at the onset they develop hyperreflexia [133, 136].

Parkin resides in the cytosol but gets recruited to the mitochondria once mitochondrial damage occurs. Parkin plays a crucial role in mitochondria quality control by promoting mitophagy, which is a form of macro-autophagy that selectively clears impaired mitochondria together with PTEN-induced putative kinase 1 (PINK1), which will be discussed in a different section.

Loss of function mutations of Parkin in *Drosophila* model led to a reduction in the flies' lifespans, male sterility, and defects in the ability of flying and climbing. Those behavioral defects were driven by cell death of muscle subsets. Additionally, mutant flies showed a reduction in mitochondria with loss of cristae structure, which leads to a dopaminergic neuronal degradation [137, 138].

Despite the impact of Parkin mutation in *Drosophila*, Parkin mutations in mice do not show significant motor alterations, reduction in nigrostriatal dopaminergic neuron or in the striatum, or abnormalities in dopamine metabolism. However, Parkin mutation affected memory and cognitive ability of mice caused by possible

deficits in hippocampus synaptic plasticity but not due to a degeneration of dopaminergic neurons in the SNpc [139-141]. In an attempt to find a better rodent model, rats with a Parkin inactivating mutation (knockout, KO) were created, but these did not display any impairment in gait, motor movements, motor strength, and motor coordination. Content of neurotransmitters dopamine and serotonin were not significantly different in Parkin KO rats compared to control. Finally, the number of TH-positive neurons in the SN were not changed at 4, 6, and 8 months of age [142].

To identify the effect of the loss of Parkin on striatal synaptic mitochondria in what animal??? as early as 3 months of age, extensive study using Seahorse XF24 to assess mitochondrial function was used. Mitochondrial function was determined by measuring the oxygen consumption rate (OCR), which did not reveal any mitochondrial dysfunction whether the respiration was driven by complex I in the presence of pyruvate or by complex II in the presence of succinate [143, 144].

#### 1.7.2.4 PARK6 (PTEN-induced putative kinase 1, PINK1)

PINK1 was the second gene to be discovered in early-onset recessive PD in 2001 in diverse populations across the world, including European and especially Italian, Japanese, Chinese, Malay, and Indians [145, 146]. Three years later, the protein encoded by PARK6 was found to be a serine-threonine kinase composed of 581 amino acids that was identified to be associated with AR-JP.

The initial report anticipated that PINK1 had an N-terminal mitochondrial membrane targeting motif and demonstrated that wild-type, but not mutant PINK1, can stabilize mitochondrial membrane potential ( $\Delta\Psi_m$ ) and protect cells from apoptosis when exposed to proteasome inhibitors [147]. Under basal conditions, endogenous PINK1 is barely detected by immunoblotting or immunofluorescence. Upon loss of  $\Delta\Psi_m$ , PINK1 accumulates on depolarized mitochondria, mediating Parkin translocation and accumulation that eventually leads to mitophagy [148-150]. PINK1 also can sense the elevation in ROS or protein misfolding to trigger mitophagy [151].

A specific mutation in PINK1, G309D, leads to complete abolition of PINK1 function, and in mice shows an age-dependent reduction in dopamine accompanied by reduced locomotor activity in aged mice (16 month-old). Neither dopaminergic neuronal loss in the SNpc nor change in the optical density of TH in the striatum were observed in those mice. Also, there were no signs of Lewy bodies or  $\alpha$ -synuclein accumulation [152, 153]. Mice that lack PINK1 showed a reduction in mitochondrial respiration, along with an increase in the susceptibility to dysfunction with any toxic effects of oxidative stress [152, 154].

Again, to try obtain a better rodent model of PD, PINK1 KO rats were created. The PINK1 KO rat model displayed abnormalities at early stage of life. Reduction in hind-limb strength, increase in the number of foot slips, and gait abnormalities were observed at 4 months of age. Additionally, progressive loss of dopaminergic neurons in the SNpc was detected at 8-months (corresponding to age between 30-40 years in humans) [142]. Loss of function of PINK1 in rats was



also used to study changes in mitochondrial function. Striatal synaptic mitochondria of 3-month old rats showed a reduction in ATP production, maximal respiration, and spare respiratory capacity (SRC). Additionally, PINK1 KO rats were also used to study the changes in cortical and striatal mitochondria isolated from 9-month old rats. Younger rats had no alteration in mitochondrial function. On the other hand, in older rats, mitochondrial oxygen consumption rate showed an increase in proton leak compared to wild-type. Mitochondrial dysfunction could result from an alteration in the protein expression in the mitochondria in PINK1 KO, which was demonstrated by proteomic analysis. SWATH-MS revealed defects in the ETC, fatty acid metabolism, oxidation reduction, and generation of precursor metabolites and energy associated with the loss of PINK1 [155, 156].

#### 1.7.2.5 Park7 (DJ-1)

Early-onset PD linked to mutation in DJ-1 are extremely rare. However, mutation within DJ-1 were identified in Italian and Dutch families [157]. DJ-1 is highly conserved protein present as a dimer and composed of 189 amino acids with seven  $\beta$ -strands and nine  $\alpha$ -helices that belongs to the superfamily of ThiJ/Pfpl [158-160]. DJ-1 is a ubiquitously expressed multifunctional redox protein participating in regulation of transcription [161-165], oxidative stress [166, 167], chaperone [168, 169], protease [170-172], and mitochondrial regulation [173-176]. DJ-1 is mainly localized in the cytoplasm, and its presence in dendrites, axons, and presynaptic terminals was previously documented [177].

Mutations of DJ-1 that have been identified in patients with PD inhibit DJ-1 localization to the mitochondria during oxidative stress, including M26I, C106A and L166P [178].

Originally, DJ-1 was identified as an oncogene and its expression was reported to be upregulated in different malignancies, e.g. breast, lung, and prostate cancer. In addition, it was implicated in other disorders such as ischemic injury, amyotrophic lateral sclerosis, and PD [179, 180]. One mutation, L166P, in addition to showing loss of function, gains a pro-apoptotic-like activity [181].

Age-dependent motor deficits in DJ-1 null mice (generated by deleting the first 5 exons and part of the promotor region) were subjected to systemic behavioral assessment of various motor functions. DJ-1 null mice (5, 9, and 11 months) locomotor and rearing activities measured in an open field chamber revealed a deficit in 11-month old mice. However, neither old mice nor the young ones displayed a change in the latency to fall when rotarod was performed [182]. In addition, deletion of DJ-1 showed no signs of dopaminergic depletion. Similarly, *Drosophila* models lacking functional DJ-1 had no neuronal loss; however, locomotor activity was either basally reduced or severely affected by oxidative stress [183, 184]. Nonetheless, in aged DJ-1 knockdown *Drosophila*, a decrease in the number of dopaminergic neurons was connected to the phosphatidyl-inositol-3 kinase (PI-3K) pathway [185, 186].

Recently, a rat model of DJ-1 KO was developed using zinc finger nuclease by the deletion of 9 bp along with the insertion of 1 bp in exon 4 of DJ-1 gene. DJ-1 KO in rats led to not only motor deficits as in mice and *Drosophila*,

but also a progressive loss of substantia nigra dopamine neurons. Despite the loss in the substantia nigra, there was no change in tyrosine hydroxylase immunoreactivity in the nerve terminal in the striatum [142]. Additionally, the assessment of respiration, an indicator of mitochondrial function, of striatal non-synaptic mitochondria from DJ-1 KO rats showed an increase in the oxygen consumption rate compared to WT. [144].

#### 1.7.2.6 Park22 (CHCHD2)

Late-onset as well as sporadic PD linked to mutation in coiled-coil-helix-coiled-coil-helix domain containing 2 (CHCHD2) was identified by Funayama and colleagues in a large Japanese family with autosomal dominant PD [36]. In addition, mutations were not only found to be linked to PD, but also with other neurodegenerative disorders, including frontal temporal dementia and amyotrophic lateral sclerosis [36, 187]. Positron transmission tomography (PET) revealed that patients with mutations in CHCHD2 had a significant reduction in DAT in the putamen and caudate nucleus similar to patients with sporadic PD [188].

The mechanism of PD pathogenesis in CHCHD2 mutation remains unclear. However functional studies suggest that CHCHD2 plays roles in regulating metabolism, oxidative phosphorylation (OXPHOS), and apoptosis mediated by mitochondria [189-191]. A study of yeast CHCHD2 (Mic17) indicated that the loss of CHCHD2 decreased OCR and changed the activity of complex III and IV [192]. In CHCHD2 mutant flies, loss of CHCHD2 impaired ATP production

as well as spare respiratory capacity. Also, it altered mitochondrial matrix structure leading to oxidative stress, neuronal loss, and motor dysfunction. As a result, flies exhibited shorter lifespan [193]. In vitro, CHCHD2 KO neuroblastoma cells (SH-SY5Y) showed a reduction in the activity of complex IV and complex I along with a reduction in ATP production, which was rescued by overexpression of wild-type CHCHD2 [194].

#### 1.7.2.7 Park5 (UCH-L1)

Humans have five different known families of de-ubiquitinating (DUB) enzymes, which are diverse in structure and function, removing either polymeric Ub or monomeric Ub [195]. Those five DUB enzymes are also conserved in mice: ubiquitin carboxy-terminal hydrolase (UCH), ubiquitin-specific protease (USP), ovarian tumor protease (OTP), Josephin, and JAMM/MPN+ [196]. Of those enzymes, UCH is the most studied in the context of neurodegenerative disorders due to its high expression in neurons, including motor and sensory neurons [197, 198]. An autosomal dominant mutation in the gene for ubiquitin carboxy-terminal hydrolase L1 (UCH-L1), also known as protein gene product (PGP9.5), was identified in 1989 in two German family members with PD [28, 199]. The affected siblings had an isoleucine to methionine substitution (I93M), which was later found to cause a decrease in enzyme activity by around 50% [200]. UCH-L1 incidence of being aggregated increased in I93M mutation and led to a change in the protein characteristics [201]. In addition, immunohistochemical (IHC) staining for UCH-L1 was observed in Lewy bodies in patients with

idiopathic PD [202]. Overexpression of UCH-L1 in mice resulted in behavioral and pathological phenotypes of parkinsonism at 20 weeks of age [200]. In addition, overexpression of  $\alpha$ -synuclein using stereotaxic injection of adeno-associated virus (AAV) into the SN in UCH-L1 transgenic mice (Ile93Met) resulted in dopaminergic neuron cell bodies loss in the SN that was confirmed by neuronal count. However, dopamine concentration in the striatum did not change [203].

## **1.8 PINK1 and Parkin importance beyond Parkinson's disease**

Mitochondria are now known to comprise a population of organelles requiring a careful balance and integration of several processes, including fusion and fission, biogenesis regulation, migration within the cell, remodeling of morphology, and autophagy [204]. These processes prompt mitochondrial recruitment to critical subcellular organelles. Well-maintained balance of mitochondria is called mitochondrial homeostasis. Mitochondrial homeostasis is critical for cellular function, such as signaling and plasticity. Based on the importance of PINK1/Parkin-mediated mitophagy for cell survival, it is not surprising that defects in the mechanism are linked to a variety of human diseases, including cancer, heart disease, and liver disease.

### **1.8.1 Cancer**

The relationship between mitophagy and cancer is complicated and possibly involves alteration in energy homeostasis and oxidative metabolites that elevate the production of ROS. Multiple studies highlighted that Parkin is one of

the commonly mutated genes in ovarian, breast, bladder, lung, ovarian, colorectal, and other cancers [205, 206]. Tumor suppression function of Parkin in Parkin KO mice is believed to contribute to spontaneous hepatocellular carcinoma [207]. However, Parkin expression restoration in vitro in breast cancer cell lines, including MCF7 cells, was found to slow the proliferation and colony formation in a clonogenic assay [208, 209]. On the other hand, mutation in mitophagy machinery, especially in PINK1, has been identified in patients with solid extracranial tumors arising from the sympathetic nervous system known as neuroblastoma [210].

#### 1.8.2 Heart Disease

The prevalence that patients with PD develop heart failure is twice as high as for the overall population. In addition, heart failure is a strong predictor of mortality among PD patients. However the reason of high mortality rate is unknown [211, 212]. The heart is one of the organs that has a high basal mitophagy rate in order to maintain mitochondria quality control [213]. One of the hypotheses suggests that mitochondria might be involved [214]. In such an organ with high energy demand, myocyte function and survival relies on the presence of healthy mitochondrial with normal function; loss of these functions could lead to different cardiac abnormalities. In mice, PINK1 deletion can lead to left ventricle dysfunction as well as hypertrophy, which is mediated by elevation in oxidative stress in cardiomyocytes [215]. Those changes in the heart occur as early as age 2 months.

### 1.8.3 Liver disease

Liver disease and liver failure caused by alcoholism and an overdose of acetaminophen are common in the United States, which has no cure [216]. However, mitochondria, through PINK1/Parkin-mediated mitophagy, have been found to have a protective effect against alcohol-induced liver injury and steatosis [217, 218]. Liver injury in control mice caused by alcohol feeding resulted in alteration in liver mitochondrial function as well as morphology [219]. In addition, liver damage induced by alcohol in Parkin KO was determined by measuring the level of alanine aminotransferase (ALT), which is a marker of liver damage. Elevation in ALT level was found in Parkin KO mice compared to control Parkin mice and control mice with liver injury [220]. In addition, double deletion of PINK1 and Parkin in mice exacerbate liver injury and mortality induced by acetaminophen [221].

## 1.9 Current Therapies for PD

### 1.9.1 Medication

Current therapies for PD address motor symptoms of the disease that can only manage the symptoms but do not halt or slow the disease progression. Dopamine itself cannot pass the blood-brain barrier (BBB), while L-DOPA easily does. While tyrosine is a precursor to dopamine, dopamine replacement therapy with L-DOPA rather than tyrosine bypasses the rate-limiting enzymatic reaction in the synthesis of dopamine, tyrosine hydroxylase (TH) (**Error! Reference source not found.**). L-DOPA or levodopa is currently the most prescribed drug for PD,

employed as dopamine replacement therapy due to its ability to cross the BBB. However, despite L-DOPA being generally well tolerated, its metabolism in the peripheral nervous system can result in unwanted side effects such as dyskinesia and reduction in the half-life of the drug, and its long-term use can lead to on-off pulsatile responses ('wearing off') [222]. L-DOPA sometimes is administered in combination with an enzyme inhibitor in order to prevent its metabolism and to prolong its duration of action, such as a catecholamine-O-methyltransferase (COMT) inhibitor, e.g. entacapone, and aromatic L-amino acid decarboxylase (AADC) inhibitor, e.g. carbidopa [223].

#### 1.9.2 Deep Brain Stimulation (DBS)

DBS is another symptom-modifying approach in the treatment of PD. This procedure involves surgical implantation of a brain pacemaker-like device. The electrode in the brain works to stimulate different regions of the basal ganglia, usually the subthalamic nucleus or the globus pallidus pars interna, by sending high frequency electrical impulses that will result in PD symptom mitigation (Figure 1.6) [224]. Since the U.S. Food and Drug Administration (FDA) approved of this procedure in 2002, the motor symptoms (bradykinesia, rigidity, tremors, and dyskinesia) as well as response to levodopa improved in patients using the device[225].



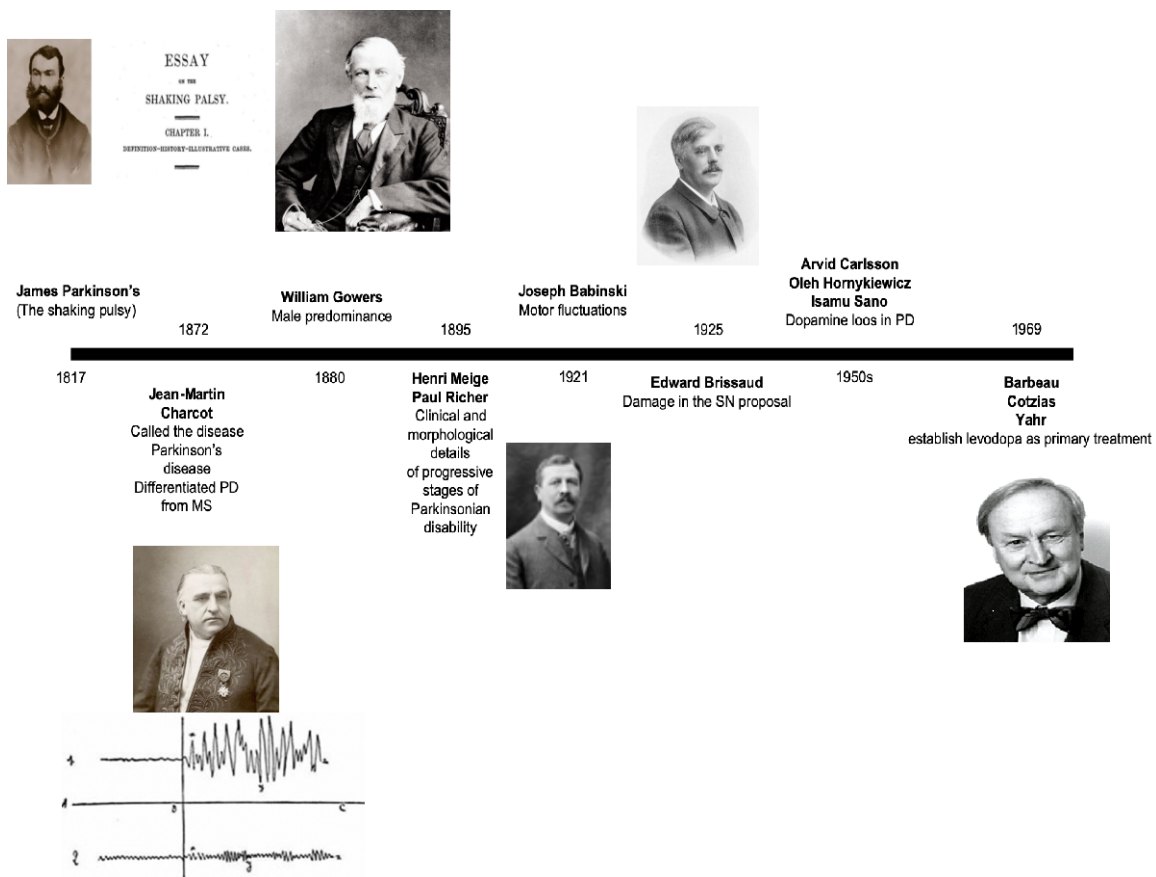


**Figure 1.1 Breakthroughs in PD history.**

This diagram illustrates the timeline of the discovery of PD and the development of our understanding of the disease.

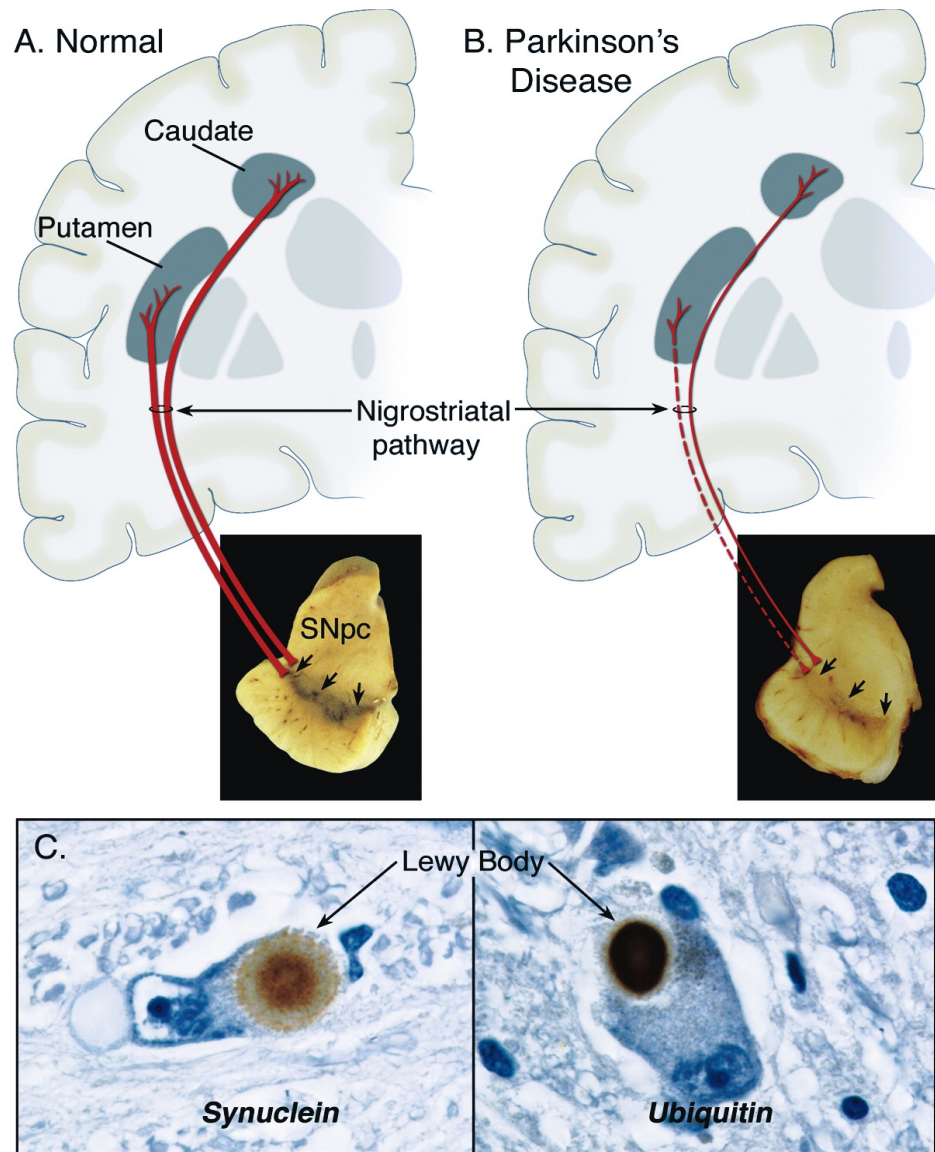


**Figure 1.2 Neuropathology of Parkinson's Disease.**

(A) Schematic representation of the normal nigrostriatal pathway (in red). It is composed of dopaminergic neurons whose cell bodies are located in the substantia nigra pars compacta (SNpc; see arrows). These neurons project (thick solid red lines) to the basal ganglia and synapse in the striatum (i.e., putamen and caudate nucleus). The photograph demonstrates the normal pigmentation of the SNpc, produced by neuromelanin within the dopaminergic neurons.

(B) Schematic representation of the diseased nigrostriatal pathway (in red). In Parkinson's disease, the nigrostriatal pathway degenerates. There is a marked loss of dopaminergic neurons that project to the putamen (dashed line) and a much more modest loss of those that project to the caudate (thin red solid line). The photograph demonstrates depigmentation (i.e., loss of dark-brown pigment neuromelanin; arrows) of the SNpc due to the marked loss of dopaminergic neurons.

(C) Immunohistochemical labeling of intraneuronal inclusions, termed Lewy bodies, in a SNpc dopaminergic neuron. Immunostaining with an antibody against  $\alpha$ -synuclein reveals a Lewy body (black arrow) with an intensely immunoreactive central zone surrounded by a faintly immunoreactive peripheral zone (left photograph). Conversely, immunostaining with an antibody against ubiquitin yields more diffuse immunoreactivity within the Lewy body (right photograph).

Reprinted by permission from Elsevier: Neuron. [226] Parkinson's disease: mechanisms and models, Dauer, W. and Przedborski, S., [4736540268459] (2003).

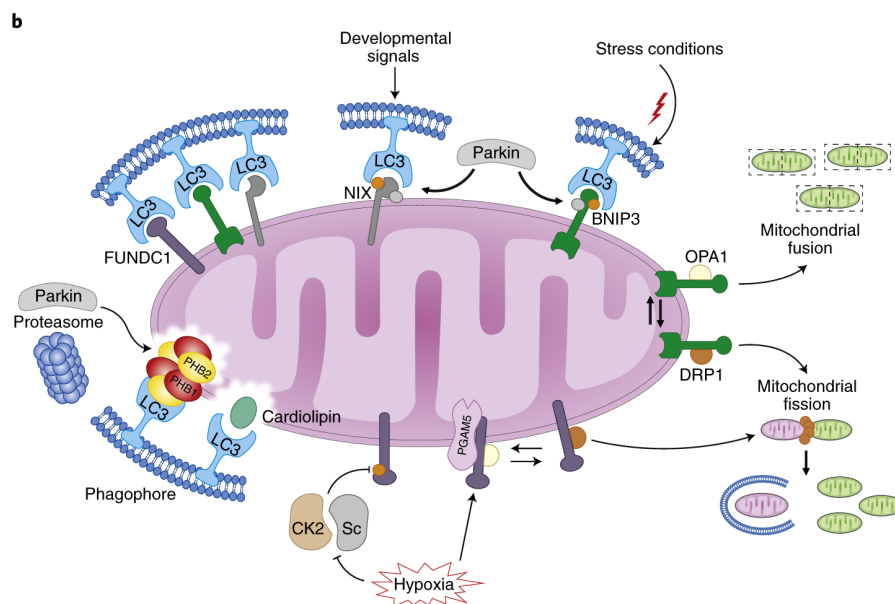
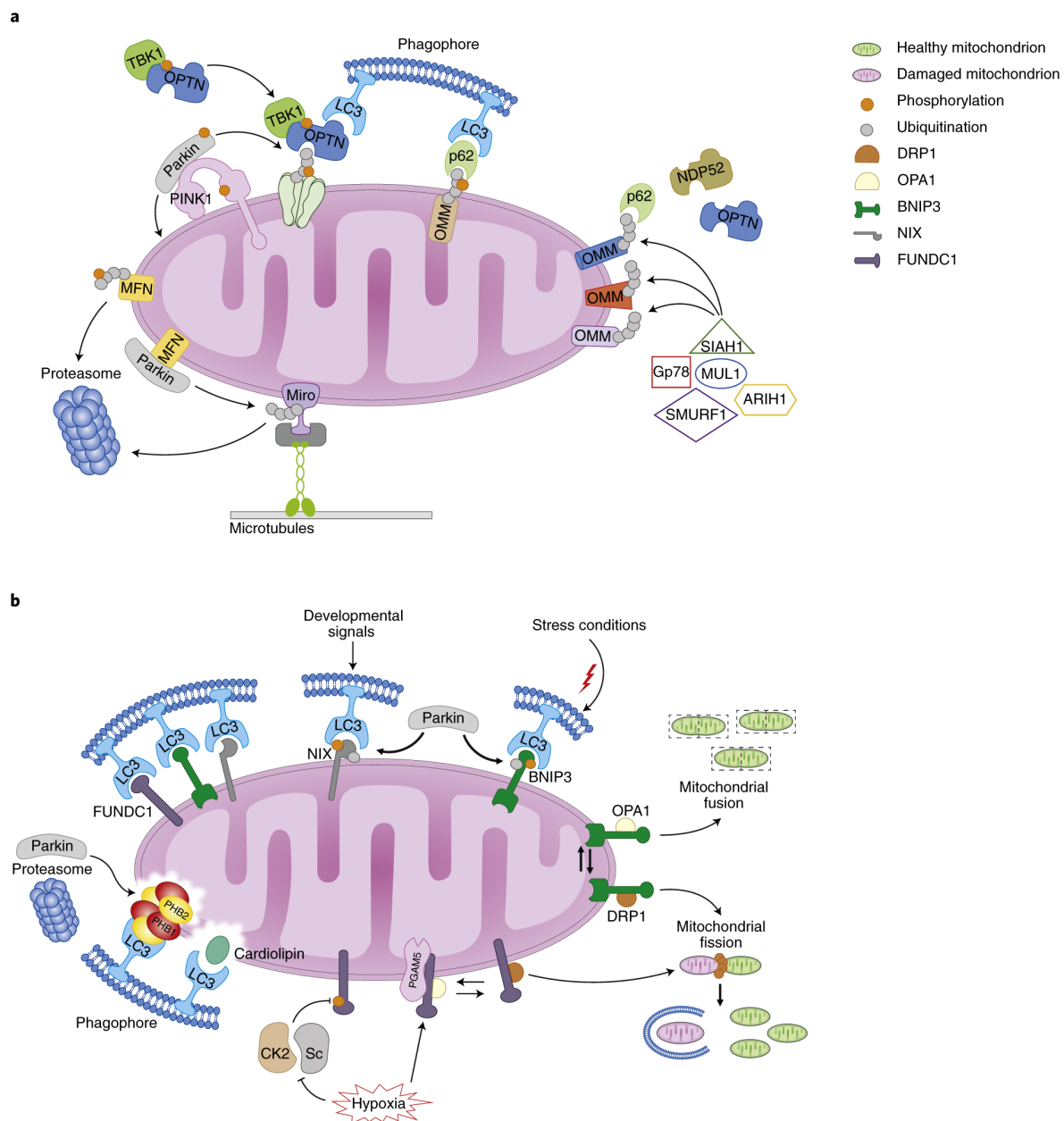


### **Figure 1.3 The PINK1–Parkin pathway of mitophagy.**

Following stress, PINK1 is stabilized on the OMM, promoting Parkin recruitment. Parkin ubiquitinates several outer membrane components. Poly-Ub chains are subsequently phosphorylated by PINK1 serving as an ‘eat me’ signal for the autophagic machinery. Adaptor proteins (p62, OPTN, NDP52) recognize phosphorylated poly-Ub chains on mitochondrial proteins and initiate autophagosome formation through binding with LC3. TBK1 phosphorylates OPTN, thereby enhancing its binding affinity to Ub chains. The OPTN–TBK1 complex establishes a feed-forward mechanism promoting mitochondrial clearance. Gp78, SMURF1, MUL1, SIAH1 and ARIH1 represent alternative E3 ubiquitin ligases targeting OMM proteins prior to mitophagy. The PINK1–Parkin pathway modulates mitochondrial dynamics and motility by targeting MFN and Miro for proteasomal degradation.

**b, Receptor-mediated mitophagy.** BNIP3, NIX and FUNDC1 mitophagy receptors localize to the OMM and interact directly with LC3 to mediate mitochondrial elimination. PHB2 and cardiolipin are externalized to OMM and interact with LC3 following mitochondrial impairment. Different receptors ensure specificity of the process in different tissues and following diverse stimuli. NIX and BNIP3 phosphorylation enhances their association with LC3. Both CK2 and Src kinases and PGAM5 phosphatase influence FUNDC1 phosphorylation status, regulating mitochondrial dynamics during hypoxia. Mitophagy receptors promote fission of damaged organelles through the disassembly and release of OPA1, and the recruitment of DRP1 on the mitochondrial surface. Parkin-dependent ubiquitination of NIX and BNIP3

highlights an intricate crosstalk between receptor-mediated mitophagy and the PINK1–Parkin pathway. Reprinted by permission from Springer Nature: Nature Cell Biology. [78]

Mechanisms of mitophagy in cellular homeostasis, physiology and pathology, Konstantinos Palikaras, Eirini Lionaki & Nektarios Tavernarakis, [4734920722703] (2018)



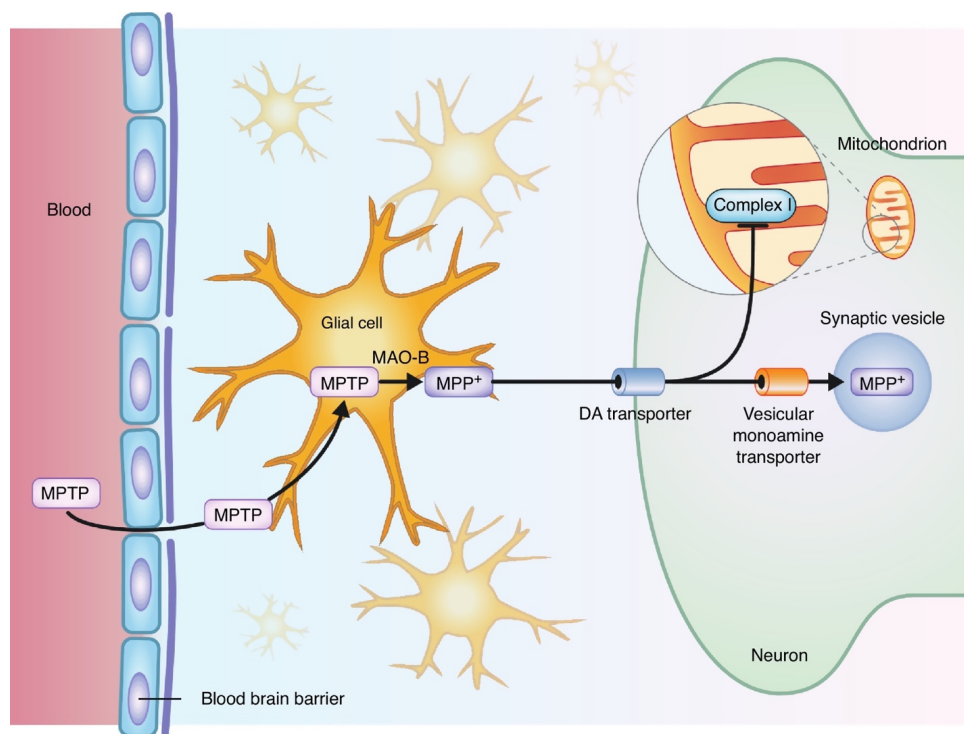


**Figure 1.4 MPTP metabolism in the brain.**

MPTP crosses the blood-brain barrier and is metabolized by MAO-B in glial cells into MPDP, which is oxidized into the toxic metabolite MPP<sup>+</sup>. After the release in the synaptic cleft, MPP<sup>+</sup> is taken up in dopaminergic neurons by DA transporters. Inside these neurons, MPP<sup>+</sup> is partly stored in the synaptic vesicles via the vesicular monoamine transporter. The toxic effect of MPP<sup>+</sup> is its blocking of complex I of the mitochondrial electron transport chain resulting in less ATP production and the formation of free radicals.

Reprinted by permission from Elsevier: Drug Discovery Today: Disease Models [227]. Mechanisms of mitophagy in cellular homeostasis, physiology and pathology, Konstantinos Palikaras, Eirini Lionaki & Nektarios Tavernarakis, [4734920722703] (2018)

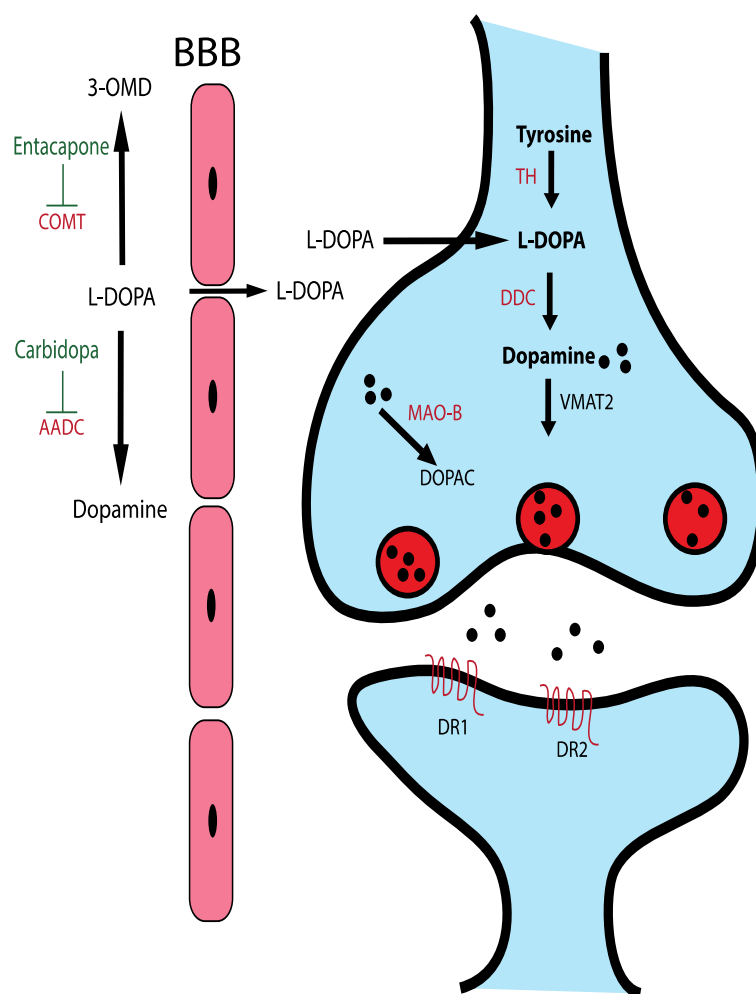


**Figure 1.5 Dopamine synthesis and common pharmacological therapeutics for PD.**

Dopamine is synthesized from tyrosine to L-DOPA by TH then to dopamine by DDC. Dopamine then gets packaged into synaptic vesicle and released into the synapse where it can bind to DR1 and DR2. Replacement therapy with L-DOPA is usually combined with COMT or DDC inhibitors to prevent peripheral degradation.

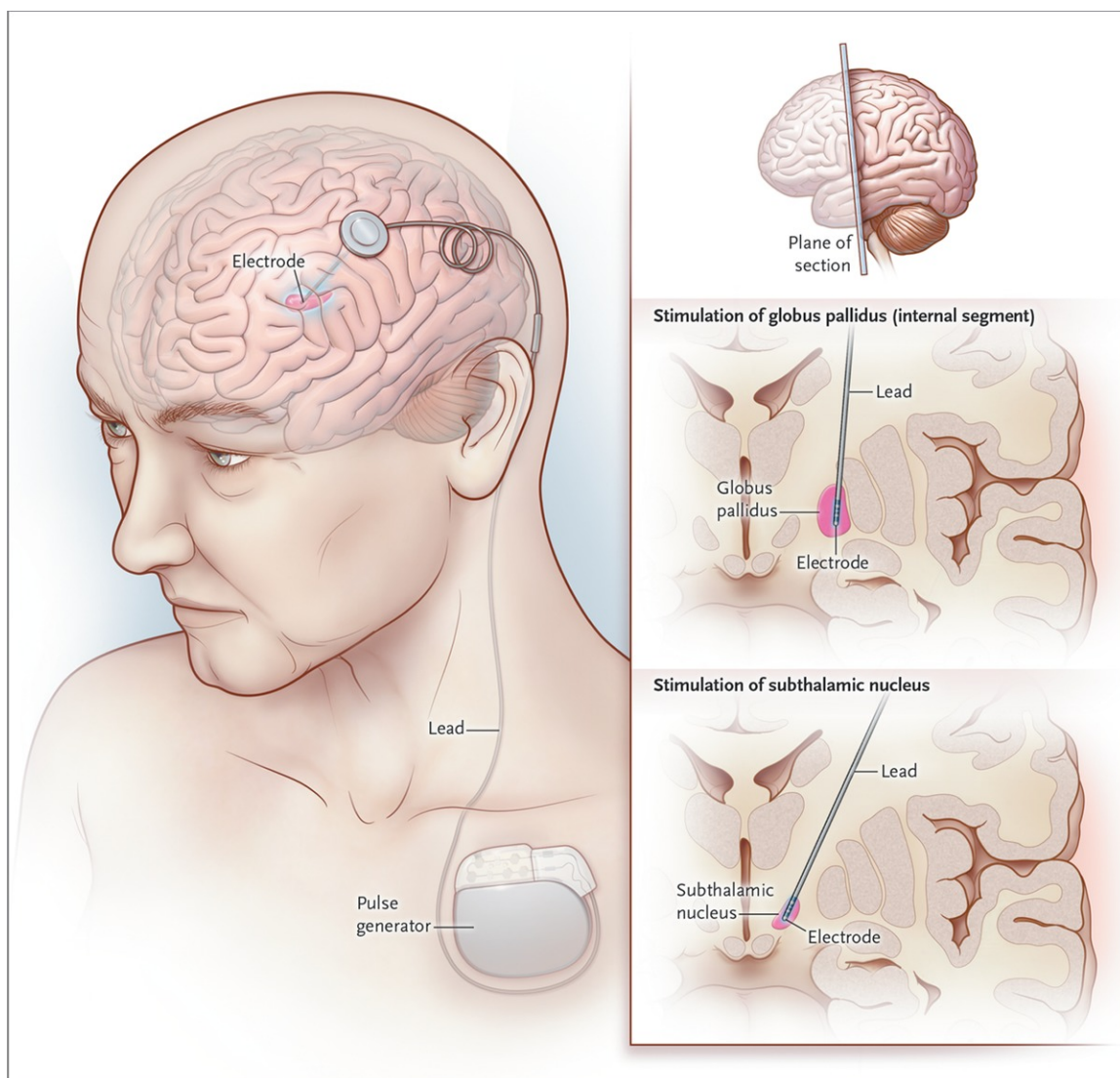


**Figure 1.6 Electrode Implantation for Deep-Brain Stimulation.**

The lead for deep-brain stimulation is implanted in either the subthalamic nucleus or the internal segment of the globus pallidus. The lead passes through a burr hole in the skull. Attached to the lead is a connecting wire, which is tunneled under the skin of the scalp and neck to the anterior chest wall, where it is connected to an impulse generator.

Reprinted by permission from [228], Copyright Massachusetts Medical Society.

# Chapter 2

Deletion of DJ-1 in rats affects protein  
abundance and mitochondrial function at  
the Synapse

## 2.1 Abstract

DJ-1 is a multifunctional protein affecting different biological and cellular processes. In addition, DJ-1 has roles in regulating mitochondrial function. Mutations in DJ-1 were found to cause an autosomal recessive form of Parkinson's disease. In order to assess the effects of DJ-1 on neuronal mitochondria, we first performed proteomic analysis of synaptic mitochondria isolated from the striatum of 3-month-old DJ-1 knockout rats. In total, 371 mitochondrial proteins were quantified and 76 proteins were found to be significantly changed due to DJ-1 deficiency. Proteins perturbed by the loss of DJ-1 were involved in several mitochondrial functional pathways, including the tricarboxylic acid cycle and electron transport chain. Second, synaptic mitochondrial respiration was measured to assess mitochondrial function, which showed a significant change due to DJ-1 knockout. The dataset generated here highlights the role of the mitochondria in PD associated with DJ-1. Furthermore, the loss of DJ-1 impacts various proteins in separate pathways. This study improves our understanding of DJ-1 effects in a complex tissue environment and the changes that accompany its loss.



## 2.2 Introduction

Parkinson's disease (PD) is a chronic neurodegenerative movement disorder that occurs in 1% of the population older than 65 years. It is characterized by a progressive loss of dopaminergic neurons in the substantia nigra pars compacta (SNpc) and their projections into the striatum, which leads to the clinical features of the disease, including rigidity, resting tremor, bradykinesia, and gait difficulty [229]. There are two types of PD, sporadic and familial/genetic. Around 90% of PD cases occur in a sporadic manner, but approximately 10% are linked to familial genetic mutations in several different protein-encoding genes [230].

DJ-1 is a highly conserved 189 amino acid protein that belongs to the superfamily proteins of DJ-1/Thi/Pfpl [231]. It is expressed in almost all cells and tissues, including the brain [232]. At the subcellular level, DJ-1 was found in the intermembrane space and the matrix of the mitochondria in addition to the cytoplasm [231]. Bonifati and his colleagues in 2003 discovered that mutations in the gene PARK7, which encodes the protein DJ-1, are linked with an early onset form of recessive PD [157]. All known DJ-1 mutations appear to act as loss-of-function mutations leading to an autosomal recessive form of the disease [233]. The physiological function of DJ-1 is not fully known. DJ-1 has been shown to be a multifunctional protein that participates in oxidative stress [167, 234-237], protein folding, glucose level, fertility, transcription and neuronal protection against oxidative stress [157, 238, 239]. Unfortunately, our knowledge about the disease mechanisms that result from loss-of-function mutations in DJ-1 are unknown, and understanding is hampered by the prior lack of valid small animal models. While

DJ-1 knockout (KO) mice do not suffer from PD [240], DJ-1 KO rats display a reduction in rearing frequency and grip strength of hind-limb. In addition, counting of dopaminergic neurons in SNpc revealed a loss of more than 50% of neurons [142].

In both familial and sporadic PD, defects in mitochondria have been well-documented, and animal models created to mimic PD similarly affect mitochondria [241-243]. In the brain, synaptic mitochondria may be a population exceptionally vulnerable to damage, due to the high energetic demands at the synapse and the distance from the soma and nucleus for repair and/or replacement of damage. The goal of this study was to assess whether the loss of DJ-1 in this rat model would result in noticeable changes in mitochondria at the striatal synapse, a key site of nigrostriatal neurotransmitter action. Therefore, we studied the bioenergetic and protein expression properties of striatal synaptic mitochondria from young adult rats, before the onset of neuronal loss due to deficiency in DJ-1.

## **2.3 Materials and Methods**

### **2.3.1 Animals**

DJ-1 KO and the congenic wild-type (WT) Long Evans Hooded (LEH) rats were obtained from SAGE Labs (and now available from Envigo) and bred and maintained at the University of Nebraska Medical Center (UNMC). Generation and characterization of the DJ-1 KO rats have been described previously [142]. Genotype was verified by Western blot (Supplemental Figure 1). Rats were kept in a temperature-controlled environment with a 12-hour light/dark cycle with free

access to rat chow and water. Three-month-old male rats were used. All experimental procedures were approved by the UNMC Institutional Animal Care and Use Committee.

### 2.3.2 Brain dissection and synaptic mitochondrial isolation

Synaptic mitochondria were isolated as previously described [244, 245]. All steps in mitochondrial isolation were performed on ice or at 4° C. Briefly, rats were anesthetized by isoflurane and sacrificed by decapitation. Immediately after euthanasia, brains were removed and placed on a pre-chilled petri dish. The petri dish was placed under a dissection microscope to dissect the striatum from the brain. The striatum was then transferred to a microcentrifuge tube containing ice-cold mitochondrial isolation medium (MSHE+BSA) containing mannitol (210 mM), sucrose (70 mM), HEPES (5 mM), EGTA (1 mM), and fatty acid free (FAF)-BSA (0.5% w/v) (pH 7.2) to prepare the striatum for homogenization. The striatum was then homogenized (10 strokes) using a Dounce homogenizer containing ice-cold MSHE+BSA buffer. The homogenate was then centrifuged at 1,300 X g for 3 minutes; the supernatant was collected, and the pellet was suspended again in MSHE+BSA and recentrifuged at 1,300 X g for 3 minutes. Both supernatants were pooled together and centrifuged at 21,000 X g for 10 minutes. The resulting supernatant was discarded, and the pellet was resuspended in Percoll to a final concentration of 15% Percoll, and layered on the top of 24% and 40% Percoll (100% Percoll was used to make the different components of the gradient, which contains MSHE+BSA, as above). Centrifugation was performed for 8 minutes at

30,700 X g. The synaptosome band (pinched-off nerve terminals containing the presynaptic components including mitochondria) migrated between the 15% and 24% layers. These were collected and diluted in MSHE+BSA.

To isolate synaptic mitochondria, the synaptosomal fraction was transferred to a nitrogen cavitation vessel (Parr Instrument Company, Moline, IL). The pressure in the vessel was calibrated to 900 psi for 15 minutes followed by depressurization to atmospheric pressure. The resulting material was then added on top of 24% Percoll and centrifuged at 30,700 X g for 10 minutes. After discarding the supernatant, the pellet containing synaptic mitochondria was resuspended in MSHE+BSA and recentrifuged at 8,000 X g for 10 minutes. Mitochondrial assay solution (MAS, 1x: 70 mM sucrose, 220 mM mannitol, 10 mM  $\text{KH}_2\text{PO}_4$ , 5 mM  $\text{MgCl}_2$ , 2 mM HEPES, 1 mM EGTA, and 0.2% (w/v) FAF-BSA PH 7.2) was used to wash the pellets twice. Pellets then were resuspended in a minimal volume of MAS. Total concentrations of mitochondria were determined using the Pierce BCA Protein Assay kit with albumin standards (Thermo Fischer Scientific, Waltham, MA). Finally, the isolated mitochondria were either lysed by sodium dodecyl sulfate (SDS) and frozen for proteomic studies or immediately used for bioenergetic analysis.

### 2.3.3 Sample preparation for SWATH-MS proteomics

Synaptic mitochondrial lysates isolated from rat striatum were prepared for analysis by digestion with trypsin (Promega, Madison, WI) using filter-aided sample preparation (FASP) on a 20- $\mu\text{m}$  filter (Pall Corporation, Ann Arbor, MI) [8].

Peptides were then desalted using Oasis mixed-mode weak cation exchange cartridges (Waters, Milford, MA), then dehydrated with a Savant ISS 110 SpeedVac concentrator (Thermo Fischer Scientific, Waltham, MA). The dried pellets were dissolved in 0.1% formic acid (FA) (Fischer Scientific, Hampton, NH) and quantified using the Scopes method [246] on a NanoDrop 2000 UV-vis Spectrophotometer (Thermo Fischer Scientific, Waltham, MA) at 205 nm absorbance.

#### 2.3.4 SWATH data acquisition

Sample peptides from the striatal synaptic mitochondrial lysates from LEH and DJ-1 KO rats were analyzed in quadruplicate by nano-LC-MS /MS in SWATH-MS mode on a 5600 TripleTOF instruments (SCIEX) and targeted data extraction was performed as previously described [144, 155]. The spectral library was generated using ProteinPilot (Version 4.5, SCIEX) where the search was performed against *Rattus norvegicus* UniProt proteome UP000002494 that contains 8023 Swiss-Prot reviewed proteins. Then, every fragment ion chromatogram was extracted and integrated automatically with PeakView (Version 2.1, SCIEX). MarkerView (Version 1.2.1) was used for data normalization to median peak ratios.

#### 2.3.5 Bioinformatic analysis

The Database for the Annotation, Visualization and Integrated Discovery (DAVID, <http://david.abcc.ncifcrf.gov>) Bioinformatics Resources 6.7 was used for functional annotation [247]. Gene Ontology (GO) was generated by STRING

version 11.0 (<https://string-db.org>) [248]. Cytoscape (<https://cytoscape.org>), an open-source software, was used to generate a molecular interaction network [249]. Reactome (<https://reactome.org>), an open-source database [250, 251], was used to generate an overview of the cellular pathways and processes affected in DJ-1 KO rats.

### 2.3.6 Mitochondrial bioenergetics assays

Oxygen consumption rates (OCR) for the isolated striatal mitochondria were measured using the Seahorse XFe24 Extracellular Flux Analyzer (Seahorse Bioscience) for electron flow and coupling assays, which were described previously [156, 244]. Each independent biological replicate (n=3 for LEH and DJ-1 KO) was measured using 3-4 technical replicate wells. In the 24-well Seahorse plate, isolated synaptic mitochondria were plated in 20  $\mu$ l MAS with the proper substrates and inhibitors for Flux assay (complex I, 10 mM pyruvate and 2 mM malate as substrate; complex II, 10 mM succinate as substrate in the presence of 2  $\mu$ M rotenone (Rot); complex IV, 10 mM ascorbate with 100  $\mu$ M tetramethylphenylenediamine (TMPD) as substrate in the presence of 4  $\mu$ M antimycin A (AA)). Data were then normalized to Rot or AA. In the mitochondrial coupling assays, 1 ml MAS (with or without inhibitors or substrates) was added to each well and incubated at 37 °C to equilibrate temperature. Final concentrations of sequential injections were 4 mM ADP, 2.5  $\mu$ M oligomycin (Oligo), 4  $\mu$ M

carbonylcyanide-p-trifluoromethoxyphenylhydrazone (FCCP), 2  $\mu$ M Rot, and 4  $\mu$ M AA. Data were then normalized to AA.

### 2.3.7 Statistical analysis

Statistical analyses and heat maps of protein expression values were generated with Prism (version 7.00 for Windows, GraphPad Software, La Jolla California USA). Briefly, DAVID was used to identify the mitochondrial proteins. The mean and the SD of all four biological replicates was used to generate a plot. Then, multiple t test correction was done using the two-stage set-up method of Benjamini, Krieger and Yekutieli (REF?). To determine the significantly changed proteins, significance was set at  $q < 0.05$ . Each row was analyzed individually, without assuming a consistent SD.

The Seahorse Wave 2.2.0 software package was used for analyzing the data and Prism (GraphPad Software) was used for graph generation. Statistical analysis was conducted in Prism using two-way ANOVA between groups corrected by the Sidak method.

## 2.4 Results

### 2.4.1 Proteomic alterations in striatal synaptic mitochondria from DJ-1 deficient rats

Since the SNpc projection of dopaminergic neuron inputs into the striatum is deficient in PD, we hypothesized that striatal synaptic mitochondria may be affected early in the disease process. We first examined the protein composition of these mitochondria, quantifying the striatal synaptic mitochondrial proteome in male WT and DJ-1 KO rats at 3 months, an age prior to reported motor deficits

that start at 6 months and prior to neuronal loss that occurs at 8 months [142]. Striatal synaptic mitochondria were isolated and lysed, the proteins were enzymatically digested, and the resultant peptides were analyzed by sequential window acquisition of all theoretical fragment-ion spectra mass spectrometry (SWATH-MS), a data-independent acquisition (DIA) technique that systematically obtains sample sets for the quantity of all fragment ions of the detectable peptide in the sample [142].

A total of 932 proteins were identified by SWATH-MS in all samples from synaptic mitochondria from the striatum of 3-month-old WT and DJ-1 KO rats (Table S1), of which 371 have been annotated as mitochondrial by the DAVID Bioinformatics Resources 6.8 database, and these were chosen for further analysis. The complete list of the 371 proteins identified and the quantification values for each biological replicate are provided in Table S2. The level of correlation to assess the reproducibility was compared among the four biological replicates in each genotype, with Pearson's correlation coefficient ( $r^2$ ) ranges between 0.90 to 0.95 for WT and 0.83 to 0.93 for DJ-1 KO (Supplemental Figure 2), which suggests a high reproducibility of the quantitative SWATH-MS data from replicates. Using a false discovery rate  $< 0.05$  for thresholds of differential expression due to loss of DJ-1, 76 differentially expressed proteins were found (Table S3). The  $\log_2$  DJ-1/WT ratio of all 371 striatal synaptic mitochondrial proteins as well as the significantly changed proteins is graphed in Figure 1A. Clustering of 76 differentially expressed proteins, and the intensity of the differentially expressed proteins in each rat, are shown as  $\log_{10}$  in the heat map.



DJ-1 deletion separated proteins into two groups, with approximately 70% of them down-regulated and 30% up-regulated (Figure 1B).

The mitochondrial localization of the altered proteins was examined (Figure 2). In general, there was no localization bias, and they approximated the representation of proteins in different mitochondrial compartments. Of the identified proteins, 30% were inner mitochondrial membrane proteins, and 37% of the significantly changed proteins were localized there. Similarly, of the identified proteins and the altered ones, outer mitochondrial membrane proteins were found at 9% and 4%, mitochondrial matrix proteins at 19% and 18%, intermembrane space proteins at 5% and 4%, and proteins in the crista at 1% and 4%, respectively.

Identification of the potential pathways affected by DJ-1 deletion in striatal mitochondria could improve our understanding of the disease caused by DJ-1 deficiency and potentially identify new targets. Reactome, a bioinformatic pathway database, revealed a large picture of the cellular processes altered by DJ-1 deficiency, likely as a result of the large number of functions performed by mitochondria. Notably, metabolism was the main cellular function to be affected (Figure 3).

Protein-protein interactions among significantly expressed proteins were investigated using STRING 11.0 ([www.string-db.org](http://www.string-db.org)). Interaction was based on experiments, databases, and co-expression with medium confidence greater than (0.400). Network information was exported to Cytoscape v. 3.7.2 for further analysis. Centrality analysis of protein-protein interaction within the network was

performed using CentiScaPe 2.2 plug-in within Cytoscape for the differentially expressed proteins based on the degree of the node, which represents the number of connections it has with other nodes [252]. Centrality highlighted proteins that are involved in several pathways in the mitochondria, including the electron transport chain (ETC) and tricarboxylic acid (TCA) cycle (Figure 4).

#### 2.4.2 Loss of DJ-1 alters striatal mitochondria in rats

Functional assessment of the mitochondria was performed to investigate the impact of changes in the expression of subunits from different complexes. Seahorse XF24 analyzer sequential measurement of the OCR of DJ-1 KO synaptic mitochondria, compared to WT synaptic mitochondria, did not show any changes in the electron flow through different ETC complexes (Figure 5A). Synaptic mitochondria from DJ-1-deficient rats consumed more oxygen throughout the conditions assessed (two-way ANOVA, effect of genotype  $p < 0.0003$ ), with the depolarizing agent FCCP, which induces maximal respiration, showing a significant increase in DJ-1 KO ( $p < 0.05$  by Sidak's post-hoc test) (Figure 5B).

The majority of the significantly altered proteins are located in the inner membrane of the mitochondria as mentioned previously. Also, several proteins that were previously pointed out to be central in the network are ETC subunits, which reside in the inner membrane. Alteration of complex I subunits represents 5.3% of the significantly expressed proteins, including Ndufs1, Ndufs2, Ndufa9, and Ndufa11. In addition, complexes II and III each have one (percentages here also??), and complexes V and VI each two (1.3%, and 2.6%, respectively), of the significantly altered proteins due to DJ-1 KO.

Mitochondrial complex II (also known as succinate dehydrogenase) has a dual function in the mitochondria. In the ETC it acts as an electron donor, facilitating the conversion of ubiquinone to ubiquinol, and is a key enzyme in the TCA cycle that uses acetyl-CoA resulting from pyruvate to metabolize succinate to fumarate [253]. One of its four subunits, succinate dehydrogenase flavoprotein subunit A (Sdha), is reduced in expression in DJ-1 KO rats, potentially linking changes in the TCA cycle to the ETC. Reductions in other enzymes involved in the TCA cycle were also found in DJ-1 KO rats, specifically isocitrate dehydrogenase 2 (Idh2) and oxoglutarate dehydrogenase (Ogdh); one enzyme, malate dehydrogenase 1 (Mdh1), was increased (Figure 7B).

## **2.5 Discussion:**

The selective, chronic, and progressive degeneration of dopaminergic neurons in the SNpc and the loss of dopaminergic nerve terminals in the striatum are responsible for motor deficits in PD patients, the most common neurodegenerative motor disorder in aging adults. This loss can be due to genetic mutations that lead to the development of PD, with one of those genes being DJ-1. Mutation in DJ-1 is linked to the early onset form of PD, but the pathological mechanism is still unknown [142]. In this study we investigated the effects of knocking out DJ-1 in rats on striatal synaptic mitochondria and the pathways affected due to this mutation. Previously, we reported that non-synaptic mitochondria isolated from the striatum of male 3-month-old DJ-1 KO rats exhibited 25 differentially expressed proteins [144]. While the proteomic analyses were

performed by different methods, only one significantly changed protein was found in both synaptic and non-synaptic mitochondria fractions, the complex III component Uqcrcq. Of note, Seahorse functional analysis revealed an elevation in OCR in the non-synaptic mitochondria from the DJ-1 KO rats [144], similar to our finding in the synaptic mitochondria studied here.

DJ-1 mutation effects on the expression of multiple subunits of the ETC complexes were particularly prominent. DJ-1 was previously found to modulate the assembly or the stability of complex I by causing reduction in Ndufs1, Ndufa9, Ndufb11, and Ndufb4 [254]. In our study, we identified a deficiency in three proteins of complex I, Ndufs1, Ndufs2, and Ndufa9, two of which were identical to those found in the prior study. In addition, patients with PD also showed similar deficiency in complex I in neurons and other peripheral tissue [255-258]. These results suggest that complex I might have a central role in DJ-1-induced PD.

SNpc neurons from subjects with idiopathic PD were previously reported to manifest a significant reduction in Sdha, one of the four subunits of complex II [259]. Similarly, we found a downregulation in Sdha in the DJ-1 KO PD rat model. In addition, reduction in mitochondrial complex III subunit Uqcrcq (which binds to ubiquinone with cytochrome b) was similar to an alteration that we previously found in non-synaptic mitochondria isolated from DJ-1 KO rats at 3 months [144]. Cytochrome c oxidase or complex IV catalyzes the transfer of electrons from reduced cytochrome c to O<sub>2</sub> to produce H<sub>2</sub>O [260]. Among complex IV subunits, Cox2 and Cox4i1 were decreased in the DJ-1 KO rats. ATP synthase (also known as Complex V) is responsible for ATP synthesis. Here, we found significant

reduction in two of its components, Atp5c1 and Atp5l, in DJ-1 KO rats. While alterations were found in additional mitochondrial proteins, our analyses indicated prominent alterations in the ETC.

We anticipated finding changes in mitochondrial energetic function based on these results. However, we found that synaptic mitochondria did not show any changes in electron flow assays. While surprising given the proteomics data, it is possible that compensatory changes took place, or that we examined a young age and defects had yet to be manifest. However, when OCR was examined using the coupling assay, DJ-1 KO mitochondria showed a significant increase in respiration, which was most prominent in the extreme condition of depolarization with FCCP. Indeed, this is similar to our findings in non-synaptic mitochondria isolated from 3-month-old DJ-1 KO rats, which showed a significant increase in OCR [144]. This is in contrast to the mouse model, where loss of DJ-1 did not result in changes in respiration of isolated cortical mitochondria at 3 months [261] or changes in mitochondria isolated from brain and muscle at 4-6-months [262]. In general, mitochondria isolated from DJ-1 KO rats displayed an increase in OCR, which would be expected to contribute to oxidative stress caused by over-production of reactive oxygen species (ROS). However, DJ-1 silencing was found to elevate the production of ROS in renal proximal tubules cells [263].

In conclusion, DJ-1 mutations are associated with the early-onset form of PD. This study documents the importance of DJ-1 in the regulation of striatal synaptic mitochondrial energy generation. While 76 mitochondrial proteins were differentially expressed, proteins of the TCA cycle and ETC appeared particularly

susceptible to changes in response to loss of DJ-1. Functionally, in the striatum of DJ-1 KO rats, synaptic mitochondrial respiration was increased, particularly manifested in the condition of maximal energy generation. This work will help in identifying new targets that would improve our understanding of DJ-1 in PD.

**Acknowledgment:**

This study was supported by a Michael J. Fox Foundation (MJFF) grant #9524 and by NIH, National Institute of Mental Health, P30MH062261. The content is solely the responsibility of the authors and does not necessarily represent the official views of the MJFF or the NIH. We are grateful for technical support received from the UNMC Mass Spectrometry and Proteomics Core Facility. The graduate studies of Mohannad Almikhlaifi were graciously supported by the Saudi Arabian Cultural Mission and Taibah University.

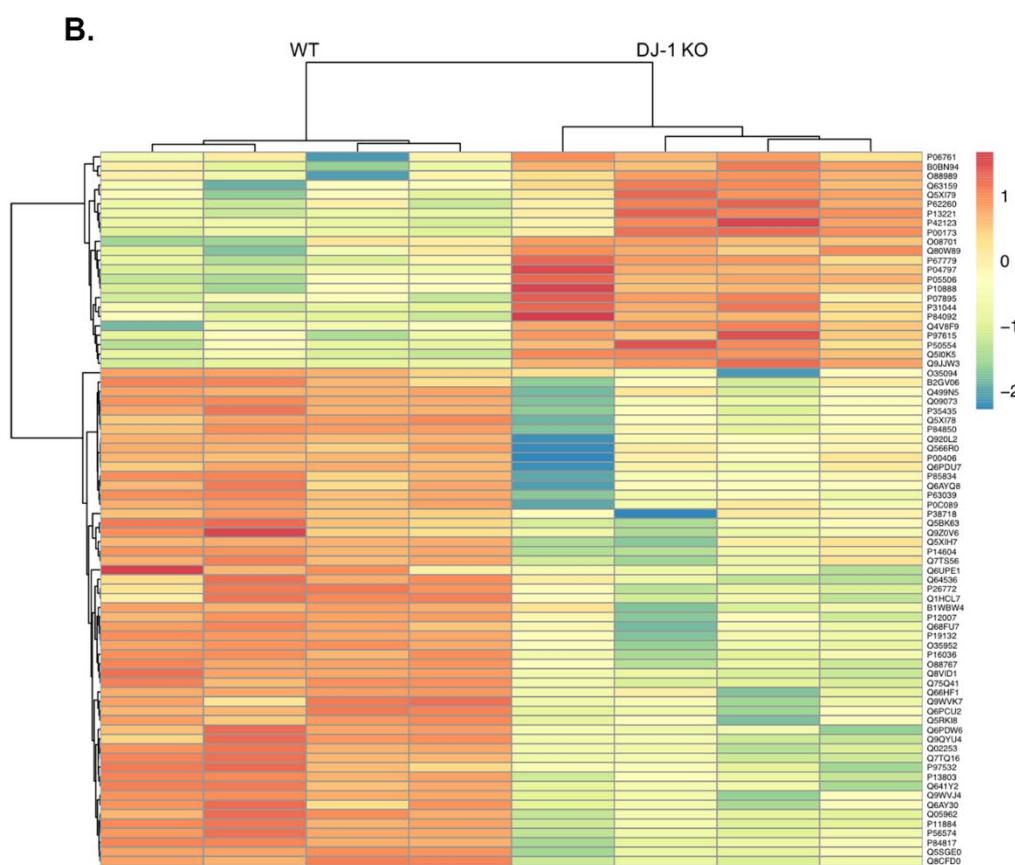
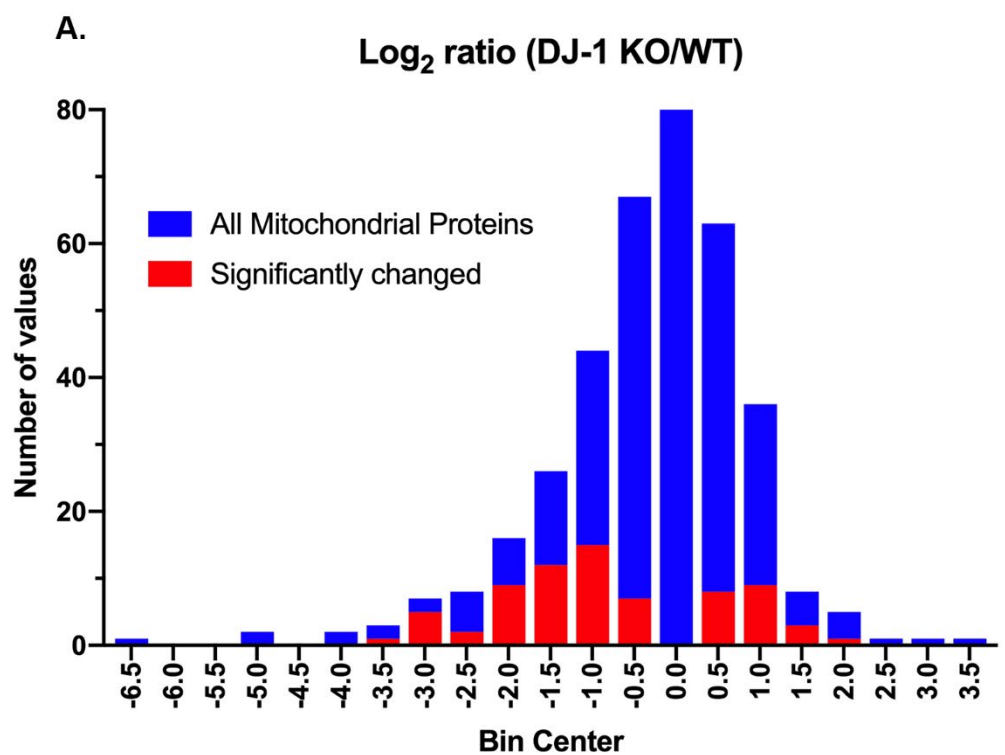


**Figure 2.1 Identification of the differentially expressed proteins in the striatal synaptic mitochondria from DJ-1 KO rats.**

(A) Histogram ratios ( $\log_2$ ) of proteins in DJ-1 KO versus WT rats showing the distribution of all 371 mitochondrial proteins and the 76 significantly differentially expressed proteins. (B) Heat map of the 76 significantly differentially expressed proteins in each biological replicate (n=4). Protein expression values are expressed in  $\log_{10}$ .



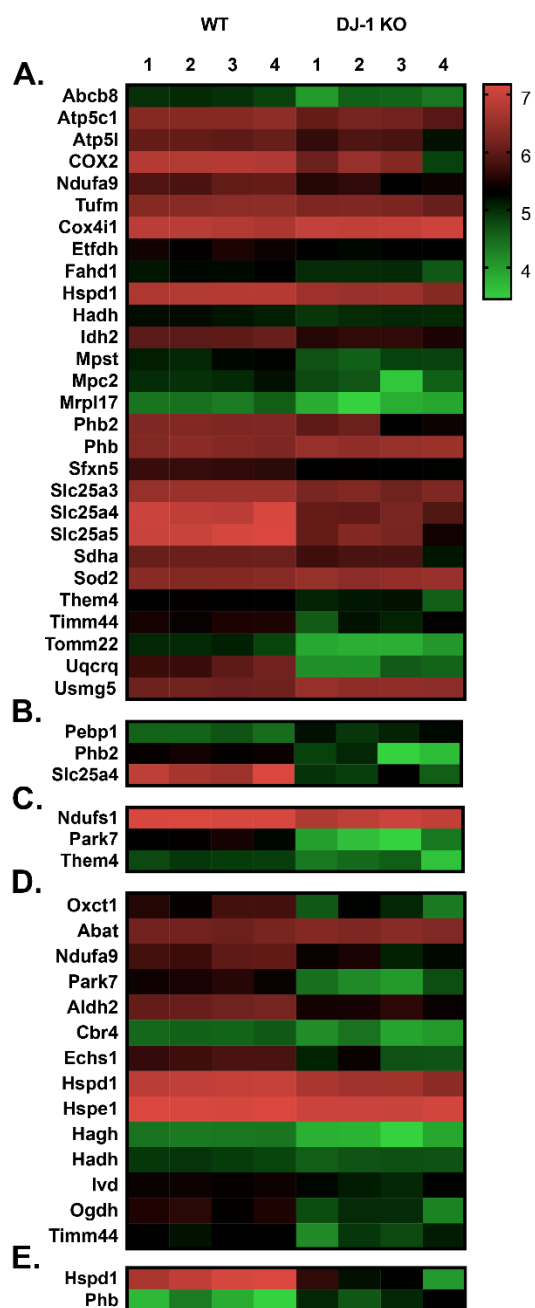


**Figure 2.2 Significant differentially expressed proteins in the striatal synaptic mitochondria from DJ-1 KO rats.**

**Heat maps depicting proteins expression in different compartments of the mitochondria in DJ-1 KO rats (A) Mitochondrial inner membrane (B) Mitochondrial outer membrane (C) Mitochondrial intermembrane space (D) Matrix (E) Crista. n=4 biological replicates for each measure. Protein expression values are expressed in  $\log_{10}$ .**

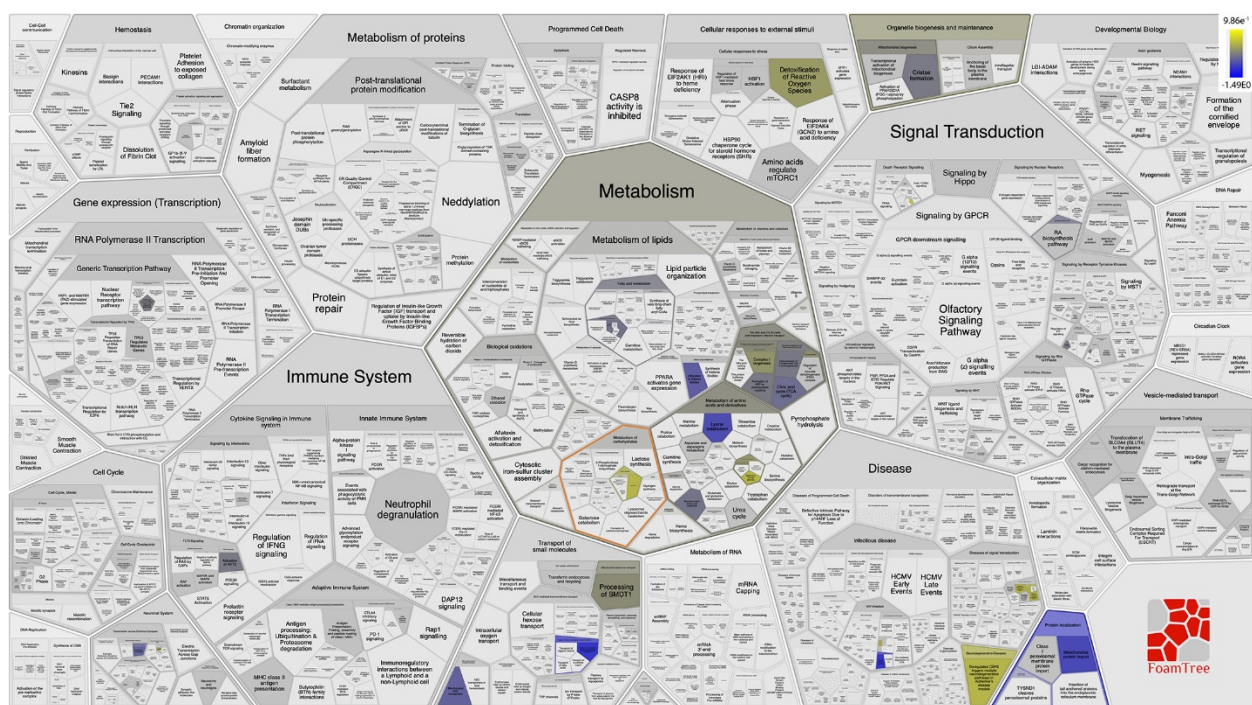


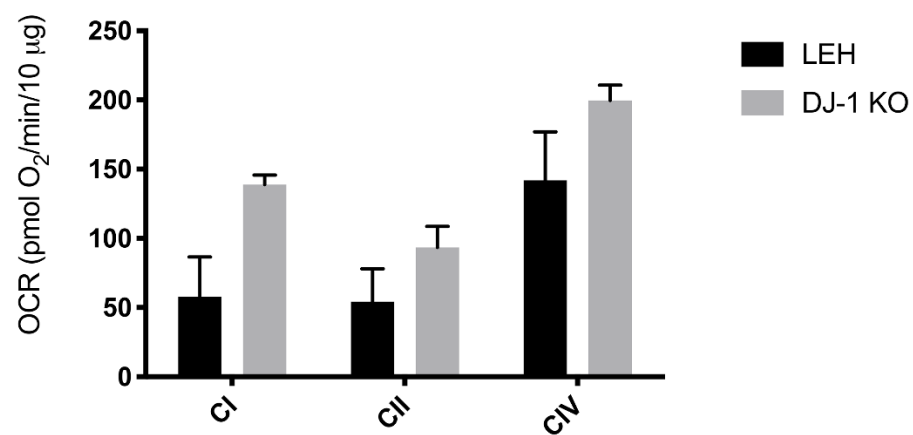
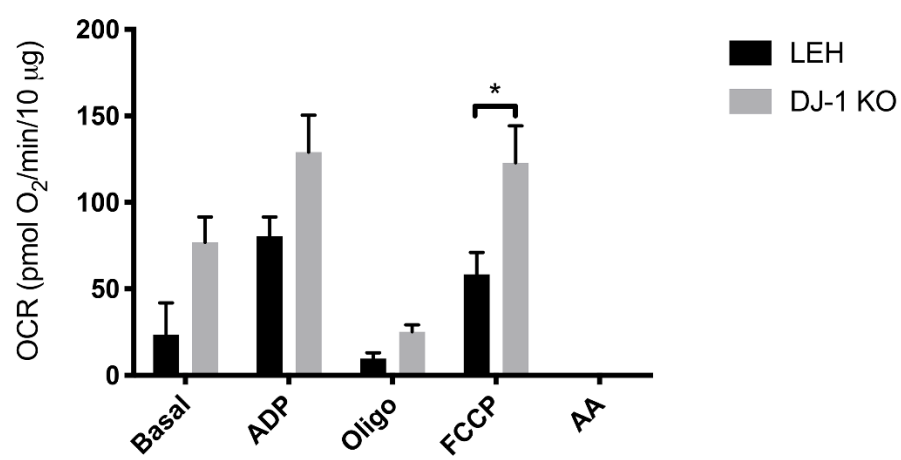
**Figure 2.3 Overview of pathways altered in DJ-1 KO rats.**

**Foam tree visualization (from reactome.org) of biological pathways and processes. Colored highlights indicated those affected by DJ-1 deficiency in synaptic mitochondria. The  $\log_{10}$  protein expression ratio of DJ-1 KO compared to WT indicates labeling color, yellow for up-regulated and blue for down-regulated pathways.**



**Figure 2.4 Centrality analysis among synaptic mitochondrial proteins differentially expressed in DJ-1 KO rats.**

CentiScaPe in Cytoscape was used to visualize the differentially expressed proteins centrality within the network based on the degree. Nodes degrees were mapped based on the size, the larger the node the higher the degree.

**A.****B.**

### **Figure 2.5 Mitochondrial bioenergetic analysis**

**Mitochondrial OCR was measured in striatal synaptic mitochondria isolated from 3-month-old WT and DJ-1 KO rats using a Seahorse XF24 analyzer (n=3). A). Electron flow assay assessing complex I- (pyruvate/malate), II- (succinate), and IV- (ascorbate/TMPD) driven respiration. Indicated are the mean  $\pm$  SEM values. Two-way ANOVA revealed a significant effect of genotype ( $p<0.0072$ ). B). Coupling assay assessing succinate-driven respiration. Mitochondria were administered sequential injections of ADP, oligomycin, FCCP, and rotenone/antimycin. Two-way ANOVA revealed a significant effect of genotype ( $p<0.0003$ ). Sidak's post-hoc comparison test revealed FCCP, a depolarizing agent inducing maximal respiration, to be significantly elevated in DJ-1 KO rats (indicated by \*,  $p<0.05$ ).**



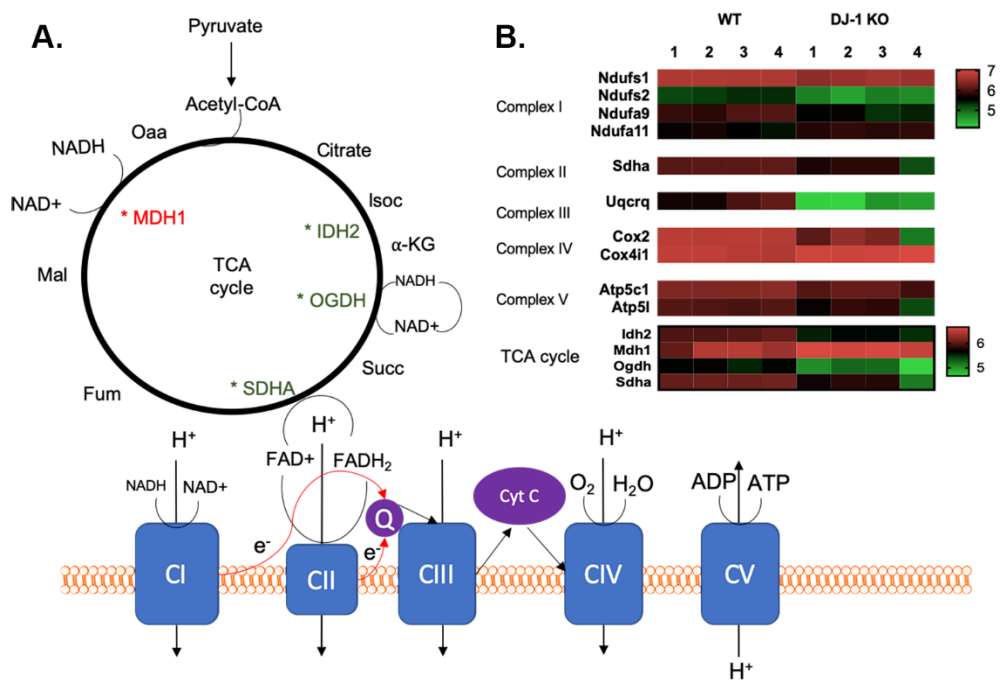


**Figure 2.6 Quantitative analysis reveals changes in the expression of protein subunits in the ETC and TCA due to DJ-1 deficiency.**

A) Schematic diagram of ETC and TCA cycle. B) Heat map of ETC proteins and TCA cycle enzymes significantly altered in expression in striatal synaptic mitochondria isolated from DJ-1 KO compared to WT rats. Protein expression values are expressed in  $\log_{10}$ .

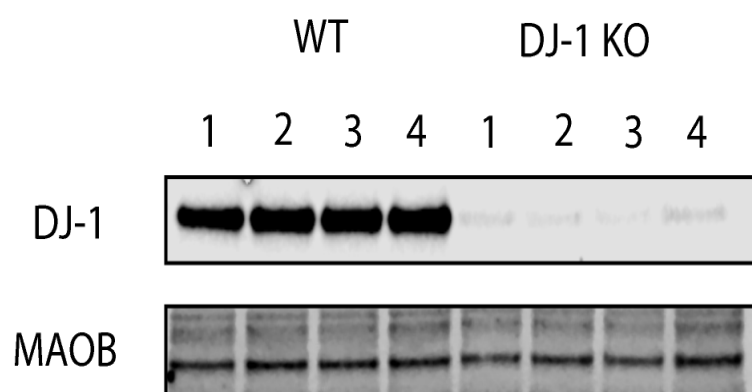


**Figure 2.7 DJ-1 protein expression.**

**Western blot confirmation of lack of expression of DJ-1 in striatal mitochondria from DJ-1 KO rats, compared to wild-type rats. The mitochondrial protein monoamine oxidase B (MAOB) was used as a loading control.**

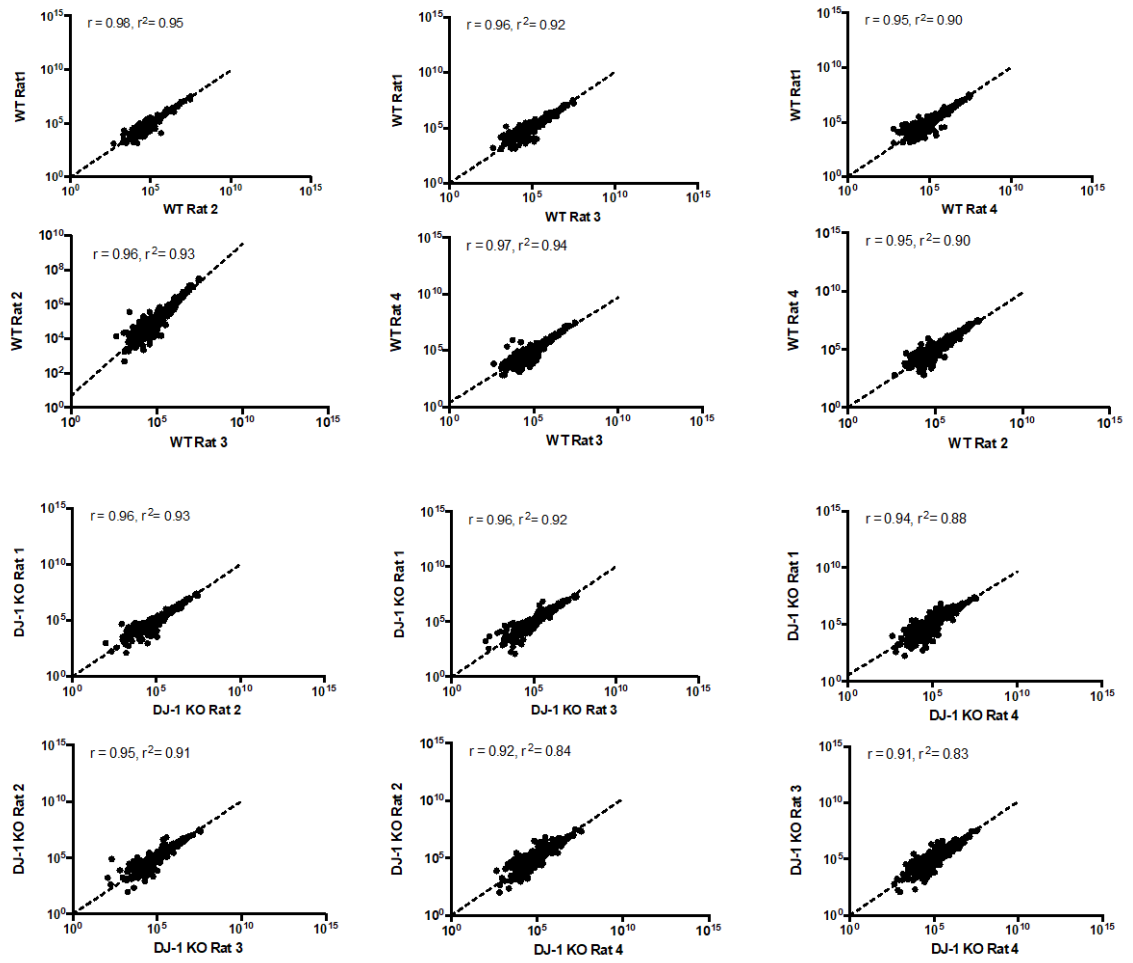


**Figure 2.8 Reproducibility of SWATH-MS proteomics between biological replicates of WT and DJ-1 KO synaptic mitochondria.**

**Scatter plot of the SWATH-MS intensity values determined in one biological replicate compared to another biological replicate for all 932 quantified proteins.**

**Table 2.1 A total of 932 proteins were quantified by SWATH-MS in all samples from synaptic mitochondria from the striatum of 3-month-old WT and DJ-1 KO rats.**

	LEH1	LEH2	LEH3	LEH4	DJ-1.1	DJ-1.2	DJ-1.3	DJ-1.4
Uniprot	Syn	Syn	Syn	Syn	Syn	Syn	Syn	Syn
P38650	109380	135950	94510	79773	147500	142880	137740	69715
P16086	76663	82446	59713	57339	105020	97927	119480	13940
P63039	5287100	5712000	6116000	6256700	3754500	3229000	3318000	2213100
P10719	17032000	29334000	31205000	28436000	15858000	29959000	30856000	16647000
Q9ER34	5837800	6147100	6175600	6553200	7289800	6689200	6635500	5502900
P15999	32412000	30641000	28717000	26553000	18860000	20560000	38021000	36926000
Q5SGE0	364140	359960	338360	339730	138230	178170	148000	98808
P15205	64242	40083	58991	24194	123670	181190	259120	17105
Q9JLT0	8683.6	7474.5	13295	46292	26545	10393	17936	19613
P10860	3566400	4964200	3338900	3793300	4426300	4729700	5072300	1579600
P11442	1630400	1802000	1495800	1607600	1141600	1380600	1264200	1647700
Q3KRE8	180360	183390	171400	159510	166190	172760	174160	361550
Q5XI78	459420	513340	342260	444660	114740	177360	174660	46916
P52873	1150800	1188000	1040900	978470	661950	956250	1211200	739440
P05708	1489200	1495900	1245900	1010200	1327400	1400100	1463900	911930
P00507	11897000	12654000	10047000	14573000	9140600	10358000	12849000	10499000
P60711	2720800	2120600	2435100	1961100	381520	157560	74998	79514
P17764	1233800	2089100	1158600	1044700	1561000	1586100	1767100	1036200
Q05962	10259000	7831900	7180800	14339000	1127100	1022000	1675100	757370
P04636	23751000	24041000	28258000	30648000	25110000	25653000	29853000	28749000
P48721	3131200	3218100	2844800	2836100	3320000	3219900	3131600	3377500
P11598	36115	18325	54672	64681	17128	23559	17543	11733
Q66HF1	5023700	5087100	4909700	4930500	2798400	3397800	4176700	3612800
P63018	2065700	1965100	2230000	1910400	2355200	2355500	2470000	468270
Q5XHZ0	722170	723480	763950	665260	1376700	1025200	1185800	464790
Q64428	589770	638580	530940	593990	709900	747620	771770	432750
Q66HD0	5917.7	14874	34348	33278	42289	31509	57752	50990
P06687	541000	643150	685240	558590	274690	297350	265810	298990

Q920L2	1163000	1226100	1229600	1311500	544570	653250	643850	140650
P50554	1481100	1478600	1360500	1596500	1990800	1760600	2133200	1862700
Q924S5	412510	421240	473500	452070	334610	338950	330640	85099
P47942	2700400	2821400	2018700	2253900	2922000	2717700	2610000	1345700
Q3KR86	1377900	1457900	1370300	1290300	1754000	1618600	1797400	1235200
Q68FY0	3258500	3299200	3594900	3358000	2630600	2568800	3146800	156700
P06761	5232.6	30389	19415	35037	69145	40887	58914	76652
Q2TA68	504860	500500	455100	263890	510930	730130	599980	232550
P82995	354200	315670	258180	353740	397390	343830	498320	248840
Q75Q39	1408000	1167200	1589100	1904700	1179300	1461800	850360	1412700
P35571	534540	578860	394070	253340	417920	422020	370580	485000
P85834	2148600	2286400	2484400	2527500	1742400	1849700	1709300	1176600
Q60587	191600	162030	201360	244500	160360	177240	60770	131140
Q9Z2L0	11975000	12148000	7986000	14963000	6973600	8399500	8655500	6877100
Q5XIN6	748470	727520	404510	489660	817340	762920	887910	586360
P29457	4346.6	8645.1	11861	14499	5001.1	10314	15095	3403.3
Q6P6R2	1347200	1381100	1104000	1145900	1352400	928530	1099000	1182600
B2GV06	495160	357030	736860	737870	93162	280220	188760	55105
Q9Z1X1	275.8	115.28	4718.7	38370	388.82	2160	348.36	0
P18484	416460	479950	239960	263040	324880	391280	395750	100740
Q641Y2	155490	177620	227080	231170	63248	34396	66106	52652
Q8VHF5	5288300	5837300	5105300	5777300	3752100	4919600	4488700	5044000
Q9QYF3	306290	210220	197870	187690	192830	210820	192490	161480
P05197	3925	7790.7	36645	19166	2126.3	4733.6	7611.6	18787
P11507	96322	88705	35593	79950	146830	92279	125780	102530
P56574	922720	922350	986280	1175600	359050	439580	427010	312470
P62630	59486	55280	95692	86257	27426	65131	18202	48748
Q02253	542010	566530	632090	726230	135680	169350	220410	226290
P08461	2000700	1959800	1821300	2943000	1210300	1503200	1157900	225790
P35565	27613	27701	9781.2	34331	42581	31402	58027	23936
P21575	864940	808990	810850	800660	499410	496810	274930	980640
P18418	33868	23548	31647	45521	65404	60807	66459	136780
P32551	2841000	2874200	2916300	2942500	2549200	3175700	3257900	2819800
P62944	380740	373830	278710	392460	340640	380070	276480	483930
P04182	294870	262360	288280	256440	365860	339650	370330	116420



P04764	1384600	1293900	1250300	1069900	2546600	1800400	2228100	2233300
P50399	103330	82210	113280	126270	150230	112080	43186	141820
P11980	1786400	1633200	1678300	1449200	2956600	2145300	2461000	1055100
Q99NA5	4161500	4423300	3764200	5006700	3401800	3518200	4121700	2765200
P45953	76884	80127	74984	36750	104880	106090	111380	20978
Q499N5	311040	328610	327290	312460	128480	191160	240200	88454
P31399	1163400	1158800	1125300	1913700	703650	972120	476350	1234700
P13596	424660	421440	533020	319870	701010	599120	573700	281990
Q62952	156020	153410	172870	43325	443670	423730	418660	363420
P46462	159470	242490	165270	180420	187920	217210	113860	229600
P13264	1217000	1308000	1316300	1343900	1049600	874670	1095500	413380
P10362	23458	10358	12643	23464	12119	11503	25372	52026
P11884	1162100	1252700	1425800	1565900	403170	413570	530500	361250
P67779	1980500	2432700	2076600	1813800	3078400	2715600	3075700	3377400
Q9QUL6	2230100	2121000	1995500	2254400	2509800	2610600	1435500	1015400
Q9JHU0	162570	137940	167690	77768	188110	224770	206260	72062
P26284	6328200	5941600	6299700	6285800	7573800	6257400	5367200	5941600
P04797	6467500	6439700	5745100	5497100	9827700	9430800	10074000	12866000
P61765	1842900	1783200	1526600	1611900	2074700	2108600	1915100	1136200
Q68FX0	1211800	1124200	803990	808170	1331200	1468000	309080	806550
P20070	41017	52274	69546	43875	21654	27078	42823	21017
P51650	491990	541060	550100	626750	391290	505190	371890	706580
P11505	22418	23410	27814	76544	850.92	20222	2854.9	3068.7
O88600	200920	186120	217730	189960	284700	230090	302110	225050
P19511	3213300	3141400	3901700	3571200	5118400	5230600	3059800	6152900
Q62950	296030	270690	244150	387930	372220	328170	435820	478180
P42676	64947	62777	24319	45455	77324	78814	96571	113420
Q66HF8	357840	361710	340450	417450	631480	574230	552710	355950
P49432	1337200	1519400	993540	1224900	1378800	1109900	329960	576260
P07153	4779.4	15475	2682.6	7664.3	24554	19233	5119.9	20241
P16036	3077500	3463600	3485600	3473600	1684500	1988000	1402200	1921000
Q05175	343200	261510	408580	197250	974430	622540	820170	437220
Q5U300	142600	156030	63612	69327	164760	125820	143430	122520
Q3KRE0	244520	330730	327590	199680	306500	289690	187770	285680
P33124	1615	14063	432.43	6750.1	730.37	1416.9	1296.6	5678.2

Q5I0C3	36085	42539	52879	11509	14509	22397	23943	25213
O70351	892780	990200	721590	840130	713560	893510	964010	496310
P04937	57308	16571	64428	114370	17065	13104	6780.1	42515
Q9JHY2	1207800	1213800	934310	610070	1171600	1464000	1337000	405360
Q68FS4	6572.1	17080	21478	16641	16965	28019	28887	20173
P05065	639790	667120	148910	462400	124330	157990	167440	167480
P06685	609180	695830	702830	634150	703980	653630	496220	221000
P53534	168360	232830	122000	107830	245960	221490	257110	231700
Q7TPB1	221670	246050	274900	298060	365050	326250	257560	397030
P97852	34700	63245	49810	21975	44518	21575	50343	22849
P81155	4532800	4551900	5114200	6332800	3927500	4466700	4462200	4692600
Q5XIH7	1854400	1970700	1828300	1917900	1004800	1254100	204300	263620
P50442	20916	30372	28947	30234	24731	31983	61481	43128
Q9JM53	147680	180550	104530	29113	177360	160540	133400	120440
Q6AXV4	794860	836070	1000900	1093700	571480	696780	744830	650860
Q64057	138100	142920	167200	88944	116730	38343	75771	16981
P97536	92732	121020	125310	127920	189200	192450	86819	177340
Q6AY23	57179	50875	74564	95536	45644	44986	16529	63216
P34926	48370	39186	2353.7	11966	176830	197600	41696	17876
P10888	7047300	6954000	5776800	5128700	8965800	8486100	8859800	11344000
Q5XIT9	134960	148990	94379	35119	142670	121910	131750	10687
O35303	424880	443730	252910	409260	306220	342530	349140	166460
Q5BK63	740440	652900	1051500	1121500	365360	434370	207460	259080
Q6P502	162780	155450	188980	71322	255150	145370	168910	200430
P62815	1093900	1038700	1368500	1153200	1904600	1593900	1843800	518790
P21707	3226900	3087600	2433400	2310500	3207200	3416000	4040700	2728000
Q05695	46518	40512	22308	50490	3826.2	5888.1	4522.5	13072
P29147	619550	653420	579550	509260	703620	896530	656750	143530
Q66HA8	114790	150170	220060	58480	41117	32679	89695	72387
P21396	1130700	1266600	1014000	1126500	1097500	1111100	1167700	369600
P14408	391910	413500	309870	400580	214810	294680	373190	233280
P14882	32562	82338	54882	42250	63160	79673	82405	36514
Q6UPE1	280810	226040	322610	262940	195810	167740	192740	200720
Q9Z1E1	3750.9	24763	11516	28805	47245	46587	49364	9353.7
Q63065	61358	28321	26528	75163	37119	36759	32928	150880

Q62717	6239.1	20187	19795	16542	3241	8005.1	6032.2	13707
P13437	304580	342040	266210	250550	305650	260410	329280	360060
Q9WTT2	32739	15120	38293	14640	43503	41847	53838	73818
P15650	532380	575610	465520	457910	417920	373650	350680	75755
Q01205	1056200	1062200	1022900	907530	1455000	1488300	697270	1418800
P45592	738190	901950	839790	631910	1261200	997790	659410	1378000
P18163	54648	13348	9469.7	2230.7	34246	48637	12321	3022.6
P13803	1305100	1347600	1461700	1431200	836000	724580	944750	741980
P62260	491680	258600	334080	260620	1104000	782630	960540	508740
Q9Z2S9	33406	28714	15110	11209	70402	65067	60951	26525
P25809	1265200	1140600	1000300	825380	1274400	1306400	1514300	1339000
Q8R500	78250	89324	12348	54720	31355	21768	31193	31867
Q63081	304590	333780	19530	17294	350080	386720	362600	45122
P50398	1285800	1335600	1128700	837410	2826000	2129900	2514900	2292200
Q09073	10052000	9896800	13275000	14886000	1107200	2101200	1596200	273900
P04897	92898	84497	87172	82863	162200	153570	174150	158910
Q4FZT0	68361	86679	62623	71402	119790	83483	103720	34704
P34058	319280	297400	171890	386810	273170	277530	419920	164600
P14604	600410	675630	776190	775410	197140	368240	105730	99519
Q9Z0V6	2775200	2605500	3417000	4336900	1724800	1855400	1302300	1766500
P09951	1105900	1625700	1076200	1027300	2086400	2015400	1756000	1394800
Q03346	88558	92636	97256	14125	146730	130980	49340	154740
P25286	902150	1032600	971470	704070	823010	829570	796780	48530
Q9R1Z0	1840800	2095200	1003200	1399800	1916000	2303200	2266800	1634700
Q6P6V0	315430	317640	526240	559790	195600	206010	205020	133740
P16617	992720	1031800	899890	1263300	887960	774820	1000400	151110
P54001	23488	10045	5196.8	4479.9	21049	28026	48558	21304
P09606	36961	20148	8654.1	26574	8199.2	22514	32489	18104
P48037	6029.9	42874	33177	46331	46264	42949	14574	9548.2
Q06647	6805700	6642100	7847500	8841200	4147400	5214100	5825700	1891700
P54921	109720	130000	59103	71943	243400	233010	189000	317180
P28480	193680	257440	52028	66127	164800	182670	138650	283590
Q5RKI0	12109	20933	3150.5	15759	38205	36392	38163	30150
P19491	50322	42571	6992	18623	54218	72819	56987	3527.7
P24329	1529700	1499200	1336500	1282200	2004300	1849600	2467200	1458700

Q794F9	208840	207160	86051	78541	297850	269600	195260	66695
Q9QXY2	261740	270790	389520	160650	360540	139650	331650	289170
P12007	374550	379810	358330	385900	279370	218340	187620	288740
P07335	2458400	2579100	1171400	821350	1541000	1518300	1329500	1286200
Q99JD4	23156	25078	2973.1	7004.5	13265	3055.6	24579	7054.9
P50137	119860	212700	127070	86652	280360	242200	277920	99399
Q05096	5349.3	13831	4041.2	10509	9963.6	15971	13663	47226
Q99PD4	122990	47095	138340	25138	185590	164860	157790	72796
O35814	139900	134580	183520	153760	73228	105540	103590	77610
Q561S0	2000100	2036800	1655900	1777100	1726600	1772800	2075500	1850200
P54311	746060	781270	784070	581690	489440	412340	470680	194000
Q6Q0N3	9625.6	12725	29027	18517	80167	69412	96140	103610
P09117	234390	273910	258350	275650	361240	267990	251560	734290
Q6AXT0	15007	15462	12897	6079.6	25450	5802.6	32008	14232
Q4V8F9	65537	85051	16624	65729	385320	217920	314700	282330
P70584	10993	51970	92506	7295.8	9753.5	7594.5	616.79	431.47
P52296	47902	32523	45909	7098.9	12204	1836	17345	13327
P31016	106140	163150	76073	95014	94263	122140	101450	257000
Q6AYH5	48683	61259	14013	56684	6789.5	14225	2219.2	14442
Q9ERH3	36633	33056	20999	9993.4	4302.5	16626	24354	5907.7
Q63198	144830	151070	197720	17112	21608	44701	56581	1204.3
P04642	638270	591630	710730	619220	1036400	370460	591630	697410
P11960	67791	70364	61426	3636.2	109620	78621	115560	9489.5
Q9JLJ3	36512	40139	43275	51538	73496	91930	40419	12882
P16638	95241	122270	140570	75691	94939	94719	83175	119240
P56571	304550	349800	39509	22111	151990	169070	139740	21552
P07633	272990	254150	162700	110590	307280	264820	139660	130960
P19643	405560	437860	276180	139560	320410	357180	299720	319510
P08413	554350	474550	661100	569980	254530	260570	302910	127930
O88778	143810	146280	96096	114740	106650	168750	166510	149050
Q62951	40828	104220	48623	52997	110800	134480	205210	117740
P21913	1160800	1328600	1039200	1125600	795310	1022400	834330	961530
Q68FU3	721990	769930	721820	674260	605340	565230	171090	443800
Q924N5	9515.7	17213	6396	32203	7068.2	14963	2165.8	6160.1
Q07936	9925.9	47846	23447	59035	25139	20877	6534	14666

P11240	2136000	1985200	1392900	1880200	1770800	1502800	1381500	1092800
P61107	204590	126740	186400	179670	138600	144010	169540	47621
P12369	136340	142950	119120	73244	117960	132670	108970	57345
Q99P39	65993	80848	49970	13349	259030	123800	379380	139620
P09527	8462.3	56053	66405	8797.7	34845	48871	80546	12154
P24268	285340	308990	330990	348190	234730	257460	296460	6110.8
P26772	9289600	9051300	8223200	9258000	7205100	6979000	6753600	7757000
Q1JU68	4791.3	8866.6	10363	3423	8356.6	15557	1365.1	278.5
P41565	1405100	1359700	1746100	2246200	1032100	1143400	1219500	1001300
Q704E8	8455	1937.9	2251.3	4422.2	1489.5	3558.2	12462	10697
P48500	1195300	1393300	1164200	1028300	1460900	1320500	1460700	985860
Q9WVC0	98048	116150	116600	67417	201890	130780	147380	24921
P37285	9433.3	3987	3301.5	2458.8	16366	23019	5212	5739.1
Q99ML5	24795	49861	55103	25656	45829	31340	37748	161290
Q5XIC0	404520	335860	299930	267170	423760	429710	389070	356950
P63004	129290	129400	117550	105060	297640	239180	282880	403190
Q7TSA0	33778	39215	5768.6	855610	45878	5937.3	1697.5	5467.2
P19332	680690	49830	439810	220750	888970	594370	925180	1184500
Q63965	850360	878710	468830	619330	851340	690320	810790	810060
P0C2X9	142620	215550	211300	204690	185630	155380	227340	100210
Q4QRB4	367420	349710	588000	639520	212790	263360	29584	33913
O88483	21334	2168.9	16926	46572	14078	16403	18753	5741
P30835	186960	229070	217090	285730	223480	248950	274380	106540
P10960	415080	417570	331350	519810	639310	558870	311080	418790
Q2TL32	164850	308860	134410	142490	15289	24728	7824.6	37165
Q3T1K5	228780	236680	197240	149590	82920	100810	73984	43902
P15651	31337	194330	17398	546860	47772	31211	40045	25642
P85845	62325	112630	102300	60905	30337	59979	42036	24709
Q63716	108410	130250	150150	121840	141590	166240	120460	292340
Q00981	254930	450570	449370	366610	663040	521590	587780	295670
P10111	1132700	1192500	1435400	1514100	1328800	1495400	1569000	871690
Q3MIB4	36563	57862	42918	12942	88609	63463	110720	99639
P97849	46419	70643	37318	7778.5	19431	2622.9	23678	8865.9
Q91ZW6	50925	180370	67580	66869	101590	165660	66034	82478
Q68FS2	12417	13455	1665.5	10741	19842	21152	20344	7570.3

Q63092	2030.4	4121	1838.4	1730.4	3514.2	2678.2	1679.1	3710.4
Q68FW7	25087	29623	28445	28832	25769	28685	2252	32627
Q9WTP0	50899	49181	64016	46968	51650	63414	46935	226350
P18886	192170	205240	424760	134920	200590	288290	265710	135280
P97700	2157800	1030500	725090	790540	1030500	1212300	1477000	1110100
P08503	35985	47443	31553	37461	64918	42907	46465	25938
P30839	141410	189420	110060	117660	77016	104000	79899	117860
Q4V8C2	13710	10948	17084	128920	363.68	5238.2	4726.5	4648
P97629	12512	1864.5	1859.5	2045.2	5009.6	1200.1	5475.5	11509
P62804	39529	57791	65360	232250	74544	40889	98018	57284
Q505J9	5991	13598	2469.2	10040	17425	17485	15259	5865.8
P20788	1246900	1074100	1349800	1393400	893610	978180	724620	1070200
Q9R063	3109600	3244500	3159900	3427600	3392000	3986600	4566400	2621200
Q9Z1Y3	33127	31700	77131	4821.4	59639	52515	51362	40261
P07895	2351000	2039800	2082900	2300000	3020100	2472900	2897700	3169800
P35435	2188200	2198600	2254800	2646100	1125000	1500400	1442900	857460
Q63028	17361	26530	7185.4	22107	31634	20297	44746	9134.5
Q704S8	165040	252870	132430	195540	168990	183070	151420	162990
P63102	1854100	1630900	2075000	1761100	1946400	1781800	881320	2937700
Q00715	83982	66788	110320	57860	37338	46417	32289	91861
P97521	131890	116320	247330	281770	77760	110730	115070	151830
Q1HCL7	72561	78422	23816	85937	10762	5231.3	6490.8	16913
B0K020	2946300	2614800	3141100	3106900	2403000	2436600	1577900	2206600
D4AAT7	97889	87965	91857	71166	85823	89607	86846	28032
P84092	490080	464770	573490	500040	703090	647070	700620	873340
P20651	97924	7204.6	20239	26032	174460	82870	138880	166290
Q5RKI8	92931	104170	91152	69365	10794	37455	34850	22912
P56558	42879	46990	4095.1	22248	51599	51871	68987	41108
P28037	14431	64829	34331	15639	21071	29087	62611	21557
O35094	296900	244370	317410	319740	41274	149710	117930	216450
P24368	25549	28501	14651	99082	38988	44670	37167	27631
Q5XIE6	209000	147380	241250	215640	116480	269690	34174	137200
Q5XI79	13538	10442	14294	7400.3	24350	23380	28892	16955
Q9WTT6	338910	303050	487670	540760	427370	414440	511120	629210
Q66H50	374830	400620	348780	563570	2279.3	149040	396180	46137

Q4V7C7	48026	52938	72783	81948	60259	67513	67481	51284
Q5FVI4	1395900	1510400	959730	1353100	1444500	2175400	2863100	491770
P51635	189220	189470	197550	228700	253200	197970	227600	330610
Q62651	254890	270020	255820	118910	151290	177580	175380	163740
Q8CFD0	492100	481780	434930	415790	193890	230030	214670	182020
P29266	434080	416400	356370	416400	473040	459390	589180	470560
Q641Y0	34022	4689.4	9544.8	12849	4282.4	3550	9126.9	11439
P07323	528100	601210	624230	720060	1236400	896180	1075400	1315400
O35095	86558	119120	100260	79067	24491	27302	12421	9389.8
P13233	394870	431470	495510	270430	167310	249780	196870	164160
P32089	494100	479080	567470	569010	525590	521010	299720	547790
B3GNI6	311840	295740	261400	330830	98190	167280	180000	109300
Q5I0K8	23262	49528	45139	160590	160890	60761	139680	152710
P42123	753840	704910	760240	786320	1398000	1150700	1218700	908290
Q5M7U6	148360	132280	153610	28841	360240	284520	219650	290500
Q3MIE4	84759	97882	99902	94303	90549	113770	141080	7636.2
P05712	433990	401450	373660	373660	534790	469130	451900	384320
Q9QUH6	349790	495900	239690	294110	362840	352000	523800	76037
P85969	403610	390180	392560	390060	553130	644970	390490	1081200
Q63537	2383300	2336900	778190	504080	1699200	1644500	1660700	127740
P97519	15661	16797	19444	3278.2	21160	16878	20716	41019
Q64548	343640	208230	38389	24045	13861	283880	171080	71104
Q64542	58506	14831	87755	12767	21765	12475	4050.9	9891
P29411	111240	112790	35149	62644	133290	120360	173870	28784
Q63060	54214	181700	101880	152880	120340	228210	132810	39054
P31044	722510	711280	830850	651860	1474900	1100800	1268100	1525300
P47858	157120	233320	132760	139600	276500	298360	344340	57607
O08701	63655	55830	9335	9066.5	99154	90757	131960	130110
P00406	6093500	5770200	6149700	5588000	1258800	3009300	2064500	68914
P46101	234500	254660	238770	246320	386030	331510	226430	322820
Q01992	1224.6	488.7	1346.9	640.02	1475.2	1450.7	1687.6	3196.8
Q63362	603700	674980	627660	684920	632320	674980	660760	149730
B5DEQ3	10215	15285	187500	30252	17367	13298	10923	7497.7
P13221	545790	545790	560230	473770	1032900	1006300	1140900	718020
Q9JIM9	1198500	1129400	1119300	1129800	939000	796890	535900	2275000

P63245	3348.7	5163.4	8108.6	13847	6122.6	5419.6	17538	11420
Q58FK9	175760	165810	174360	213830	91407	117680	30199	138910
P0C1X8	68157	87381	171630	54845	129040	118450	115510	63225
Q6AY30	255460	302960	304210	332770	148900	203310	191780	172330
P63036	38817	46629	7860.8	44546	15652	5669.8	13755	29150
Q66H15	38120	93108	42468	50092	18214	16964	23038	26595
Q68FX9	92251	84506	78788	26732	149120	118500	137280	37063
P15087	79126	69981	81716	116510	104640	110940	103510	100610
B2RYW9	373430	454620	419740	679850	237800	276580	293690	51779
Q9JLH5	238110	4787.1	367790	2182.8	25636	11498	21544	2551.1
P51583	60782	14441	236830	280570	3915.2	55531	34331	82963
P08592	5773.5	4668.2	11703	7098.3	2093.7	3673.5	22954	42337
O08839	87481	79422	62219	77730	231180	159430	214440	186780
P54313	797760	835660	686460	638880	594680	661310	555320	150490
F1LU71	553540	544480	485520	551910	1148300	977580	803880	338550
A1L1L2	65913	10568	26063	21631	82888	18396	66052	48001
A0JPJ7	64704	69396	72401	85856	101100	99803	94708	124510
Q498R3	46977	4019.9	7283	11815	11977	8480.9	34473	33202
Q63569	62007	96864	47876	17062	54845	39419	99964	56389
Q9Z1N4	303240	310010	300320	325780	181380	192240	172120	141740
P05426	252380	272120	11653	32708	158220	246490	181770	355410
P19234	3604400	4226800	3438300	3400400	3192300	3740000	4214100	305730
Q9Z269	463.22	15546	10910	8849.3	10652	890.7	18010	4071.8
Q6P7S1	1794.5	7402.6	21030	4627.8	2643.5	4974.5	4008.9	35343
Q68FT3	40088	43779	29886	5465.4	53770	41228	41093	58679
Q9QXU8	20231	23021	23207	4776.8	14128	20847	22320	28337
Q64536	246240	274960	209700	301580	103730	99485	131680	185230
Q64605	18158	19410	21411	27725	3302.8	14073	5688.8	6035.5
F1LMZ8	18398	4107.8	23917	12282	17333	5901.7	8422.5	7763.2
Q08163	182260	161160	215540	202660	203970	159110	157180	101130
P97576	100300	19744	103970	89941	47411	842.6	18817	10645
Q9WVK								
7	154380	157990	144240	124820	84049	101650	107400	103560
Q6AXR4	29122	29117	50029	33357	37912	34110	22031	59504
P63331	57219	114030	127070	140060	83169	83578	94603	22577



Q9WTV0	17568	9458.3	26657	23540	20143	32059	26393	125690
O55171	141490	153730	44820	111680	49007	68278	44643	45391
Q62936	62229	57248	61183	6389.6	133510	101820	106840	102460
Q62889	53472	48563	57687	51250	7854.2	6720	3756.1	10007
Q5RKI1	407620	401680	40814	582710	337420	362180	397950	31191
Q5XI22	181580	45822	63672	316590	48733	44388	51322	37419
P02091	60049	43021	28673	44467	136210	120650	79093	146370
Q5U2V8	1742.1	4419.1	3662.4	2105.5	4172.1	6051.8	4276.9	2150.6
Q4G064	1394.3	14860	9437.6	6533.3	11650	3197.5	6235	13890
O88989	1126600	2875100	3014800	2195900	4718500	4209900	4541800	3585600
P69897	1462700	1399400	1541500	1368400	1279100	1102500	929550	1519600
B1WBW4	97277	81454	90503	77838	5964.1	11357	2061	37211
Q05140	224120	255680	192630	167120	575130	498790	624620	420910
P68255	66220	24591	60140	47258	91735	57346	106530	67594
Q5XI32	139600	94734	129490	78191	123410	85069	59419	67717
Q5PPN7	110160	117190	82548	54624	75058	85534	60911	164210
P62982	836360	715620	744530	587280	1913400	1258500	1387900	940090
Q5I0K5	94972	90039	101620	111340	174550	155820	181350	179110
P62898	5312700	5303200	6316500	7494300	7143100	6495500	343210	298500
Q6AXT5	13735	250250	33876	38818	32169	30846	34754	10853
Q62915	13395	7721.8	15042	25141	31030	28683	15108	23311
P19490	152860	137880	128200	107030	102940	92257	77809	35295
P60905	273200	317310	249640	201500	195770	217610	117090	303220
Q5EB81	121850	147260	139230	171530	54515	54257	58309	132790
Q9R080	79232	102100	16790	89587	59647	92863	92623	435630
P35434	330690	82838	70317	76795	160580	69314	157270	96920
Q91ZW1	36399	33163	27976	107810	89647	79706	88390	54218
Q68FR9	18747	11947	21406	28605	26105	28525	19801	59484
O35547	23685	15542	9199.8	12863	13267	25207	41740	134560
P14669	53607	53632	6575.5	50805	70920	68163	44448	15224
P85971	81092	78188	51881	71492	135710	135430	112640	182890
P70483	75408	63446	83003	53367	45684	51389	42182	14805
P59215	1474100	1449500	1260300	803050	2474500	2011400	2519600	2136500
P55053	20748	15256	19071	5745.3	16446	16033	20416	18966
P61265	707960	723010	614880	469540	1473600	1114800	1077400	689480

P23965	699480	683930	536810	1004600	430190	657500	679880	354430
Q5FVJ0	5255.8	2854.5	49555	36056	37550	3141.4	16479	8530.2
P68511	38238	6501.4	24913	58693	82939	102080	57714	18696
P51647	205960	202230	160970	197960	63299	44483	84281	146830
Q0ZHH6	83030	64711	76762	69031	72744	85810	75465	121030
Q9WV63	52443	53124	21556	15591	22362	42743	42289	12911
P45479	69933	56019	48871	74479	140690	100890	132820	110850
Q7M0E3	199060	181540	258980	196170	460230	343380	427630	315400
O08873	40714	44371	25229	15290	92874	92593	28403	118960
Q75Q40	203630	169640	161680	151330	252250	218580	222750	78845
P47727	334610	300100	302610	354010	246860	240640	240640	260680
Q6AY19	12431	12313	14198	1224.8	936.53	94.953	1752.9	631.49
Q68FR6	52462	54933	57522	78123	84633	71262	63229	219070
Q9QZR6	264170	4613.7	107190	118740	348710	46322	12807	306690
Q5XIC2	12283	11912	7284.6	6244.2	22821	16721	28958	4377.9
Q5U2X7	96176	95603	84282	115930	132920	119600	85901	127330
O35796	195180	219610	230980	205280	249590	333790	320180	183300
Q6P7B0	11089	25103	26623	38262	16746	10782	10860	20980
P61206	1653600	1608700	1387500	1510100	1278900	1466400	688160	886860
P60881	624210	579370	580330	450260	1283000	914970	1026100	406520
Q07116	10604	4281.8	3029	2957.1	1743.7	971.76	1442.9	1304.8
Q5FVH2	91639	80249	25439	73580	191960	150130	97879	175320
P10536	129980	131740	26893	36589	12870	11017	14319	36825
Q4KM98	23705	23039	21292	13681	25914	25589	36553	62915
P25113	344010	396150	319400	164470	139370	235440	243420	32677
P97532	124730	108460	168280	180230	51816	37067	68827	66827
P0DP31	996880	870170	807830	510620	1811400	1610600	743830	152310
Q64119	51805	71523	45894	48588	129250	105230	82476	125170
P07150	39975	5895.5	4477.2	10800	31513	5155.2	2703.6	7457.8
P85970	61993	75792	16933	69994	77300	82332	67932	19822
P35738	302990	325700	422220	161930	323260	350130	385650	166670
P63086	91326	48344	20037	23420	50675	58404	53421	11839
Q9QZM5	53699	43853	53149	30380	108760	93487	90437	124710
P13832	100210	83226	79835	66102	175130	82681	124430	37845
O55096	26948	26746	16954	22033	76311	58710	66433	51320

P04177	506380	443430	545140	386730	420880	385120	500370	120850
Q9WVB								
1	319980	340540	245680	298590	144280	138420	82688	401660
Q5XII9	48490	70597	39598	101440	55941	54910	45721	32293
P24473	47673	50863	68922	86779	47297	42186	42014	10132
P35171	1834200	1848600	2127700	2500500	1849900	2205700	1997800	968490
Q9WUS0	251130	260370	275840	329420	227430	224000	125590	152290
Q64559	562470	591690	616120	556950	354420	388500	376820	168390
Q4V8B7	46171	61779	140710	12775	4734.9	78316	201.61	7368.5
Q4FZT8	59536	53901	11144	84946	40065	15146	29675	17372
P21571	138320	353510	2632.1	229710	40149	77613	56758	4686.3
Q9Z214	228750	227710	201650	209650	333520	252070	247380	183490
O88994	542260	405280	545120	588030	463120	497560	544800	304590
Q66HG9	23159	17537	36693	6116.7	13718	4641.7	45353	25943
P11730	2249.1	23052	41650	12264	2192.2	5052	5667.7	13908
O08618	60258	97229	35415	104900	41361	42122	102950	92879
Q5HZV9	115380	109260	124420	81606	118230	140380	75956	195990
B5DFN2	33914	24305	29345	50015	6282.9	9227.5	5901.9	6237
Q64591	617020	587440	597430	583800	577450	584330	554310	447860
Q9QYU2	9288.4	19873	2202.3	1531	2363.6	13864	23680	5370.8
D4A7N1	217760	221080	156230	119440	342330	342840	348640	91342
Q9QX74	1157.8	4368.3	20899	14760	5924.4	4468.3	1170.9	24169
P54690	10306	34101	53635	17131	10147	93856	55691	15562
O88767	386820	435550	505030	363840	65607	40853	31833	110050
O70511	156340	98680	89004	112730	188040	195350	253270	48443
P04041	86291	75096	77511	107250	20116	75099	74731	67483
P68403	60484	61798	7096.6	5937.6	156490	121230	131830	40293
Q05764	12424	12030	5170.1	5646.2	25426	21673	13889	11627
Q99MZ4	11673	12813	5042.1	13187	1056.3	5647.1	4523.8	2278.3
Q62636	89940	79212	101630	44430	125810	65607	124830	58379
Q52KK3	40338	670.72	90743	13549	3611.6	1599.1	737.91	0
Q505J6	812390	798690	795360	894310	1204600	1080400	1367200	696590
P12075	572600	778230	409760	237400	961720	609830	427990	316680
Q5U2R4	5685.3	15368	128560	266120	16438	18724	8760.4	32807
O35179	222400	253770	218740	8500.2	204560	168960	156840	308910

Q3B7U9	27318	16376	21841	21657	15515	12217	50578	14997
P57113	11224	11079	13007	10037	1854.2	9928.8	3957.7	36670
P32851	111750	140890	98537	72354	339930	258540	311250	25625
Q9JIR4	3053.7	18041	5719.6	3574.6	22306	17621	182.38	4025.5
Q5I0L3	12541	12784	67587	95834	4106.6	3131.9	6031.9	4588.6
Q9JHL4	12667	1738.6	2590.6	2942.4	33648	27451	28725	23680
P56603	117840	104070	47004	178890	107000	86713	124050	80380
P62963	318130	289650	362030	421360	298560	222160	163550	411180
Q6PDU7	1133700	1076400	950400	1142600	452290	728670	659840	151510
P07340	2644800	2639800	2594000	2295600	2387700	2643200	1722500	3658800
Q5RKH6	7843.8	7742.2	8282.2	13228	7772	4185.9	8638.2	10087
Q03555	53469	57960	53528	25409	58317	61312	6674.6	87593
Q4V888	55460	80674	226100	10257	62065	44689	24929	32394
P39069	1385900	270210	1366800	1108400	2415800	1707700	1243200	4472500
Q63621	26289	28963	29478	208540	151950	10524	11142	280850
Q63560	47029	48980	39772	39233	167150	139170	159980	39477
Q920F5	1603.9	1758.9	1389.5	6429.2	4437.1	1598.4	3927.9	12343
Q4QQT4	2315.9	3149.5	42150	8451.9	9712.6	1863.6	13131	26526
P11661	12962	17603	13864	3414.4	1941.9	14926	4353.6	2999.6
Q5M818	114780	94289	63440	80045	94880	116640	45931	54286
O08838	424210	404540	378760	377810	882400	726850	839220	964950
Q63633	27774	33911	17788	77999	25961	43325	51933	5389.5
O08557	37517	37736	44409	19280	58951	59165	57468	34384
P84850	135690	134460	118490	143270	59087	72420	85373	40813
P07632	246030	329410	321520	530700	569240	366960	163290	336700
P85968	1417400	35575	13907	1257200	77787	59032	37493	45125
P04906	110640	128620	120470	64548	172110	122410	103540	135020
P10818	104240	40159	90024	202140	22602	19374	7705.8	11923
P70619	78354	84924	109600	11080	129610	123160	67653	130940
P16446	48746	66561	144610	32059	118140	75425	30724	53004
O55012	330.8	4743.4	1469.8	3311.4	263.3	2726.5	3791.3	1769
Q9ESW0	15661	17053	22880	26553	22177	23394	928.27	4115.8
Q6RUV5	561920	590360	631940	606350	394780	415460	215930	394060
P12368	4430.4	3038	2698.4	95037	2478.1	374	1499.1	415.79
P37805	106660	136700	112110	103130	311020	303860	282830	102030

P40329	3381.4	8697.3	7604.9	55900	33154	6445.7	8848.4	22778
Q6PEC4	20964	21549	20298	8627.3	94535	61656	73435	63739
P62828	145350	213020	240770	250530	286020	242620	216780	304650
Q66HR2	26790	27782	16571	2981.3	62737	51819	32924	53171
Q9WU34	505640	489220	552900	466990	520930	469850	67318	1080100
Q75Q41	108820	105130	123910	64879	7663.1	6715.2	6684	12025
B5DF41	10659	9447.9	17723	34577	10820	13422	12774	69916
Q4QQV3	141530	163330	87958	147710	26245	7229.5	101200	42520
P13086	1127000	1176400	1059700	1061900	1214200	1323800	1628300	1494700
P27615	47046	65339	96109	25625	26496	16228	39132	55080
P82471	161170	162080	132020	75118	293020	261440	313120	199540
P62762	191320	186470	90222	136130	401840	288750	315110	3589.9
Q9Z272	68794	13664	10900	47214	57133	95616	115980	59271
Q62910	129080	134680	99221	63366	106990	97885	76844	20643
P32232	7603.2	6323.1	3556.1	2247.5	1535.8	1194	2171.9	16393
P35213	74906	90651	29567	22847	196420	162750	195980	172210
O08679	19166	861.05	23521	18615	12284	14256	634.08	14633
P08753	50942	62752	73322	60500	81977	81198	66356	122990
Q8VI04	52802	52720	59762	32039	75454	50308	49760	66199
P11030	51410	59873	21361	2346.8	84071	58436	5522.6	24201
P52555	48702	54658	54873	57757	35243	38623	46826	22083
Q5XI73	544010	594600	544520	449290	1258400	949250	1205600	1183600
Q6PCU2	780530	749910	577590	584230	147670	308740	252450	221110
P62076	643810	668290	672410	695120	488530	590740	616760	258960
P08009	10404	22400	3119.1	12526	28179	2206	28477	16509
Q9EPH2	2310.7	219.54	704.68	612.53	1278.3	2063.8	418.66	3138.2
P16067	102880	50633	25496	119380	11790	114710	114510	62913
P27605	104890	97723	107180	132810	4938.7	13043	25471	22904
P11275	2267400	2285600	2199100	1999600	2716400	2806500	3579500	4009800
P63012	1776400	1667100	1996800	1966200	2532300	2217900	1500300	2763500
Q566R0	191990	234310	222570	216890	112260	133150	149750	39526
P02770	265080	280700	217220	74382	289940	342770	118560	581520
B2RYT9	48748	48847	54354	104780	911.76	30701	17746	39854
Q5RK00	37308	8706.3	40789	41361	29134	21394	6767.7	21841
Q5BK26	8788	2153.3	22282	6318.1	1184.8	9679.4	2894	8464.7

D3ZW55	49647	49392	26175	27342	95602	108830	52103	109520
Q9Z0J8	88640	91645	87600	6624	88855	85997	113420	54559
Q5M7W5	41866	32032	31185	8372	6926.5	54420	46059	74503
Q63377	60204	99805	59957	103710	86016	107530	80122	123520
Q9JJ19	2355.2	37610	25152	13211	3875.4	4823.1	3821.6	2387.4
Q05683	236780	205150	208220	157460	273830	263930	280890	109000
Q6AYQ8	139700	172240	161990	202870	99451	102770	105230	44234
Q5U2U2	5631.9	9289.1	1651.1	7352.5	15565	16368	11684	4540.3
D3ZAA9	39241	5591	16182	13768	6048.1	39063	9564.4	79011
Q5EB62	14910	21846	1220.6	2897.8	1462.6	12035	7790.4	4518.2
O70257	162200	105180	66281	26957	275700	184770	259780	343050
Q5XII0	127360	127530	149890	186070	132620	139130	107660	249280
Q5XIF6	3333300	2493400	2801000	3395200	446860	344850	594580	2187100
Q5XIN7	3590	1535.2	2314	1077.9	5684.9	6551.5	2641.8	9701.2
Q5BJQ0	27688	6805.2	5083.7	7988.2	43134	4381	36184	10175
P18266	15531	12599	11772	6686.3	34193	28912	33719	2022.8
Q9Z1M9	124210	117280	165950	145620	20807	40285	22339	288910
P0DJJ3	24778	19551	3252.6	24310	48393	41195	40315	36433
P63329	1741900	1705200	1154200	1239100	1675500	1790500	1405600	1698400
Q02769	3114.2	5535	6125.6	6959.1	1817.6	3393.4	1889.1	4916.1
Q5FVI6	133850	103520	141170	104230	11152	47476	15869	11114
Q6AYG5	1395.8	4726	1382.6	152810	11883	135.9	1033.3	7823.4
P18421	2583.3	8470.8	9699.5	2865.4	11589	1566.3	16685	10261
Q99N27	28904	44074	2412.9	3808.8	48699	45432	17999	56837
Q9ES71	38547	70697	15129	34199	73507	84089	46512	8414.2
Q9Z311	23263	32731	15332	17897	5205.3	30555	2160.3	7983.1
P26453	28106	38345	51381	23215	46887	40059	65590	85708
Q566E5	10205	19628	14789	14991	8774.5	2120.4	13832	6500.3
Q68FU7	76847	53235	81020	107730	11771	8705.5	1799.2	19876
Q6Q7Y5	2251500	2163100	2648100	2145200	1092100	1082200	573520	1402600
P51146	19177	20314	10192	32785	28159	32604	25010	99584
P11348	64719	59476	11109	51847	79624	64637	95385	31991
Q66HA6	227050	231900	347090	397570	85454	59095	20006	135690
P70580	4880.2	9351.2	3964.8	8057.8	20352	2412.9	5126	22653
P53676	92736	93418	19331	44102	94353	128900	18652	18790

Q5GFD9	31392	50360	28711	35037	48373	14039	30981	26610
P97615	80146	98832	93634	110410	189760	141550	143330	158950
Q8CHM								
7	2856.8	2516.6	9960.1	29763	3778	11124	5471.4	1426.4
Q9Z2F5	290540	122040	325270	187060	519510	500920	366150	363840
P61589	601230	262590	561790	447690	259330	271660	256410	148270
P37377	1052200	1124200	1290100	1372800	1699000	1545800	1262600	829990
P19686	1534.3	18089	998.25	1797.7	8038.1	13970	468.65	2030
P05369	8170.4	32050	72086	29091	11502	7759.2	7101.6	32133
Q9Z270	344140	202850	111450	136270	157620	176010	139940	55896
B0BNM1	89898	99545	29705	27919	24424	42521	38043	21847
P07936	480310	392600	487750	332500	1486900	923850	1090000	770260
Q62658	241700	204820	171370	175950	371990	316700	301750	119170
Q6P7Q4	170240	159060	87152	189950	159160	219840	172480	15560
A8WCF8	27085	19896	57971	11737	148410	56654	161110	157430
G3V7P1	59375	66075	99549	63546	270180	219580	255000	105290
Q6MGB5	29862	31663	27942	37715	15285	17868	24714	4538.1
P22062	66657	84697	99019	120340	13368	18585	5388.5	11514
P30904	1183300	1263900	1027900	1336600	1527300	1684300	1680000	69817
Q9EPJ3	32762	64840	37615	29901	85363	82193	89250	35403
Q3B8Q0	4330.8	8639.9	10930	10424	532.12	1009.4	1499.1	6995.8
P18422	11737	7034.6	3171.7	5497	3366	4750.1	4338.9	5391.1
P84087	325660	383830	368310	352630	460770	344630	146500	432140
Q02563	163350	212880	119100	70270	324250	304470	265230	196220
P09216	15990	21863	9338.5	2145.7	35619	24048	33959	8409.5
Q62813	81763	87796	38401	7280.8	180370	139280	104660	183150
P01946	41576	113910	43224	76212	60033	33825	104900	264870
Q5FWU3	69918	59786	74875	69168	51673	5060.7	32960	49949
Q5XFX0	43962	3045.9	4544.2	7149.7	832.28	365.1	214.4	1285.6
P28075	41115	21917	32815	152020	13255	13536	11745	13987
Q8CGU4	9976	8669.2	6163.9	18707	9520.8	13979	14513	6983.3
P97697	251200	234970	220890	185220	465370	312100	252700	389060
P62243	23043	3181.4	3654.1	3979.1	1612.9	28311	1766.9	7473.2
P13668	91011	143240	20632	150480	49800	41783	52931	23323
P12711	2799.2	3810.2	15545	21115	61038	49787	58125	4564.1

Q04970	73512	103690	119630	133010	100640	75259	62264	174520
Q6RJR6	89973	111680	61235	49417	57182	74761	42726	102680
P07943	109810	134190	98227	34151	70827	66572	27095	32656
Q07647	14050	3211	19509	25936	6949	33076	6540.5	17762
Q99MZ8	189270	160720	186630	150800	326140	224620	335850	448550
P29419	2786500	2261500	2742700	2745700	2350600	2568100	1617600	3677700
Q920J4	70640	84416	70621	64109	188110	127240	18137	123560
Q00238	11533	4968.5	7357.1	4476.7	11817	14977	10839	29684
Q1WIM2	12192	16478	10386	4796.6	2122.8	26682	27194	21019
P03889	52695	46741	85051	123770	21751	32601	7165.4	8092.2
Q568Z9	83431	102410	105200	166940	155020	120730	144180	45853
P29315	9310.3	2615.2	6000.5	5182.3	62577	51864	61519	23800
Q8CFN2	59331	51296	151890	180630	26031	29116	33468	48856
Q8CGU6	24007	8288	27259	28669	28192	1876.3	28764	13151
Q00566	0	3347.4	3597.6	6609.5	1728.4	1721.7	116.37	917.28
Q4QQW4	11533	44398	64119	70487	152020	103360	73484	161090
Q9EQX9	259690	213890	316590	222980	300840	246550	116710	558590
Q5XIF3	697860	600700	601730	638690	803180	963330	1071000	113370
Q66H47	6445.9	17886	7262.6	27608	12874	1823.2	897.56	27542
P31422	12252	11905	1889	7760.6	10602	3674.3	9284.4	32158
Q9WU70	38587	12061	45798	22145	30436	30230	14358	14137
P97612	3929.8	4836.5	9976.2	143100	1364.8	584.32	4235.2	29378
P14173	122540	120680	104040	46369	113900	85014	74265	94839
P36201	46231	37399	34540	20748	94557	73986	73545	18308
Q62768	13780	5723.5	5246	11431	27094	22262	538.03	43782
B0BN94	1376.5	3036	5895.8	2449.6	15063	11662	9499.2	10522
B2RYG6	72288	69903	41025	36076	150040	105350	129400	104620
Q4FZT2	16436	48164	14400	35188	74707	78764	77796	134130
Q4QQW3	3991.7	4709.2	39593	37087	4812.3	2863.8	10202	3016.8
P36970	54732	53685	26990	10556	12297	109670	29148	176440
O35331	54886	67091	52512	40714	124260	95570	121260	42655
Q63468	60258	97229	35415	104900	41361	42122	102950	92879
Q792I0	47019	858.98	46472	178700	1341.9	3542.4	2102.4	2649.3
P0C643	1473.7	2463.8	3360.2	13745	10895	4355.6	254.07	1134.4
P61023	2676.4	2062.3	766.42	4121.1	5018.5	2202.2	4069.7	5435.6



P14668	8514.3	4432	68239	18156	13552	6507.4	392.36	11330
B2GV71	81630	75010	40470	27157	29662	12185	26358	32902
P62074	26625	31459	13522	66686	20530	25799	2294.8	27478
P31596	28122	20228	100230	104410	49572	50227	61300	36441
P01830	376840	359670	525710	579710	211390	303460	240800	71682
Q7TS56	74055	80405	76993	93061	38420	61735	25925	31846
Q4KM73	128740	155110	296180	398970	97072	75739	81037	49423
P29117	91599	50492	76841	101440	119190	10164	103440	14251
Q80W89	441980	527640	389070	308140	585910	687480	633610	681310
P18420	34052	11044	40646	26660	43435	36512	53624	31297
Q8R553	46043	39923	106530	22692	43045	41946	49939	21394
Q497B0	24573	52828	32766	115010	12680	33325	30151	220200
B4F7A1	101940	66057	89632	40176	78643	74232	85845	61896
P63322	11098	82836	48933	10839	201090	130680	165090	20395
D3ZPG5	18265	16898	6374.4	16299	29178	13028	23994	35133
P0C2C0	15644	15333	13887	40629	61649	19711	59966	62579
Q63754	903990	1011400	1170800	1422900	1058800	882750	602790	1145100
Q9WV97	79733	71505	84224	22729	136500	141310	83128	95076
P38718	98640	91384	103950	151290	59567	46695	3701.8	38041
A2RUW1	31781	36301	16490	5653.4	7277.7	2923.6	8940.3	5131.6
P37996	71147	81557	35529	81973	191250	88711	168140	79321
O35353	3320.7	12710	25915	138390	637.89	991.94	1324.7	2513.4
Q9Z1P3	23338	22792	1884.2	636.51	128.42	1607.1	7164.6	0
Q9QYU4	81329	88112	45483	126760	6769.7	6025.8	14702	13533
P97546	330950	289830	309820	243440	328320	254250	338230	247440
P63045	1866600	1629300	443720	1346500	1497800	1055300	1223400	170030
Q9WVJ4	220060	231190	269550	279230	22971	83589	62052	43306
P62882	34880	82131	48663	60470	104260	85762	96384	39932
P47709	68157	15431	39322	11816	134700	92934	124650	29648
Q9ES53	3857.6	2835.2	7346.4	198260	243.09	1443.2	1857.4	2186.5
Q641X9	9123.8	13529	7136	21548	8972.5	8877.3	7280.4	18246
Q6P799	37581	33666	52499	108690	22316	36931	33405	44375
Q6AYN4	36246	15782	30039	33250	89951	37052	20518	54553
P20156	14395	12448	8613.7	23589	61076	3204.1	48186	36850
Q8R431	21505	5293.5	5705.2	12721	1516.4	818.2	2486.2	1929.8

Q6AYR2	67547	57272	69781	67056	140460	112010	79362	172530
P62824	163490	161100	230810	51582	274520	226740	202120	201600
P34064	15653	49704	15218	33135	57306	56643	28077	118110
Q9Z173	13810	4018.1	14191	6556.1	2559.1	12199	786.97	52262
O08722	40163	11430	10927	120660	2438	7308.6	7310.4	20770
Q4KLY0	14871	96174	159740	203810	6081.5	424.81	2893.9	4581.3
Q8VID1	64756	68053	85151	66873	21546	19480	24879	27783
P19132	54439	54021	63583	59841	16110	14904	6001.2	20152
D4ACN8	381430	393050	297770	378020	359350	347780	355380	48522
P04644	841.58	805.61	2809.1	3355	839.59	3099.4	2657.2	9904
P80254	64056	71790	101520	11312	152520	115000	80976	168220
B0LT89	13979	14328	43523	19248	11519	9542.8	6516.4	6609.5
Q03114	4111.3	4047.9	9408	5433.2	932.39	12227	8190.9	3219.6
Q62718	299400	111580	113000	25747	309630	176080	215290	169580
P11232	42382	26883	52062	27477	85416	57942	53861	83174
Q4FZY0	114990	178080	137290	99295	392030	290230	261170	309030
O35764	73725	5767.3	39935	150750	3406.6	3972.5	11685	102890
Q8R491	55196	36763	37462	58536	28105	25963	8663.8	45748
Q924S1	497.64	3247.5	3547.8	6305.1	9645.2	10757	8183.5	2747
F1LP90	18758	21892	5396.4	7539.9	33863	30436	36034	6698.2
P04166	305320	293070	305670	407770	287490	328280	270960	78699
Q9EPC6	685700	640660	597810	571180	491690	481220	307350	500580
Q56A18	9106.6	17103	6557.8	7271.3	14390	1702	10823	8534.6
Q5PQL5	29283	58716	53370	46730	81524	83436	61731	28257
Q4V7F3	20511	76693	22583	38546	22467	22832	59481	24513
P0C089	63586	71753	69405	75164	50404	37765	35692	18337
Q812E9	662920	643460	766060	577820	1132300	983650	467950	964470
P28042	343220	102720	70516	82232	181130	128070	334000	126540
P60901	24609	24991	38103	47556	3355.8	12941	1817.4	7772.3
Q6NYB7	196510	254850	174340	124180	43294	51172	45762	59317
Q64122	5251.1	91474	20755	4991.5	64097	4774.9	75202	28239
O70277	24137	19749	5167	18556	37539	22180	30917	44872
P09495	37995	39356	43470	55533	45513	2838	5753.7	19050
Q8VD48	10287	7000.9	9155	21481	2226.2	6260.2	1614.9	4452.1
P62250	240160	228580	221670	235190	69993	110100	365490	744970

P62332	64436	172100	266490	376860	36449	19402	46480	130220
P42893	4289.7	1548.2	11291	9298.9	17970	2661.9	777.75	1824.2
M0RC99	108300	288510	219400	146380	337770	272470	200660	337090
P58405	16556	7610.6	9093.4	5472.1	24375	21943	22678	51894
A0MZ67	4889	4125.2	10266	16658	1248.7	2335.7	4704	5137.4
Q6IRK9	51816	128350	16461	20838	66037	66490	2420.7	9179.2
P49242	7720	7028.8	23776	33224	4372.4	4985.9	16191	10012
Q63692	14032	10993	19644	29367	64256	55218	53404	36404
Q62784	21599	30627	10289	15536	21116	1868.2	23819	100410
O35987	18382	55345	12989	10290	122140	97962	110410	44266
Q5U1X1	48378	52400	23947	124300	23571	17754	21298	12835
Q9NQR8	28026	26623	39575	60532	549.48	2183.4	5515	26905
O88775	36977	16924	17647	25055	25301	12599	15977	22925
Q63228	28792	27686	34023	9729.5	82590	54537	1113.1	1060.2
Q08851	769.92	3607.5	5053	8331.4	4103.2	1738.6	2432	50397
Q9WVA1	230850	272770	257500	285250	305360	321500	171400	116520
P36876	62220	69156	72426	70360	112670	90246	64819	138710
Q4G069	37597	55724	31920	99619	3472.2	8627.9	2414.6	20194
P61227	2666.5	1221.6	6523.3	40697	41163	10852	31273	2975.9
P00786	26239	7910.7	39105	5691.9	508.22	6621.6	4573.3	7764
Q5XIH4	26537	22829	22341	7725.6	40088	54258	46958	19463
P23978	90451	92309	87562	69111	279070	189110	190350	146850
Q7M0E7	27431	24494	4343	6072.9	17197	18121	7686.5	14491
Q920Q0	102350	86790	78562	82301	172790	80962	76971	20057
Q91ZN1	33018	35776	39686	5394.5	46244	45716	50140	49056
Q9JID2	30083	25881	31273	34059	46583	43467	58795	15717
Q5MPA9	10067	59502	68977	85504	8306.2	19258	16375	241770
Q6AY84	24100	12445	16073	40014	7961.4	6194.3	7145.8	774.23
P18265	10517	6281.2	2176.7	9910.5	30811	12814	10030	23024
P50408	168230	154630	221660	263650	194260	155980	97709	158290
Q01066	325570	317360	427870	477970	655580	705610	226430	2305000
B0BNE5	85955	26556	58804	34484	177280	125850	175440	195920
P62959	358700	358010	395090	375500	459450	420730	228450	894340
Q641Z2	9469	16719	8934.1	4319.8	12591	13751	14979	10729
P35439	18904	8502.6	29517	8857.2	47473	35564	28574	22735

Q5BJU7	54064	32169	109390	66432	50382	68479	64273	191150
D3ZYW7	59977	45233	51891	67943	73855	71794	139550	92788
Q63159	54544	53790	50841	27891	95308	80763	100480	73119
Q68FT1	2930.8	9356.5	4770.5	5500.1	17069	17201	13653	2796.3
Q91Y78	48149	3496.8	42712	11511	15718	20125	19693	26242
Q5XIQ4	5773.1	36344	49389	17804	52526	39443	33405	27258
P62138	33204	36895	43315	16279	48803	57211	53726	12928
B0BNF1	60146	40762	81775	28046	74954	115800	94331	205880
Q08415	12516	29714	21915	5778.2	16273	6259.6	23786	10641
P70605	78817	120630	9672.2	149900	29937	17606	37009	52103
Q6KC51	28873	24329	27101	645870	2305.4	1063	1577.3	19905
Q5HZE0	6744.4	23129	23653	17858	9694.3	7522.8	11754	18532
P62775	45141	37398	43787	34421	137470	76882	79569	120240
P14841	4363.8	22822	8529.8	1750	27936	28067	20161	39822
O35458	37233	33039	39957	31480	154860	69423	83202	79384
B5DFN3	48507	35685	50758	17042	48871	59020	58856	8885.7
Q62745	49521	35924	85518	82698	21201	35116	43998	63784
Q5PQJ6	19281	17774	34284	36427	58042	6668.6	37556	29266
Q80W83	159550	97048	120690	149130	25129	35820	9348.9	20035
B0BN85	10254	41227	3356.7	25952	55361	44019	49515	60285
Q5I0P2	95724	125430	102450	215170	165570	138280	132160	10841
P32736	15013	14562	1260.3	897.55	42180	34038	39243	28167
P97710	32325	21700	43663	15285	33837	32505	43803	24467
P42667	26782	12666	19443	13742	8362.4	58487	16837	5671.2
Q9WTT7	73333	2190500	95212	478380	2569500	3075900	1700100	143110
O89046	11872	119950	19540	19563	126440	5702.5	193340	86860
Q5HZY2	14751	139150	30259	140600	185490	169970	172420	79125
Q6Q0N1	77691	7193.8	86223	63159	145030	83154	121110	179600
P52303	74299	68165	81780	92015	57157	63027	5683.7	125300
P62744	398800	317800	475540	508860	108420	122010	27276	44220
P10760	111880	16496	102350	19528	59920	70392	50836	126360
Q3KRD8	38162	21684	177910	36574	859580	296860	527460	1445200
Q5HZA4	4069.3	6186.2	21146	55814	3763	390.89	837.71	8073.8
D4A6D7	61599	30105	35202	36095	52867	35169	141980	97140
Q6PDW6	25734	27479	21237	39696	7216.2	2835.8	6875.2	7951.7

Q6AXN3	10724	12525	3100.7	11821	2663.5	3062.2	4286.2	12645
P11506	22418	23410	27814	76544	850.92	20222	2854.9	3068.7
Q6DGG0	65424	130980	30188	66543	198040	166870	195090	104760
P63319	45719	51351	4622.7	10779	24573	18437	25620	13362
P20236	1180.7	711.96	7076.6	1106.2	844.16	3082	2353.9	8046.9
P13383	2613.6	1308.7	2267.4	3100.3	191.55	373.87	6793	13293
P61983	358010	418940	371740	263590	1220400	791830	494470	1035700
F1LQY6	19255	18004	7696.5	41211	7957.6	8334.5	18865	12676
P07825	6436600	6029100	8374000	9072100	3492800	4162100	2211200	4246100
P70583	42040	37530	33111	18467	46587	8439.1	53059	36534
Q7TNY6	9822.6	11014	33229	38679	173.49	212.5	4067.9	2275.2
P84817	129400	117520	247100	240350	6319.3	11364	4576.8	1411.8
P15943	9331.4	6972.4	5139.9	8534.9	6142.7	9349.8	11399	13636
O89049	22273	13968	22102	17799	3862.9	45855	4332.7	54304
P97526	4384.8	108390	57063	16400	190560	154100	86202	9432.9
P05503	48597	146250	120390	94848	24299	32193	32865	60571
Q5M9I5	269120	397320	137970	168990	230040	146250	112910	10152
O35952	61616	54693	56338	60144	20008	18505	10635	24902
Q62673	27657	31078	19627	123540	21779	15504	13292	27870
Q4KLH5	17414	15166	35038	13383	26236	22751	22669	3657.2
Q499T2	7324.5	5577.9	22572	9171.6	173.57	8734.9	10786	2721.4
P41498	1136.6	3735.4	4861.2	5398.3	22737	18798	30794	8226.5
B5DEN9	3455.6	5406.6	9307.9	9513.4	8513.2	19208	11118	879.25
Q4KLY4	11731	13968	275060	30446	36549	42056	29886	18395
Q62698	5095.9	17976	15757	31010	23648	17855	23463	58106
Q5M821	38669	37246	29868	64955	62560	54224	66125	28079
Q63564	43215	26868	70045	12807	51799	35591	82244	37892
Q9QXU9	298940	295900	276910	327860	421260	396860	395380	586830
Q4V7D2	711050	201100	821090	876440	5908.4	118670	10778	40005
P37136	21819	15911	24843	15184	46745	39340	29028	104000
A2VCX1	5282.5	1708.7	4531.7	7691.3	4682.9	3888.1	6158.6	10606
P52759	74540	61627	39662	111390	20643	39609	29561	47631
Q6IMX7	3997.7	103130	43734	18543	4773	10112	12649	56176
Q5FWY5	17371	3917.5	12606	14872	44448	33078	40448	5492.6
P52481	124910	126320	75448	14793	159760	142040	117950	75271

Q9ES40	34504	96092	97972	37973	7552.4	309.58	467.37	1625.3
A9CMA6	26618	14432	8889.2	4136.1	23767	4310.5	16171	2960.5
P14562	7389.8	16413	9761.2	12528	8812	13514	4504.7	24067
P00173	10874	8379.6	8347.3	11816	29213	29146	24604	25088
P10824	134240	122240	109630	76662	196980	184380	249950	203200
Q5U316	1102500	729350	1223400	1430800	1020700	1030700	924790	2551900
P53042	4123.6	17732	11694	12208	10106	3696.3	15188	15659
P20280	7747.1	1819.8	13948	10576	869.15	189.52	1290.1	5380.5
Q62634	265480	287850	267370	217370	621670	504740	380990	337060
Q6AY04	71097	86122	84321	90890	40843	114840	91038	32749
P24050	4203.8	3860.8	22176	13685	8789.4	18180	15164	519.73
D3ZAF6	4551500	4817900	5493000	5663300	3292000	4298000	216310	775980
O35264	97169	99490	157370	167600	7763.4	12974	24837	1595.2
Q9JKW1	147240	167990	87828	101290	185880	195130	182370	217300
P22831	307730	335580	220190	343830	627240	462540	434600	381580
Q8CHJ1	24976	14694	569570	1047400	27333	29922	15791	40615
P0DN35	358820	375820	379100	326340	303110	331220	180740	452600
P15791	284760	360710	284160	209250	5210.7	8019.6	9199.2	22768
P49088	3522.2	2177	2354.1	918.87	4469.3	1845.9	1937	12097
P97838	74423	53798	53878	136030	64852	63542	58271	60703
A4F267	21113	46099	45931	43409	63569	61810	28368	7432.8
Q6P9U8	39900	107660	82770	67094	336330	292200	286960	316150
P39052	622260	563450	493990	603740	439840	432090	346630	1017500
P01041	54562	63737	11062	10709	50468	54039	46289	73881
Q9Z0W5	265390	299050	243860	194140	603640	358450	326480	478320
P06907	16062	16156	20811	28407	22720	7408.3	11922	15767
Q5HZA9	11519	15066	36652	12080	4613.2	33209	3532.9	23292
Q5D006	14620	13676	5646.5	51204	9531	20275	2739.5	22420
P04905	2045.9	13593	9635.2	90254	104.2	7005.5	806.05	5063.1
Q9R1B1	22589	33463	16341	28967	56510	15898	42681	12787
O70593	15322	32828	29821	29092	76641	51915	26365	76717
O35964	65732	65743	50759	30999	79963	55064	62436	21110
P48768	67059	63397	46328	43893	37010	37693	20098	13713
P85108	1427900	1384200	1223600	1214800	1183100	1242400	1471500	1070800
P18088	20981	17812	23014	12827	10955	1672.1	19296	27154

A0JPM9	7976.7	11387	6455.6	6438.8	26646	21685	17322	43187
Q9JJW3	1356500	1397300	1242100	1362900	3115000	2612500	2700400	2512100
Q6MGD0	68841	74611	8028	70646	10402	4229.8	8013.5	126680
Q8VHW5	1592.3	11005	13525	7943.2	2312.8	14718	13786	5243.3
B2DD29	1228.7	1220.8	4370.8	11312	66840	61399	33909	87514
P09456	17278	17922	11447	39500	30682	31786	16640	36670
B2RZ78	20180	94761	88669	112450	24088	1884.3	52679	39196
Q5FVI3	26815	23898	23967	19619	30547	37418	38789	2590.9
P20673	26075	17198	69139	85478	10955	41120	30077	11086
P0C6S7	100730	104400	105140	105650	55494	78372	86706	5709.4
P97685	75827	69128	71965	8002.1	166880	121680	107030	167430
Q6P9T8	2197500	1980700	1845200	1336900	2205200	3285700	3554900	1130800
P83868	37855	36051	7893.7	22380	45197	49556	52857	18095
Q6AYZ1	19601	14769	84665	55228	19598	8532.6	13251	83029
Q9JJZ1	4692.9	9079.7	271480	291060	8197.2	6442.2	14525	291090
P31662	58743	60287	67875	5106.8	141290	124720	73350	158290
O35092	3732.3	2019.1	2012.4	4080.8	3508.9	997.23	1631.5	2898.6
Q9JHZ4	44572	11454	63134	29177	8552.5	11402	8200.1	9233.3
O35263	22549	28640	35864	35131	21791	4652.5	23099	20176
P68035	113670	1507500	17528	30388	3023800	2283200	2591000	35530
Q68FS3	38368	12353	56483	5068.1	62790	5621.6	10714	26432
P70500	83341	67467	64374	100930	139700	134950	124130	145510
P63041	44659	71446	89117	72193	153330	95780	91284	81364
P62914	6977.4	39327	6353.8	13170	30406	26838	32937	16576
Q9QZA6	12060	31801	23589	30383	13226	2569.6	5195.4	9598.1
Q6AXS4	7293.8	9417.4	4780.9	24427	11289	24230	80602	31241
P63259	1311100	1137600	1177100	1069100	161650	1212900	271600	52216
O35509	71461	63942	87137	52320	54034	64071	8631.8	12716
Q5PPM8	23773	23590	30213	27238	8553.1	2375.7	10418	12686
Q78P75	46600	44929	40982	21990	115050	86435	40173	5462.7
Q80WL2	167070	166010	58186	255890	61019	58990	25064	52518
B2RZD7	188320	362380	157940	59034	181730	256150	400620	129520
Q5XI72	10414	38643	6591.1	36225	44440	45949	56321	13329
P05508	223760	249220	219050	249880	278590	320370	330070	73659
P60203	184110	165340	244200	214490	105510	169380	133130	184740

P62634	40522	3878	12182	22436	10777	65033	30131	16297
P11951	267380	242420	101920	126110	394380	394000	439520	53886
Q62760	121010	114840	186080	67711	216800	196590	177820	181550
A1L108	95563	104590	109040	137710	85055	118860	142900	5785.2
Q91XV6	4360.9	4145.6	1915	2534.4	1169	3811.9	1116.4	4608.8
Q641Z7	43964	2761.8	6232.9	4954	85475	75519	82039	73798
D3ZVR7	11367	7093.5	5146	3503.9	881.47	1609	3920.9	8366.5
Q9JHW0	100730	12497	5407.9	32065	25427	29109	10670	7571.4
P69682	154840	112210	130470	124950	181160	187540	166790	155000
P29101	89323	51871	97951	82091	112450	113970	63683	191530
Q9JLU4	40220	69629	41029	16647	28953	30867	44950	18299
Q8VD52	56730	64567	16653	8909.7	125030	4201.8	101850	83056
B0BN86	12414	438570	120750	237430	241860	276860	939320	1581200
Q68FP1	1910.2	7837.9	4323.9	5181.5	11275	3080.4	3575.8	15612
P13852	53497	50454	40699	2323.9	81779	64372	43783	96116
P97829	213350	209880	281120	75998	411560	376320	5121	118020
P02688	197990	151570	237760	130410	174940	117520	163910	12710
P62839	61548	68874	83934	114230	83318	81060	17593	110410
Q1M168	20288	95196	9656.2	23901	109110	78250	78586	7767.4
O54858	19383	6675.2	25448	36188	11246	14430	60263	21828
P09759	21414	32099	29051	65295	61286	62847	12738	139170
Q6PCT3	52647	41203	52107	48727	62286	78885	43293	134320
Q7TQ16	497700	491400	1004000	1408400	14067	13710	43342	35744
P19492	716.91	60018	5253	2890.7	1858.5	1473.7	803.64	11388
Q5XIT1	1776.5	21487	44131	7281.1	48716	35754	8121.2	25909
P63081	64697	90437	76909	71061	4683.4	6114.4	2525.3	11158
D3ZAT9	22172	5465.2	9895.3	10055	5305.1	4211.4	7787.3	6546.6
A4L9P7	4847.1	117820	7051.4	244250	51345	7331.1	14221	3554.4
Q08013	4344.7	9135.5	7549.3	8386.3	5286.8	2869.1	7965.5	56813
P52504	252250	64127	329650	382380	34041	40314	38129	41146
Q9EQS0	29563	26217	39857	10065	6296.5	32753	35385	4938.6
P85007	8972.7	3792	6090.5	11485	2182.2	15609	11769	3948.8
Q69BT7	6932.8	11644	7062.1	9620.6	11018	6428.3	14995	25118
P49803	25421	40703	54068	16471	43856	45576	37877	12194
P80202	21759	19379	4215.7	43108	23501	24042	2635.2	9467.3



P63088	42691	37225	33265	16287	23852	2131.8	57948	22968
Q5XIP6	4019	11772	4723.6	4778.4	2406.6	1345.9	2948.6	7519.3
Q63941	76103	107370	112570	120860	13872	22988	28719	16903
P63025	777290	625700	592130	471320	29366	404430	552490	6327
A1EC95	1842.8	30316	55212	15029	789.67	591.23	4519.4	415.62
Q9ES39	64916	38599	3845.3	3352.2	422.05	729.14	310.05	2518.8
O09014	41610	57708	4386.5	14650	164.97	922.45	321.61	449.17
Q5XI06	165300	125940	9397.6	52636	6880.1	12281	10829	105970
D4A6D8	6989.4	10034	5448	27072	1497.1	4748.8	5271.2	11127
Q6QIX3	38790	41622	715.24	13874	32725	38702	45392	38896
Q6BBI8	26094	25062	18796	180300	9483.4	40112	3239.8	16109
Q5U2V5	20571	20263	3715.1	13089	37350	63393	77457	10537
Q6PCU8	58975	76256	53113	61766	160620	75850	51093	24235
Q63690	1736.1	7822.9	4965.1	12299	3386.7	111520	6619.7	108840
Q71UE8	72445	92475	104350	45024	83832	68707	126280	42305
Q9JJK1	148420	173720	208740	31536	130190	10309	8892.1	26306
P05505	62795	25767	21576	18027	366.6	424.31	177.24	684.39
P80432	178750	152690	17246	84966	49805	23667	45166	180660
Q10758	9604.7	25342	128020	129530	7652.5	11895	5422	332080
P08082	396610	348290	433190	486290	189590	196760	120630	364180
P43425	116250	84293	121760	134150	13625	22620	31154	3410.3
P05506	401440	398560	285410	266950	624700	608500	591470	756240
Q6P777	10856	4075.7	28962	10889	14757	18300	1836.2	19956
P0CD94	22085	30654	39437	49702	34346	42753	60343	21995
Q7M767	285300	303770	104860	101800	101430	92765	10997	7250.9
P02651	69885	79322	151180	145260	99309	106320	131880	50676
Q9EPX4	77451	73164	47857	20162	15112	69723	23598	16517
Q3B8N8	36426	29629	57150	72641	49775	51318	69708	47218
D3Z9R8	815340	634790	173720	211130	89178	115570	66357	111940
D4AC13	9502.5	7242.3	3714.3	4047.8	24516	4434	5731	6265.2
Q63279	11667	10235	31334	6774.6	50420	29606	37181	229850
Q9QYP2	38191	22647	56908	96540	4168.7	5154.6	10161	108980

**Table 2.2 The complete list of the 371 proteins identified and the quantification values for each biological replicate.**

Uniprot	Wild-type				DJ-1 KO			
Q64591	617020	587440	597430	583800	577450	584330	554310	447860
P29147	619550	653420	579550	509260	703620	896530	656750	143530
P29266	434080	416400	356370	416400	473040	459390	589180	470560
Q5XIE6	209000	147380	241250	215640	116480	269690	34174	137200
P97519	15661	16797	19444	3278.2	21160	16878	20716	41019
B2GV06	495160	357030	736860	737870	93162	280220	188760	55105
P50554	1481100	1478600	1360500	1596500	1990800	1760600	2133200	1862700
Q1M168	20288	95196	9656.2	23901	109110	78250	78586	7767.4
Q704E8	8455	1937.9	2251.3	4422.2	1489.5	3558.2	12462	10697
Q5RKI8	92931	104170	91152	69365	10794	37455	34850	22912
P16638	95241	122270	140570	75691	94939	94719	83175	119240
Q06647	6805700	6642100	7847500	8841200	4147400	5214100	5825700	1891700
P15999	32412000	30641000	28717000	26553000	18860000	20560000	38021000	36926000
P10719	17032000	29334000	31205000	28436000	15858000	29959000	30856000	16647000
P35434	330690	82838	70317	76795	160580	69314	157270	96920
P35435	2188200	2198600	2254800	2646100	1125000	1500400	1442900	857460
P19511	3213300	3141400	3901700	3571200	5118400	5230600	3059800	6152900
P29419	2786500	2261500	2742700	2745700	2350600	2568100	1617600	3677700
D3ZAF6	4551500	4817900	5493000	5663300	3292000	4298000	216310	775980
P21571	138320	353510	2632.1	229710	40149	77613	56758	4686.3
Q6PDU7	1133700	1076400	950400	1142600	452290	728670	659840	151510
P31399	1163400	1158800	1125300	1913700	703650	972120	476350	1234700
Q6PCU2	780530	749910	577590	584230	147670	308740	252450	221110
Q505J9	5991	13598	2469.2	10040	17425	17485	15259	5865.8
Q3KRE0	244520	330730	327590	199680	306500	289690	187770	285680
F1LU71	553540	544480	485520	551910	1148300	977580	803880	338550
Q8CGU4	9976	8669.2	6163.9	18707	9520.8	13979	14513	6983.3
Q63690	1736.1	7822.9	4965.1	12299	3386.7	111520	6619.7	108840
Q9Z1P3	23338	22792	1884.2	636.51	128.42	1607.1	7164.6	0
B0K020	2946300	2614800	3141100	3106900	2403000	2436600	1577900	2206600

P00406	6093500	5770200	6149700	5588000	1258800	3009300	2064500	68914
Q9WTT2	32739	15120	38293	14640	43503	41847	53838	73818
P84850	135690	134460	118490	143270	59087	72420	85373	40813
P63036	38817	46629	7860.8	44546	15652	5669.8	13755	29150
P60905	273200	317310	249640	201500	195770	217610	117090	303220
Q5XIC2	12283	11912	7284.6	6244.2	22821	16721	28958	4377.9
Q68FS3	38368	12353	56483	5068.1	62790	5621.6	10714	26432
Q3B7U9	27318	16376	21841	21657	15515	12217	50578	14997
P97576	100300	19744	103970	89941	47411	842.6	18817	10645
B4F7A1	101940	66057	89632	40176	78643	74232	85845	61896
Q1HCL7	72561	78422	23816	85937	10762	5231.3	6490.8	16913
D4AAT7	97889	87965	91857	71166	85823	89607	86846	28032
B0BNM1	89898	99545	29705	27919	24424	42521	38043	21847
Q66HF1	5023700	5087100	4909700	4930500	2798400	3397800	4176700	3612800
Q641Y2	155490	177620	227080	231170	63248	34396	66106	52652
P03889	52695	46741	85051	123770	21751	32601	7165.4	8092.2
P05506	401440	398560	285410	266950	624700	608500	591470	756240
P05508	223760	249220	219050	249880	278590	320370	330070	73659
P11661	12962	17603	13864	3414.4	1941.9	14926	4353.6	2999.6
Q9NQR8	28026	26623	39575	60532	549.48	2183.4	5515	26905
B2GV71	81630	75010	40470	27157	29662	12185	26358	32902
Q5XI79	13538	10442	14294	7400.3	24350	23380	28892	16955
P19234	3604400	4226800	3438300	3400400	3192300	3740000	4214100	305730
Q80W89	441980	527640	389070	308140	585910	687480	633610	681310
Q63362	603700	674980	627660	684920	632320	674980	660760	149730
Q5BK63	740440	652900	1051500	1121500	365360	434370	207460	259080
Q5XIF3	697860	600700	601730	638690	803180	963330	1071000	113370
P52504	252250	64127	329650	382380	34041	40314	38129	41146
Q6PCU8	58975	76256	53113	61766	160620	75850	51093	24235
Q99P39	65993	80848	49970	13349	259030	123800	379380	139620
P56558	42879	46990	4095.1	22248	51599	51871	68987	41108
Q4V7F3	20511	76693	22583	38546	22467	22832	59481	24513
Q2TA68	504860	500500	455100	263890	510930	730130	599980	232550
O88767	386820	435550	505030	363840	65607	40853	31833	110050
O35509	71461	63942	87137	52320	54034	64071	8631.8	12716

P10536	129980	131740	26893	36589	12870	11017	14319	36825
Q5U316	1102500	729350	1223400	1430800	1020700	1030700	924790	2551900
P51146	19177	20314	10192	32785	28159	32604	25010	99584
Q5U1X1	48378	52400	23947	124300	23571	17754	21298	12835
Q6AXV4	794860	836070	1000900	1093700	571480	696780	744830	650860
Q4FZT8	59536	53901	11144	84946	40065	15146	29675	17372
Q5XHZ0	722170	723480	763950	665260	1376700	1025200	1185800	464790
Q9QYU2	9288.4	19873	2202.3	1531	2363.6	13864	23680	5370.8
P85834	2148600	2286400	2484400	2527500	1742400	1849700	1709300	1176600
Q5BJU7	54064	32169	109390	66432	50382	68479	64273	191150
B5DEQ3	10215	15285	187500	30252	17367	13298	10923	7497.7
Q5I0K5	94972	90039	101620	111340	174550	155820	181350	179110
P17764	1233800	2089100	1158600	1044700	1561000	1586100	1767100	1036200
Q5XI22	181580	45822	63672	316590	48733	44388	51322	37419
P13437	304580	342040	266210	250550	305650	260410	329280	360060
Q9ER34	5837800	6147100	6175600	6553200	7289800	6689200	6635500	5502900
Q7TNY6	9822.6	11014	33229	38679	173.49	212.5	4067.9	2275.2
P15651	31337	194330	17398	546860	47772	31211	40045	25642
P08503	35985	47443	31553	37461	64918	42907	46465	25938
P15650	532380	575610	465520	457910	417920	422020	370580	485000
P70584	10993	51970	92506	7295.8	9753.5	7594.5	616.79	431.47
P45953	76884	80127	74984	36750	104880	106090	111380	20978
Q499N5	311040	328610	327290	312460	128480	191160	240200	88454
P18163	54648	13348	9469.7	2230.7	34246	48637	12321	3022.6
O35547	23685	15542	9199.8	12863	13267	25207	41740	134560
P33124	1615	14063	432.43	6750.1	730.37	1416.9	1296.6	5678.2
O55171	141490	153730	44820	111680	49007	68278	44643	45391
P84092	490080	464770	573490	500040	703090	647070	700620	873340
P29411	111240	112790	35149	62644	133290	120360	173870	28784
Q9WUS0	251130	260370	275840	329420	227430	224000	125590	152290
P12711	2799.2	3810.2	15545	21115	61038	49787	58125	4564.1
Q4QQW3	3991.7	4709.2	39593	37087	4812.3	2863.8	10202	3016.8
Q66HF8	357840	361710	340450	417450	631480	574230	552710	355950
P28037	14431	64829	34331	15639	21071	29087	62611	21557
P11884	1162100	1252700	1425800	1565900	403170	413570	530500	361250

P30839	141410	189420	110060	117660	77016	104000	79899	117860
P0C2X9	142620	215550	211300	204690	185630	155380	227340	100210
P51650	491990	541060	550100	626750	391290	505190	371890	706580
Q02253	542010	566530	632090	726230	135680	169350	220410	226290
Q64057	138100	142920	167200	88944	116730	38343	75771	16981
Q9JLJ3	36512	40139	43275	51538	73496	91930	40419	12882
P05065	639790	667120	148910	462400	124330	157990	167440	167480
P09117	234390	273910	258350	275650	361240	267990	251560	734290
P48037	6029.9	42874	33177	46331	46264	42949	14574	9548.2
Q9JM53	147680	180550	104530	29113	177360	160540	133400	120440
O08701	63655	55830	9335	9066.5	99154	90757	131960	130110
P40329	3381.4	8697.3	7604.9	55900	33154	6445.7	8848.4	22778
B1WBW4	97277	81454	90503	77838	5964.1	11357	2061	37211
P26453	28106	38345	51381	23215	46887	40059	65590	85708
P54690	10306	34101	53635	17131	10147	93856	55691	15562
P35738	302990	325700	422220	161930	323260	350130	385650	166670
P11960	67791	70364	61426	3636.2	109620	78621	115560	9489.5
P11275	2267400	2285600	2199100	1999600	2716400	2806500	3579500	4009800
Q7TS56	74055	80405	76993	93061	38420	61735	25925	31846
Q5U2V5	20571	20263	3715.1	13089	37350	63393	77457	10537
Q704S8	165040	252870	132430	195540	168990	183070	151420	162990
P18886	192170	205240	424760	134920	200590	288290	265710	135280
P24268	285340	308990	330990	348190	234730	257460	296460	6110.8
Q8VHF5	5288300	5837300	5105300	5777300	3752100	4919600	4488700	5044000
P11442	1630400	1802000	1495800	1607600	1141600	1380600	1264200	1647700
Q63159	54544	53790	50841	27891	95308	80763	100480	73119
Q4G064	1394.3	14860	9437.6	6533.3	11650	3197.5	6235	13890
Q68FU7	76847	53235	81020	107730	11771	8705.5	1799.2	19876
Q5BJQ0	27688	6805.2	5083.7	7988.2	43134	4381	36184	10175
Q6AY19	12431	12313	14198	1224.8	936.53	94.953	1752.9	631.49
Q68FT1	2930.8	9356.5	4770.5	5500.1	17069	17201	13653	2796.3
Q5PPN7	110160	117190	82548	54624	75058	85534	60911	164210
D4A7N1	217760	221080	156230	119440	342330	342840	348640	91342
O35796	195180	219610	230980	205280	249590	333790	320180	183300
P07335	2458400	2579100	1171400	821350	1541000	1518300	1329500	1286200

P25809	1265200	1140600	1000300	825380	1274400	1306400	1514300	1339000
Q9QYU4	81329	88112	45483	126760	6769.7	6025.8	14702	13533
Q5EB81	121850	147260	139230	171530	54515	54257	58309	132790
P20070	41017	52274	69546	43875	21654	27078	42823	21017
P00173	10874	8379.6	8347.3	11816	134700	92934	124650	29648
P04166	305320	293070	305670	407770	287490	328280	270960	78699
P05503	48597	146250	120390	94848	24299	32193	32865	60571
P05505	62795	25767	21576	18027	366.6	424.31	177.24	684.39
P10888	7047300	6954000	5776800	5128700	8965800	8486100	8859800	11344000
P11240	2136000	1985200	1392900	1880200	1770800	1502800	1381500	1092800
P12075	572600	778230	409760	237400	961720	609830	427990	316680
P10818	104240	40159	90024	202140	22602	19374	7705.8	11923
P11951	267380	242420	101920	126110	394380	394000	439520	53886
P80432	178750	152690	17246	84966	49805	23667	45166	180660
P35171	1834200	1848600	2127700	2500500	1849900	2205700	1997800	968490
P62898	5312700	5303200	6316500	7494300	7143100	6495500	343210	298500
Q8VID1	64756	68053	85151	66873	21546	19480	24879	27783
P70583	42040	37530	33111	18467	46587	8439.1	53059	36534
P11030	51410	59873	21361	2346.8	84071	58436	5522.6	24201
P08461	2000700	1959800	1821300	2943000	1210300	1503200	1157900	225790
Q01205	1056200	1062200	1022900	907530	1455000	1488300	697270	1418800
Q6P6R2	1347200	1381100	1104000	1145900	1352400	928530	1099000	1182600
P47942	2700400	2821400	2018700	2253900	2922000	2717700	2610000	1345700
O08557	37517	37736	44409	19280	58951	59165	57468	34384
O35303	424880	443730	252910	409260	306220	342530	349140	166460
P13803	1305100	1347600	1461700	1431200	836000	724580	944750	741980
Q68FU3	721990	769930	721820	674260	605340	565230	171090	443800
Q6UPE1	280810	226040	322610	262940	195810	167740	192740	200720
P14604	600410	675630	776190	775410	197140	368240	105730	99519
P23965	699480	683930	536810	1004600	430190	657500	679880	354430
Q5XIC0	404520	335860	299930	267170	423760	429710	389070	356950
Q62651	254890	270020	255820	118910	151290	177580	175380	163740
B0BN94	1376.5	3036	5895.8	2449.6	15063	11662	9499.2	10522
Q4QQV3	141530	163330	87958	147710	26245	7229.5	101200	42520
P05369	8170.4	32050	72086	29091	11502	7759.2	7101.6	32133

P19132	54439	54021	63583	59841	16110	14904	6001.2	20152
P84817	129400	117520	247100	240350	6319.3	11364	4576.8	1411.8
Q5XIP6	4019	11772	4723.6	4778.4	2406.6	1345.9	2948.6	7519.3
D3ZYW7	59977	45233	51891	67943	73855	71794	139550	92788
P14408	391910	413500	309870	400580	214810	294680	373190	233280
Q6AYQ8	139700	172240	161990	202870	99451	102770	105230	44234
B2RYW9	373430	454620	419740	679850	237800	276580	293690	51779
P18088	20981	17812	23014	12827	10955	1672.1	19296	27154
P10860	3566400	4964200	3338900	3793300	4426300	4729700	5072300	1579600
P09606	36961	20148	8654.1	26574	8199.2	22514	32489	18104
P13221	545790	545790	560230	473770	1032900	1006300	1140900	718020
P00507	11897000	12654000	10047000	14573000	9140600	10358000	12849000	10499000
P13264	1217000	1308000	1316300	1343900	1049600	874670	1095500	413380
P24473	47673	50863	68922	86779	47297	42186	42014	10132
P04906	110640	128620	120470	64548	172110	122410	103540	135020
P57113	11224	11079	13007	10037	1854.2	9928.8	3957.7	36670
P04041	86291	75096	77511	107250	20116	75099	74731	67483
P36970	54732	53685	26990	10556	12297	109670	29148	176440
P70619	78354	84924	109600	11080	129610	123160	67653	130940
P04797	6467500	6439700	5745100	5497100	9827700	9430800	10074000	12866000
Q63060	54214	181700	101880	152880	120340	228210	132810	39054
P35571	534540	578860	394070	253340	417920	422020	370580	485000
Q9ES71	38547	70697	15129	34199	73507	84089	46512	8414.2
P50442	20916	30372	28947	30234	24731	31983	61481	43128
Q5I0P2	95724	125430	102450	215170	165570	138280	132160	10841
P18265	10517	6281.2	2176.7	9910.5	30811	12814	10030	23024
P18266	15531	12599	11772	6686.3	34193	28912	33719	2022.8
P34058	319280	297400	171890	386810	273170	277530	419920	164600
P06761	5232.6	30389	19415	35037	69145	40887	58914	76652
P48721	3131200	3218100	2844800	2836100	3320000	3219900	3131600	3377500
P63039	5287100	5712000	6116000	6256700	3754500	3229000	3318000	2213100
P26772	9289600	9051300	8223200	9258000	7205100	6979000	6753600	7757000
P05708	1489200	1495900	1245900	1010200	1327400	1400100	1463900	911930
P56571	304550	349800	39509	22111	151990	169070	139740	21552
O35952	61616	54693	56338	60144	20008	18505	10635	24902

Q9WVK7	154380	157990	144240	124820	84049	101650	107400	103560
Q64428	589770	638580	530940	593990	709900	747620	771770	432750
Q60587	191600	162030	201360	244500	160360	177240	60770	131140
O70351	892780	990200	721590	840130	713560	893510	964010	496310
P97852	34700	63245	49810	21975	44518	21575	50343	22849
Q6MGB5	29862	31663	27942	37715	15285	17868	24714	4538.1
Q4V8B7	46171	61779	140710	12775	4734.9	78316	201.61	7368.5
Q4V8F9	65537	85051	16624	65729	385320	217920	314700	282330
Q3KR86	1377900	1457900	1370300	1290300	1754000	1618600	1797400	1235200
P56574	922720	922350	986280	1175600	359050	439580	427010	312470
P41565	1405100	1359700	1746100	2246200	1032100	1143400	1219500	1001300
Q99NA5	4161500	4423300	3764200	5006700	3401800	3518200	4121700	2765200
Q68FX0	1211800	1124200	803990	808170	1331200	1468000	309080	806550
P12007	374550	379810	358330	385900	279370	218340	187620	288740
Q08415	12516	29714	21915	5778.2	16273	6259.6	23786	10641
Q58FK9	175760	165810	174360	213830	91407	117680	30199	138910
P04642	638270	591630	710730	619220	1036400	370460	591630	697410
P42123	753840	704910	760240	786320	1398000	1150700	1218700	908290
Q68FS4	6572.1	17080	21478	16641	16965	28019	28887	20173
Q5XIN6	748470	727520	404510	489660	817340	762920	887910	586360
Q5SGE0	364140	359960	338360	339730	138230	178170	148000	98808
Q5XIH4	26537	22829	22341	7725.6	40088	54258	46958	19463
Q924S5	412510	421240	473500	452070	334610	338950	330640	85099
O88989	1126600	2875100	3014800	2195900	4718500	4209900	4541800	3585600
P04636	23751000	24041000	28258000	30648000	25110000	25653000	29853000	28749000
Q920F5	1603.9	1758.9	1389.5	6429.2	4437.1	1598.4	3927.9	12343
P97532	124730	108460	168280	180230	51816	37067	68827	66827
Q00566	0	3347.4	3597.6	6609.5	1728.4	1721.7	116.37	917.28
Q5I0C3	36085	42539	52879	11509	14509	22397	23943	25213
Q5XIT9	134960	148990	94379	35119	142670	121910	131750	10687
O88994	542260	405280	545120	588030	463120	497560	544800	304590
Q66HG9	23159	17537	36693	6116.7	13718	4641.7	45353	25943
Q4KM98	23705	23039	21292	13681	25914	25589	36553	62915
Q5XII9	48490	70597	39598	101440	55941	54910	45721	32293
Q01992	1224.6	488.7	1346.9	640.02	1475.2	1450.7	1687.6	3196.8



P38718	98640	91384	103950	151290	59567	46695	3701.8	38041
Q7M0E7	27431	24494	4343	6072.9	17197	18121	7686.5	14491
Q5M818	114780	94289	63440	80045	94880	116640	45931	54286
Q6PDW6	25734	27479	21237	39696	7216.2	2835.8	6875.2	7951.7
P0C2C0	15644	15333	13887	40629	61649	19711	59966	62579
Q66H47	6445.9	17886	7262.6	27608	12874	1823.2	897.56	27542
Q6AXT0	15007	15462	12897	6079.6	25450	5802.6	32008	14232
Q5RK00	37308	8706.3	40789	41361	29134	21394	6767.7	21841
Q641X9	9123.8	13529	7136	21548	8972.5	8877.3	7280.4	18246
Q9EPJ3	32762	64840	37615	29901	85363	82193	89250	35403
Q5I0K8	23262	49528	45139	160590	160890	60761	139680	152710
Q9Z311	23263	32731	15332	17897	5205.3	30555	2160.3	7983.1
Q8R500	78250	89324	12348	54720	31355	21768	31193	31867
P63086	91326	48344	20037	23420	50675	58404	53421	11839
P21396	1130700	1266600	1014000	1126500	1097500	1111100	1167700	369600
P19643	405560	437860	276180	139560	320410	357180	299720	319510
Q9JLT0	8683.6	7474.5	13295	46292	26545	10393	17936	19613
P42676	64947	62777	24319	45455	77324	78814	96571	113420
Q497B0	24573	52828	32766	115010	12680	33325	30151	220200
P04182	294870	262360	288280	256440	365860	339650	370330	116420
Q5XI78	459420	513340	342260	444660	114740	177360	174660	46916
Q03346	88558	92636	97256	14125	146730	130980	49340	154740
Q6DGG0	65424	130980	30188	66543	198040	166870	195090	104760
P29117	91599	50492	76841	101440	55941	54910	45721	32293
Q63716	108410	130250	150150	121840	141590	166240	120460	292340
Q9Z0V6	2775200	2605500	3417000	4336900	1724800	1855400	1302300	1766500
Q9R063	3109600	3244500	3159900	3427600	3392000	3986600	4566400	2621200
P31044	722510	711280	830850	651860	1474900	1100800	1268100	1525300
Q6AYN4	36246	15782	30039	33250	89951	37052	20518	54553
D4ACN8	381430	393050	297770	378020	359350	347780	355380	48522
Q5XIH7	1854400	1970700	1828300	1917900	1004800	1254100	204300	263620
P67779	1980500	2432700	2076600	1813800	3078400	2715600	3075700	3377400
P54001	23488	10045	5196.8	4479.9	21049	28026	48558	21304
P14882	32562	82338	54882	42250	63160	79673	82405	36514
P07633	272990	254150	162700	110590	307280	264820	139660	130960

P10960	415080	417570	331350	519810	639310	558870	311080	418790
P11598	36115	18325	54672	64681	17128	23559	17543	11733
P09216	15990	21863	9338.5	2145.7	35619	24048	33959	8409.5
P63088	42691	37225	33265	16287	23852	2131.8	57948	22968
P63329	1741900	1705200	1154200	1239100	1675500	1790500	1405600	1698400
P0C089	63586	71753	69405	75164	50404	37765	35692	18337
Q9EPX4	77451	73164	47857	20162	15112	69723	23598	16517
Q6AY23	57179	50875	74564	95536	45644	44986	16529	63216
P52873	1150800	1188000	1040900	978470	661950	956250	1211200	739440
P26284	6328200	5941600	6299700	6285800	7573800	6257400	5367200	5941600
P49432	1337200	1519400	993540	1224900	1378800	1109900	329960	576260
Q63065	61358	28321	26528	75163	37119	36759	32928	150880
Q64536	246240	274960	209700	301580	103730	99485	131680	185230
O88483	21334	2168.9	16926	46572	14078	16403	18753	5741
P11980	1786400	1633200	1678300	1449200	2956600	2145300	2461000	1055100
P11348	64719	59476	11109	51847	79624	64637	95385	31991
P61589	601230	262590	561790	447690	259330	271660	256410	148270
Q7TSA0	33778	39215	5768.6	855610	45878	5937.3	1697.5	5467.2
P52759	74540	61627	39662	111390	20643	39609	29561	47631
P63245	3348.7	5163.4	8108.6	13847	6122.6	5419.6	17538	11420
Q4G069	37597	55724	31920	99619	3472.2	8627.9	2414.6	20194
Q66H15	38120	93108	42468	50092	18214	16964	23038	26595
Q6AY30	255460	302960	304210	332770	148900	203310	191780	172330
Q6P799	37581	33666	52499	108690	22316	36931	33405	44375
Q63965	850360	878710	468830	619330	851340	690320	810790	810060
Q9JHY2	1207800	1213800	934310	610070	1171600	1464000	1337000	405360
Q8CFD0	492100	481780	434930	415790	193890	230030	214670	182020
Q6AY04	71097	86122	84321	90890	40843	114840	91038	32749
P28042	343220	102720	70516	82232	181130	128070	334000	126540
Q68FX9	92251	84506	78788	26732	149120	118500	137280	37063
P32089	494100	479080	567470	569010	525590	521010	299720	319510
P97700	2157800	1030500	725090	790540	1030500	1212300	1477000	1110100
P97521	131890	116320	247330	281770	77760	110730	115070	151830
Q5HZE0	6744.4	23129	23653	17858	9694.3	7522.8	11754	18532
P16036	3077500	3463600	3485600	3473600	1684500	1988000	1402200	1921000

Q05962	10259000	7831900	7180800	14339000	1127100	1022000	1675100	757370
Q09073	10052000	9896800	13275000	14886000	1107200	2101200	1596200	273900
Q5EB62	14910	21846	1220.6	2897.8	1462.6	12035	7790.4	4518.2
P97849	46419	70643	37318	7778.5	19431	2622.9	23678	8865.9
P48768	67059	63397	46328	43893	37010	37693	20098	13713
Q4FZT0	68361	86679	62623	71402	119790	83483	103720	34704
Q920L2	1163000	1226100	1229600	1311500	544570	653250	643850	140650
P21913	1160800	1328600	1039200	1125600	795310	1022400	834330	961530
P13086	1127000	1176400	1059700	1061900	1214200	1323800	1628300	1494700
Q07116	10604	4281.8	3029	2957.1	1743.7	971.76	1442.9	1304.8
P07632	246030	329410	321520	530700	569240	366960	163290	336700
P07895	2351000	2039800	2082900	2300000	3020100	2472900	2897700	3169800
Q9WVJ4	220060	231190	269550	279230	22971	83589	62052	43306
B5DF41	10659	9447.9	17723	34577	10820	13422	12774	69916
P61765	1842900	1783200	1526600	1611900	2074700	2108600	1915100	1136200
P37377	1052200	1124200	803990	808170	1331200	1468000	309080	806550
Q63754	903990	1011400	1170800	1422900	1058800	882750	602790	1145100
Q5U2R4	5685.3	15368	128560	266120	16438	18724	8760.4	32807
D4A6D7	61599	30105	35202	36095	52867	35169	141980	97140
Q566R0	191990	234310	222570	216890	112260	133150	149750	39526
P11232	42382	26883	52062	27477	85416	57942	53861	83174
P97615	80146	98832	93634	110410	189760	141550	143330	158950
O89049	22273	13968	22102	17799	3862.9	45855	4332.7	54304
Q920J4	70640	84416	70621	64109	188110	224770	206260	72062
P24329	1529700	1499200	1336500	1282200	2004300	1849600	2467200	1458700
Q68FW7	25087	29623	28445	28832	25769	28685	2252	32627
Q91ZW1	36399	33163	27976	107810	89647	79706	88390	54218
B2RYT9	48748	48847	54354	104780	911.76	30701	17746	39854
P62074	26625	31459	13522	66686	20530	25799	2294.8	27478
Q9R1B1	22589	33463	16341	28967	56510	15898	42681	12787
P62076	643810	668290	672410	695120	488530	590740	616760	258960
O35092	3732.3	2019.1	2012.4	4080.8	3508.9	997.23	1631.5	2898.6
Q5U2X7	96176	95603	84282	115930	132920	119600	85901	127330
Q9JKW1	147240	167990	87828	101290	185880	195130	182370	217300
O35094	296900	244370	317410	319740	41274	149710	117930	216450

Q9WVA1	230850	272770	257500	285250	305360	321500	171400	116520
Q9WV97	79733	71505	84224	22729	136500	141310	83128	95076
Q62760	121010	114840	186080	67711	216800	196590	177820	181550
Q75Q41	108820	105130	123910	64879	7663.1	6715.2	6684	12025
A4F267	21113	46099	45931	43409	63569	61810	28368	7432.8
Q75Q40	203630	169640	161680	151330	252250	218580	222750	78845
Q75Q39	1408000	1167200	1589100	1904700	1179300	1461800	850360	1412700
B0BN86	12414	438570	120750	237430	241860	276860	939320	1581200
Q5HZA9	11519	15066	36652	12080	4613.2	33209	3532.9	23292
Q91ZW6	50925	180370	67580	66869	101590	165660	66034	82478
P62260	491680	258600	334080	260620	1104000	782630	960540	508740
P63102	1854100	1630900	2075000	1761100	1946400	1781800	881320	2937700
P04177	506380	443430	545140	386730	420880	385120	500370	120850
Q5I0L3	12541	12784	67587	95834	4106.6	3131.9	6031.9	4588.6
P32551	2841000	2874200	2916300	2942500	2549200	3175700	3257900	2819800
B5DFN3	48507	35685	50758	17042	48871	59020	58856	8885.7
Q68FY0	3258500	3299200	3594900	3358000	2630600	2568800	3146800	156700
Q5M9I5	269120	397320	137970	168990	230040	146250	112910	10152
P20788	1246900	1074100	1349800	1393400	893610	978180	724620	1070200
Q7TQ16	497700	491400	1004000	1408400	14067	13710	43342	35744
D3ZPG5	18265	16898	6374.4	16299	29178	13028	23994	35133
Q5U300	142600	156030	63612	69327	164760	125820	143430	122520
Q9JJW3	1356500	1397300	1242100	1362900	3115000	2612500	2700400	2512100
Q9Z2L0	11975000	12148000	7986000	14963000	6973600	8399500	8655500	6877100
P81155	4532800	4551900	5114200	6332800	3927500	4466700	4462200	4692600
Q9R1Z0	1840800	2095200	1003200	1399800	1916000	2303200	2266800	1634700

**Table 2.3. Differentially expressed proteins in striatal mitochondria of DJ-1 KO rats.**

Uniprot	Name	Symbol	Mean1 (WT)	Mean2 (DJ-1 KO)	Difference	SE of difference
	family with sequence similarity 136,					
B0BN94	member A	Fam136a	3189	11687	-8497	1547
B1WBW4	armadillo repeat containing 10	Armc10	86768	14148	72620	9061
B2GV06	3-oxoacid CoA transferase 1	Oxct1	581730	154312	427418	106868
O08701	arginase 2	Arg2	34472	112995	-78524	18083
	translocase of inner mitochondrial					
O35094	membrane 44	Timm44	294605	131341	163264	40367
O35952	hydroxyacyl glutathione hydrolase	Hagh	58198	18513	39685	3371
O88767	Parkinsonism associated deglycase	Park7	422810	62086	360724	35794
	230310					
O88989	malate dehydrogenase 1	Mdh1	0	4263950	-1960850	498016
P00173	cytochrome b5 type A	Cyb5a	9854	95483	-85629	23697
	590035					
P00406	COXII	COX2	0	1600379	4299972	637476
	glyceraldehyde-3-phosphate					
	603735					
P04797	dehydrogenase	Gapdh	0	10549625	-4512275	821023
P05506	NADH dehydrogenase subunit 3	ND3	338090	645228	-307138	52034
P06761	heat shock protein family A member 5	Hspa5	22518	61400	-38881	10193
	219342					
P07895	superoxide dismutase 2, mitochondrial	Sod2	5	2890125	-696700	168634
	protein tyrosine phosphatase, mitochondrial					
P0C089	1	Ptpmt1	69977	35550	34428	7030
	622670					
P10888	cytochrome c oxidase subunit 4i1	Cox4i1	0	9413925	-3187225	801264
	aldehyde dehydrogenase 2 family					
	135162					
P11884	(mitochondrial)	Aldh2	5	427123	924503	96999
P12007	isovaleryl-CoA dehydrogenase	Ivd	374648	243518	131130	25014
P13221	glutamic-oxaloacetic transaminase 1	Got1	531395	974530	-443135	92403
	138640					
P13803	electron transfer flavoprotein alpha subunit	Etfa	0	811828	574573	62273

	enoyl CoA hydratase, short chain,					
P14604	1,mitochondrial	Echs1	706910	192657	514253	75770
			337507			
P16036	solute carrier family 25 member 3	Slc25a3	5	1748925	1626150	165692
P19132	ferritin heavy chain 1	Fth1	57971	14292	43679	3762
			895552			
P26772	heat shock protein family E member 1	Hspe1	5	7173675	1781850	329670
P31044	phosphatidylethanolamine binding protein 1	Pebp1	729125	1342275	-613150	104714
	ATP synthase, H+ transporting,					
	mitochondrial F1 complex, gamma		232192			
P35435	polypeptide 1	Atp5c1	5	1231440	1090485	185052
P38718	mitochondrial pyruvate carrier 2	Mpc2	111316	37001	74315	18081
P42123	lactate dehydrogenase B	Ldhb	751328	1168923	-417595	102746
			147917			
P50554	4-aminobutyrate aminotransferase	Abat	5	1936825	-457650	93932
	isocitrate dehydrogenase (NADP(+)) 2,		100173			
P56574	mitochondrial	Idh2	8	384528	617210	66889
	tyrosine 3-monooxygenase/tryptophan 5-					
P62260	monooxygenase activation protein, epsilon	Ywhae	336245	838978	-502733	139391
			584295			
P63039	heat shock protein family D member 1	Hspd1	0	3128650	2714300	392397
			207590			
P67779	prohibitin	Phb	0	3061775	-985875	188200
	adaptor-related protein complex 2, mu 1					
P84092	subunit	Ap2m1	507095	731030	-223935	54426
P84817	fission, mitochondrial 1	Fis1	183593	5918	177675	34891
P84850	D-2-hydroxyglutarate dehydrogenase	D2hgdh	132978	64423	68554	10856
	Tu translation elongation factor,		236172			
P85834	mitochondrial	Tufm	5	1619500	742225	174630
P97532	mercaptopyruvate sulfurtransferase	Mpst	145425	56134	89291	18677
P97615	thioredoxin 2	Txn2	95756	158398	-62642	12804
	aldehyde dehydrogenase 6 family, member					
Q02253	A1	Aldh6a1	616715	187933	428783	46486
			990267			
Q05962	solute carrier family 25 member 4	Slc25a4	5	1145393	8757283	1631752
			120274			
Q09073	solute carrier family 25 member 5	Slc25a5	50	1269625	10757825	1290535

Q1HCL7	NAD kinase 2, mitochondrial	Nadk2	65184	9849	55335	14303
Q499N5	acyl-CoA synthetase family member 2	Acsf2	319850	162074	157777	33865
Q4V8F9	hydroxysteroid dehydrogenase like 2	Hsd12	58235	300068	-241832	37755
Q566R0	thioesterase superfamily member 4	Them4	216440	108672	107769	25877
	NADH:ubiquinone oxidoreductase subunit					
Q5BK63	A9	Ndufa9	891585	316568	575018	125737
Q5I0K5	abhydrolase domain containing 10	Abhd10	99493	172708	-73215	7410
	ATP binding cassette subfamily B member					
Q5RKI8	8	Abcb8	89405	26503	62902	9506
	leucine-rich pentatricopeptide repeat					
Q5SGE0	containing	Lrpprc	350548	140802	209746	17695
Q5XI78	oxoglutarate dehydrogenase	Ogdh	439920	128419	311501	47165
	NADH:ubiquinone oxidoreductase complex					
Q5XI79	assembly factor 7	Ndufaf7	11419	23394	-11976	2922
			189282			
Q5XIH7	prohibitin 2	Phb2	5	681705	1211120	265686
Q63159	coenzyme Q3 methyltransferase	Coq3	46767	87418	-40651	8964
	NADH dehydrogenase (ubiquinone) Fe-S					
Q641Y2	protein 2	Ndufs2	197840	54101	143740	19972
Q64536	pyruvate dehydrogenase kinase 2	Pdk2	258120	130031	128089	27887
	NADH dehydrogenase (ubiquinone) Fe-S		498775			
Q66HF1	protein 1	Ndufs1	0	3496425	1491325	287781
Q68FU7	coenzyme Q6 monooxygenase	Coq6	79708	10538	69170	11777
Q6AY30	saccharopine dehydrogenase (putative)	Sccpdh	298850	179080	119770	19966
	fumarylacetoacetate hydrolase domain					
Q6AYQ8	containing 1	Fahd1	169200	87921	81279	19636
Q6PCU2	ATPase H+ transporting V1 subunit E1	Atp6v1e1	673065	232493	440573	63244
	ATP synthase, H+ transporting,		107577			
Q6PDU7	mitochondrial Fo complex, subunit G	Atp5l	5	498078	577698	136957
Q6PDW6	mitochondrial ribosomal protein L17	Mrpl17	28537	6220	22317	4110
	electron transfer flavoprotein					
Q6UPE1	dehydrogenase	Etfdh	273100	189253	83848	21366
	translocase of outer mitochondrial					
Q75Q41	membrane 22	Tomm22	100685	8272	92413	12672
	ubiquinol-cytochrome c reductase, complex					
Q7TQ16	III subunit VII	Uqcrc	850375	26716	823659	221533
Q7TS56	carbonyl reductase 4	Cbr4	81129	39482	41647	8890

	NADH:ubiquinone oxidoreductase subunit					
Q80W89	A11	Ndufa11	416708	647078	-230370	51819
Q8CFD0	sideroflexin 5	Sfxn5	456150	205153	250998	21213
Q8VID1	dehydrogenase/reductase 4	Dhrs4	71208	23422	47786	5041
	succinate dehydrogenase complex		123255			
Q920L2	flavoprotein subunit A	Sdha	0	495580	736970	124613
	up-regulated during skeletal muscle growth		133970			
Q9JJW3	5 homolog (mouse)	mouse	0	2735000	-1395300	136611
Q9QYU4	crystallin, mu	Usmg5	85421	10258	75163	16804
Q9WVJ4	synaptojanin 2 binding protein	Synj2bp	250008	52980	197028	19365
Q9WVK7	hydroxyacyl-CoA dehydrogenase	Hadh	145358	99165	46193	9064
			328365			
Q9Z0V6	peroxiredoxin 3	Prdx3	0	1662250	1621400	411013



# Chapter 3

Neurodegeneration in PINK1/Parkin double  
knockout rats

### 3.1 Abstract

Introduction: Animals are important tools to study pathological and behavioral abnormalities and to test therapeutics in Parkinson's disease (PD), which is characterized by loss of dopaminergic neurons in the substantia nigra (SN).

Mutation in PTEN-induced putative kinase 1 (PINK1) and Parkin, autosomal recessive mutations found in human PD, did not affect dopaminergic neurons in the SN in mice. In rats, mutation in PINK1 displayed progressive neurodegeneration but mutation in Parkin did not. For a better understanding of genetic PD, we generated a PINK1/Parkin double-knockout (DKO) rat model.

Hypothesis: Given the roles of PINK1 and Parkin in mitochondrial bioenergetics and integrity, we hypothesized that DKO rats would have mitochondrial dysfunction leading to a loss in dopaminergic neurons in the SN causing motor deficits.

Methods: Immunohistochemistry for stereological counting and behavioral assessments of motor coordination, bradykinesia/agility, hind-limb strength, and gait were performed for WT and DKO rats.

Results: DKO at 6 and 8 months showed 23% and 45% reductions, respectively, in dopaminergic neurons in the SN, compared to control wild-type rats. A reduction in the number of neurons was found in the ventral tegmental area of DKO at 8 months. Motor coordination assessed by rotarod showed a reduction in the latency to fall in both 6- and 8-month-old rats. Bradykinesia and agility were tested by pole test that showed an increase in the time the rat required to turn and to walk down the pole at 6- and 9-month old rats. Cylinder test showed a

significant reduction in hind-limb strength when rearing frequency was measured at both 6 and 8 months. Finally, gait abnormalities were also present at 8 months, including reduction in hind-limb step length, reduction in fore- and hind-limb step pressure, and an increase in step angle.

Conclusion: PP-DKO is a novel genetic model with reproducible neuropathology and motor abnormalities of PD that may provide new insights into the mechanisms by which these genes produce PD and a novel model for testing preventative and potential therapeutic paradigms.

### 3.2 Introduction

Parkinson's disease (PD) is a neurodegenerative disorder that affects 1-3% of the population over 60 years of age worldwide [12]. The etiology of the disease is not well understood. There are two forms of PD: sporadic, with likely multiple gene-environmental causative factors; and familial, genetically inherited in either an autosomal recessive or dominant fashion. The majority of PD cases occur in a sporadic manner, with only ~10 % of all PD cases being familial, many with identified genetic mutations [230]. Pathologically, PD is characterized by the loss of dopaminergic neurons in the substantia nigra pars compacta (SNpc) and the presence of eosinophilic inclusions known as Lewy bodies containing alpha-synuclein and ubiquitin. This loss in dopaminergic neurons leads to a reduction in the release of dopamine; as an outcome, symptoms of PD become apparent [14, 264].

Overwhelming evidence indicates that mitochondrial dysfunction plays a critical role in the pathology of PD. The neurotoxin methyl-4-phenyl-1,2,3,6-tetrahydropyridine (MPTP) was found to induce PD in humans, and experiments revealed that it can induce Parkinson's-like symptoms in mice by inhibiting mitochondrial complex I. Another neurotoxin, 6-hydroxydopamine (6-OHDA), which inhibits mitochondrial complex I and IV, also results in PD-like symptoms in rats [22, 265]. Numerous studies in human PD have revealed mitochondrial deficits associated with disease [266]. Furthermore, investigation of familial PD has revealed additional linkage to mitochondria. Two autosomal recessive causes of PD, mutations in *PARK6* (which encodes PTEN-induced

putative kinase 1, PINK1) and PARK2 (which encodes PARKIN) have been found to act together in the mitochondrial quality control pathway of mitophagy, which acts to clear damaged mitochondria. Once there is damage to the mitochondria, PINK1 accumulates on the outer membrane of mitochondria, where it recruits and activates Parkin, resulting in auto-ubiquitination of Parkin and ubiquitination of Parkin targets on the outer membrane of the mitochondria. Eventually, this leads to recruitment of autophagosomes to clear defective mitochondria [267]. Animal models are important tools to further our understanding of the pathology of disease in order to discover new therapeutic targets. In *Drosophila*, PINK1 mutant flies show a reduction in life span and degeneration of muscles and dopaminergic neurons [268, 269]. Loss of function mutations of Parkin in *Drosophila* led to a defect in their ability to fly and to climb. These behavioral defects were driven by cell death of muscle subsets and dopaminergic neuronal degradation [137, 138]. In contrast, knockout mouse models of PINK1 or Parkin, or the combined double mutant, surprisingly, did not show dopaminergic neuronal loss in the SNpc or other neuropathological signs of PD [152, 270, 271]. Behavioral studies in single and combined KOs revealed findings ranging from mild abnormalities to normal, and neurochemical analysis of dopamine and its metabolites were indistinguishable from wild-type mice [141, 153, 272]. Importantly, PINK1 knockout (KO) rats were found to exhibit motor abnormalities starting at 4 months, including reduction in total distance traveled and rearing frequency, grip strength reduction in the hind-limbs, and an increase in the number of foot slips while walking on a balance beam. In addition, PINK1

KO rats exhibited 50% reduction in SNpc dopaminergic neurons at 8 months [142]. Unlike PINK1 KO rats, Parkin KO rats did not exhibit behavioral, neurochemical or pathological abnormalities [142].

Functional healthy mitochondria are critical for the release of neurotransmitter from the synaptic nerve terminal [273]. Nevertheless, synaptic mitochondria isolated from 3-month-old PINK1-deficient rats exhibited a reduction in complex I-driven respiration and an increase in complex II-mediated respiration [155]. In contrast, synaptic mitochondria isolated from the same age in Parkin KO rats did not display alteration of either respiration or electron transport chain function [143].

We hypothesized that since PINK1 and Parkin act in the same mitophagy pathway, a combined knockout of PINK1 and Parkin (PINK1/Parkin double-knockout, DKO) would provide a more robust and reproducible model of PD. Indeed, the data here with this DKO rat model show a progressive loss of dopaminergic neurons, with significant loss starting at 6 months of age, significant loss of neurons in the ventral tegmental area (VTA) at 8 months of age, and motor abnormalities at both 6 and 8 months. Further studies of this model should help in providing preventative and potential therapeutic paradigms to treat PD.

### 3.3 MATERIALS AND METHODS

#### 3.3.1 Generation of DKO rats

The generation and characterization of PINK1 and Parkin single KO rats has been described previously [142]. The PINK1 and Parkin single KO rats were obtained from SAGE Labs (City State Country). DKO rats were generated by crossing PINK1<sup>-/-</sup> rats with Parkin<sup>-/-</sup> rats to obtain PINK1<sup>+/-</sup>; Parkin<sup>+/-</sup> rats, which were interbred to obtain PINK1<sup>-/-</sup>; Parkin<sup>-/-</sup> rats. To confirm the deletion of 26 bp in PINK1, genotyping was performed using 5'-CCCTGGCTGACTATCCTGAC-3' forward and 5'-CCACCACCCACTACCACTTACT-3' reverse primers. Deletion of 5 bp in Parkin was tested after DNA was amplified using a forward 5'-GGTGTCTTGGCTCAGTGTGA-3' and reverse 5'-GCCACCCAGAATAGCATCTC-3'. Polymerase Chain Reaction (PCR) was amplified and sent to ACGT Inc (Wheeling, IL) for sequencing (Figure 3.1). All rats were on the Long Evans Hooded (LEH) background. Only male rats were utilized in these experiments. Rats were kept in a temperature-controlled environment with a 12-hour light/dark cycle and free access to rat chow and water. All experimental procedures were approved by the University of Nebraska Medical Center Institutional Animal Care and Use Committee (IACUC).

#### 3.3.2 Weight

All rats were weighed at 3, 6 and 8 months of age.

### 3.3.3 Brain collection for stereology

Brains were rapidly collected following sacrifice and fixed in Formal Fixx (Thermo Scientific, Rockford, IL) overnight at 4° C. The next day, brains were immersed in 30% sucrose solution in 0.1 M phosphate-buffered saline (PBS) for 48 hours at 4° C. Then, each brain was dipped in 2-methylbutane for snap freezing and stored at -80° C.

### 3.3.4 Stereology tissue processing

Cryostat serial sections (50 µm) were collected in 48-well plates containing 0.1 M phosphate buffer at pH 7.4. Plates were stored at 4° C. Immunostaining of sections was done by collecting every 8<sup>th</sup> section. Sections were washed in 0.1 M PBS three times for 10 min each wash.. Sections were then incubated in 3% hydrogen peroxide for 30 minutes to eliminate endogenous peroxidase. This was followed by incubation in blocking buffer containing 10% normal goat serum (NGS) (Vector Laboratories, S-1000) and 0.3% Triton X-100 in PBS for 2 hours at room temperature. Next, sections were incubated with mouse monoclonal primary antibody against tyrosine hydroxylase (TH) (anti-TH, 1:2000; EMD/Millipore, MAB318) in PBS containing 3% NGS and 0.3% Triton X-100, overnight in 4° C on a rocker. After incubation in primary antibody, sections were washed three times in PBS solution followed by incubation with goat anti-mouse IgG secondary antibody / HRP polymer (ImmPRESS, Vector Laboratories, MP-7452) for 2 hours followed by three PBS rinses. Finally, ImmPACT DAB peroxidase (ImmPACT, Vector Laboratories, SK-4105) was used



to develop a dark brown color. After mounting sections on slides, sections were counterstained with Nissl.

### 3.3.5 Stereology

Stereology was performed to quantify the number of TH<sup>+</sup> neurons in the SN and the VTA using Stereo Investigator software with the optical fractionator module (MBF Bioscience) (Figure 3.9). First, the anatomic area of interest was outlined at low magnification (4x), which was divided into small counting frames of 120  $\mu$ m x 100  $\mu$ m. Next, TH<sup>+</sup> neurons were marked in every section. Finally, after counting all images, the software calculated the total number of neurons and the coefficient of error (CE). Counting with CE<0.2 was accepted as valid quantification.

### 3.3.6 Nerve terminal isolation

Rats were euthanized with isoflurane and decapitated to remove the striata. Then, nerve terminals were isolated using a previously described method [274]. Briefly, the striatum was rapidly removed and homogenized with a pre-chilled Dounce homogenizer containing 320 mM sucrose, 1 mM EDTA, 0.25 mM dithiothreitol, pH 7.4. Tissue was then homogenized using 10 strokes in a Dounce homogenizer. The homogenate was then centrifuged at 1000 x g for 10 minutes. The supernatant was layered on the top of a Percoll gradient of 3, 10, and 30% followed by centrifugation at 31,000 x g for 10 minutes. Then, the band between 10% and 23% that contains the nerve terminals was collected. This nerve terminal suspension was then diluted with medium containing 20 mM HEPES, 10 mM D-glucose, 1.2 mM Na<sub>2</sub>HPO<sub>4</sub>, 1 mM MgCl<sub>2</sub>, 5 mM NaHCO<sub>3</sub>, 5

mM KCl, 140 mM NaCl, pH 7.4, followed by centrifugation at 15,000 x g for 15 minutes. Finally, the nerve terminal pellet was suspended in 3.5 mM KCl, 120 mM NaCl, 1.3 mM CaCl<sub>2</sub>, 0.4 mM KH<sub>2</sub>PO<sub>4</sub>, 1.2 mM Na<sub>2</sub>SO<sub>4</sub>, 2 mM MgSO<sub>4</sub>, 15 mM D-glucose, pH 7.4, and the protein concentration was measured using Pierce BCA Protein Assay.

### 3.3.7 Mitochondrial Respiration

Oxygen consumption rate (OCR) and extracellular acidification rate (ECAR) were used to monitor mitochondrial respiration within the nerve terminals using microplate respirometry as described previously [274, 275]. Briefly, 15 µg protein/well of nerve preparation was placed in a poly-D-lysine-coated 96-well cell culture microplate (Seahorse XF<sup>e</sup>96 Analyzer; Agilent Technologies, Santa Clara, CA) and attached to the plate by centrifugation. Assay buffer contained 3.5 mM KCl, 120 mM NaCl, 1.3 mM CaCl<sub>2</sub>, 0.4 mM KH<sub>2</sub>PO<sub>4</sub>, 1.2 mM Na<sub>2</sub>SO<sub>4</sub>, 2 mM MgSO<sub>4</sub>, 15 mM D-glucose, 10 mM pyruvate, and 4 mg/ml fatty acid-free bovine serum albumin, pH 7.4. The microplate was then incubated for 2 hours at 37°C followed by sequential addition of drugs to measure different mitochondrial respiration parameters. Drugs were 5 µM oligomycin (complex V inhibitor), 4 µM carbonyl cyanide 4-(trifluoromethoxy) phenylhydrazone (FCCP) (uncoupler of oxidative phosphorylation), 2 µM rotenone (complex I inhibitor) in combination with 2 µM antimycin A (AA; complex III inhibitor). The respiration parameters measured were basal respiration (the average of the first three measurements prior to the injection of oligomycin), ATP production (the difference between the average of the basal respiration and the average of the three measurements

after the injection of oligomycin), maximal respiration (the average of three measurements after the injection of FCCP), spare respiratory capacity (the difference between maximal respiration and basal respiration), non-mitochondrial respiration (the difference between the average of three measurements ?? before and after rotenone/antimycin), and proton leak (the difference between non-mitochondrial respiration and the average of three measurements after the injection of antimycin A).

The rates of O<sub>2</sub> consumption for each well were normalized to protein concentration that was determined by Pierce BCA Protein Assay (Thermo Fisher Scientific, Rochester, NY). Respiration data analyses are presented as the means  $\pm$  SEM of 2 to 3 experiments with nerve terminal preparations from 6 to 9 rats (n = 3 technical replicates, containing 2 technical replicates).

### 3.3.8 Cylinder Test

This test was used to assess asymmetry of forelimb function by measuring the number of touches and the hind-limb strength by measuring rearing frequency. In brief, rats were placed in a transparent cylinder with a mirror at a 45° angle placed below the cylinder. Rats were placed in the cylinder for 3 minutes, and activity was recorded using a Sony video camera. The cylinder was cleaned with 70% ethanol between animals. Recordings were analyzed blindly with respect to animal genotype.

### 3.3.9 Gait

A method was developed by our group to measure gait in rats based on equipment and a technique developed for mice by a group at Columbia University [276]. The equipment is composed of three parts: background light, the walking floor and mirror, and a video camera. Detailed description of the machine and different parts can be found in the supplement (Figure 3.10 to Figure 3.13).

For experiments, rats were transferred individually to a new cage. This home cage was placed at the end of the walker so the rats could walk freely on the walking floor toward their home cage without turning. Rat gait was captured from a mirror at a 45° angle beneath the walking floor using GoPro Hero6 (camera? Software?) that was set to record 120 frames/second. Videos were then converted into a series of images and uploaded to the MouseWalker software written in MATLAB [276]. The software was able to measure different parameters of the gait, including step length, angle, and step pressure.

### 3.3.10 Pole test

Pole test has been used to assess basal ganglia-related motor movement deficits in rodents [277]. In this test the pole was wrapped with Grip non-adhesive shelf liner to provide grip so the rats would not slide down the pole. All rats received one day of training at the age of 2 months, which consisted of five trials with 30 minutes between trials. During training, rats were placed at the middle of the pole and then the top of the pole. After each animal, the pole was wiped with

70% ethanol. On the test day, the animals received 5 trials, and time to orient downward ( $T_{\text{Turn}}$ ) and time to descend ( $T_{\text{Des}}$ ) were measured with a maximum time of 60 seconds to perform each task. Scoring started when the animal initiated the turning movement. The time to make a complete 180° turn ( $T_{\text{turn}}$ ) and latency to reach the ground ( $T_{\text{Des}}$ ) were recorded. If the animal did not turn but instead descended with a lateral body position, then  $T_{\text{Des}}$  was attributed to  $T_{\text{turn}}$ . When an animal made a turn, descended part-way and fell, 30 seconds was added to the time at which the fall occurred. However, if the rat fell down the pole immediately, the maximum duration was recorded for both  $T_{\text{Des}}$  and  $T_{\text{turn}}$ .

#### 3.3.11 Accelerating Rotarod

Rotarod was used to assess motor coordination and balance alterations. An accelerated rotarod (Accurotor Rotarod, AccuScan Instruments, Inc., Columbus, OH) was set to increase at a constant acceleration rate from 0 to 40 rpm over a period of 60 seconds. On the day of the experiment, rats were placed on the treadmill facing opposite the direction of the rotation and the latency to fall was recorded. The treadmill was wiped with 70% ethanol after each animal. Each animal was given 3 trials with 30 minutes between experiments and the mean was used for comparison.

### 3.3.12 Statistical analysis

All values are expressed as means  $\pm$  SEM. The difference between groups was analyzed using unpaired t test with Welch's correction (GraphPad Software 8).

## 3.4 RESULTS

### 3.4.1 Behavioral characteristics of DKO rats

Since motor behavior could be influenced by body weight, we first assessed the weight of WT and DKO rats. A significant increase in DKO body weights was found at all three ages tested -- , by 30%, 20%, and 24% in DKO compared to WT in 3, 6, and 8 month-old rats, respectively (Figure 3.2).

To investigate whether the loss of Pink1 and Parkin in DKO rats affected the motor behavior, behavioral characterization was performed at 3, 6 and 8 months of age. Two groups of rats ( $n = 9/\text{age/genotype}$ ) were tested in both cylinder and gait tests. The cylinder test measured hind-limb strength as well as the symmetry of wall touching. Briefly, animals were placed in a cylinder for 3 minutes and the rearing frequency and the number of wall-touching by right or left paw were counted. At 3 months of age there was no change in the rearing frequency between WT and DKO rats. However at 6 months of age, rearing in DKO rats was significantly reduced compared to WT. The mean ( $\pm$  SEM) of DKO rears was  $6.78 \pm 7.10$  compared to  $18.44 \pm 6.24$  in WT; the DKO reared only 37% as much as WT (Figure 3.3). This deficit in the rearing frequency persisted

in 8-month-old DKO rats, with a mean of  $8.42 \pm 2.64$  compared to  $15.92 \pm 3.29$  in WT; the DKO reared only 53% as much as WT.

In asymmetry tests in 3, 6, and 8 months old rats, right paw touches did not show any significant difference in the number of wall touches executed by DKO and WT rats. On the other hand, while no difference was detected at 3 or 6 months of age, the number of left paw touches was significantly less in DKO compared to WT in 8 month old rats (DKO  $15.5 \pm 13.93$ , WT  $32.0 \pm 19.03$ ), with DKO left paw touching only 47% of that for WT.

Gait in rats was assessed at 3, 6, and 8 months of age. Young DKO rats at the age of 3 months did not exhibit abnormality in their step length or step angle of either fore- or hind-limb (Figure 3.4). However, DKO exhibited an increase in their hind-limb step pressure ( $622 \pm 72$ ) compared to WT ( $488 \pm 136$ ), while fore-limb showed normal step pressure. Complicating gait analysis was that at 6 months of age, the DKO rats manifested relative loss of control of their hind limbs and decreased overall muscle control as reported previous for the single PINK1 KO rats [142], but here affecting 100% of DKO rats. The duration of this impairment varies, with some rats recovering after a week whereas other rats taking up to one month. Still, gait analysis of 3- and 6-month old rats did not show any abnormality in the step length, pressure or angle. Finally, at 8 months of age, DKO rats exhibited abnormal gait in both their fore- as well as hind-limbs. Fore-limb analysis showed a normal step length but showed an increase in the step angle that was wider and towards the outside ( $91.6 \pm 3.3$ ) compared to WT ( $89.4 \pm 3.5$ ). Also, fore-limbs of DKO were not able to exert as much pressure on

the walking floor as the WT rats from the same age (DKO  $1280 \pm 620$ , WT  $831 \pm 368$ ). On the other hand, hind-limbs of DKO had a shorter step length (DKO  $6.25 \pm 1.32$ , WT  $7.46 \pm 0.44$ ) , less step pressure (DKO  $815 \pm 409$ , WT  $1309 \pm 664$ ), and step angle was different from WT (DKO  $91.41 \pm 3.22$ , WT  $89.35 \pm 3.3$ ).

#### 3.4.2 Effect of aging on DKO behavior

Vertical pole test and rotarod experiments were performed to test the effect of aging on the behavior of WT and DKO rats. Behaviors were tested when they were 3 months old and then retested when they became 6 and 9 months.

Bradykinesia and the loss of agility are important characteristic abnormalities seen in PD patients. In rodents, the vertical pole test is used to assess agility and bradykinesia. Results indicated an increase in the time DKO required to turn and descend at 6 and 9 months with no difference at 3months. At the age of 6 months, when all DKO rats lose control on their hind-limbs, it was not possible to perform either task. The time WT took to turn was  $4.75 \pm 1.43$  seconds, while DKO took 60 seconds. In addition, the time WT took to descend was  $3.42 \pm 1.56$  seconds, while DKO took  $60 \pm 0$  seconds. When the rats were aged to 9 months, the hind-limbs of the DKO recovered, but they still did not have the agility of the WT. The mean of the time to turn was  $4.89 \pm 3.09$  seconds in WT compared to  $18.9 \pm 5.32$  seconds in DKO (mean difference was 14.01 seconds). On the other hand, WT time to descend was  $4.46 \pm 2.93$  seconds compared to  $28.77 \pm 14.52$  seconds in the DKO (mean difference was 24.31 seconds) (Figure 3.5).



Then motor coordination was assessed by rotarod. The latency to fall did not show a difference when rats were 3 months old. However, at 6 months and 9 months, there were significant differences between WT and DKO. At 6-month, the latency to fall was  $39.41 \pm 6.82$  seconds in WT, while it was  $10.95 \pm 4.63$  seconds in DKO. At 9-month, WT mean latency to fall was  $40.6 \pm 9.73$  seconds and  $24.36 \pm 8.1$  seconds in the DKO (Figure 3.6).

### 3.4.3 Pathological phenotyping of DKO rats.

The day following behavioral assessment, mid- to hind-brain specimens were collected for immunohistochemistry for tyrosine hydroxylase (TH) to determine whether the loss of PINK1 and Parkin would negatively impact the number of neurons in the substantia nigra and the ventral tegmental area (VTA). Unbiased stereology revealed no difference at 3 months, but a significant loss in the number of dopaminergic neurons in the substantia nigra in 6- and 8-month old rats. At 6 months, the average total number of neurons in WT was 33,026 plus minus ?? compared to 23,891 (SEM  $-9135 \pm 3269$ ) in DKO, indicating that DKO lost approximately 30% of their neurons. The loss of neurons was more significant with aging in DKO rats, especially at 8 months (23,856 in WT and 13,853 in DKO plus minus values). At this age DKO rats lost almost 45% of their dopaminergic neurons (Figure 3.7 A-C). In the VTA, TH+ neuron number was not significantly different in 3 or 6 month old DKO compared to WT. However, 8-month old DKO rats showed a significant loss in the number of neurons in the VTA (45,245 in WT and 35,251 in DKO plus minus values). The loss was approximately 22% (Figure 3.7 D-E).

#### 3.4.4 Functional assessment of the mitochondria

To examine the effect of the deletion of PINK1 and Parkin on striatal nerve terminal function, mitochondrial respiration was measured using SeahorseXF<sup>96</sup> extracellular flux analyzer for both WT and DKO animals of 3, 6, and 8 months of age.

At 3 months, DKO did not show any significant change in the OCR until FCCP was injected. After injection of the uncoupler, DKO exhibited an 18.2% reduction in OCR compared to WT ( $P < 0.01$ ). Don't we need to know the values before and after for both??. When mitochondrial parameters were calculated, no change was found in the DKO except a reduction in the maximal respiration (12%;  $P < 0.001$ ) and SRC (11%;  $P < 0.05$ ) (Figure 3.8A). Glycolysis measured by ECAR did not show any significant alterations. Older rats at 6 and 8 months did not display any significant change in the OCR or ECAR (Figure 3.8 B and Figure 3.8 C).

### 3.5 DISCUSSION

To gain insight into the early-onset form of PD caused by PINK1 and Parkin mutations, this study evaluated motor functions and neurodegeneration in a newly generated rat model in comparison with WT. We hypothesized that PINK1/Parkin DKO would have progressive loss of motor functions due to a loss of dopaminergic neurons in the SN and the VTA. These data demonstrate that the loss of PINK1 and Parkin in those rats resulted in motor impairments in both strength and gait. These abnormalities were accompanied by a decline in the number of dopaminergic neurons. Thus, PINK1/Parkin DKO appears to be a

useful animal model, with reproducible motor deficit and early loss of neurons in the SN.

Genetic mutations leading to PD take place in less than 10% of all cases. PINK1 and Parkin mutation incidences in patients are higher in early-onset PD (<40 years old). The 581-amino acid protein encoded by the PINK1 gene is the serine/threonine kinase PINK1, which protects the cell against oxidative stress, with the help of the PARK2 gene that encodes Parkin, an E3 ubiquitin ligase, that ubiquitinates substrates. Both proteins are important for mitochondria quality control via inducing mitophagy, thus maintaining neuronal homeostasis [278].

To help understand of the pathophysiological changes associated with mutations in PINK1 and Parkin, several different animal models knockouts have been generated and characterized. While the mouse knockout model of PINK1 displayed some motor abnormalities, those deficits were mild and there was no sign of dopaminergic neuronal loss in the SN or dopamine loss in the striatum [153]. On the other hand, despite the fact that Parkin mutations are the most common autosomal recessive form of PD in human, neither mouse nor rat models showed substantial abnormalities, although a slight impairment in dopamine release was found in some of the models [140, 279, 280]. The PINK1 KO rat (as well as a second rat KO, in the DJ-1/PARK7 gene) was the first in mammals to show significant PD-like changes [142].

In the current study, a PINK-1 Parkin DKO rat model was generated. Those rats exhibited an increase in weight compared to WT at 3, 6 and 8 months. This is most likely due to PINK1, as an increase in weight was also

observed in the PINK1 single knockout but not the Parkin KO (unpublished findings). This finding raises the intriguing question regarding a possible metabolic abnormality.

Assessment of behavior in the DKO was performed by cylinder tests, gait tests, pole tests, and rotarod.

Hind-limb muscle strength was assessed using cylinder test by measuring the rearing frequency. Reduction in the rearing frequency was found in DKO at 6 months and persisted at 8 months of age. Similarly, results were found at 6 and 8 months old PINK1 KO (but not Parkin KO) rats when the test was performed in an open field [142]. However, the mouse model did not show any change in the number of rears in the cylinder test [281].

Gait abnormalities were also evaluated, revealing a significant increase in the foot step pressure at 3 months, which may be due to the weight of PINK1/Parkin DKO rats, since the average weight difference between the WT and the DKO was 100 g, a 25% increase. Gait abnormalities in DKO were expected to be a consequence of dopaminergic neuronal loss in the SN. Furthermore, longitudinal experiments on DKO rats revealed a loss of motor coordination and loss of agility that start at 6 months and continues at 8 months. Taking all these behavioral abnormalities together suggests that knocking out Parkin in addition to PINK1 magnifies the behavioral abnormalities that arise, in parallel to neurodegeneration of neurons in the SN.

In order to determine if these abnormalities align with degeneration of dopaminergic neurons in the SNpc, unbiased stereological counting was used.

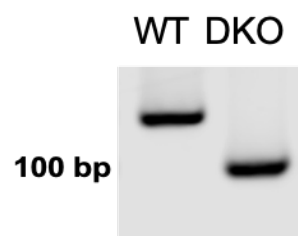
Interestingly, counting revealed a reduction in the number of neurons that started early, at 6 months, and increased at 8 months. In addition, a reduction in the number of TH<sup>+</sup> neurons in the VTA was found at 8 months. It is worth noting that PINK1 KO, but not Parkin KO, exhibited a loss in dopaminergic neurons at 8 months in SN without any change in the VTA staining intensity of TH [142]. These findings suggest a link between the motor abnormalities present in the model and dopaminergic neuronal loss.

To uncover one of the possible underlying reasons behind the neurodegeneration, mitochondrial function was measured using Seahorse XF<sup>®</sup>96 analyzer. Rats at the age of 3 months exhibited a significant reduction in the maximal respiration of the mitochondria at the nerve terminal, which means that when ATP demand is increased, for example when the nerve terminal should release neurotransmitter, the mitochondria are not able to keep up with that increase in the energy demand. In addition, SRC was also reduced, meaning that when the mitochondria start to work in full power, they will not provide the needed amount of ATP. On the contrary, older DKO rats showed normal mitochondrial function. A possible explanation is that following neuronal death caused by mitochondrial dysfunction, only mitochondria in healthy neurons remained present.

In summary, this PINK1/Parkin DKO rat animal model shows pathological characteristics as well as phenotypic abnormalities similar to those in PD. Our findings demonstrate that deletion of PINK1 and Parkin can cause an early degeneration of dopaminergic neurons that becomes more significant with age.

Furthermore, gross neurodegeneration were contributing to mitochondria dysfunction in the DKO. This model may provide an important tool to explore new therapeutic strategies for patients with PD and expand our knowledge about the importance of mitophagy in the brain. Since this is a global DKO's animal model not brain specific, it would also improve our understanding of the importance of PINK1 and Parkin beyond the brain.

A



B

CAG CCT GGG AAA CTC CGA GTT **CAG T** GC GGC ACC TGC AGA CAA GCA ACC CTC ACC TTG GCC CA GG TAA GGA AGC  
 CAG CCT GGG AAA CTC CGA GT GC GGC ACC TGC AGA CAA GCA ACC CTC ACC TTG GCC CA GG TAA GGA AGC

**Figure 3.1 Genotyping of DKO rats.**

A. Representative result of polymerase chain reaction (PCR) to confirm the deletion of 26 bp in the PINK1 in DKO rat model in comparison with WT. B. Sequencing of DKO rats to confirm the deletion of 5 bp.



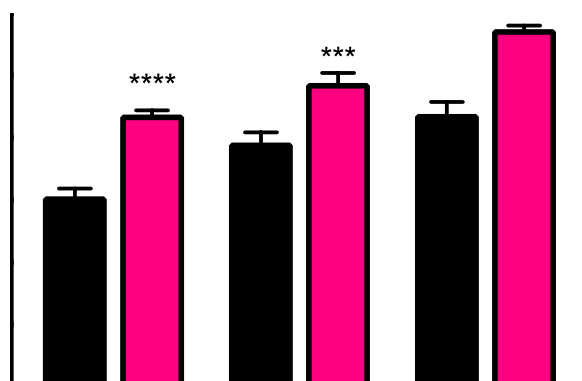


**Figure 3.2 Weight change in WT and PINK1/Parkin DKO rats.**

Weights were measured in WT and PINK1/Parkin DKO at 3, 6, and 8 month old rats. \*\*\*( $p < 0.001$ ), \*\*\*\*( $p < 0.0001$ ), significantly different. All values are expressed as means  $\pm$  SEM. The differences between groups were analyzed using unpaired t test with Welch's correction ( $n = 9-12$ ).

Put the raw values here, not in text.

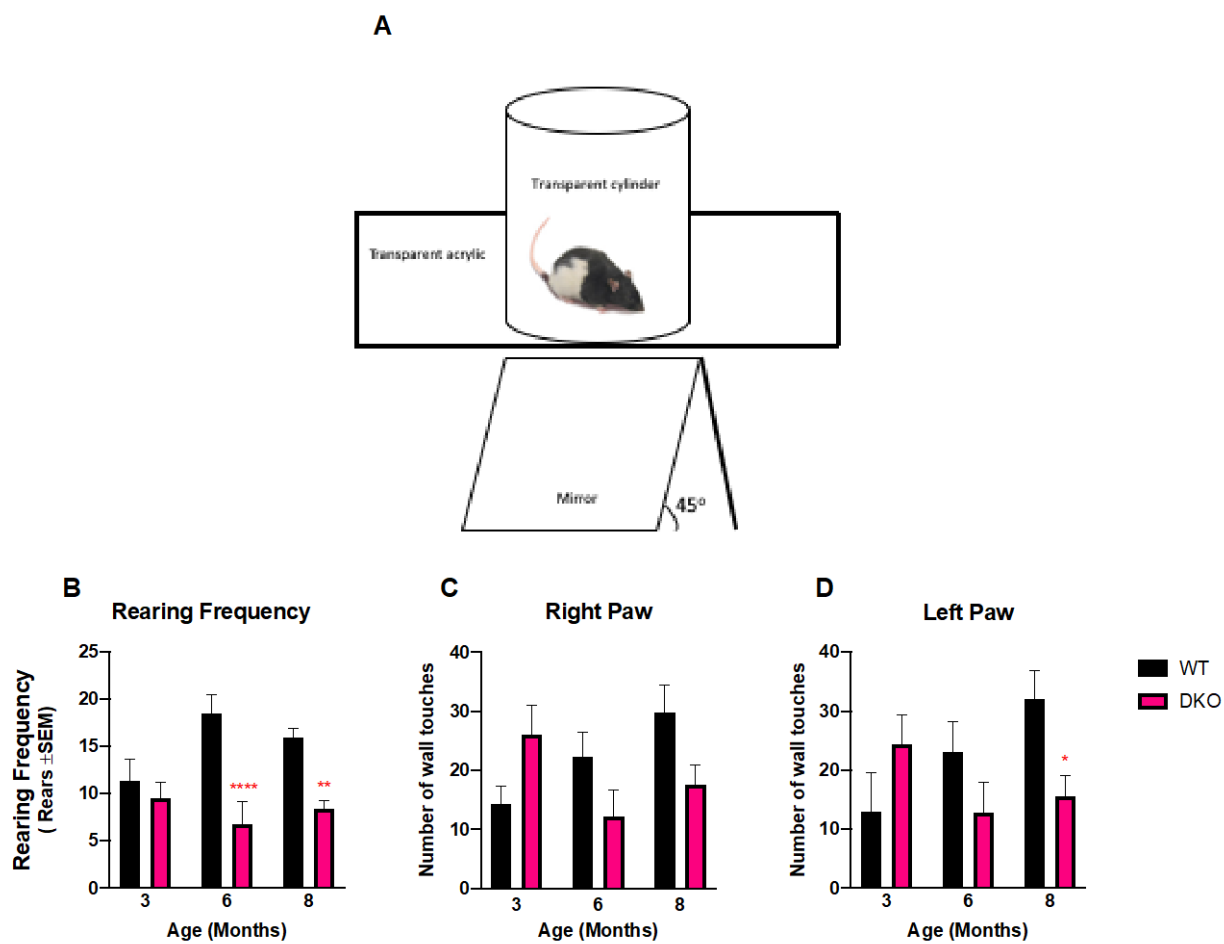
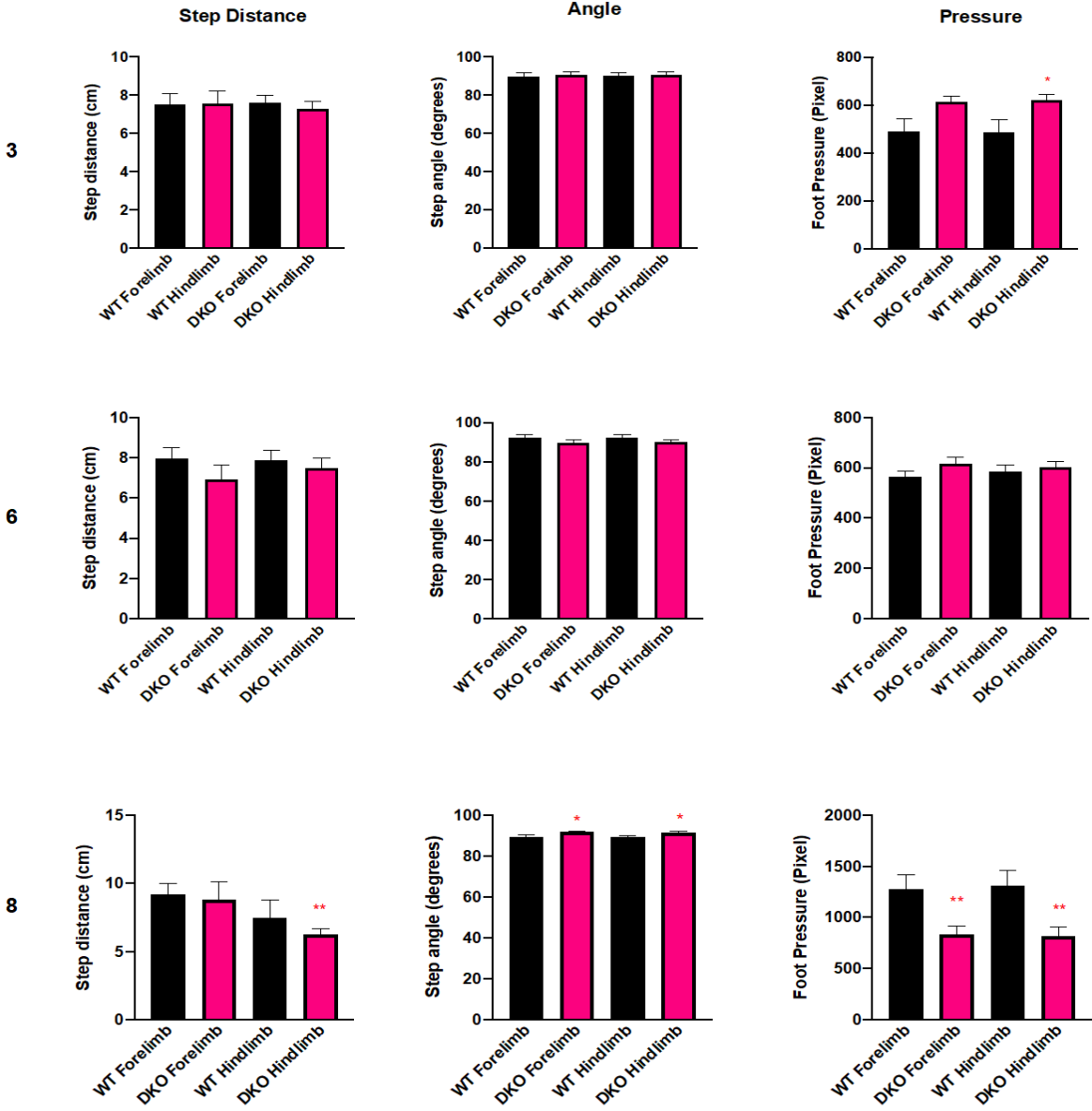


**Figure 3.3 Reduction hind-limb strength and presence of fore-limb asymmetry.**

Hind-limb strength was determined by measuring rearing frequency, while asymmetry of forelimb by measuring the number of wall touches. In brief, rats were placed in a transparent cylinder with a mirror at 45° angle placed below the cylinder. Rats were placed in the cylinder for 3 minutes. \*( $p < 0.05$ ); \*\*( $p < 0.01$ ); \*\*\*\*( $p < 0.0001$ ) significantly different. All values are expressed as the mean  $\pm$  SEM. The difference between groups was analyzed using unpaired t test with Welch's correction ( $n=9-12$ ).

A      Age



B

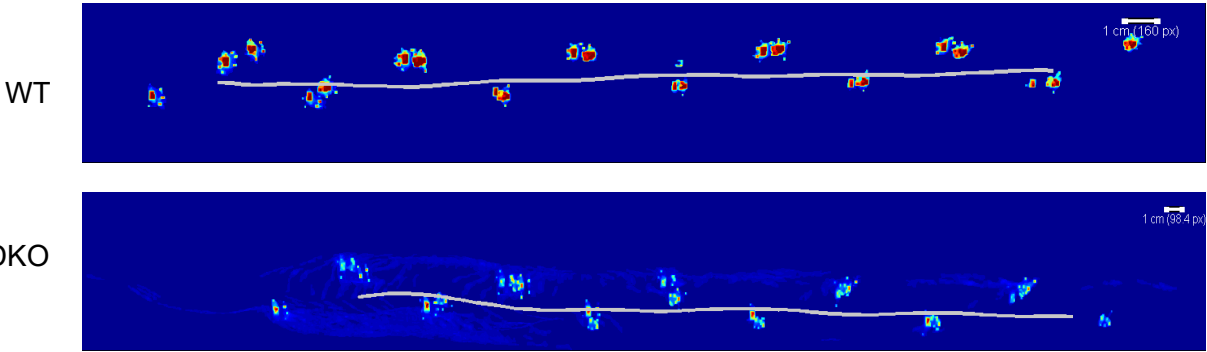


**Figure 3.4 Gait abnormality of fore- and hind-limbs of DKO.**

Gait was evaluated by RatWalker, a method that was developed by our group to measure gait in rats. In the beginning rats were transferred individual to a new cage that was placed at the end of the walker so the rats would walk freely on the walking floor toward their home cage without turning. Rats' gait was captured from a mirror at 45° angle beneath the walking floor using GoPro Hero6 that was set to record 120 frame/second. Videos were then converted into a series of images and were then uploaded to the MouseWalker software. (A) Step distance, angle, and pressure evaluation in WT and DKO at different ages. (B) Foot step heatmap of 8 month old WT and DKO. \*( $p < 0.05$ ); \*\*( $p < 0.01$ ) significantly different. All values are expressed as the mean  $\pm$  SEM. The difference between groups was analyzed using unpaired t test with Welch's correction (n=9-12)

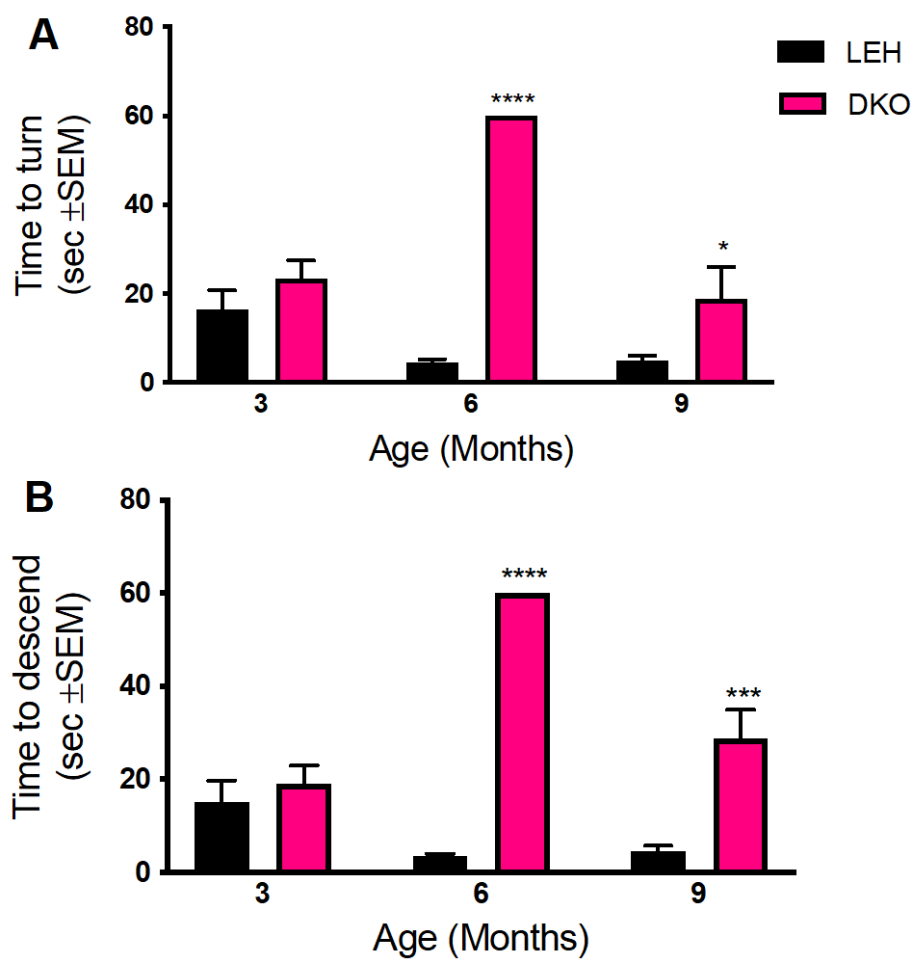


**Figure 3.5 Increase in bradykinesia and decrease in the agility in DKO.**

The agility and bradykinesia was assessed in rats using pole test. In this test rats were placed on the pole facing upward and the time it takes to turn and face downward is the time to turn figure (A). The time it takes to descend to the floor is the time to descend figure (B). The failure in performing one or both of the tasks will be recorded as 60 sec. Each rat repeated the task five times. \*( $p < 0.05$ ), \*\*\*( $p < 0.001$ ), \*\*\*\*( $p < 0.0001$ ), significantly different from WT, 2-way Repeated Measure ANOVA, followed by Bonferroni multiple comparisons. Data are represented as mean  $\pm$  SEM (n=6)



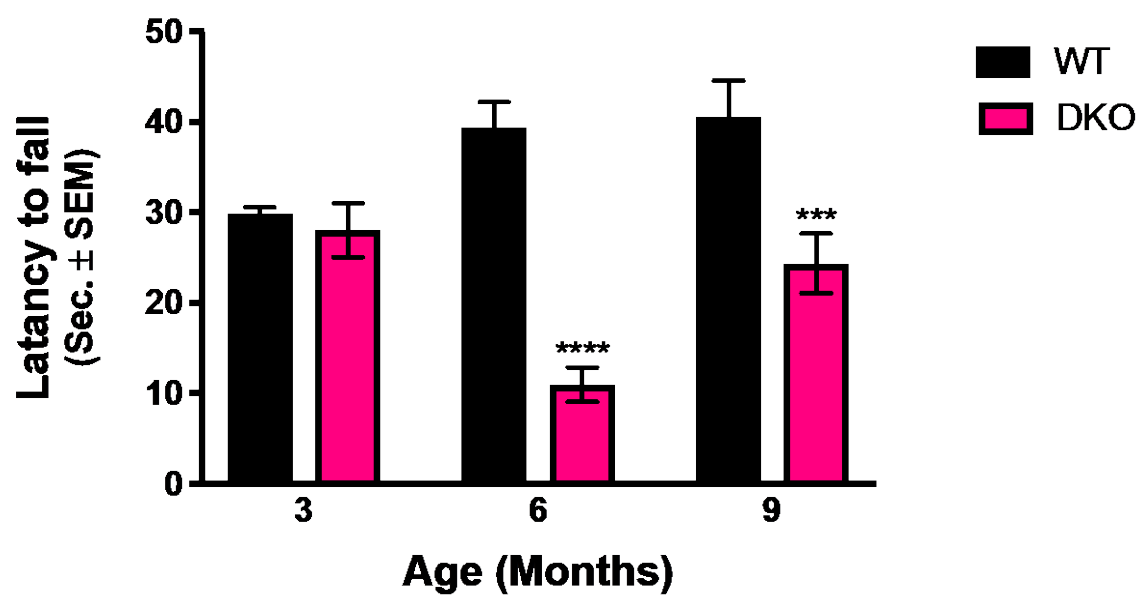


**Figure 3.6 Motor coordination deficit in DKO.**

Motor coordination was accessed using rotarod. Each rat was tested three times with half an hour in between tests. \*\*\*( $p < 0.001$ ), \*\*\*\*( $p < 0.0001$ ), significantly different from WT, 2-way Repeated Measure ANOVA, followed by Bonferroni multiple comparisons. Data are represented as mean  $\pm$  SEM (n=6)

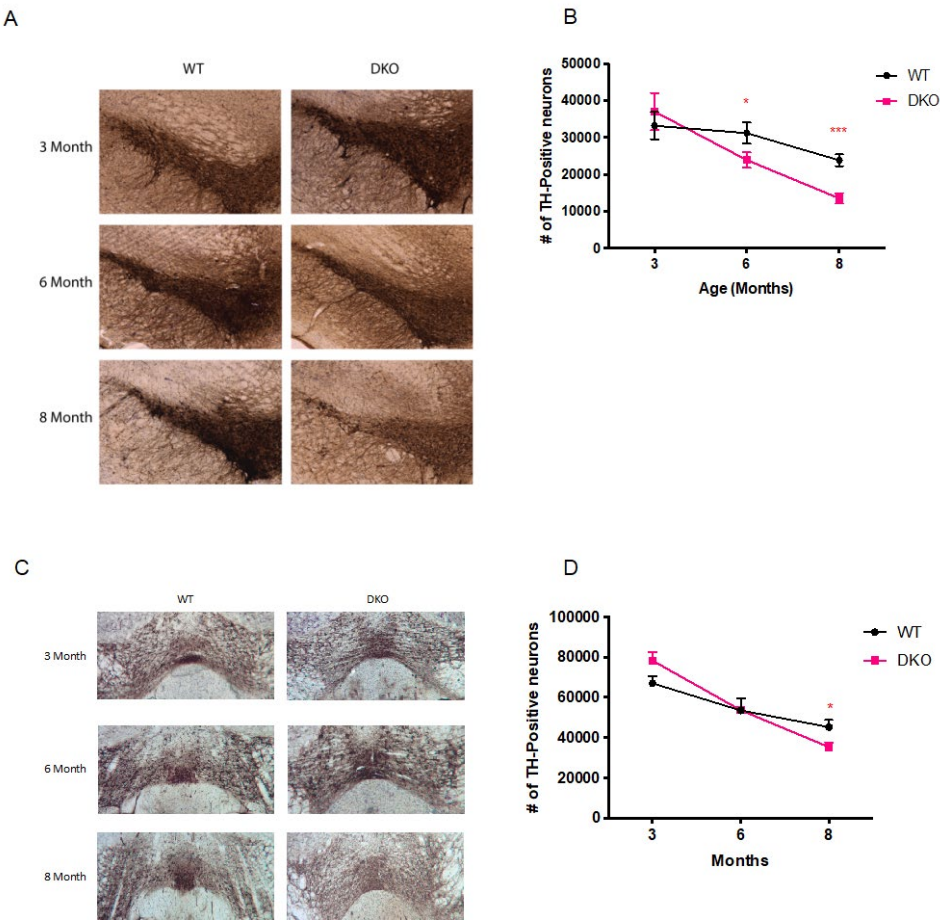
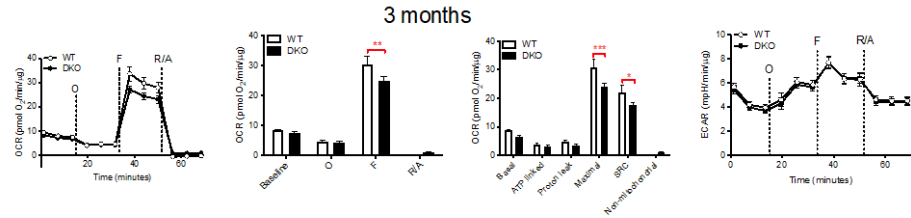


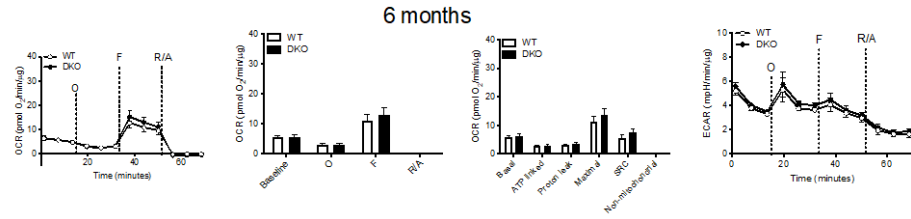
**Figure 3.7 Progressive loss of dopaminergic neuron in the SNpC and the VTA.**

Dopaminergic neuron in the SNpc (A and B) and the VTA (B and C) were counted at 3, 6 and 8 months old wild-type and PINK1/Parkin DKO. Fixed brains were sectioned and stained against tyrosine hydroxylase (TH). Then the number of dopaminergic neurons was determined using stereological counting. \*( $p < 0.05$ ); \*\*\*( $p < 0.001$ ) significantly different. All values are expressed as the mean  $\pm$  SEM. The difference between groups was analyzed using unpaired t test with Welch's correction (n=9-12).

A



B



C

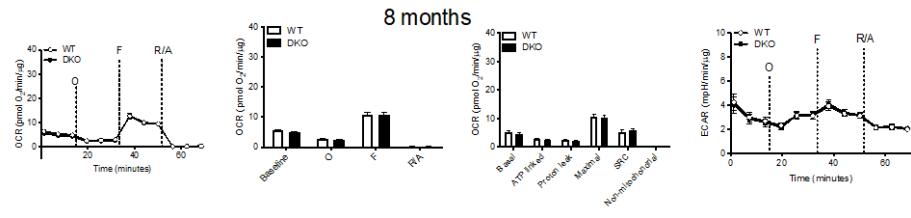


**Figure 3.8 Effect of PINK1/Parkin deletion on mitochondrial respiration at the nerve terminal.**

The OCR was measured in striatal nerve terminal over time at baseline or after the injection of series of drugs: 5  $\mu$ M Oligomycin (O), 4  $\mu$ M FCCP (F), and 2  $\mu$ M Rotenone in combination with 2  $\mu$ M Antimycin A (R/A) at (A) 3 months, (B) 6 months and (C) 8 months. \*( $p < 0.05$ ); \*\*( $p < 0.01$ ); \*\*\*( $p < 0.001$ ) significantly different from WT, 2-way ANOVA followed by Sidak's multiple comparisons test. Data are presented as mean  $\pm$  SEM (n=4-6).

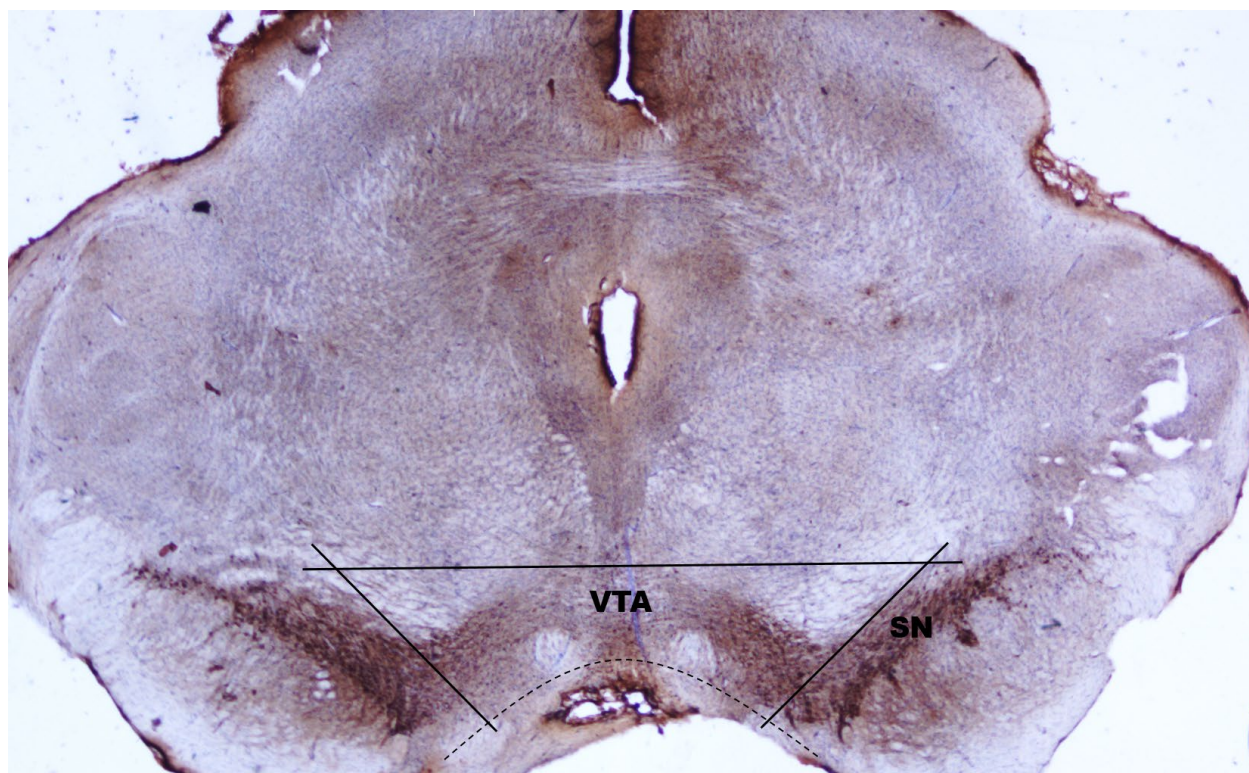


**Figure 3.9 Supplement stereology counting areas**



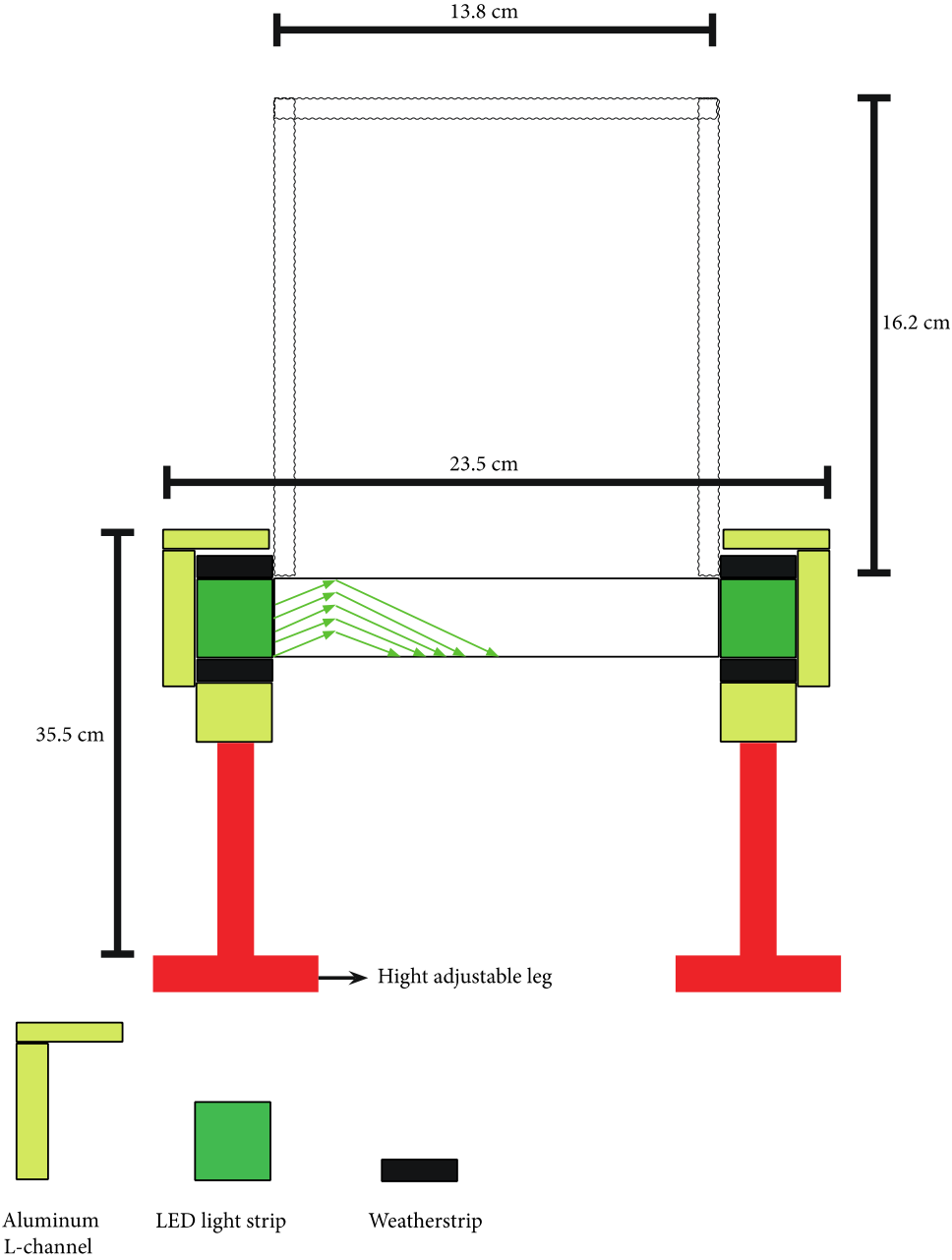


**Figure 3.10 Supplement walking floor design**

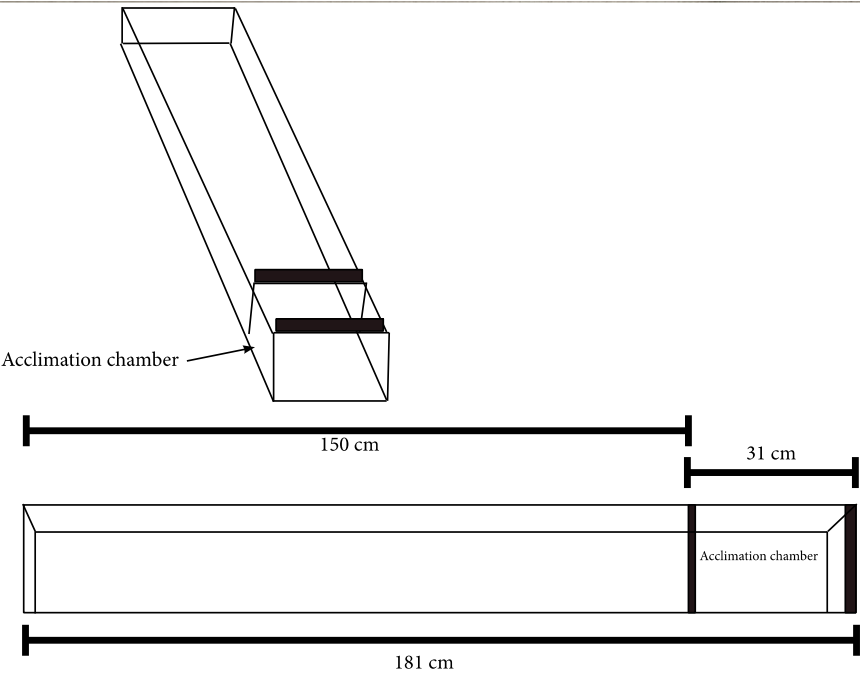


**Figure 3.11 Supplement walking floor cover design.**

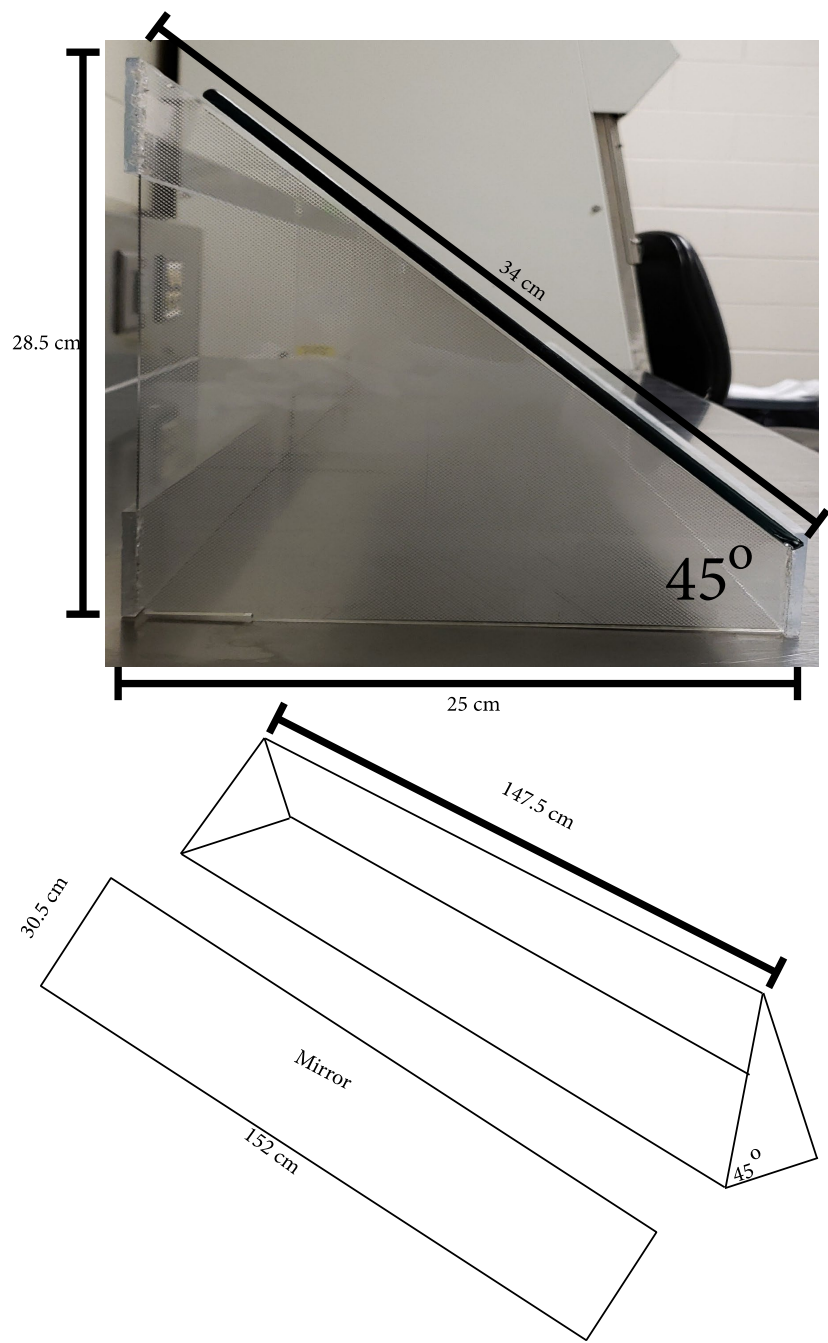


**Figure 3.12 Supplement mirror holder design.**

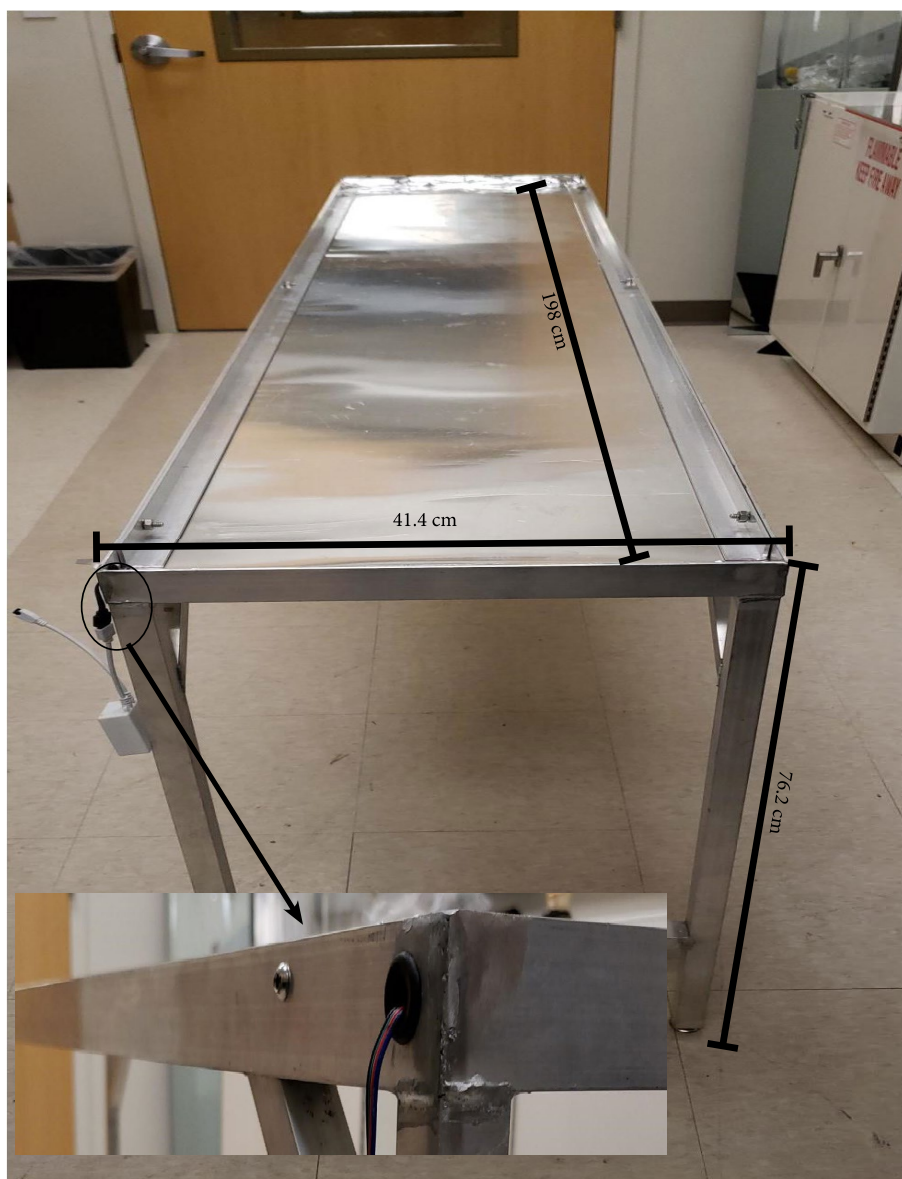


**Figure 3.13 Supplement background light design**



# Chapter 4

Other studies on male and female

PINK1/Parkin DKO rats

## 4.1 Introduction

In this section of the dissertation, additional studies relevant to our PD studies are described, in three parts: nigrostriatal terminal studies, mitochondrial deoxynucleic acid (mtDNA), and female DKO behavior.

The nigrostriatal pathway is the projection of dopaminergic neuron axons from the SN via the medial forebrain bundle to the dorsal striatum. Post mortem studies revealed that motor symptoms onset in PD occurs together with extensive degeneration of dopaminergic axonal projections occur. This suggests that damage is not only in the cell body in the SN, but also involves the nerve terminals in the striatum [59, 282]. PINK1 and DJ-1 KO rats exhibited loss of dopaminergic neurons in the SN. However, no change in striatal TH was observed in either of the models. In addition, Parkin KO rats did not show any change in the SN or in the striatum [142]. Similar to Parkin KO rats, mouse models of PINK1 KO, Parkin KO, DJ-1 KO, and PINK1/Parkin/DJ-1 triple KO did not show any changes in the nigrostriatal neurons.

While most of the deoxyribonucleic acid (DNA) in a cell is packaged in chromosomes within the nucleus, mitochondria also have their own DNA. Mitochondria have a circular double-stranded DNA containing 37 genes that encode 13 proteins essential for oxidative phosphorylation (OXPHOS) [283]. Accumulation of mutated mtDNA requires clearing by mitophagy. However, in the absence of PINK1 and Parkin, uncleared mutations in the mtDNA were found to be linked to PD-like neurodegeneration [284].

Finally, despite the fact that the risk of developing PD is twice as high in males as in females, the mortality rate in females is higher than in males. In addition, the progression of the disease is faster in females. The female sex is underrepresented in PD research, and studies in female animals are warranted [285].

## **4.2 Methods**

### **4.2.1 Animals**

PINK1/Parkin DKO and the congenic wild-type (WT) Long Evans Hooded (LEH) rats were obtained from SAGE Labs (and now available from Envigo) and bred and maintained at the University of Nebraska Medical Center (UNMC). Generation and characterization of the DKO rats have been described previously (Chapter 3). Rats were kept in a temperature-controlled environment with a 12-hour light/dark cycle and free access to rat chow and water. All experimental procedures were approved by the UNMC Institutional Animal Care and Use Committee (IACUC).

### **4.2.2 Immunoblotting**

Striata was dissected from 3, 6, and 8 month old WT and DKO (n=5), homogenized, and lysed in SDS-based lysis buffer (4% SDS, 100 mM Tris, 0.1 M DTT). Protein concentration was determined in the samples using 660 nm Protein Assay (SOURCE???) and 10 µg of each sample was separated by SDS-PAGE on NuPAGE 4%-12% Bis-Tris gel (Invitrogen Novex, CITY STATE). Following electrophoresis, transfer of proteins onto nitrocellulose membranes

was performed using iBlot®2 System (Thermo Fisher Scientific, Rockford, IL) followed by blocking of nonspecific binding sites for an hour at room temperature using SuperBlock Blocking Buffer (Thermo Fisher Scientific, Rockford, IL). Overnight incubation of the membrane at 4° C was with primary antibody for TH (anti-TH, 1:1000; EMD/Millipore) and dopamine transporter (DAT) (anti DAT, 1:200; Alomone Labs CITY STATE FOR ALL OF THESE). IRDye 680RD goat anti-rabbit and IRDye 800RD goat anti-mouse fluorescent secondary antibodies (LI-COR, Lincoln, NE) were used at a dilution of 1:20,000. Finally, blots were imaged using Odyssey Fc imaging system (LI-COR, Lincoln, NE).

#### 4.2.3 DNA extraction

DNA was extracted and purified using QIAamp DNA Micro Kit according to the manufacturer's protocol (Qiagen, Inc., Valencia, CA). Briefly, 50 µl of striatal homogenate from 3 and 6 month-old male WT and DKO were treated with 20 µl of proteinase K and 180 µl of ATL buffer and incubated at 65 °C overnight in a heated orbital incubator. After the homogenates were completely lysed, 200 µl ATL buffer was added followed by vortexing for 15 seconds. Then, 200 µl ethanol was added and the tube was vortexed again for 15 seconds. After 5 minutes incubation, the lysate was transferred on to a QIAamp MinElute column. Then, it was washed with AW1 and AW2 buffers. Next, 20 µl of AE buffer was added and genomic DNA was collected in the eluted solution.

#### 4.2.4 Real Time PCR (RT-PCR)

Deletion frequency and copy number of mtDNA was quantified using RT-PCR using TaqMan master mix (Applied Biosystems, Foster City, CA). Briefly,

mtDNA copy number was determined by amplification of the mitochondrial D-loop, the region surrounding the consensus deletion, and normalized to quantification of a nuclear gene,  $\beta$ -actin. Amplifications were performed using 10 ng of DNA. The primers used were as follows:

Mitochondrial D-loop

Forward (50 nM): GGTTCTTACTTCAGGGCCATCA

Reverse (50 nM): GATTAGACCCGTTACCATCGAGAT

Probe (2  $\mu$ M): 6FAM-TTGGTTCATCGTCCATACGTTCCCCTTA-TAMRA

Mitochondrial deletion

Forward (200 nM): AAGGACGAACCTGAGCCCTAATA

Reverse (200 nM): CGAAGTAGATGATCCGTATGCTGTA

Probe (2  $\mu$ M): 6FAM-TCACTTTAATCGCCACATCCATAACTGCTGT-TAMRA

$\beta$ -actin

Forward (200 nM): GGGATGTTTGCTCCAACCAA

Reverse (200 nM): GCGCTTTTGACTCAAGGATTAA

Probe (2  $\mu$ M): 6FAM-CGGTCGCCTTCACCGTTCCAGTT-TAMRA

Data acquisition and analyses were performed with a Step One Real-Time PCR System using StepOne Real-Time PCR System (Applied Biosystems, Foster City, CA).

#### 4.2.5 Fluorescence immunostaining

Staining was performed similar to staining for stereology previously described using the same reagents with a few modifications. Sections were

washed three times for 10 min each in 0.1 M PBS containing 0.3% Triton X-100. Sections were then incubated in 3% hydrogen peroxide followed by incubation in blocking buffer containing 10% NGS and 0.3% Triton X-100 in PBS for 2 hours at room temperature. Then, sections were incubated in mouse monoclonal primary antibody against TH (as above) and rabbit polyclonal primary antibody against dopamine transporter (DAT) (anti-DAT, AMT-003, 1:200; Alomone Labs, CITY STATE,) in PBS containing 3% NGS and 0.3% Triton X-100 overnight at 4° C on a rocker. After incubation in primary antibody, sections were washed three times in PBS solution containing 0.3% Triton X-100 followed by incubation with goat anti-mouse IgG (H+L) secondary antibody Alexa Fluor Plus 488 (1:2000; Thermo Fisher Scientific, A32723) and F(ab')<sub>2</sub>-goat anti-rabbit IgG (H+L) secondary antibody Alexa Fluor Plus 568 (1:2000; Thermo Fisher Scientific, A21069) for 2 hours followed by two 0.1 M PBS rinses and one 0.001 M PBS rinse. Finally, slides were mounted using Fluoromount-G (SouthernBiotech, 0100-01).

#### 4.2.6 Rearing test

In this test, rats were placed in a cylinder for 5 min and the rearing frequency and the total rearing time were measured, as described previously.

### 4.3 Results

#### 4.3.1 Striatal and cortical dopaminergic neurons terminal

Dopaminergic neuron projections in the cortex and the striatum of WT and DKO rats were quantified at 3, 6 and 8 month-old rats by immunoblotting proteins

from these regions for TH and DAT. TH and DAT expression showed no change in cortical homogenate at any of the tested ages (Figure 4.1 to Figure 4.3). However, up-regulation in the expression level of DAT was found in striatal homogenates of 3- and 6-month old DKO, but not 8-month. In addition, a significant up-regulation of TH (12 %;  $P=0.0013$ ) was found in 3-month DKO rats (Figure 4.4 to Figure 4.6).

#### 4.3.2 Striatal mtDNA

Mitochondrial DNA in 3 and 6 months old male rats was examined to identify the frequency of deletion and mtDNA copy number. Quantitative PCR did not reveal any change in either the copy number or in deletion frequency (Figure 4.7).

#### 4.3.3 Longitudinal behavior examination in female DKO

In order to study the effects of aging in female DKO rats, behavior tests were performed at 3, 6, and 9 months, including pole test, rotarod, and cylinder test as previously described (Methods , Chapter 3). Animal weight was also recorded.

##### 4.3.3.1 Weight change in DKO females

A significant 23% increase in DKO weight was found at 3 months (

Figure 4.9). There were no significant differences in the weight of 6 and 8 month rats.

#### 4.3.3.2 Agility, bradykinesia, and motor coordination in females

A distinct difference in the DKO versus wild-type rats was found in the two measures of the pole test in: time to turn (P value = 0.0113) and time to descend (P value = 0.049). Unlike in the male rats (Figure 3.5), females showed a change in the time to turn only at 6 month, 5.5 seconds for WT and 24.25 seconds for DKO  $18.76 \pm 4.04$  seconds. On the other hand, time to descend did not show any change at any age (Figure 4.10). In addition, when motor coordination was assessed by rotarod as previously described, females did not show any significant change in latency to fall at any age (Figure 4.11).

#### 4.3.3.3 Hind-limb strength assessment in female DKO

Hind-limb strength was assessed by two parameters, rearing frequency and rearing duration. Rearing frequency showed a significantly fewer rearing's performed during the test at 3 months (32 in WT, 16 in DKO). When rats were aged to 6 months, the difference was greater, 37 in WT vs 18 in DKO. At 9 months the difference in the rearing frequency persisted and the values were 38 in WT and 20 in DKO (Figure 4.12 A). On the other hand, a difference in the duration of the total rears appeared at 6 month (95.3 seconds in WT vs 41 seconds in DKO) and continued at 8-month old DKO (105 seconds in WT vs 42 seconds in DKO) (Figure 4.12 B). These data indicate that DKO females also exhibit behavioral abnormalities that need to be further investigated.



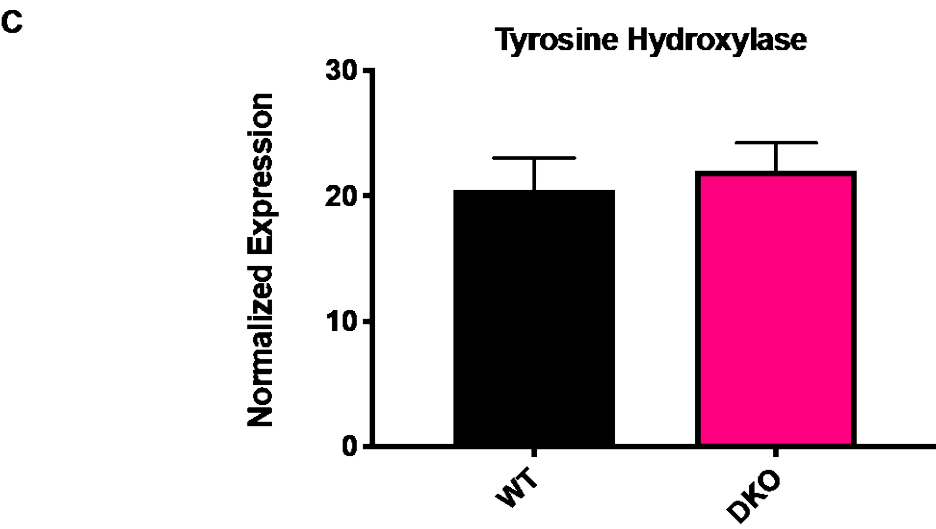
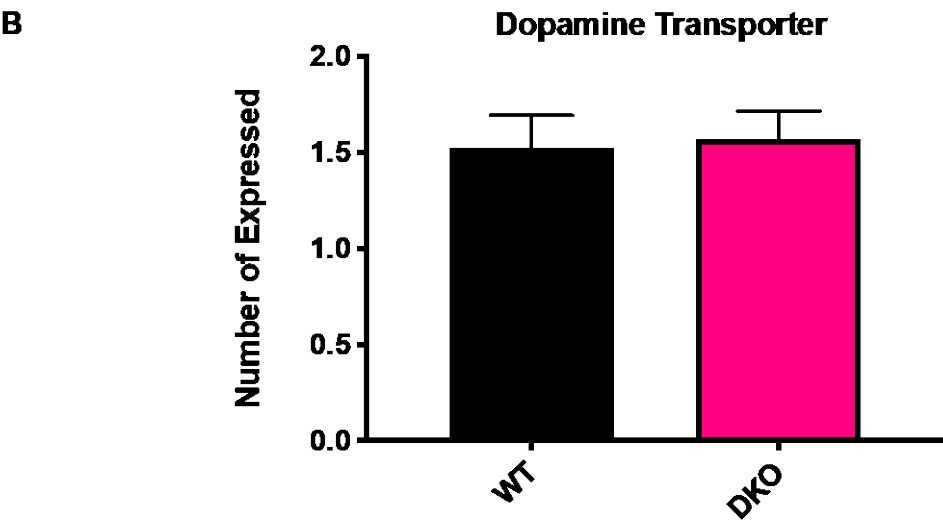
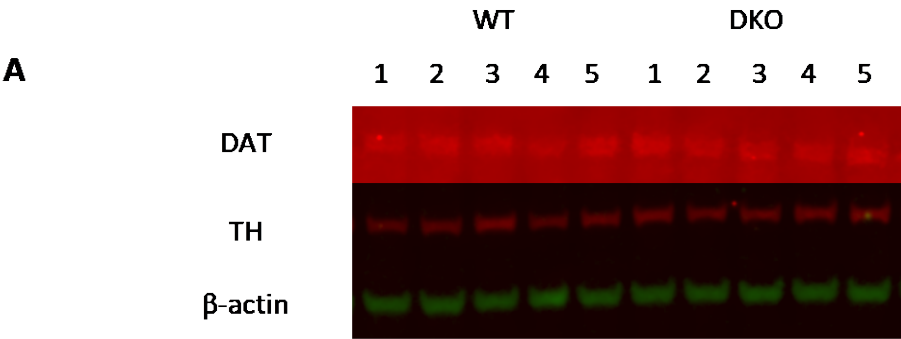


**Figure 4.1 Western blot and quantification of cortical homogenate of 3 month old rats.**

Representative western blot of DAT and TH in cortical homogenate from 3-month old WT and DKO rats (A), quantification of DAT and TH western blot (B) and (C).

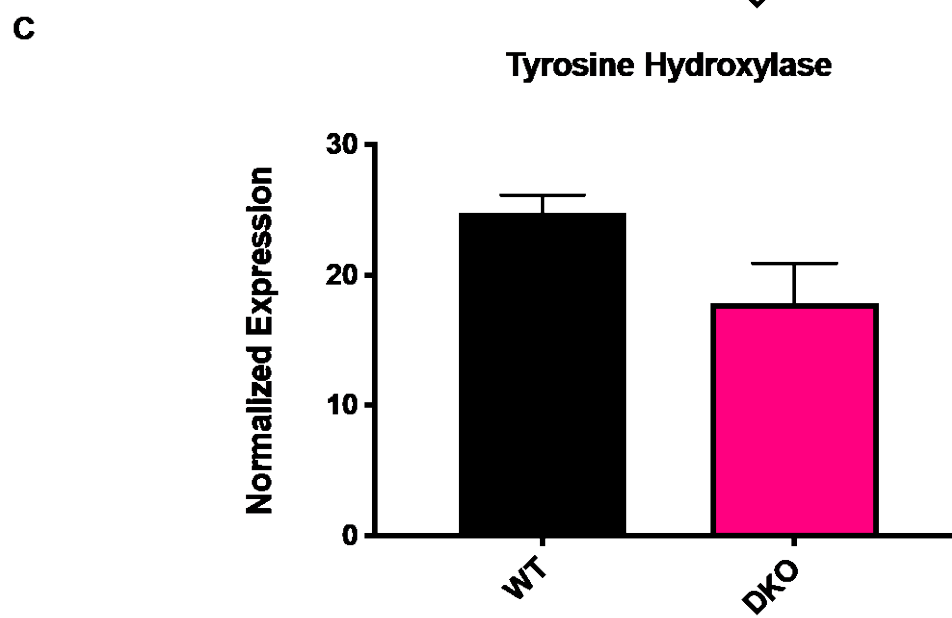
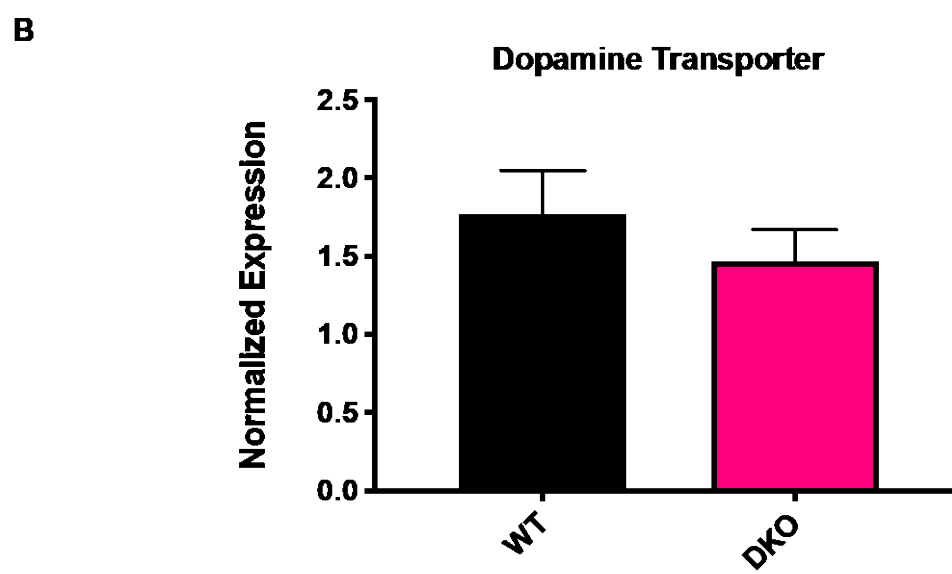
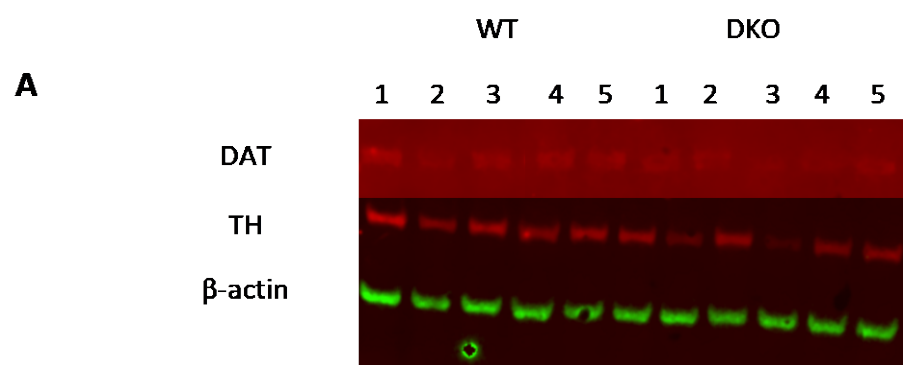


**Figure 4.2 Western blot and quantification of cortical homogenate of 6 month old rats.**

Representative western blot of DAT and TH in cortical homogenate from 6-month old WT and DKO rats, (A); quantification of DAT and TH western blots, (B) and (C).

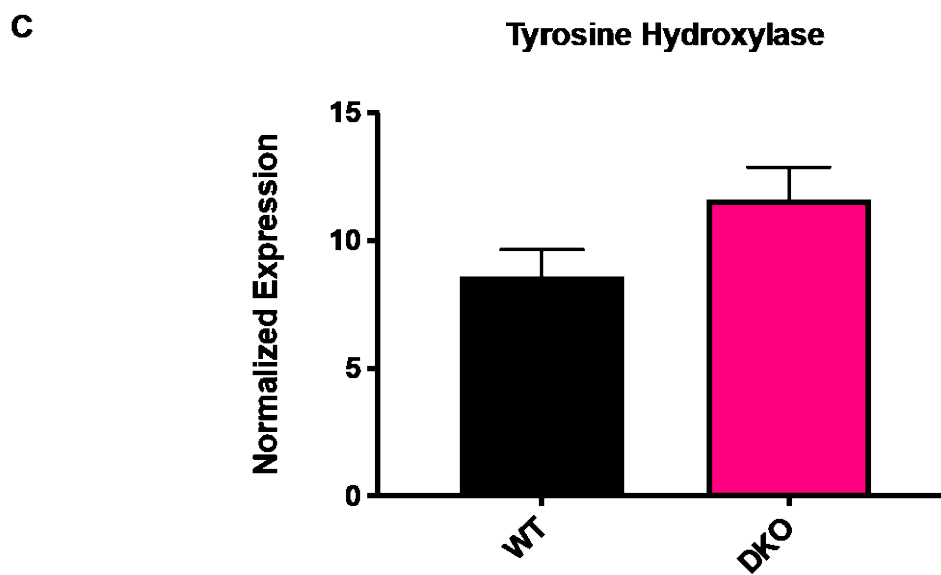
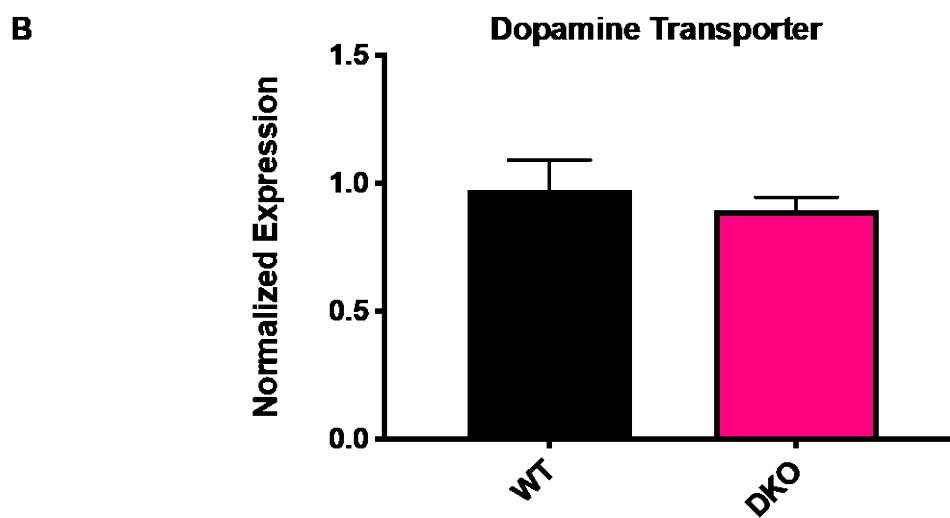
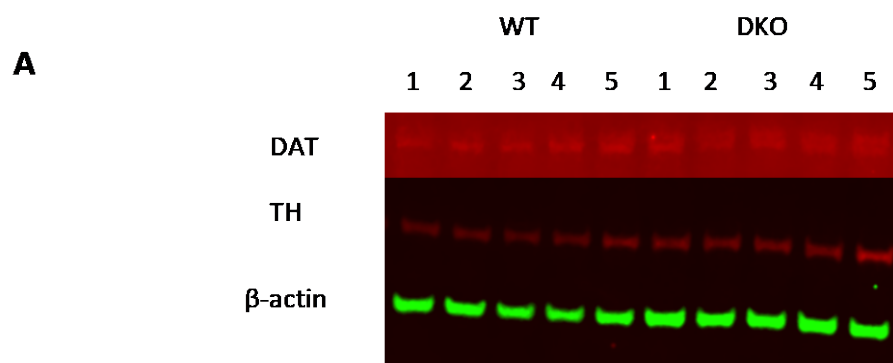


**Figure 4.3 Western blot and quantification of cortical homogenate of 8 month old rats.**

Representative western blot of DAT and TH in cortical homogenate from 8-month old WT and DKO rats (A), quantification of DAT and TH western blot (B) and (C).

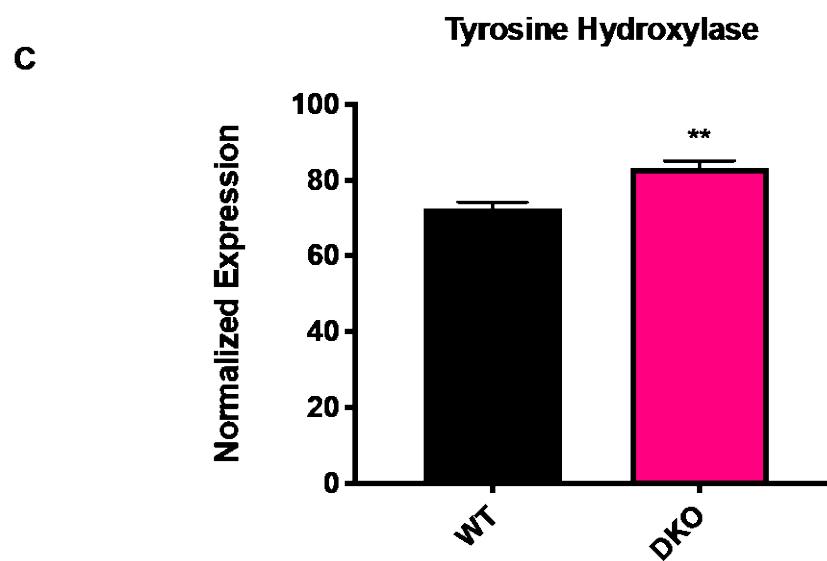
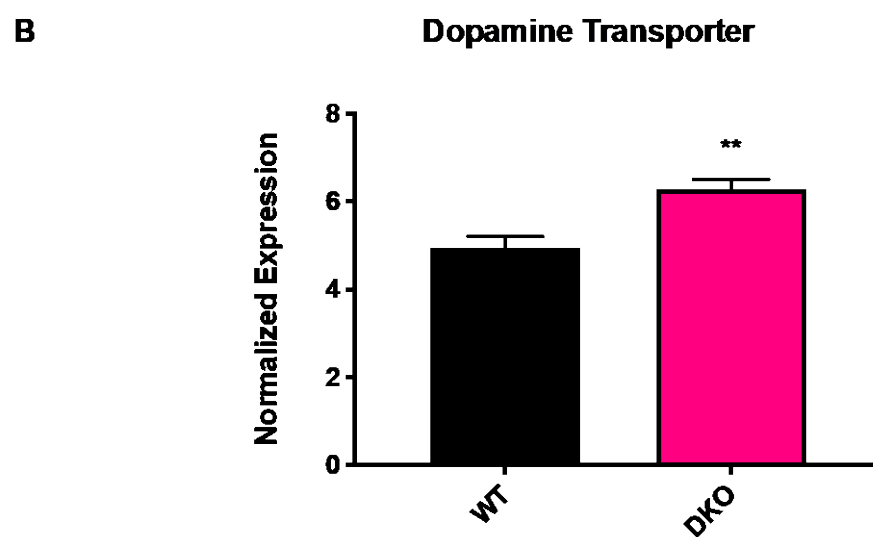
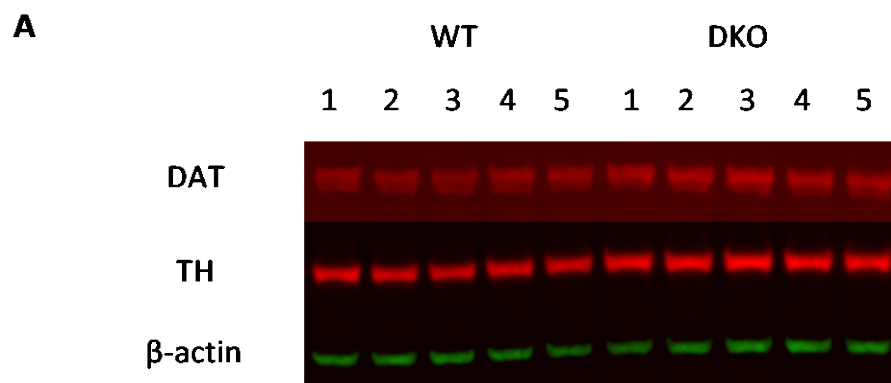


**Figure 4.4 Western blot and quantification of striatal homogenate of 3 month old rats.**

Representative western blot of DAT and TH in striatal homogenate from 3-month old WT and DKO rats (A), quantification of DAT and TH western blot (B) and (C).



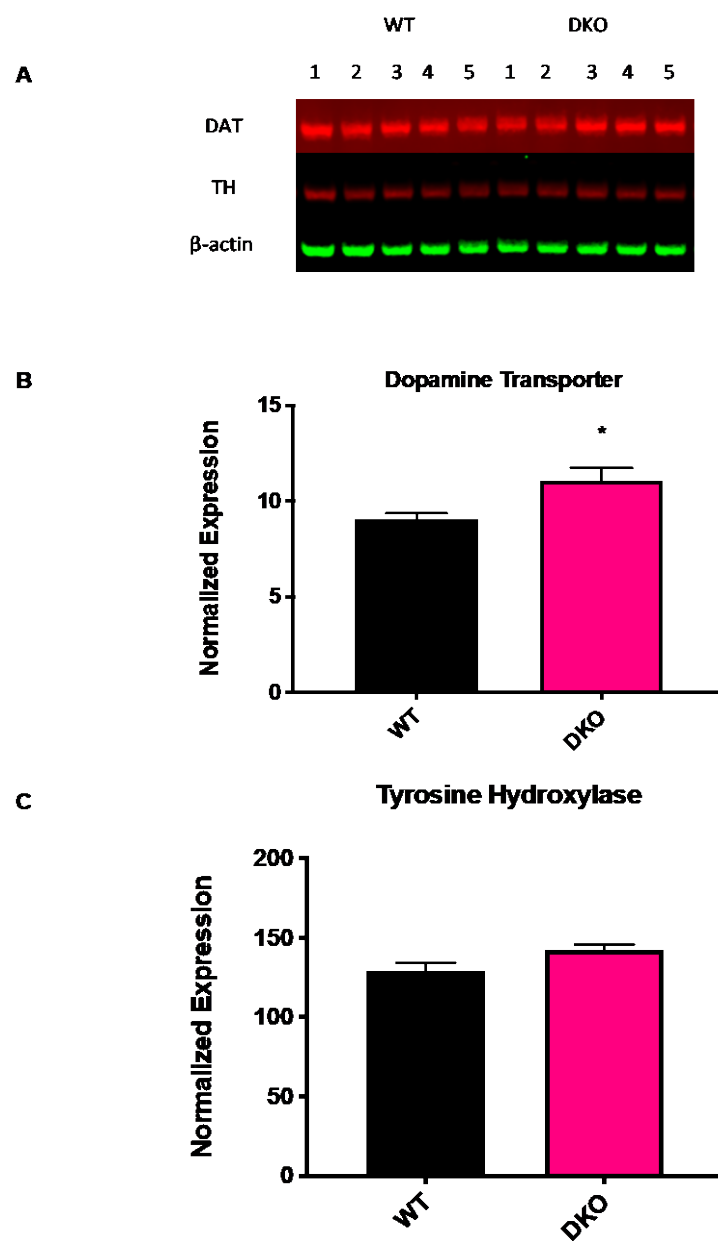


**Figure 4.5 Western blot and quantification of striatal homogenate of 6 month old rats.**

Representative western blot of DAT and TH in striatal homogenate from 6-month old WT and DKO rats (A), quantification of DAT and TH western blot (B) and (C).

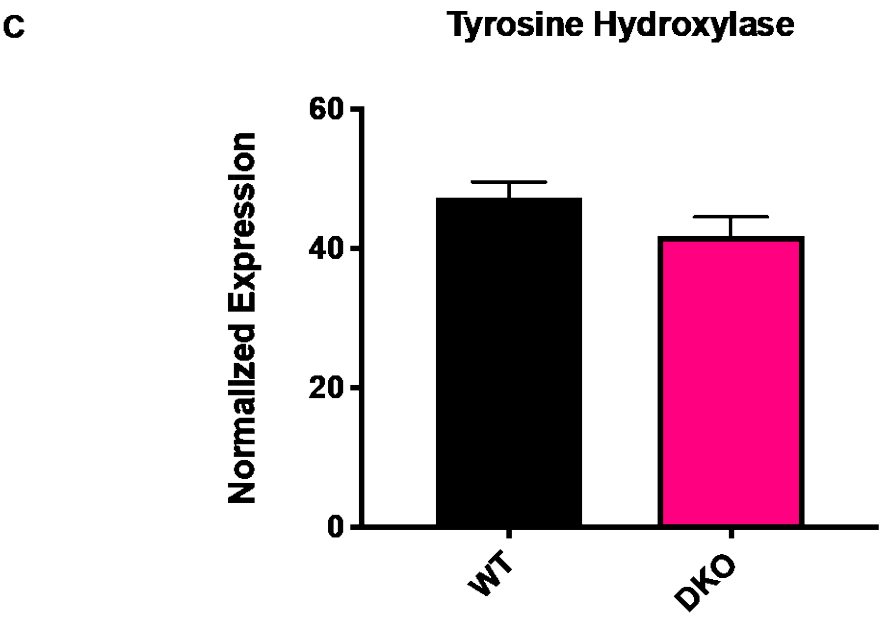
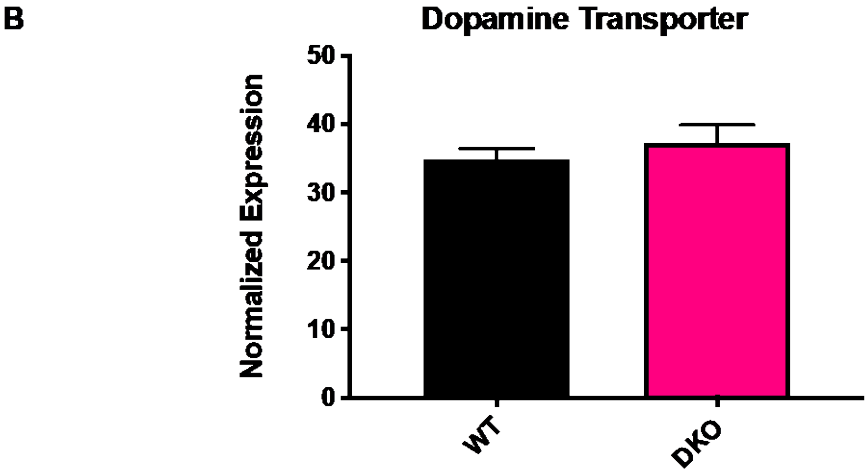
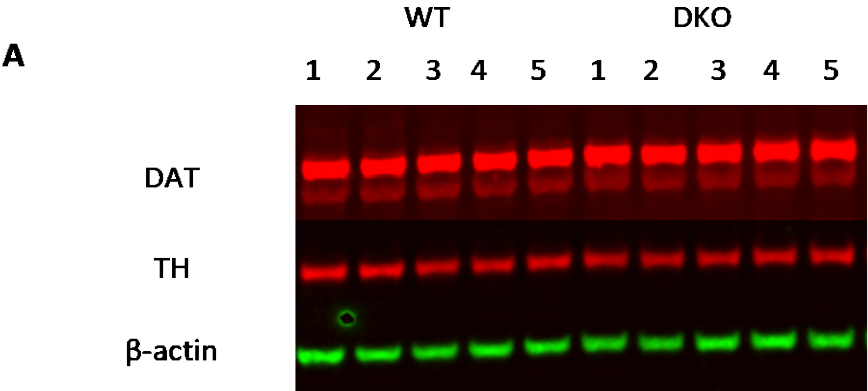


**Figure 4.6 Western blot and quantification of striatal homogenate of 8 month old rats.**

Representative western blot of DAT and TH in striatal homogenate from 8-month old WT and DKO rats (A), quantification of DAT and TH western blot (B) and (C).

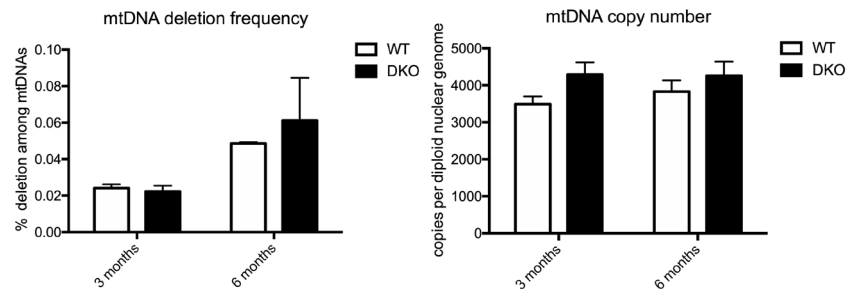
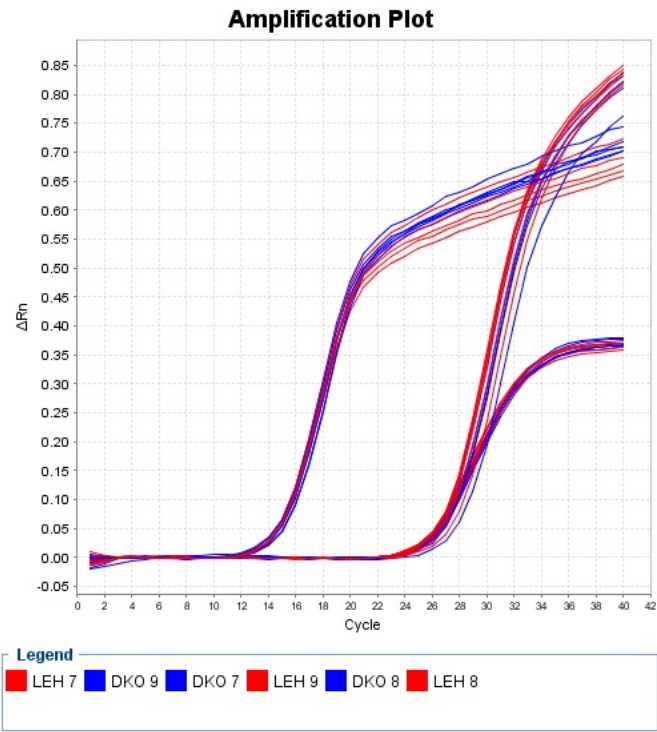


**Figure 4.7 Absence of mtDNA alterations.**

mtDNA deletion frequency and mtDNA copy number. All values are expressed as the mean  $\pm$  SEM. The difference between groups was analyzed using unpaired t test with Welch's correction (n=3).

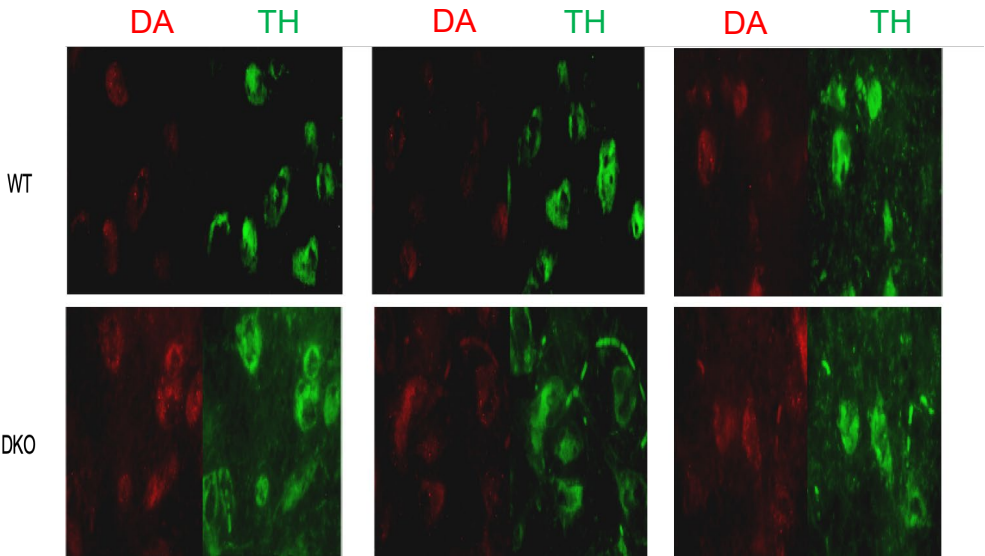


**Figure 4.8 Upregulation in the expression of dopamine transporter in the SNpc.**

Brains from 8 months old wild-type and PINK1/Parkin DKO rats were isolated. Fixed brains were sectioned and stained against TH and DAT. Images were captured at 40x.



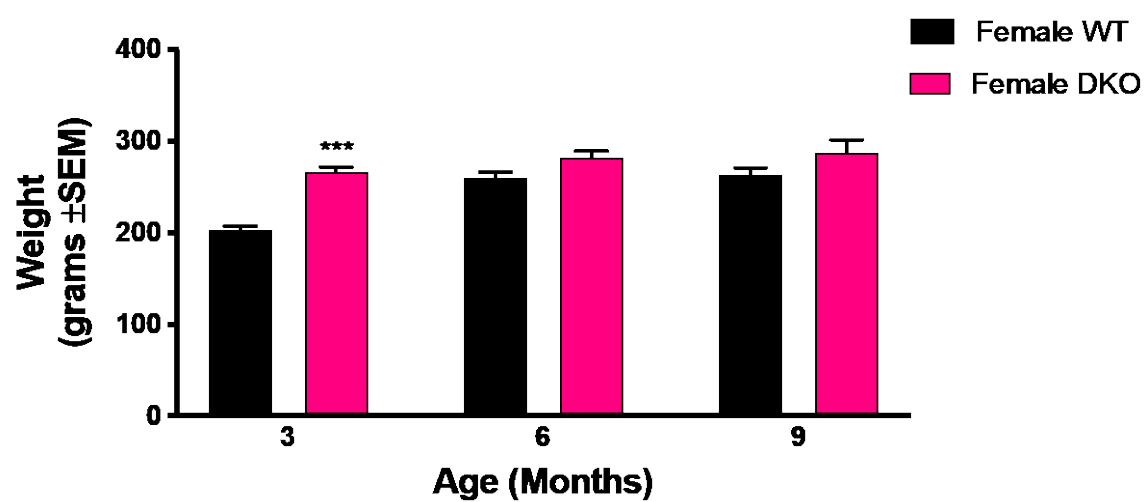


**Figure 4.9 Weight change in WT and PINK1/Parkin DKO females.**

Weights were measured in WT and DKO at 3, 6, and 9 month. \*\*\*( $p < 0.001$ ), significantly different from WT, 2-way Repeated Measure ANOVA, followed by Sidak multiple comparisons. Data are represented as mean  $\pm$  SEM (n = 4-6).

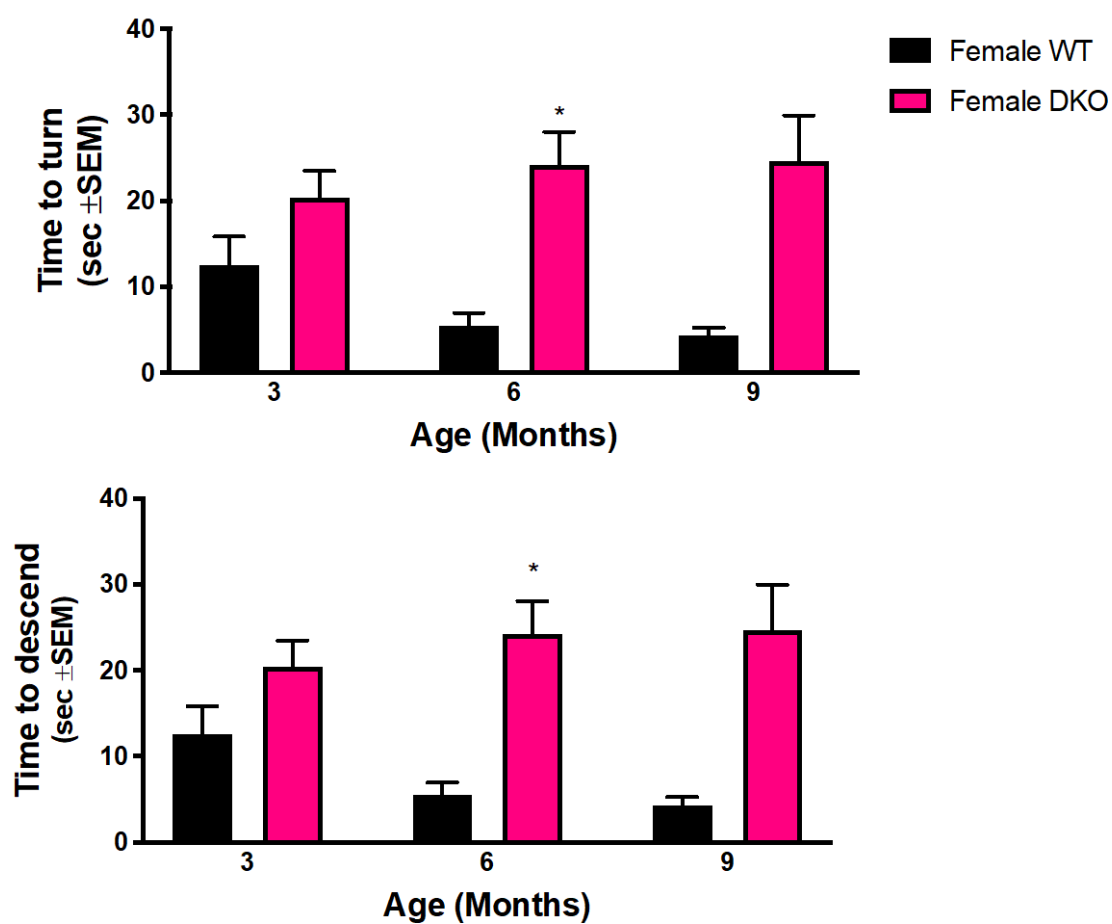


**Figure 4.10 Agility and bradykinesia in DKO females.**

Pole test time to turn values (A). Pole test time to descend (B). Failure in performing one or both tasks was recorded as 60 sec. Each rat repeated the task five times. \*( $p < 0.05$ ), significantly different from WT, 2-way Repeated Measure ANOVA, followed by Sidak multiple comparisons. Data are represented as mean  $\pm$  SEM (n=4-6).

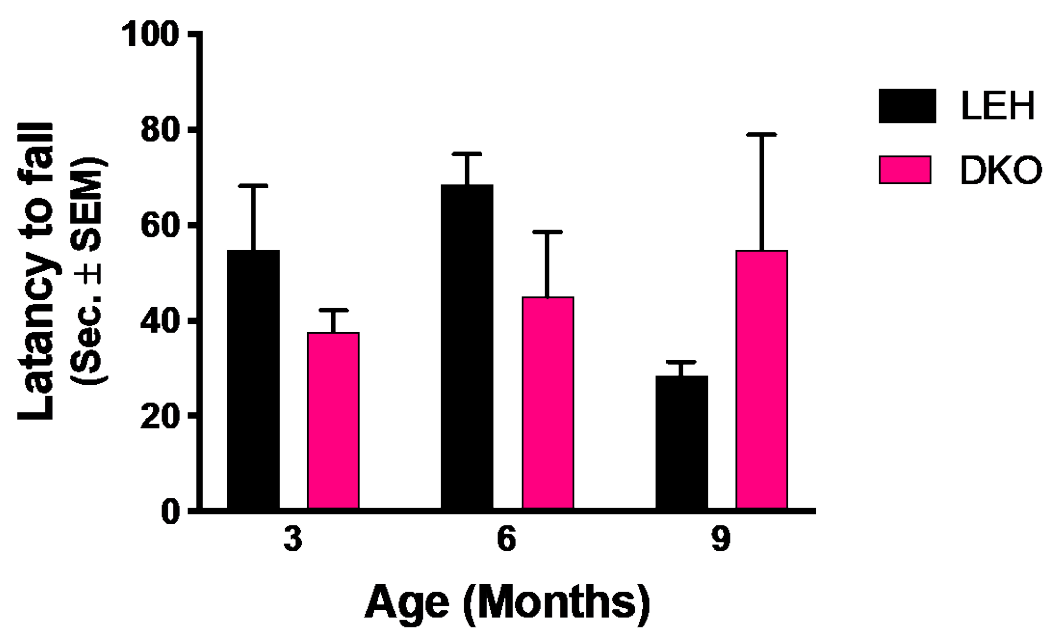


**Figure 4.11 Motor coordination in DKO females.**

Motor coordination was assessed using rotarod and latency to fall values are shown. Data are from 4-6 rats, with each rat tested three times. Two-way Repeated Measure ANOVA, followed by Sidak multiple comparisons. Data are represented as mean  $\pm$  SEM (n=4-6).

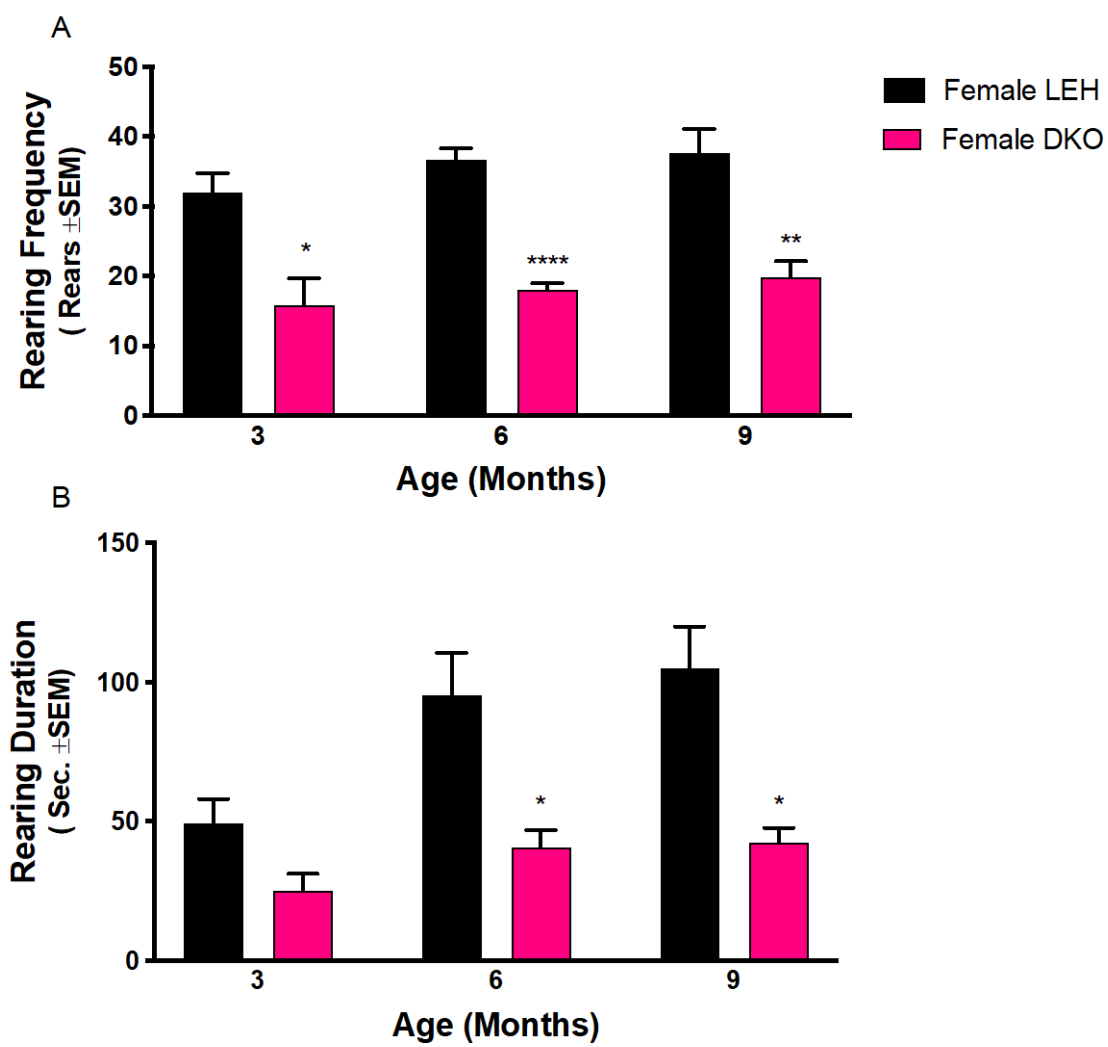


**Figure 4.12 Reduction in hind-limb strength of female DKO.**

Hind-limb strength determined by measuring rearing frequency (A) and rearing duration (B) over 3 minutes. \*( $p < 0.05$ ); \*\*( $p < 0.01$ ); \*\*\*\*( $p < 0.0001$ ) significantly different. All values are expressed as the mean  $\pm$  SEM. The difference between groups was analyzed using unpaired t test with Welch's correction ( $n=4-6$ ).



# Chapter 5

## Summary and Future Directions

## 5.1 Conclusions

Throughout this dissertation, much effort has been made to describe the development in PD research from model generation to characterization. The reason and excuses behind this effort is the amount of neurotoxin induced end-stage PD research, which proven unproductive at least nowadays in curative therapies. At least two centuries have passed since James Parkinson described the disease in 1817; we still do not know the exact etiology of the disease, and we are still describing symptomatic treatments that have many side effects. So, patients do not only suffer from the disease itself, but also side effects from what is supposed to improve their condition. I believe that this deficiency of our knowledge comes from our limited understanding of the disease. Unfortunately, this is applicable not to PD only but to many other neurodegenerative disorders.

It would not be fair to completely ignore the importance of end-stage PD models in what we have already learned so far. Nonetheless, these models are not useful to understand the progression and neurobiology of the PD that could help identify pathways or specific proteins that could be a potential therapeutic target to stop or slow down the progression of the disease, or help in the diagnosis of PD. To achieve this goal, an animal model with high reproducibility rate is required.

Neurotoxins have emphasized the importance of the mitochondria in the disease. The generation of single KO models of mitochondrial genes was the first step to emphasize the importance of mitochondrial health in PD. Also, the generation of PINK1 KO and Parkin KO shed the light over the importance of the

quality control mechanisms of the mitochondria. Despite that the presence of both genes is critical to clear damaged mitochondria via mitophagy, rats KO of PINK1 or Parkin do not exhibit similar pathological characteristics since PINK1 KO rat exhibited motor deficits and degeneration in dopaminergic neurons while Parkin KO did not. Those results raised questions about Parkin importance and whether neurons have alternative mechanisms to overcome the loss of Parkin. To answer those questions, a DKO of both PINK1 and Parkin in a rat model was generated. We found that DKO neurodegeneration and motor deficits happened earlier than in PINK1 KO, which means that knocking out Parkin alone is not as crucial as in the absence of PINK1. In this study we focused on characterizing the motor behavior; however, degeneration in the VTA found requires extensive examination of the rat's memory, reward, and other non-motor behavior.

Since Pink1 and Parkin are important for mitochondrial quality control and neurotransmitter release is bioenergetically demanding, striatal nerve terminals (a portion which would be derived from SNpc projections) were isolated and metabolic function was measured using the Seahorse XF<sup>®</sup>96 analyzer. Only 3-month-old rats exhibited mitochondrial dysfunction without changes in ECAR (glycolysis). Thus, an energetic crisis due to mitochondrial dysfunction at the nerve terminal precedes and may contribute to dopaminergic neuron death in the SNpc. On the contrary, striatal nerve terminals from older (6 and 8 months) DKO rats show bioenergetic function (mitochondrial and glycolytic) similar to age-matched WT rats. Since dopaminergic neuronal death is significant at 6 and 8 months in DKO rats, it is possible that the associated nerve terminals in the

striatum containing dysfunctional mitochondria at 3 months have already deteriorated and been cleared by microglia leaving only nerve terminals with healthy mitochondria. Alternatively, the nerve terminals containing dysfunctional mitochondria might have become more fragile and been lost during the isolation procedure in the older animals. It is also possible that compensatory mechanisms in the context of Pink1 and Parkin deficiency have resulted in a return of the dysfunctional mitochondria to a functional state. Future work is required to uncover the exact mechanism of bioenergetic dysfunction in these rats. Additionally, synaptic mitochondria isolated from 3-month-old PINK1 deficient rats exhibited a reduction in complex I-driven respiration and an increase in complex II-mediated respiration. In contrary, synaptic mitochondria isolated from the same age in Parkin KO did not display alteration of either the respiration or the electron transport chain function.

## **5.2 Stress**

Oxidative stress contributes to the cascade causing dopaminergic neurons' death in PD. However, it has been found that there is higher basal level of oxidative stress in the SNpc in PD patients compared to a normal brain [286]. I think future experiments using DKO rats should involve the administration of drugs known to induce stress, e.g. methamphetamine, which also affects dopaminergic systems. All behavioral experiments conducted by us were done under normal conditions, or in another words, in the absence of external stressors. I think studying the function, morphology, and proteome of the

mitochondria following stress will help us see how the mitochondria will handle the stress. Also, it will be exciting to see if stress would accelerate the degeneration of dopaminergic neurons in the SNpc, leading to earlier motor deficits. Clearly, people with PD have been exposed to a variety of stressors throughout life, and such studies may help clarify which ones contribute to the pathogenesis of the disease.

### **5.3 Exercise**

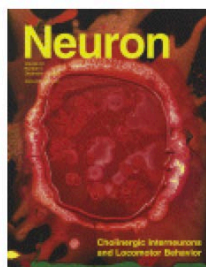
So far, there is no cure for PD, and treatments (e.g. dopamine replacement with L-DOPA and deep brain stimulation affecting neuronal networks) help with symptoms but do not affect the course of disease. Interestingly, exercise and physical activity has been shown to be beneficial in the management of PD by affecting different neurotransmitters including dopamine [287, 288]. In addition to PD, the variety of animal models of brain injury have shown that exercise can promote neuroplasticity and behavioral recovery in different areas of the brain like the hippocampus, cortex, and spinal cord, but the mechanism how training can do so is still to be explored [289]. Furthermore, exercise can significantly improve skeletal muscle's mitochondrial functions in PD patients exposed to high-intensity exercise compared to pre-training mitochondrial function [290]. Finally, the mechanism of how exercise can promote mitochondrial function is not yet known, and I think this future experiment idea may give a new insight on how exercise triggers mitochondrial function.

#### **5.4 Ideal animal model**

In general, there is no best model PD and it all depends on what we are trying to study. For example, MPTP works greatly to test dopamine replacement therapy, but if we wanted to study the disease progression it may not be very helpful. However, I think in order to be both a good model of human PD and good test model for new therapies, the model should have number of characteristic features. First, the model should have normal dopaminergic neuronal count in their early stage of life, which gradually decreased in adulthood. Second, the model should display motor deficits, including the cardinal symptoms of PD in human: bradykinesia, rigidity, resting tremor, and gait abnormality. Third, presence of Lewy bodies neuropathology. Fourth, the model should have a relatively short disease course.

In order to better understand a better animal model was required. The studies here generated and used a novel rat models of specific mitochondrial proteins mutations to assess neurodegeneration, motor deficits, proteomics and mitochondrial function. These models will help improving our understanding of the neuropathology and it could be a candidate to examine new therapeutic strategies.

# Appendix



## Thank you for your order!

Dear Mr. Mohannad Almikhlafi,

Thank you for placing your order through Copyright Clearance Center's RightsLink® service.

### Order Summary

Licensee:	University of Nebraska Medical Center
Order Date:	Dec 26, 2019
Order Number:	4736540268459
Publication:	Neuron
Title:	Parkinson's Disease Mechanisms and Models
Type of Use:	reuse in a thesis/dissertation
Order Total:	0.00 USD

View or [print](#) complete [details \[s100.copyright.com\]](https://s100.copyright.com/details) of your order and the publisher's terms and conditions.

Sincerely,

Copyright Clearance Center





## Thank you for your order!

Dear Mr. Mohannad Almikhlafi,

Thank you for placing your order through Copyright Clearance Center's RightsLink® service.

### Order Summary

Licensee: University of Nebraska Medical Center  
Order Date: Dec 23, 2019  
Order Number: 4734971413271  
Publication: Drug Discovery Today: Disease Models  
Title: Refinement of the MPTP model for Parkinson's disease in the marmoset  
Type of Use: reuse in a thesis/dissertation  
Order Total: 0.00 USD

View or [print](#) complete [details \[s100.copyright.com\]](https://s100.copyright.com) of your order and the publisher's terms and conditions.

Sincerely,

Copyright Clearance Center



## Thank you for your order!

Dear Mr. Mohannad Almikhlaifi,

Thank you for placing your order through Copyright Clearance Center's RightsLink® service.

### Order Summary

Licensee: University of Nebraska Medical Center  
Order Date: Dec 23, 2019  
Order Number: 4734920722703  
Publication: Nature Cell Biology  
Title: Mechanisms of mitophagy in cellular homeostasis, physiology and pathology  
Type of Use: Thesis/Dissertation  
Order Total: 0.00 USD

View or [print](#) complete [details \[s100.copyright.com\]](https://s100.copyright.com) of your order and the publisher's terms and conditions.

Sincerely,

Copyright Clearance Center

## References:

1. Parkinson, J., An essay on the shaking palsy. 1817. *J Neuropsychiatry Clin Neurosci*, 2002. 14(2): p. 223-36; discussion 222.
2. J-M, C., On Parkinson's disease. In *Lectures on diseases of the nervous system delivered at the Salpêtrière*. New Sydenham Society, London, 1872: p. pp. 129–156.
3. Richer, P. and H. Meige, *Etude morphologique sur la maladie de Parkinson*. *Nouvelle iconographie de la Salpêtrière*, 1895. 8: p. 361-371.
4. Babinski, J., B. Jarkowski, and X. Plichet, Kinésie paradoxale. Mutisme parkinsonien. *Rev Neurol*, 1921. 37: p. 1266-1270.
5. E, B., *Leçons sur les maladies nerveuses*. Masson, Paris, 1925.
6. C, T., Contribution à l'étude de l'anatomie du locus niger. *Rev Neurol*, 1921. 37: p. 592–608.
7. Foix MC, N.J., *Les noyaux gris centraux et la région mesencéphalo-sous-optique*. Masson, Paris. 1925.
8. Greenfield, J.G. and F.D. Bosanquet, The brain-stem lesions in Parkinsonism. *J Neurol Neurosurg Psychiatry*, 1953. 16(4): p. 213-26.
9. Cotzias, G.C., P.S. Papavasiliou, and R. Gellene, Modification of Parkinsonism—chronic treatment with L-dopa. *New England Journal of Medicine*, 1969. 280(7): p. 337-345.
10. Barbeau, A., L-dopa therapy in Parkinson's disease: a critical review of nine years' experience. *Canadian Medical Association Journal*, 1969. 101(13): p. 59.

11. Yahr, M.D., et al., Treatment of parkinsonism with levodopa. Archives of neurology, 1969. 21(4): p. 343-354.
12. Miller, D.B. and J.P. O'Callaghan, Biomarkers of Parkinson's disease: present and future. Metabolism, 2015. 64(3 Suppl 1): p. S40-6.
13. Miller, I.N. and A. Cronin-Golomb, Gender differences in Parkinson's disease: clinical characteristics and cognition. Mov Disord, 2010. 25(16): p. 2695-703.
14. Hirsch, L., et al., The Incidence of Parkinson's Disease: A Systematic Review and Meta-Analysis. Neuroepidemiology, 2016. 46(4): p. 292-300.
15. Marras, C., et al., Prevalence of Parkinson's disease across North America. NPJ Parkinsons Dis, 2018. 4: p. 21.
16. Van Den Eeden, S.K., et al., Incidence of Parkinson's disease: variation by age, gender, and race/ethnicity. Am J Epidemiol, 2003. 157(11): p. 1015-22.
17. Pringsheim, T., et al., The prevalence of Parkinson's disease: a systematic review and meta-analysis. Mov Disord, 2014. 29(13): p. 1583-90.
18. Seidler, A., et al., Possible environmental, occupational, and other etiologic factors for Parkinson's disease: a case-control study in Germany. Neurology, 1996. 46(5): p. 1275-84.
19. Gatto, N.M., et al., Well-water consumption and Parkinson's disease in rural California. Environ Health Perspect, 2009. 117(12): p. 1912-8.
20. Ziering, A. and J. Lee, Piperidine derivatives; 1,3-dialkyl-4-aryl-4-acyloxypiperidines. J Org Chem, 1947. 12(6): p. 911-4.

21. Langston, J.W., et al., 1-Methyl-4-phenylpyridinium ion (MPP<sup>+</sup>): identification of a metabolite of MPTP, a toxin selective to the substantia nigra. *Neurosci Lett*, 1984. 48(1): p. 87-92.
22. Langston, J.W., et al., Chronic Parkinsonism in humans due to a product of meperidine-analog synthesis. *Science*, 1983. 219(4587): p. 979-80.
23. Watanabe, Y., T. Himeda, and T. Araki, Mechanisms of MPTP toxicity and their implications for therapy of Parkinson's disease. *Med Sci Monit*, 2005. 11(1): p. RA17-23.
24. Polymeropoulos, M.H., et al., Mutation in the alpha-synuclein gene identified in families with Parkinson's disease. *Science*, 1997. 276(5321): p. 2045-7.
25. Kitada, T., et al., Mutations in the parkin gene cause autosomal recessive juvenile parkinsonism. *Nature*, 1998. 392(6676): p. 605-8.
26. Gasser, T., et al., A susceptibility locus for Parkinson's disease maps to chromosome 2p13. *Nat Genet*, 1998. 18(3): p. 262-5.
27. Singleton, A.B., et al., alpha-Synuclein locus triplication causes Parkinson's disease. *Science*, 2003. 302(5646): p. 841.
28. Leroy, E., et al., The ubiquitin pathway in Parkinson's disease. *Nature*, 1998. 395(6701): p. 451-2.
29. Valente, E.M., et al., Hereditary early-onset Parkinson's disease caused by mutations in PINK1. *Science*, 2004. 304(5674): p. 1158-60.
30. Bonifati, V., et al., DJ-1 ( PARK7), a novel gene for autosomal recessive, early onset parkinsonism. *Neurol Sci*, 2003. 24(3): p. 159-60.

31. Paisan-Ruiz, C., et al., Cloning of the gene containing mutations that cause PARK8-linked Parkinson's disease. *Neuron*, 2004. 44(4): p. 595-600.
32. Ramirez, A., et al., Hereditary parkinsonism with dementia is caused by mutations in ATP13A2, encoding a lysosomal type 5 P-type ATPase. *Nat Genet*, 2006. 38(10): p. 1184-91.
33. Hicks, A.A., et al., A susceptibility gene for late-onset idiopathic Parkinson's disease. *Ann Neurol*, 2002. 52(5): p. 549-55.
34. Pankratz, N., et al., Genome screen to identify susceptibility genes for Parkinson disease in a sample without parkin mutations. *Am J Hum Genet*, 2002. 71(1): p. 124-35.
35. Strauss, K.M., et al., Loss of function mutations in the gene encoding Omi/HtrA2 in Parkinson's disease. *Hum Mol Genet*, 2005. 14(15): p. 2099-111.
36. Funayama, M., et al., CHCHD2 mutations in autosomal dominant late-onset Parkinson's disease: a genome-wide linkage and sequencing study. *Lancet Neurol*, 2015. 14(3): p. 274-82.
37. Gelb, D.J., E. Oliver, and S. Gilman, Diagnostic criteria for Parkinson disease. *Arch Neurol*, 1999. 56(1): p. 33-9.
38. Weintraub, D., C.L. Comella, and S. Horn, Parkinson's disease--Part 1: Pathophysiology, symptoms, burden, diagnosis, and assessment. *Am J Manag Care*, 2008. 14(2 Suppl): p. S40-8.

39. Gibb, W.R. and A.J. Lees, The relevance of the Lewy body to the pathogenesis of idiopathic Parkinson's disease. *J Neurol Neurosurg Psychiatry*, 1988. 51(6): p. 745-52.
40. Hoehn, M.M. and M.D. Yahr, Parkinsonism: onset, progression and mortality. *Neurology*, 1967. 17(5): p. 427-42.
41. Remy, P., et al., Depression in Parkinson's disease: loss of dopamine and noradrenaline innervation in the limbic system. *Brain*, 2005. 128(Pt 6): p. 1314-22.
42. Bowers, D., et al., Startling facts about emotion in Parkinson's disease: blunted reactivity to aversive stimuli. *Brain*, 2006. 129(Pt 12): p. 3356-65.
43. Chen, J.J., Parkinson's disease: health-related quality of life, economic cost, and implications of early treatment. *Am J Manag Care*, 2010. 16 Suppl Implications: p. S87-93.
44. Cools, R., et al., Mechanisms of cognitive set flexibility in Parkinson's disease. *Brain*, 2001. 124(Pt 12): p. 2503-12.
45. Shulman, L.M., et al., Non-recognition of depression and other non-motor symptoms in Parkinson's disease. *Parkinsonism Relat Disord*, 2002. 8(3): p. 193-7.
46. Bernheimer, H., et al., Brain dopamine and the syndromes of Parkinson and Huntington. Clinical, morphological and neurochemical correlations. *J Neurol Sci*, 1973. 20(4): p. 415-55.
47. Braak, H. and E. Braak, Pathoanatomy of Parkinson's disease. *J Neurol*, 2000. 247 Suppl 2: p. II3-10.

48. De Boer, W.J., P.J. Besten, and C.F. Ter Braak, Statistical analysis of sediment toxicity by additive monotone regression splines. *Ecotoxicology*, 2002. 11(6): p. 435-50.
49. Doty, R.L., Olfaction in Parkinson's disease and related disorders. *Neurobiol Dis*, 2012. 46(3): p. 527-52.
50. Ross, G.W., et al., Association of olfactory dysfunction with risk for future Parkinson's disease. *Ann Neurol*, 2008. 63(2): p. 167-73.
51. Amara, A.W., et al., Longitudinal assessment of excessive daytime sleepiness in early Parkinson's disease. *J Neurol Neurosurg Psychiatry*, 2017. 88(8): p. 653-662.
52. Hawkes, C.H., K. Del Tredici, and H. Braak, A timeline for Parkinson's disease. *Parkinsonism Relat Disord*, 2010. 16(2): p. 79-84.
53. Edwards, L.L., E.M. Quigley, and R.F. Pfeiffer, Gastrointestinal dysfunction in Parkinson's disease: frequency and pathophysiology. *Neurology*, 1992. 42(4): p. 726-32.
54. Abbott, R.D., et al., Bowel movement frequency in late-life and incidental Lewy bodies. *Mov Disord*, 2007. 22(11): p. 1581-6.
55. Sutcliffe, J.G. and L. de Lecea, The hypocretins: excitatory neuromodulatory peptides for multiple homeostatic systems, including sleep and feeding. *J Neurosci Res*, 2000. 62(2): p. 161-8.
56. Kayama, Y. and Y. Koyama, Control of sleep and wakefulness by brainstem monoaminergic and cholinergic neurons. *Acta Neurochir Suppl*, 2003. 87: p. 3-6.



57. Klimek, V., et al., Reduced levels of norepinephrine transporters in the locus coeruleus in major depression. *J Neurosci*, 1997. 17(21): p. 8451-8.
58. Ben-Shlomo, Y. and M.G. Marmot, Survival and cause of death in a cohort of patients with parkinsonism: possible clues to aetiology? *J Neurol Neurosurg Psychiatry*, 1995. 58(3): p. 293-9.
59. Fearnley, J.M. and A.J. Lees, Ageing and Parkinson's disease: substantia nigra regional selectivity. *Brain*, 1991. 114 ( Pt 5): p. 2283-301.
60. Chateau, D. and C.L. Aron, Heterotypic sexual behavior in male rats after lesions in different amygdaloid nuclei. *Horm Behav*, 1988. 22(3): p. 379-87.
61. Weiss, F. and G.F. Koob, Drug addiction: functional neurotoxicity of the brain reward systems. *Neurotox Res*, 2001. 3(1): p. 145-56.
62. Braak, H., et al., Stages in the development of Parkinson's disease-related pathology. *Cell Tissue Res*, 2004. 318(1): p. 121-34.
63. Baba, M., et al., Aggregation of alpha-synuclein in Lewy bodies of sporadic Parkinson's disease and dementia with Lewy bodies. *Am J Pathol*, 1998. 152(4): p. 879-84.
64. Spillantini, M.G., et al., Alpha-synuclein in Lewy bodies. *Nature*, 1997. 388(6645): p. 839-40.
65. Kuzuhara, S., et al., Lewy bodies are ubiquitinated. A light and electron microscopic immunocytochemical study. *Acta Neuropathol*, 1988. 75(4): p. 345-53.

66. Uhl, G.R., et al., Dopamine transporter messenger RNA in Parkinson's disease and control substantia nigra neurons. *Ann Neurol*, 1994. 35(4): p. 494-8.
67. Marsden, C.D., Neuromelanin and Parkinson's disease. *J Neural Transm Suppl*, 1983. 19: p. 121-41.
68. Caminiti, S.P., et al., Axonal damage and loss of connectivity in nigrostriatal and mesolimbic dopamine pathways in early Parkinson's disease. *Neuroimage Clin*, 2017. 14: p. 734-740.
69. Uhl, G.R., J.C. Hedreen, and D.L. Price, Parkinson's disease: loss of neurons from the ventral tegmental area contralateral to therapeutic surgical lesions. *Neurology*, 1985. 35(8): p. 1215-8.
70. Gibb, W.R. and A.J. Lees, Anatomy, pigmentation, ventral and dorsal subpopulations of the substantia nigra, and differential cell death in Parkinson's disease. *J Neurol Neurosurg Psychiatry*, 1991. 54(5): p. 388-96.
71. Calabresi, P., et al., Direct and indirect pathways of basal ganglia: a critical reappraisal. *Nat Neurosci*, 2014. 17(8): p. 1022-30.
72. Dyall, S.D., M.T. Brown, and P.J. Johnson, Ancient invasions: from endosymbionts to organelles. *Science*, 2004. 304(5668): p. 253-7.
73. Wallace, D.C., A mitochondrial paradigm of metabolic and degenerative diseases, aging, and cancer: a dawn for evolutionary medicine. *Annu Rev Genet*, 2005. 39: p. 359-407.

74. Lin, M.T. and M.F. Beal, Mitochondrial dysfunction and oxidative stress in neurodegenerative diseases. *Nature*, 2006. 443(7113): p. 787-95.
75. Rugarli, E.I. and T. Langer, Mitochondrial quality control: a matter of life and death for neurons. *EMBO J*, 2012. 31(6): p. 1336-49.
76. Rolfe, D.F. and G.C. Brown, Cellular energy utilization and molecular origin of standard metabolic rate in mammals. *Physiol Rev*, 1997. 77(3): p. 731-58.
77. Mattson, M.P., M. Gleichmann, and A. Cheng, Mitochondria in neuroplasticity and neurological disorders. *Neuron*, 2008. 60(5): p. 748-66.
78. Palikaras, K., E. Lionaki, and N. Tavernarakis, Mechanisms of mitophagy in cellular homeostasis, physiology and pathology. *Nat Cell Biol*, 2018. 20(9): p. 1013-1022.
79. Lewis, M.R. and W.H. Lewis, Mitochondria in Tissue Culture. *Science*, 1914. 39(1000): p. 330-3.
80. Ashford, T.P. and K.R. Porter, Cytoplasmic components in hepatic cell lysosomes. *J Cell Biol*, 1962. 12: p. 198-202.
81. Scott, S.V. and D.J. Klionsky, Delivery of proteins and organelles to the vacuole from the cytoplasm. *Curr Opin Cell Biol*, 1998. 10(4): p. 523-9.
82. Khaminets, A., C. Behl, and I. Dikic, Ubiquitin-Dependent And Independent Signals In Selective Autophagy. *Trends Cell Biol*, 2016. 26(1): p. 6-16.
83. Shen, R.S., et al., Serotonergic conversion of MPTP and dopaminergic accumulation of MPP+. *FEBS Lett*, 1985. 189(2): p. 225-30.

84. Hasegawa, E., et al., 1-Methyl-4-phenylpyridinium (MPP+) induces NADH-dependent superoxide formation and enhances NADH-dependent lipid peroxidation in bovine heart submitochondrial particles. *Biochem Biophys Res Commun*, 1990. 170(3): p. 1049-55.
85. Chiueh, C.C., H. Miyake, and M.T. Peng, Role of dopamine autoxidation, hydroxyl radical generation, and calcium overload in underlying mechanisms involved in MPTP-induced parkinsonism. *Adv Neurol*, 1993. 60: p. 251-8.
86. Chiueh, C.C. and P. Rauhala, Free radicals and MPTP-induced selective destruction of substantia nigra compacta neurons. *Adv Pharmacol*, 1998. 42: p. 796-800.
87. Bezard, E., C. Imbert, and C.E. Gross, Experimental models of Parkinson's disease: from the static to the dynamic. *Rev Neurosci*, 1998. 9(2): p. 71-90.
88. Przedborski, S., et al., The parkinsonian toxin 1-methyl-4-phenyl-1,2,3,6-tetrahydropyridine (MPTP): a technical review of its utility and safety. *J Neurochem*, 2001. 76(5): p. 1265-74.
89. Langston, J.W., E.B. Langston, and I. Irwin, MPTP-induced parkinsonism in human and non-human primates--clinical and experimental aspects. *Acta Neurol Scand Suppl*, 1984. 100: p. 49-54.
90. Burns, R.S., et al., The neurotoxicity of 1-methyl-4-phenyl-1,2,3,6-tetrahydropyridine in the monkey and man. *Can J Neurol Sci*, 1984. 11(1 Suppl): p. 166-8.

91. Riachi, N.J., et al., On the mechanisms underlying 1-methyl-4-phenyl-1,2,3,6-tetrahydropyridine neurotoxicity. II. Susceptibility among mammalian species correlates with the toxin's metabolic patterns in brain microvessels and liver. *J Pharmacol Exp Ther*, 1988. 244(2): p. 443-8.
92. Riachi, N.J., J.C. LaManna, and S.I. Harik, Entry of 1-methyl-4-phenyl-1,2,3,6-tetrahydropyridine into the rat brain. *J Pharmacol Exp Ther*, 1989. 249(3): p. 744-8.
93. Ungerstedt, U., 6-Hydroxy-dopamine induced degeneration of central monoamine neurons. *Eur J Pharmacol*, 1968. 5(1): p. 107-10.
94. Blum, D., et al., Molecular pathways involved in the neurotoxicity of 6-OHDA, dopamine and MPTP: contribution to the apoptotic theory in Parkinson's disease. *Prog Neurobiol*, 2001. 65(2): p. 135-72.
95. Bezard, E. and S. Przedborski, A tale on animal models of Parkinson's disease. *Mov Disord*, 2011. 26(6): p. 993-1002.
96. Malmfors, T. and C. Sachs, Degeneration of adrenergic nerves produced by 6-hydroxydopamine. *Eur J Pharmacol*, 1968. 3(1): p. 89-92.
97. Faull, R.L. and R. Lavery, Changes in dopamine levels in the corpus striatum following lesions in the substantia nigra. *Exp Neurol*, 1969. 23(3): p. 332-40.
98. Jeon, B.S., V. Jackson-Lewis, and R.E. Burke, 6-Hydroxydopamine lesion of the rat substantia nigra: time course and morphology of cell death. *Neurodegeneration*, 1995. 4(2): p. 131-7.

99. Angioni, A., L. Porcu, and F. Pirisi, LC/DAD/ESI/MS method for the determination of imidacloprid, thiacloprid, and spinosad in olives and olive oil after field treatment. *J Agric Food Chem*, 2011. 59(20): p. 11359-66.
100. Betarbet, R., et al., Chronic systemic pesticide exposure reproduces features of Parkinson's disease. *Nat Neurosci*, 2000. 3(12): p. 1301-6.
101. Higgins, D.S., Jr. and J.T. Greenamyre, [3H]dihydrorotenone binding to NADH: ubiquinone reductase (complex I) of the electron transport chain: an autoradiographic study. *J Neurosci*, 1996. 16(12): p. 3807-16.
102. Heikkila, R.E., et al., Dopaminergic toxicity of rotenone and the 1-methyl-4-phenylpyridinium ion after their stereotaxic administration to rats: implication for the mechanism of 1-methyl-4-phenyl-1,2,3,6-tetrahydropyridine toxicity. *Neurosci Lett*, 1985. 62(3): p. 389-94.
103. Ferrante, R.J., et al., Systemic administration of rotenone produces selective damage in the striatum and globus pallidus, but not in the substantia nigra. *Brain Res*, 1997. 753(1): p. 157-62.
104. Zhu, C., et al., Variable effects of chronic subcutaneous administration of rotenone on striatal histology. *J Comp Neurol*, 2004. 478(4): p. 418-26.
105. Vaccari, C., R. El Dib, and J.L.V. de Camargo, Paraquat and Parkinson's disease: a systematic review protocol according to the OHAT approach for hazard identification. *Syst Rev*, 2017. 6(1): p. 98.
106. Richardson, J.R., et al., Paraquat neurotoxicity is distinct from that of MPTP and rotenone. *Toxicol Sci*, 2005. 88(1): p. 193-201.

107. Kang, M.J., S.J. Gil, and H.C. Koh, Paraquat induces alternation of the dopamine catabolic pathways and glutathione levels in the substantia nigra of mice. *Toxicol Lett*, 2009. 188(2): p. 148-52.
108. Corasaniti, M.T., et al., Evidence that paraquat is able to cross the blood-brain barrier to a different extent in rats of various age. *Funct Neurol*, 1991. 6(4): p. 385-91.
109. McCormack, A.L., et al., Environmental risk factors and Parkinson's disease: selective degeneration of nigral dopaminergic neurons caused by the herbicide paraquat. *Neurobiol Dis*, 2002. 10(2): p. 119-27.
110. Thiruchelvam, M., et al., Age-related irreversible progressive nigrostriatal dopaminergic neurotoxicity in the paraquat and maneb model of the Parkinson's disease phenotype. *Eur J Neurosci*, 2003. 18(3): p. 589-600.
111. Fleming, S.M., et al., Early and progressive sensorimotor anomalies in mice overexpressing wild-type human alpha-synuclein. *J Neurosci*, 2004. 24(42): p. 9434-40.
112. Rockenstein, E., et al., Differential neuropathological alterations in transgenic mice expressing alpha-synuclein from the platelet-derived growth factor and Thy-1 promoters. *J Neurosci Res*, 2002. 68(5): p. 568-78.
113. Yamada, M., et al., Overexpression of alpha-synuclein in rat substantia nigra results in loss of dopaminergic neurons, phosphorylation of alpha-synuclein and activation of caspase-9: resemblance to pathogenetic changes in Parkinson's disease. *J Neurochem*, 2004. 91(2): p. 451-61.

114. Xu, J., et al., Dopamine-dependent neurotoxicity of alpha-synuclein: a mechanism for selective neurodegeneration in Parkinson disease. *Nat Med*, 2002. 8(6): p. 600-6.
115. Kamp, F., et al., Inhibition of mitochondrial fusion by alpha-synuclein is rescued by PINK1, Parkin and DJ-1. *EMBO J*, 2010. 29(20): p. 3571-89.
116. Martin, L.J., et al., Parkinson's disease alpha-synuclein transgenic mice develop neuronal mitochondrial degeneration and cell death. *J Neurosci*, 2006. 26(1): p. 41-50.
117. Caughey, B. and P.T. Lansbury, Protofibrils, pores, fibrils, and neurodegeneration: separating the responsible protein aggregates from the innocent bystanders. *Annu Rev Neurosci*, 2003. 26: p. 267-98.
118. Gisbert, S., et al., Transgenic mice expressing mutant A53T human alpha-synuclein show neuronal dysfunction in the absence of aggregate formation. *Mol Cell Neurosci*, 2003. 24(2): p. 419-29.
119. Funayama, M., et al., A new locus for Parkinson's disease (PARK8) maps to chromosome 12p11.2-q13.1. *Ann Neurol*, 2002. 51(3): p. 296-301.
120. Wszolek, Z.K., et al., German-Canadian family (family A) with parkinsonism, amyotrophy, and dementia - Longitudinal observations. *Parkinsonism Relat Disord*, 1997. 3(3): p. 125-39.
121. Wszolek, Z.K., et al., Western Nebraska family (family D) with autosomal dominant parkinsonism. *Neurology*, 1995. 45(3 Pt 1): p. 502-5.
122. De Wit, T., V. Baekelandt, and E. Lobbestael, LRRK2 Phosphorylation: Behind the Scenes. *Neuroscientist*, 2018. 24(5): p. 486-500.



123. Mandemakers, W., et al., LRRK2 expression is enriched in the striosomal compartment of mouse striatum. *Neurobiol Dis*, 2012. 48(3): p. 582-93.
124. Moehle, M.S., et al., LRRK2 inhibition attenuates microglial inflammatory responses. *J Neurosci*, 2012. 32(5): p. 1602-11.
125. Piccoli, G., et al., LRRK2 controls synaptic vesicle storage and mobilization within the recycling pool. *J Neurosci*, 2011. 31(6): p. 2225-37.
126. Gloeckner, C.J., et al., The Parkinson disease-associated protein kinase LRRK2 exhibits MAPKKK activity and phosphorylates MKK3/6 and MKK4/7, in vitro. *J Neurochem*, 2009. 109(4): p. 959-68.
127. Lee, J.W., et al., Behavioral, neurochemical, and pathologic alterations in bacterial artificial chromosome transgenic G2019S leucine-rich repeated kinase 2 rats. *Neurobiol Aging*, 2015. 36(1): p. 505-18.
128. Herzig, M.C., et al., LRRK2 protein levels are determined by kinase function and are crucial for kidney and lung homeostasis in mice. *Hum Mol Genet*, 2011. 20(21): p. 4209-23.
129. Smith, W.W., et al., Kinase activity of mutant LRRK2 mediates neuronal toxicity. *Nat Neurosci*, 2006. 9(10): p. 1231-3.
130. Wang, X., et al., LRRK2 regulates mitochondrial dynamics and function through direct interaction with DLP1. *Hum Mol Genet*, 2012. 21(9): p. 1931-44.
131. Matsumine, H., et al., Localization of a gene for an autosomal recessive form of juvenile Parkinsonism to chromosome 6q25.2-27. *Am J Hum Genet*, 1997. 60(3): p. 588-96.

132. Hristova, V.A., et al., Identification of a novel Zn<sup>2+</sup>-binding domain in the autosomal recessive juvenile Parkinson-related E3 ligase parkin. *J Biol Chem*, 2009. 284(22): p. 14978-86.
133. Lucking, C.B., et al., Association between early-onset Parkinson's disease and mutations in the parkin gene. *N Engl J Med*, 2000. 342(21): p. 1560-7.
134. Khan, N.L., et al., Parkin disease: a phenotypic study of a large case series. *Brain*, 2003. 126(Pt 6): p. 1279-92.
135. Hedrich, K., et al., Distribution, type, and origin of Parkin mutations: review and case studies. *Mov Disord*, 2004. 19(10): p. 1146-57.
136. Pramstaller, P.P., et al., Lewy body Parkinson's disease in a large pedigree with 77 Parkin mutation carriers. *Ann Neurol*, 2005. 58(3): p. 411-22.
137. Greene, J.C., et al., Mitochondrial pathology and apoptotic muscle degeneration in *Drosophila* parkin mutants. *Proc Natl Acad Sci U S A*, 2003. 100(7): p. 4078-83.
138. Whitworth, A.J., et al., Increased glutathione S-transferase activity rescues dopaminergic neuron loss in a *Drosophila* model of Parkinson's disease. *Proc Natl Acad Sci U S A*, 2005. 102(22): p. 8024-9.
139. Rial, D., et al., Behavioral phenotyping of Parkin-deficient mice: looking for early preclinical features of Parkinson's disease. *PLoS One*, 2014. 9(12): p. e114216.

140. Itier, J.M., et al., Parkin gene inactivation alters behaviour and dopamine neurotransmission in the mouse. *Hum Mol Genet*, 2003. 12(18): p. 2277-91.
141. Perez, F.A. and R.D. Palmiter, Parkin-deficient mice are not a robust model of parkinsonism. *Proc Natl Acad Sci U S A*, 2005. 102(6): p. 2174-9.
142. Dave, K.D., et al., Phenotypic characterization of recessive gene knockout rat models of Parkinson's disease. *Neurobiol Dis*, 2014. 70: p. 190-203.
143. Villeneuve, L.M., et al., Proteomic and functional data sets on synaptic mitochondria from rats with genetic ablation of Parkin. *Data Brief*, 2018. 20: p. 568-572.
144. Stauch, K.L., et al., SWATH-MS proteome profiling data comparison of DJ-1, Parkin, and PINK1 knockout rat striatal mitochondria. *Data Brief*, 2016. 9: p. 589-593.
145. Valente, E.M., et al., Localization of a novel locus for autosomal recessive early-onset parkinsonism, PARK6, on human chromosome 1p35-p36. *Am J Hum Genet*, 2001. 68(4): p. 895-900.
146. Abou-Sleiman, P.M., M.M. Muqit, and N.W. Wood, Expanding insights of mitochondrial dysfunction in Parkinson's disease. *Nat Rev Neurosci*, 2006. 7(3): p. 207-19.
147. Silvestri, L., et al., Mitochondrial import and enzymatic activity of PINK1 mutants associated to recessive parkinsonism. *Hum Mol Genet*, 2005. 14(22): p. 3477-92.

148. Jin, S.M., et al., Mitochondrial membrane potential regulates PINK1 import and proteolytic destabilization by PARL. *J Cell Biol*, 2010. 191(5): p. 933-42.
149. Geisler, S., et al., PINK1/Parkin-mediated mitophagy is dependent on VDAC1 and p62/SQSTM1. *Nat Cell Biol*, 2010. 12(2): p. 119-31.
150. Geisler, S., et al., The PINK1/Parkin-mediated mitophagy is compromised by PD-associated mutations. *Autophagy*, 2010. 6(7): p. 871-8.
151. Shiriha, O.S., M. Song, and G.W. Dorn, 2nd, How mitochondrial dynamism orchestrates mitophagy. *Circ Res*, 2015. 116(11): p. 1835-49.
152. Gispert, S., et al., Parkinson phenotype in aged PINK1-deficient mice is accompanied by progressive mitochondrial dysfunction in absence of neurodegeneration. *PLoS One*, 2009. 4(6): p. e5777.
153. Kitada, T., et al., Impaired dopamine release and synaptic plasticity in the striatum of PINK1-deficient mice. *Proc Natl Acad Sci U S A*, 2007. 104(27): p. 11441-6.
154. Gautier, C.A., T. Kitada, and J. Shen, Loss of PINK1 causes mitochondrial functional defects and increased sensitivity to oxidative stress. *Proc Natl Acad Sci U S A*, 2008. 105(32): p. 11364-9.
155. Stauch, K.L., et al., Loss of Pink1 modulates synaptic mitochondrial bioenergetics in the rat striatum prior to motor symptoms: concomitant complex I respiratory defects and increased complex II-mediated respiration. *Proteomics Clin Appl*, 2016. 10(12): p. 1205-1217.

156. Villeneuve, L.M., et al., Early Expression of Parkinson's Disease-Related Mitochondrial Abnormalities in PINK1 Knockout Rats. *Mol Neurobiol*, 2016. 53(1): p. 171-186.
157. Bonifati, V., et al., Mutations in the DJ-1 gene associated with autosomal recessive early-onset parkinsonism. *Science*, 2003. 299(5604): p. 256-9.
158. Lucas, J.I. and I. Marin, A new evolutionary paradigm for the Parkinson disease gene DJ-1. *Mol Biol Evol*, 2007. 24(2): p. 551-61.
159. Honbou, K., et al., The crystal structure of DJ-1, a protein related to male fertility and Parkinson's disease. *J Biol Chem*, 2003. 278(33): p. 31380-4.
160. Tao, X. and L. Tong, Crystal structure of human DJ-1, a protein associated with early onset Parkinson's disease. *J Biol Chem*, 2003. 278(33): p. 31372-9.
161. Takahashi, K., et al., DJ-1 positively regulates the androgen receptor by impairing the binding of PIASx alpha to the receptor. *J Biol Chem*, 2001. 276(40): p. 37556-63.
162. Niki, T., et al., DJBP: a novel DJ-1-binding protein, negatively regulates the androgen receptor by recruiting histone deacetylase complex, and DJ-1 antagonizes this inhibition by abrogation of this complex. *Mol Cancer Res*, 2003. 1(4): p. 247-61.
163. Shinbo, Y., et al., DJ-1 restores p53 transcription activity inhibited by Topors/p53BP3. *Int J Oncol*, 2005. 26(3): p. 641-8.

164. Xu, J., et al., The Parkinson's disease-associated DJ-1 protein is a transcriptional co-activator that protects against neuronal apoptosis. *Hum Mol Genet*, 2005. 14(9): p. 1231-41.
165. Zhong, N., et al., DJ-1 transcriptionally up-regulates the human tyrosine hydroxylase by inhibiting the sumoylation of pyrimidine tract-binding protein-associated splicing factor. *J Biol Chem*, 2006. 281(30): p. 20940-8.
166. Taira, T., et al., DJ-1 has a role in antioxidative stress to prevent cell death. *EMBO Rep*, 2004. 5(2): p. 213-8.
167. Canet-Aviles, R.M., et al., The Parkinson's disease protein DJ-1 is neuroprotective due to cysteine-sulfinic acid-driven mitochondrial localization. *Proc Natl Acad Sci U S A*, 2004. 101(24): p. 9103-8.
168. Shendelman, S., et al., DJ-1 is a redox-dependent molecular chaperone that inhibits alpha-synuclein aggregate formation. *PLoS Biol*, 2004. 2(11): p. e362.
169. Zhou, W., et al., The oxidation state of DJ-1 regulates its chaperone activity toward alpha-synuclein. *J Mol Biol*, 2006. 356(4): p. 1036-48.
170. Olzmann, J.A., et al., Familial Parkinson's disease-associated L166P mutation disrupts DJ-1 protein folding and function. *J Biol Chem*, 2004. 279(9): p. 8506-15.
171. Koide-Yoshida, S., et al., DJ-1 degrades transthyretin and an inactive form of DJ-1 is secreted in familial amyloidotic polyneuropathy. *Int J Mol Med*, 2007. 19(6): p. 885-93.

172. Chen, J., L. Li, and L.S. Chin, Parkinson disease protein DJ-1 converts from a zymogen to a protease by carboxyl-terminal cleavage. *Hum Mol Genet*, 2010. 19(12): p. 2395-408.
173. Ooe, H., et al., Induction of reactive oxygen species by bisphenol A and abrogation of bisphenol A-induced cell injury by DJ-1. *Toxicol Sci*, 2005. 88(1): p. 114-26.
174. Li, H.M., et al., Association of DJ-1 with chaperones and enhanced association and colocalization with mitochondrial Hsp70 by oxidative stress. *Free Radic Res*, 2005. 39(10): p. 1091-9.
175. Junn, E., et al., Mitochondrial localization of DJ-1 leads to enhanced neuroprotection. *J Neurosci Res*, 2009. 87(1): p. 123-9.
176. Thomas, K.J., et al., DJ-1 acts in parallel to the PINK1/parkin pathway to control mitochondrial function and autophagy. *Hum Mol Genet*, 2011. 20(1): p. 40-50.
177. Olzmann, J.A., et al., Selective enrichment of DJ-1 protein in primate striatal neuronal processes: implications for Parkinson's disease. *J Comp Neurol*, 2007. 500(3): p. 585-99.
178. Kyung, J.W., et al., DJ-1 deficiency impairs synaptic vesicle endocytosis and reavailability at nerve terminals. *Proc Natl Acad Sci U S A*, 2018. 115(7): p. 1629-1634.
179. Annesi, G., et al., DJ-1 mutations and parkinsonism-dementia-amyotrophic lateral sclerosis complex. *Ann Neurol*, 2005. 58(5): p. 803-7.

180. Lev, N., et al., DJ-1 changes in G93A-SOD1 transgenic mice: implications for oxidative stress in ALS. *J Mol Neurosci*, 2009. 38(2): p. 94-102.
181. Fu, K., et al., Familial Parkinson's Disease-Associated L166P Mutant DJ-1 is Cleaved by Mitochondrial Serine Protease Omi/HtrA2. *Neurosci Bull*, 2017. 33(6): p. 685-694.
182. Chen, L., et al., Age-dependent motor deficits and dopaminergic dysfunction in DJ-1 null mice. *J Biol Chem*, 2005. 280(22): p. 21418-26.
183. Meulener, M., et al., Drosophila DJ-1 mutants are selectively sensitive to environmental toxins associated with Parkinson's disease. *Curr Biol*, 2005. 15(17): p. 1572-7.
184. Park, J., et al., Drosophila DJ-1 mutants show oxidative stress-sensitive locomotive dysfunction. *Gene*, 2005. 361: p. 133-9.
185. Yang, Y., et al., Inactivation of Drosophila DJ-1 leads to impairments of oxidative stress response and phosphatidylinositol 3-kinase/Akt signaling. *Proc Natl Acad Sci U S A*, 2005. 102(38): p. 13670-5.
186. Kim, R.H., et al., DJ-1, a novel regulator of the tumor suppressor PTEN. *Cancer Cell*, 2005. 7(3): p. 263-73.
187. Straub, I.R., et al., Loss of CHCHD10-CHCHD2 complexes required for respiration underlies the pathogenicity of a CHCHD10 mutation in ALS. *Hum Mol Genet*, 2018. 27(1): p. 178-189.
188. Shi, C.H., et al., CHCHD2 gene mutations in familial and sporadic Parkinson's disease. *Neurobiol Aging*, 2016. 38: p. 217 e9-217 e13.



189. Aras, S., et al., Oxygen-dependent expression of cytochrome c oxidase subunit 4-2 gene expression is mediated by transcription factors RBPJ, CXXC5 and CHCHD2. *Nucleic Acids Res*, 2013. 41(4): p. 2255-66.
190. Aras, S., et al., MNRR1 (formerly CHCHD2) is a bi-organellar regulator of mitochondrial metabolism. *Mitochondrion*, 2015. 20: p. 43-51.
191. Liu, Y., et al., CHCHD2 inhibits apoptosis by interacting with Bcl-x L to regulate Bax activation. *Cell Death Differ*, 2015. 22(6): p. 1035-46.
192. Longen, S., et al., Systematic analysis of the twin cx(9)c protein family. *J Mol Biol*, 2009. 393(2): p. 356-68.
193. Meng, H., et al., Loss of Parkinson's disease-associated protein CHCHD2 affects mitochondrial crista structure and destabilizes cytochrome c. *Nat Commun*, 2017. 8: p. 15500.
194. Funayama, M., et al., CHCHD2 deficiency leads to mitochondrial dysfunction and increasing oxidative stress in human neuroblastoma SH-SY5Y cells. *Journal of the Neurological Sciences*, 2017. 381: p. 226.
195. Todi, S.V. and H.L. Paulson, Balancing act: deubiquitinating enzymes in the nervous system. *Trends Neurosci*, 2011. 34(7): p. 370-82.
196. Eletr, Z.M. and K.D. Wilkinson, Regulation of proteolysis by human deubiquitinating enzymes. *Biochim Biophys Acta*, 2014. 1843(1): p. 114-28.
197. Ann, E.S., et al., Motor axon terminal regeneration as studied by protein gene product 9.5 immunohistochemistry in the rat. *Arch Histol Cytol*, 1994. 57(4): p. 317-30.

198. Hirata, K., et al., Postnatal development of Schwann cells at neuromuscular junctions, with special reference to synapse elimination. *J Neurocytol*, 1997. 26(12): p. 799-809.
199. Chen, F., et al., Ubiquitin carboxyl-terminal hydrolase L1 is required for maintaining the structure and function of the neuromuscular junction. *Proc Natl Acad Sci U S A*, 2010. 107(4): p. 1636-41.
200. Setsuie, R., et al., Dopaminergic neuronal loss in transgenic mice expressing the Parkinson's disease-associated UCH-L1 I93M mutant. *Neurochem Int*, 2007. 50(1): p. 119-29.
201. Kabuta, T., et al., Aberrant interaction between Parkinson disease-associated mutant UCH-L1 and the lysosomal receptor for chaperone-mediated autophagy. *J Biol Chem*, 2008. 283(35): p. 23731-8.
202. Lowe, J., et al., Ubiquitin carboxyl-terminal hydrolase (PGP 9.5) is selectively present in ubiquitinated inclusion bodies characteristic of human neurodegenerative diseases. *J Pathol*, 1990. 161(2): p. 153-60.
203. Yasuda, T., et al., Effects of UCH-L1 on alpha-synuclein over-expression mouse model of Parkinson's disease. *J Neurochem*, 2009. 108(4): p. 932-44.
204. Smith, J.B. and L. Smith, Energy dependence of sodium-calcium exchange in vascular smooth muscle cells. *Am J Physiol*, 1990. 259(2 Pt 1): p. C302-9.
205. Gong, Y., et al., Pan-cancer genetic analysis identifies PARK2 as a master regulator of G1/S cyclins. *Nat Genet*, 2014. 46(6): p. 588-94.

206. Cesari, R., et al., Parkin, a gene implicated in autosomal recessive juvenile parkinsonism, is a candidate tumor suppressor gene on chromosome 6q25-q27. *Proc Natl Acad Sci U S A*, 2003. 100(10): p. 5956-61.
207. Fujiwara, M., et al., Parkin as a tumor suppressor gene for hepatocellular carcinoma. *Oncogene*, 2008. 27(46): p. 6002-11.
208. Tay, S.P., et al., Parkin enhances the expression of cyclin-dependent kinase 6 and negatively regulates the proliferation of breast cancer cells. *J Biol Chem*, 2010. 285(38): p. 29231-8.
209. Veeriah, S., et al., The familial Parkinson disease gene PARK2 is a multisite tumor suppressor on chromosome 6q25.2-27 that regulates cyclin E. *Cell Cycle*, 2010. 9(8): p. 1451-2.
210. Pugh, T.J., et al., The genetic landscape of high-risk neuroblastoma. *Nat Genet*, 2013. 45(3): p. 279-84.
211. Zesiewicz, T.A., et al., Heart failure in Parkinson's disease: analysis of the United States medicare current beneficiary survey. *Parkinsonism Relat Disord*, 2004. 10(7): p. 417-20.
212. Pennington, S., et al., The cause of death in idiopathic Parkinson's disease. *Parkinsonism Relat Disord*, 2010. 16(7): p. 434-7.
213. Sun, N., et al., Measuring In Vivo Mitophagy. *Mol Cell*, 2015. 60(4): p. 685-96.
214. Zhou, B. and R. Tian, Mitochondrial dysfunction in pathophysiology of heart failure. *J Clin Invest*, 2018. 128(9): p. 3716-3726.

215. Billia, F., et al., PTEN-inducible kinase 1 (PINK1)/Park6 is indispensable for normal heart function. *Proc Natl Acad Sci U S A*, 2011. 108(23): p. 9572-7.
216. Rehm, J., A.V. Samokhvalov, and K.D. Shield, Global burden of alcoholic liver diseases. *J Hepatol*, 2013. 59(1): p. 160-8.
217. Ding, W.X., et al., Autophagy reduces acute ethanol-induced hepatotoxicity and steatosis in mice. *Gastroenterology*, 2010. 139(5): p. 1740-52.
218. King, A.L., et al., Involvement of the mitochondrial permeability transition pore in chronic ethanol-mediated liver injury in mice. *Am J Physiol Gastrointest Liver Physiol*, 2014. 306(4): p. G265-77.
219. Han, D., et al., Dynamic adaptation of liver mitochondria to chronic alcohol feeding in mice: biogenesis, remodeling, and functional alterations. *J Biol Chem*, 2012. 287(50): p. 42165-79.
220. Williams, J.A., et al., Parkin regulates mitophagy and mitochondrial function to protect against alcohol-induced liver injury and steatosis in mice. *Am J Physiol Gastrointest Liver Physiol*, 2015. 309(5): p. G324-40.
221. Wang, H., et al., Double deletion of PINK1 and Parkin impairs hepatic mitophagy and exacerbates acetaminophen-induced liver injury in mice. *Redox Biol*, 2019. 22: p. 101148.
222. Olanow, C.W., J.A. Obeso, and F. Stocchi, Drug insight: Continuous dopaminergic stimulation in the treatment of Parkinson's disease. *Nat Clin Pract Neurol*, 2006. 2(7): p. 382-92.

- 223. Whone, A.L., et al., Slower progression of Parkinson's disease with ropinirole versus levodopa: The REAL-PET study. *Ann Neurol*, 2003. 54(1): p. 93-101.
- 224. Benabid, A.L., et al., Combined (thalamotomy and stimulation) stereotactic surgery of the VIM thalamic nucleus for bilateral Parkinson disease. *Appl Neurophysiol*, 1987. 50(1-6): p. 344-6.
- 225. Bronstein, J.M., et al., Deep brain stimulation for Parkinson disease: an expert consensus and review of key issues. *Arch Neurol*, 2011. 68(2): p. 165.
- 226. Dauer, W. and S. Przedborski, Parkinson's disease: mechanisms and models. *Neuron*, 2003. 39(6): p. 889-909.
- 227. Philippens, I.H., Refinement of the MPTP model for Parkinson's disease in the marmoset. *Drug Discovery Today: Disease Models*, 2017. 25: p. 53-61.
- 228. Okun, M.S., Deep-brain stimulation for Parkinson's disease. *N Engl J Med*, 2012. 367(16): p. 1529-38.
- 229. Jankovic, J., Parkinson's disease: clinical features and diagnosis. *J Neurol Neurosurg Psychiatry*, 2008. 79(4): p. 368-76.
- 230. Klein, C. and A. Westenberger, Genetics of Parkinson's disease. *Cold Spring Harb Perspect Med*, 2012. 2(1): p. a008888.
- 231. Zhang, L., et al., Mitochondrial localization of the Parkinson's disease related protein DJ-1: implications for pathogenesis. *Hum Mol Genet*, 2005. 14(14): p. 2063-73.

232. Nagakubo, D., et al., DJ-1, a novel oncogene which transforms mouse NIH3T3 cells in cooperation with ras. *Biochem Biophys Res Commun*, 1997. 231(2): p. 509-13.
233. Pankratz, N., et al., Mutations in DJ-1 are rare in familial Parkinson disease. *Neurosci Lett*, 2006. 408(3): p. 209-13.
234. Yanagida, T., et al., Oxidative stress induction of DJ-1 protein in reactive astrocytes scavenges free radicals and reduces cell injury. *Oxid Med Cell Longev*, 2009. 2(1): p. 36-42.
235. Mitsumoto, A., et al., Oxidized forms of peroxiredoxins and DJ-1 on two-dimensional gels increased in response to sublethal levels of paraquat. *Free Radic Res*, 2001. 35(3): p. 301-10.
236. Yokota, T., et al., Down regulation of DJ-1 enhances cell death by oxidative stress, ER stress, and proteasome inhibition. *Biochem Biophys Res Commun*, 2003. 312(4): p. 1342-8.
237. Kinumi, T., et al., Cysteine-106 of DJ-1 is the most sensitive cysteine residue to hydrogen peroxide-mediated oxidation in vivo in human umbilical vein endothelial cells. *Biochem Biophys Res Commun*, 2004. 317(3): p. 722-8.
238. Cookson, M.R., Parkinsonism due to mutations in PINK1, parkin, and DJ-1 and oxidative stress and mitochondrial pathways. *Cold Spring Harb Perspect Med*, 2012. 2(9): p. a009415.
239. Dias, V., E. Junn, and M.M. Mouradian, The role of oxidative stress in Parkinson's disease. *J Parkinsons Dis*, 2013. 3(4): p. 461-91.

- 240. Chandran, J.S., et al., Progressive behavioral deficits in DJ-1-deficient mice are associated with normal nigrostriatal function. *Neurobiol Dis*, 2008. 29(3): p. 505-14.
- 241. Grunewald, A., K.R. Kumar, and C.M. Sue, New insights into the complex role of mitochondria in Parkinson's disease. *Prog Neurobiol*, 2018.
- 242. Helley, M.P., et al., Mitochondria: A Common Target for Genetic Mutations and Environmental Toxicants in Parkinson's Disease. *Front Genet*, 2017. 8: p. 177.
- 243. Bose, A. and M.F. Beal, Mitochondrial dysfunction in Parkinson's disease. *J Neurochem*, 2016. 139 Suppl 1: p. 216-231.
- 244. Stauch, K.L., P.R. Purnell, and H.S. Fox, Quantitative proteomics of synaptic and nonsynaptic mitochondria: insights for synaptic mitochondrial vulnerability. *J Proteome Res*, 2014. 13(5): p. 2620-36.
- 245. Stauch, K.L., P.R. Purnell, and H.S. Fox, Aging synaptic mitochondria exhibit dynamic proteomic changes while maintaining bioenergetic function. *Aging (Albany NY)*, 2014. 6(4): p. 320-34.
- 246. Scopes, R.K., Measurement of protein by spectrophotometry at 205 nm. *Anal Biochem*, 1974. 59(1): p. 277-82.
- 247. Huang da, W., B.T. Sherman, and R.A. Lempicki, Systematic and integrative analysis of large gene lists using DAVID bioinformatics resources. *Nat Protoc*, 2009. 4(1): p. 44-57.

- 248. Szklarczyk, D., et al., STRING v11: protein-protein association networks with increased coverage, supporting functional discovery in genome-wide experimental datasets. *Nucleic Acids Res*, 2019. 47(D1): p. D607-D613.
- 249. Shannon, P., et al., Cytoscape: a software environment for integrated models of biomolecular interaction networks. *Genome Res*, 2003. 13(11): p. 2498-504.
- 250. Jassal, B., et al., The reactome pathway knowledgebase. *Nucleic Acids Res*, 2020. 48(D1): p. D498-D503.
- 251. Fabregat, A., et al., The Reactome Pathway Knowledgebase. *Nucleic Acids Res*, 2018. 46(D1): p. D649-D655.
- 252. Scardoni, G., et al., Biological network analysis with CentiScaPe: centralities and experimental dataset integration. *F1000Res*, 2014. 3: p. 139.
- 253. Stepanova, A., et al., Differential susceptibility of mitochondrial complex II to inhibition by oxaloacetate in brain and heart. *Biochim Biophys Acta*, 2016. 1857(9): p. 1561-1568.
- 254. Di Nottia, M., et al., DJ-1 modulates mitochondrial response to oxidative stress: clues from a novel diagnosis of PARK7. *Clin Genet*, 2017. 92(1): p. 18-25.
- 255. Schapira, A.H., et al., Mitochondrial complex I deficiency in Parkinson's disease. *Lancet*, 1989. 1(8649): p. 1269.



256. Benecke, R., P. Strumper, and H. Weiss, Electron transfer complexes I and IV of platelets are abnormal in Parkinson's disease but normal in Parkinson-plus syndromes. *Brain*, 1993. 116 ( Pt 6): p. 1451-63.
257. Parker, W.D., Jr. and R.H. Swerdlow, Mitochondrial dysfunction in idiopathic Parkinson disease. *Am J Hum Genet*, 1998. 62(4): p. 758-62.
258. Ambrosi, G., et al., Bioenergetic and proteolytic defects in fibroblasts from patients with sporadic Parkinson's disease. *Biochim Biophys Acta*, 2014. 1842(9): p. 1385-94.
259. Grunewald, A., et al., Mitochondrial DNA Depletion in Respiratory Chain-Deficient Parkinson Disease Neurons. *Ann Neurol*, 2016. 79(3): p. 366-78.
260. Welchen, E., et al., Coordination of plant mitochondrial biogenesis: keeping pace with cellular requirements. *Front Plant Sci*, 2014. 4: p. 551.
261. Giaime, E., et al., Loss of DJ-1 does not affect mitochondrial respiration but increases ROS production and mitochondrial permeability transition pore opening. *PLoS One*, 2012. 7(7): p. e40501.
262. Hao, L.Y., B.I. Giasson, and N.M. Bonini, DJ-1 is critical for mitochondrial function and rescues PINK1 loss of function. *Proc Natl Acad Sci U S A*, 2010. 107(21): p. 9747-52.
263. Cuevas, S., et al., Role of renal DJ-1 in the pathogenesis of hypertension associated with increased reactive oxygen species production. *Hypertension*, 2012. 59(2): p. 446-52.

264. Exner, N., et al., Mitochondrial dysfunction in Parkinson's disease: molecular mechanisms and pathophysiological consequences. *EMBO J*, 2012. 31(14): p. 3038-62.
265. Glinka, Y., M. Gassen, and M.B. Youdim, Mechanism of 6-hydroxydopamine neurotoxicity. *J Neural Transm Suppl*, 1997. 50: p. 55-66.
266. Thomas, B. and M.F. Beal, Parkinson's disease. *Hum Mol Genet*, 2007. 16 Spec No. 2: p. R183-94.
267. Sekine, S. and R.J. Youle, PINK1 import regulation; a fine system to convey mitochondrial stress to the cytosol. *BMC Biol*, 2018. 16(1): p. 2.
268. Clark, I.E., et al., *Drosophila* pink1 is required for mitochondrial function and interacts genetically with parkin. *Nature*, 2006. 441(7097): p. 1162-6.
269. Park, J., et al., Mitochondrial dysfunction in *Drosophila* PINK1 mutants is complemented by parkin. *Nature*, 2006. 441(7097): p. 1157-61.
270. Von Coelln, R., et al., Loss of locus coeruleus neurons and reduced startle in parkin null mice. *Proc Natl Acad Sci U S A*, 2004. 101(29): p. 10744-9.
271. Kitada, T., et al., Absence of nigral degeneration in aged parkin/DJ-1/PINK1 triple knockout mice. *J Neurochem*, 2009. 111(3): p. 696-702.
272. Goldberg, M.S., et al., Parkin-deficient mice exhibit nigrostriatal deficits but not loss of dopaminergic neurons. *J Biol Chem*, 2003. 278(44): p. 43628-35.
273. Devine, M.J. and J.T. Kittler, Mitochondria at the neuronal presynapse in health and disease. *Nat Rev Neurosci*, 2018. 19(2): p. 63-80.

- 274. Stauch, K.L., et al., Central nervous system-penetrating antiretrovirals impair energetic reserve in striatal nerve terminals. *J Neurovirol*, 2017. 23(6): p. 795-807.
- 275. Gerencser, A.A., et al., Quantitative microplate-based respirometry with correction for oxygen diffusion. *Anal Chem*, 2009. 81(16): p. 6868-78.
- 276. Mendes, C.S., et al., Quantification of gait parameters in freely walking rodents. *BMC Biol*, 2015. 13: p. 50.
- 277. Ogawa, N., et al., A simple quantitative bradykinesia test in MPTP-treated mice. *Res Commun Chem Pathol Pharmacol*, 1985. 50(3): p. 435-41.
- 278. Pickles, S., P. Vigie, and R.J. Youle, Mitophagy and Quality Control Mechanisms in Mitochondrial Maintenance. *Curr Biol*, 2018. 28(4): p. R170-R185.
- 279. Periquet, M., et al., Parkin mutations are frequent in patients with isolated early-onset parkinsonism. *Brain*, 2003. 126(Pt 6): p. 1271-8.
- 280. Kitada, T., et al., Impaired dopamine release and synaptic plasticity in the striatum of parkin<sup>-/-</sup> mice. *J Neurochem*, 2009. 110(2): p. 613-21.
- 281. Oliveras-Salva, M., et al., Alpha-synuclein-induced neurodegeneration is exacerbated in PINK1 knockout mice. *Neurobiol Aging*, 2014. 35(11): p. 2625-2636.
- 282. Tagliaferro, P. and R.E. Burke, Retrograde Axonal Degeneration in Parkinson Disease. *J Parkinsons Dis*, 2016. 6(1): p. 1-15.
- 283. Taylor, R.W. and D.M. Turnbull, Mitochondrial DNA mutations in human disease. *Nat Rev Genet*, 2005. 6(5): p. 389-402.

- 284. Newman, L.E. and G.S. Shadel, Pink1/Parkin link inflammation, mitochondrial stress, and neurodegeneration. *J Cell Biol*, 2018. 217(10): p. 3327-3329.
- 285. Dahodwala, N., et al., Sex disparities in access to caregiving in Parkinson disease. *Neurology*, 2018. 90(1): p. e48-e54.
- 286. Fahn, S., Levodopa-induced neurotoxicity. *CNS drugs*, 1997. 8(5): p. 376-393.
- 287. Fisher, B.E., et al., Exercise-induced behavioral recovery and neuroplasticity in the 1-methyl-4-phenyl-1,2,3,6-tetrahydropyridine-lesioned mouse basal ganglia. *J Neurosci Res*, 2004. 77(3): p. 378-90.
- 288. Petzinger, G.M., et al., Effects of treadmill exercise on dopaminergic transmission in the 1-methyl-4-phenyl-1,2,3,6-tetrahydropyridine-lesioned mouse model of basal ganglia injury. *J Neurosci*, 2007. 27(20): p. 5291-300.
- 289. Kempermann, G., H. van Praag, and F.H. Gage, Activity-dependent regulation of neuronal plasticity and self repair. *Prog Brain Res*, 2000. 127: p. 35-48.
- 290. Kelly, N.A., et al., Novel, high-intensity exercise prescription improves muscle mass, mitochondrial function, and physical capacity in individuals with Parkinson's disease. *J Appl Physiol (1985)*, 2014. 116(5): p. 582-92.